# ECE453 Spring 2019 Course Info

- Instructor: Professor Steven Franke
- Office: 5048 ECEB, s-franke@illinois.edu
- Office Hours: 10-11am M-F
- Purchase Course Notes from ECE Store or download from 453 web site

# Course Grading Policy

- Hour Exams (2): 20% each. (One 8.5”x11” sheet of notes allowed per exam)
    - Exam 1: Friday, March 1 (in class)
    - Exam 2: Friday, April 12 (in class)
- Homework: 5%
- Final Exam: 30% (Tues, May 7, 7-10 pm, 2015 ECEB --- 3 sheets of notes allowed.)
- Lab Grade: 25% (assigned by your lab instructor)

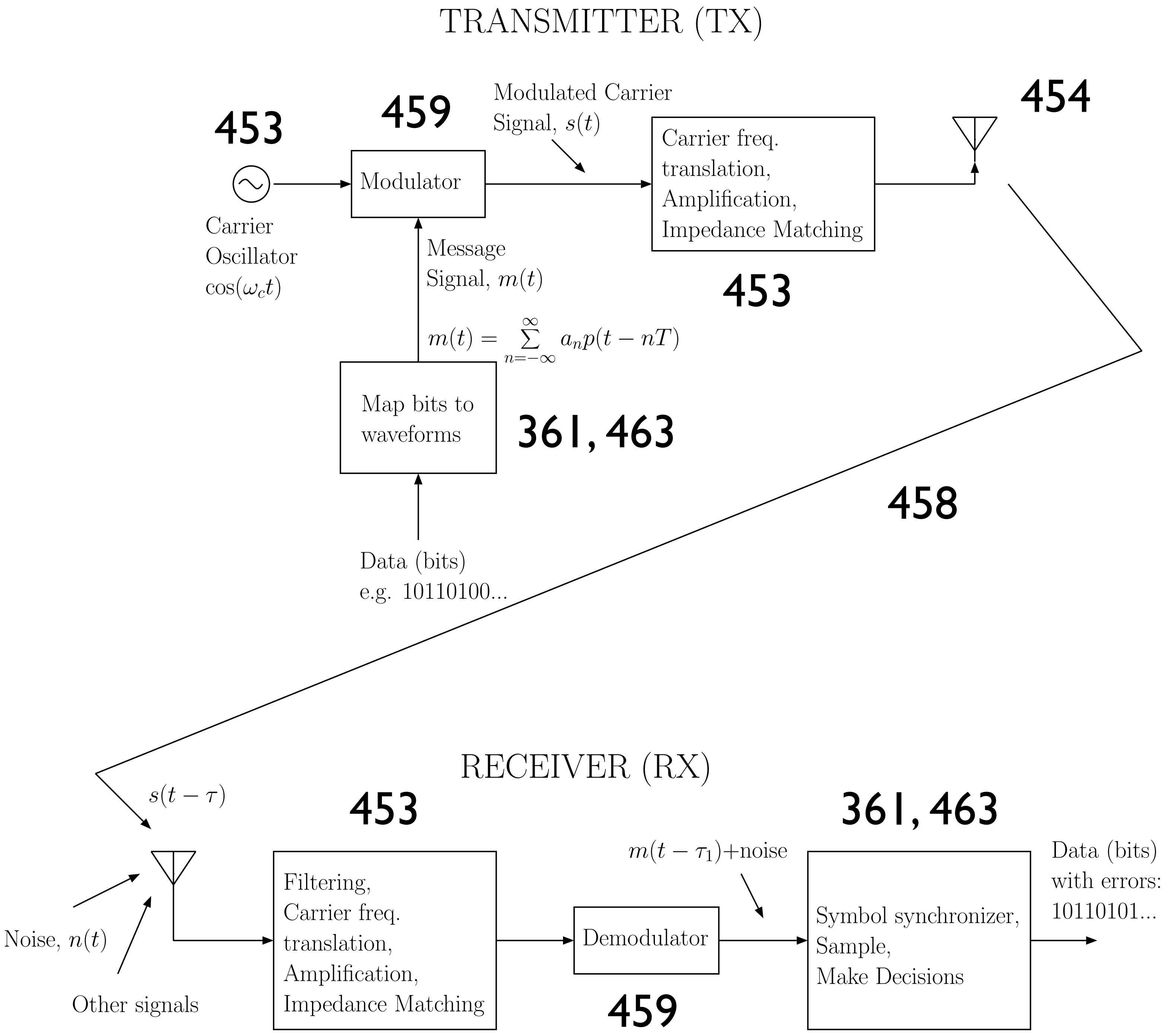
TRANSMITTER (TX)
453
459
Modulated Carrier Signal, $s(t)$
454
Modulator
Carrier freq. translation, Amplification, Impedance Matching
Carrier Oscillator $\cos(\omega_c t)$
Message Signal, $m(t)$
453
$m(t) = \sum_{n=-\infty}^{\infty} a_n p(t - nT)$
Map bits to waveforms
361, 463
458
Data (bits) e.g. 10110100...
RECEIVER (RX)
$s(t - \tau)$
453
361, 463
$m(t - \tau_1)$+noise
Data (bits) with errors: 10110101...
Noise, $n(t)$
Other signals
Filtering, Carrier freq. translation, Amplification, Impedance Matching
Demodulator
Symbol synchronizer, Sample, Make Decisions
459

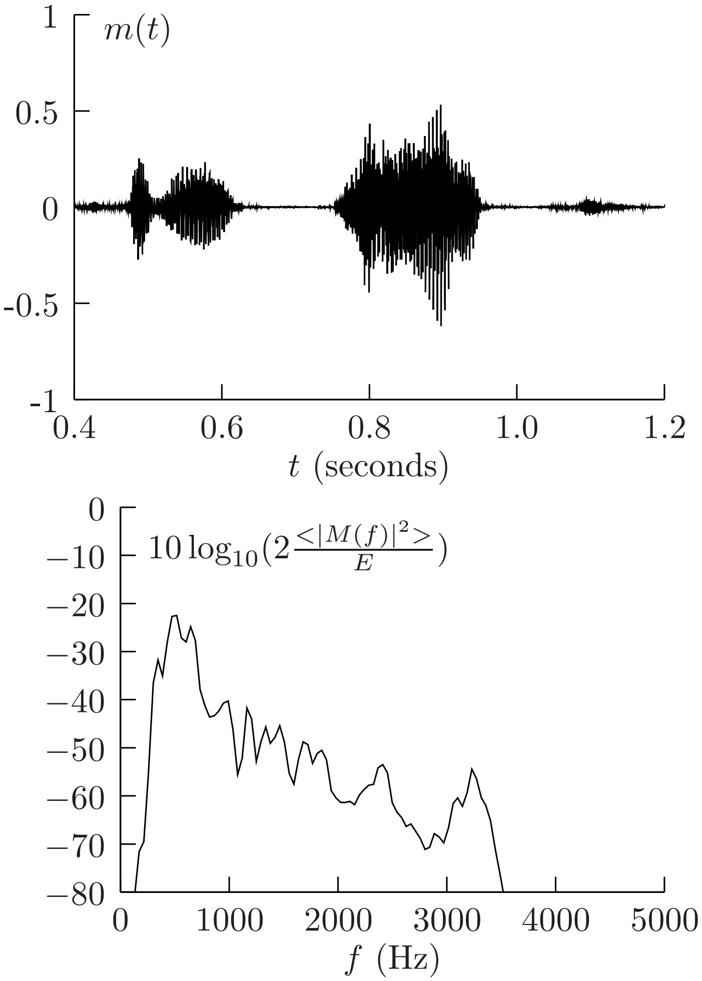

Figure 1.7: Top: message signal consisting of 0.8 seconds of audio from a radio talk show. Bottom: normalized average energy spectrum (in dB) of a 15-second segment of audio from the same talk show. The average energy spectrum was calculated by segmenting the original time series, sampled at 44.1 ksamples/s, into 512 point segments. The discrete Fourier transform (DFT) was calculated for each segment, and the squared magnitude of each DFT was averaged.

In a digital communication system the message signal will typically be formed from a superposition of pulses with amplitudes chosen to represent a sequence of information bits. In this case $m(t)$ can be written

$$m(t) = \sum_n a_n p(t - nT)$$

where:

$p(t)$ is a pulse function chosen to control the shape of the spectrum of $m(t)$

$a_n$ is a sequence of pulse amplitudes chosen from a finite set of possible values

$T$ is the signaling interval, and $T^{-1}$ is then the signaling rate — the rate at which pulses are transmitted.

$a_n \in \{-1, 1\}$: binary pulse amplitudes, $\log_2(2) = 1$ bit of information per pulse $\rightarrow \frac{1}{T}$ bits/sec

$a_n \in \{-1, 0, 1\}$: ternary pulse amplitudes, $\log_2(3) = 1.585$ bits per pulse $\rightarrow \frac{1.585}{T}$ bits/sec

$a_n \in \{-1.5, -0.5, 0.5, 1.5\}$: 4-ary pulse amplitudes, $\log_2(4) = 2$ bits per pulse $\rightarrow \frac{2}{T}$ bits/sec

$a_n \in \{-3.5, -2.5, -1.5, -0.5, 0.5, 1.5, 2.5, 3.5\}$: 8-ary pulse amplitudes, $\log_2(8) = 3$ bits per pulse $\rightarrow \frac{3}{T}$ bits/sec

bits per second = pulses per second x bits per pulse

$$\mathcal{F}(m(t)) = M(f) = \int_{-\infty}^{\infty} m(t) e^{-j2\pi f t} dt$$

$$M(f) = \int_{-\infty}^{\infty} [\sum_n a_n p(t - nT)] e^{-j2\pi f t} dt$$

$$M(f) = P(f) \sum_n a_n e^{-j2\pi f n T}$$

$$< |M(f)|^2 >= |P(f)|^2 \underbrace{< |\sum_n a_n e^{-j2\pi f n T}|^2 >}_{\text{a constant}}$$

If the pulses, $p(t)$, have bandwidth $W$ then the message signal, $m(t)$, will also have bandwidth $W$.

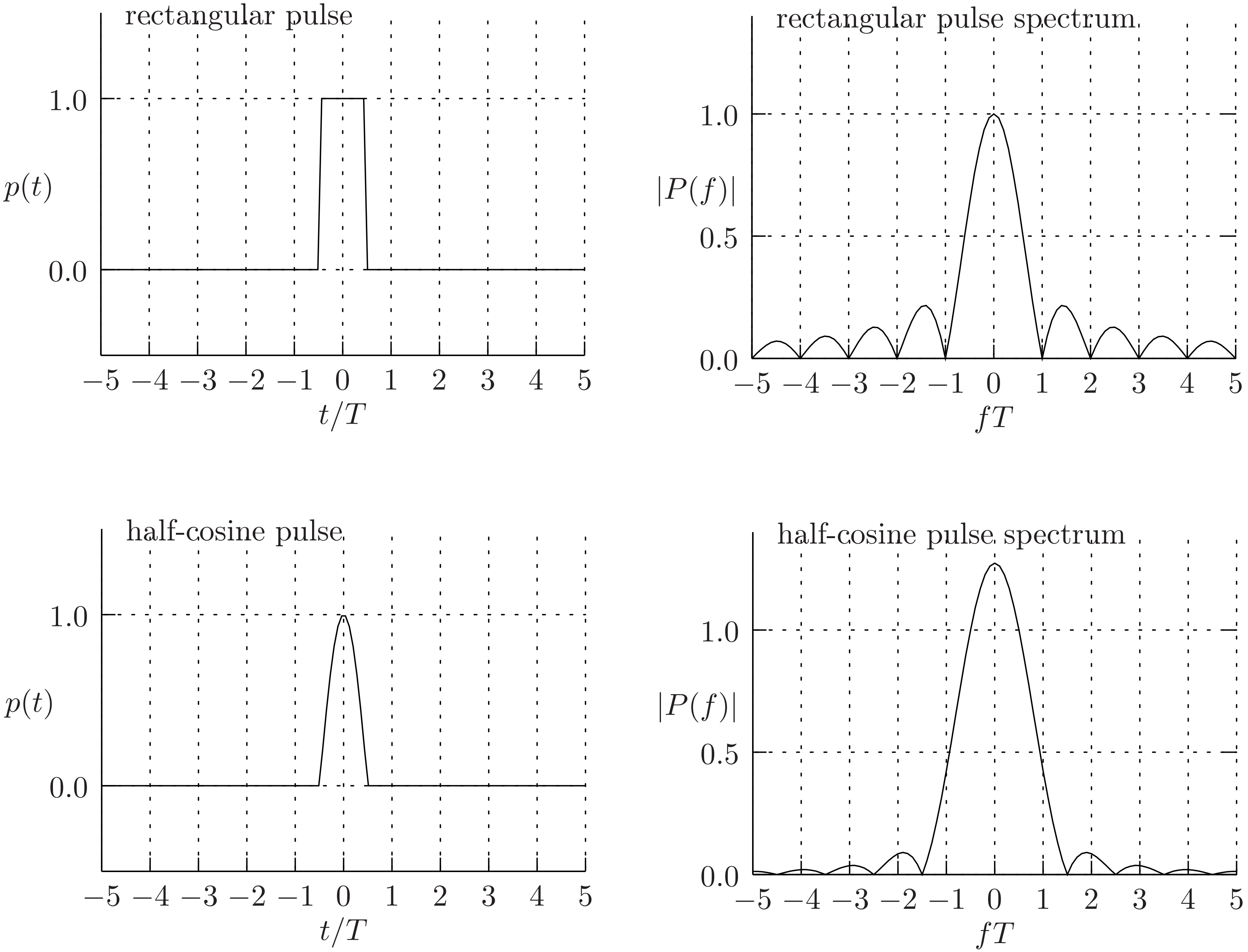
rectangular pulse
1.0
0.0
p(t)
−5 −4 −3 −2 −1 0 1 2 3 4 5
t/T
rectangular pulse spectrum
1.0
0.5
0.0
|P(f)|
−5 −4 −3 −2 −1 0 1 2 3 4 5
fT
half-cosine pulse
1.0
0.0
p(t)
−5 −4 −3 −2 −1 0 1 2 3 4 5
t/T
half-cosine pulse spectrum
1.0
0.5
0.0
|P(f)|
−5 −4 −3 −2 −1 0 1 2 3 4 5
fT

In practice, communication channels have finite bandwidth, $W$, so it is best to use pulses that have finite bandwidth.

If pulses are bandlimited, then successive pulses in the message signal $m(t) = \sum a_n p(t - nT)$ will overlap. This is called *intersymbol interference.*

In 1928 Harry Nyquist showed that:

> it is possible to design bandlimited (finite bandwidth) pulse waveforms that go to zero at multiples of $T$ seconds, so that inter symbol interference vanishes at discrete times $0, T, 2T, \ldots.$ Pulses that pass through zero at multiples of $T$ are called *Nyquist pulses.*
>
> given a channel with bandwidth $W$, it is possible to send pulses at a maximum rate of $2W$ pulses per second with no intersymbol interference using Nyquist pulses.
>
> if we want to send pulses at a given rate, say $1/T$ pulses per second, then the minimum bandwidth required for no intersymbol interference is $1/2T$ Hz.

Nyquist's 1928 signaling-rate results were cited by Claude Shannon in 1945 when Shannon derived the Nyquist-Shannon sampling theorem.

# Certain Topics in Telegraph Transmission Theory

BY H. NYQUIST[1]
Member, A. I. E. E.

***Synopsis.***—*The most obvious method for determining the distortion of telegraph signals is to calculate the transients of the telegraph system. This method has been treated by various writers, and solutions are available for telegraph lines with simple terminal conditions. It is well known that the extension of the same methods to more complicated terminal conditions, which represent the usual terminal apparatus, leads to great difficulties.*

*The present paper attacks the same problem from the alternative standpoint of the steady-state characteristics of the system. This method has the advantage over the method of transients that the complication of the circuit which results from the use of terminal apparatus does not complicate the calculations materially. This method of treatment necessitates expressing the criteria of distortionless transmission in terms of the steady-state characteristics. Accordingly, a considerable portion of the paper describes and illustrates a method for making this translation.*

*A discussion is given of the minimum frequency range required for transmission at a given speed of signaling. In the case of carrier telegraphy, this discussion includes a comparison of single-sideband and double-sideband transmission. A number of incidental topics is also discussed.*

* * * * *

## SCOPE

THE purpose of this paper is to set forth the results of theoretical studies of telegraph systems which have been made from time to time. These results are naturally disconnected and in order to make a connected story it has been necessary to include a certain amount of material which is already well known to telegraph engineers. The following topics are discussed:

1. The required frequency band is directly proportional to the signaling speed.

2. A repeated telegraph signal (of any length) may be considered as being made up of sinusoidal components. When the amplitude and phase, or real and imaginary parts, of these components are plotted as ordinates with their frequencies as abscissas, and when the frequency axis is divided into parts each being a frequency band of width numerically equal to the speed of signaling, it is found that the information conveyed in any band is substantially identical with

is shown that the usual carrier telegraph requires twice as much frequency range as the corresponding d-c. telegraph, other things being equal.

8. A discussion is given of two alternative methods for overcoming this inefficiency of carrier telegraphy, namely, the use of phase discrimination and of a single sideband.

9. After the d-c. and carrier waves have thus been analyzed a corresponding analysis is given of an arbitrary wave shape, including these two as special cases. Calculations are given on the shaping of the transmitted wave so as to make the received wave perfect.

10. A discussion is given of the dual aspect of the telegraph wave. The wave may be looked on either as a function of $\omega$, requiring the so-called steady-state method of treatment, or as a function of $t$ requiring the so-called method of transients. It is shown that the steady-state theory can be made to yield the information necessary to specify the characteristics of an

A very useful family of pulses with finite bandwidth is obtained by defining the pulse such that its Fourier transform transitions from a constant (flat) central region to zero through a smooth transition region having a raised cosine shape. These pulses are called *raised-cosine pulses* (Figure 1.8(c-e)). The Fourier transform of the raised-cosine pulse is

$$P(f) = \begin{cases} T & |fT| \leq \frac{1}{2}(1-\beta) \\ \frac{T}{2}\{1+\cos[\frac{\pi}{\beta}(|fT| - \frac{1}{2}(1-\beta)]\} & \frac{1}{2}(1-\beta) < |fT| \leq \frac{1}{2}(1+\beta) \\ 0 & |fT| > \frac{1}{2}(1+\beta) \end{cases} , \qquad (1.6)$$

where $0 \leq \beta \leq 1$. The dimensionless parameter $\beta$ controls the width of the raised-cosine transition region. The time-domain pulse shape of the raised-cosine pulse is

$$p(t) = \frac{\sin(\pi t/T)}{\pi t/T} \frac{\cos(\pi\beta t/T)}{1-(2\beta t/T)^2}. \qquad (1.7)$$

The bandwidth of these pulses is $W = \frac{1}{2T}(1+\beta)$. The parameter $\beta$ is called the fractional *excess bandwidth* and it is often expressed as a percentage. The minimum possible bandwidth results when $\beta = 0$ which results in $W = \frac{1}{2T}$. In this case, the spectrum becomes rectangular and the pulse shape is a sinc function with relatively large sidelobes that extend over many signaling intervals on either side of the center of the pulse. For $0 < \beta \leq 1$, the amplitude spectrum exhibits a gradual transition to zero. As $\beta$ increases, the sidelobes are increasingly damped and the time-domain pulse becomes more compact and extends over fewer signaling intervals.

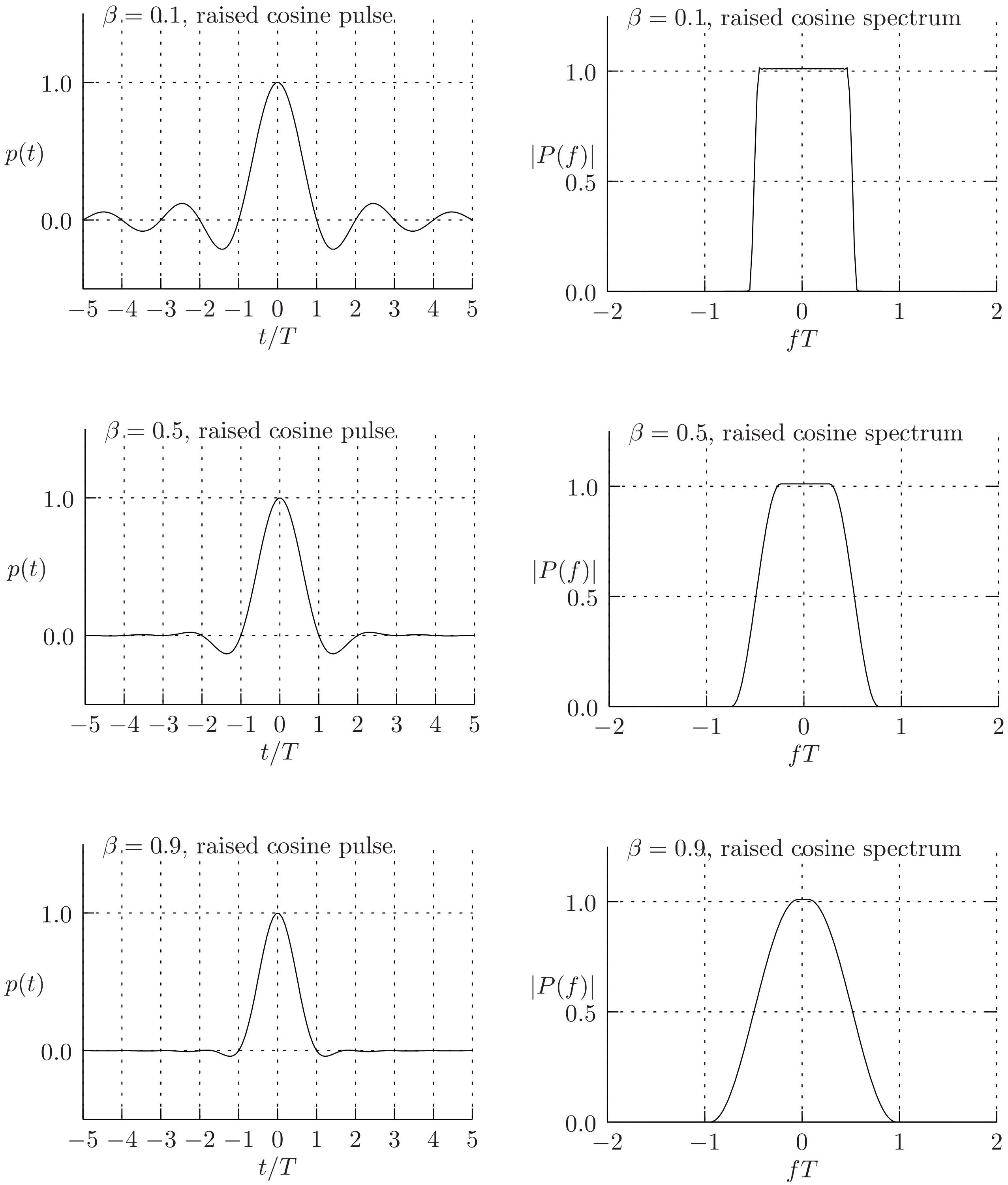
$\beta = 0.1$, raised cosine pulse
$\beta = 0.1$, raised cosine spectrum
$\beta = 0.5$, raised cosine pulse
$\beta = 0.5$, raised cosine spectrum
$\beta = 0.9$, raised cosine pulse
$\beta = 0.9$, raised cosine spectrum
$p(t)$
1.0
0.0
$t/T$
$-5$ $-4$ $-3$ $-2$ $-1$ 0 1 2 3 4 5
$|P(f)|$
1.0
0.5
0.0
$fT$
$-2$ $-1$ 0 1 2

Message signal $$m(t) = \sum_{n=-\infty}^{\infty} a_n\, p(t - nT)$$

Raised – cosine (spectrum) pulse $$p(t) = \frac{\sin(\frac{\pi t}{T})}{\frac{\pi t}{T}} \frac{\cos(\pi \beta \frac{t}{T})}{1 - 4\beta^2 (\frac{t}{T})^2}$$

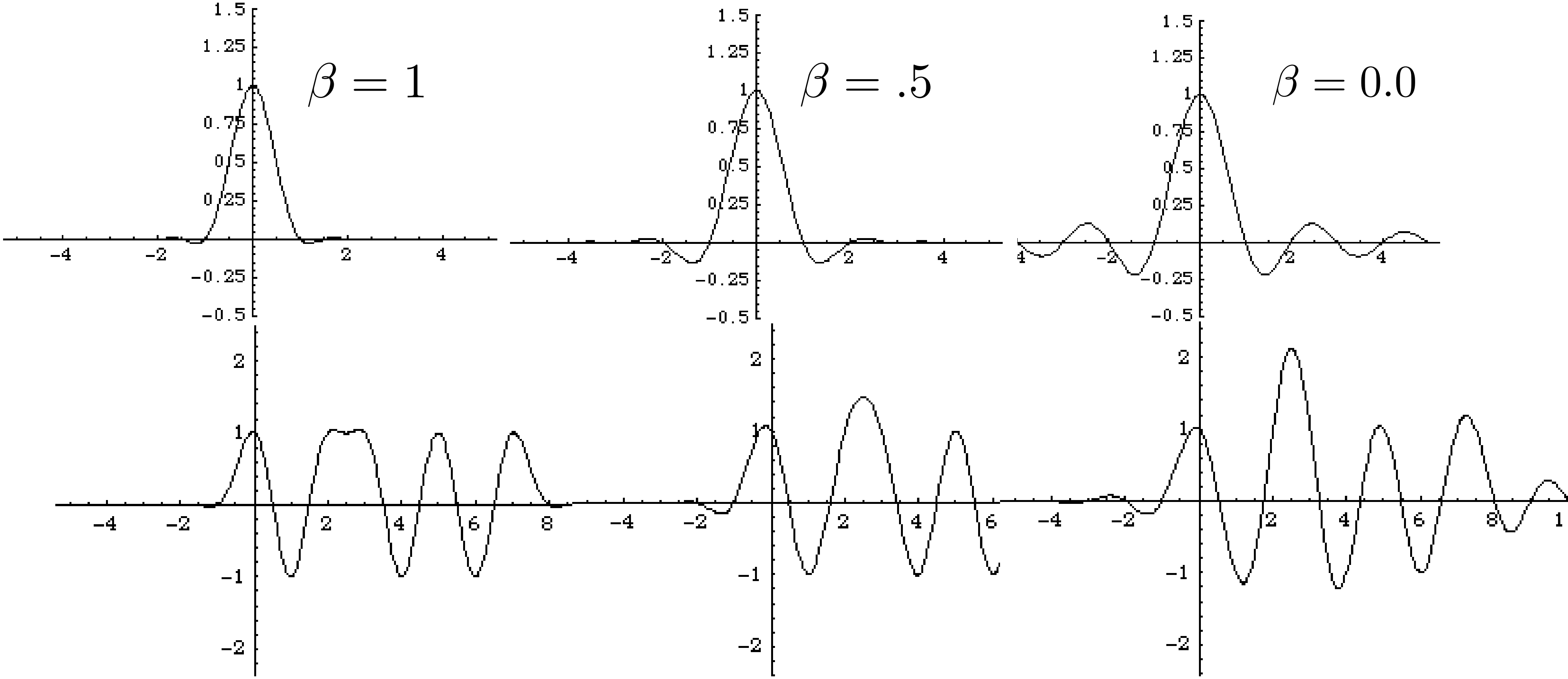

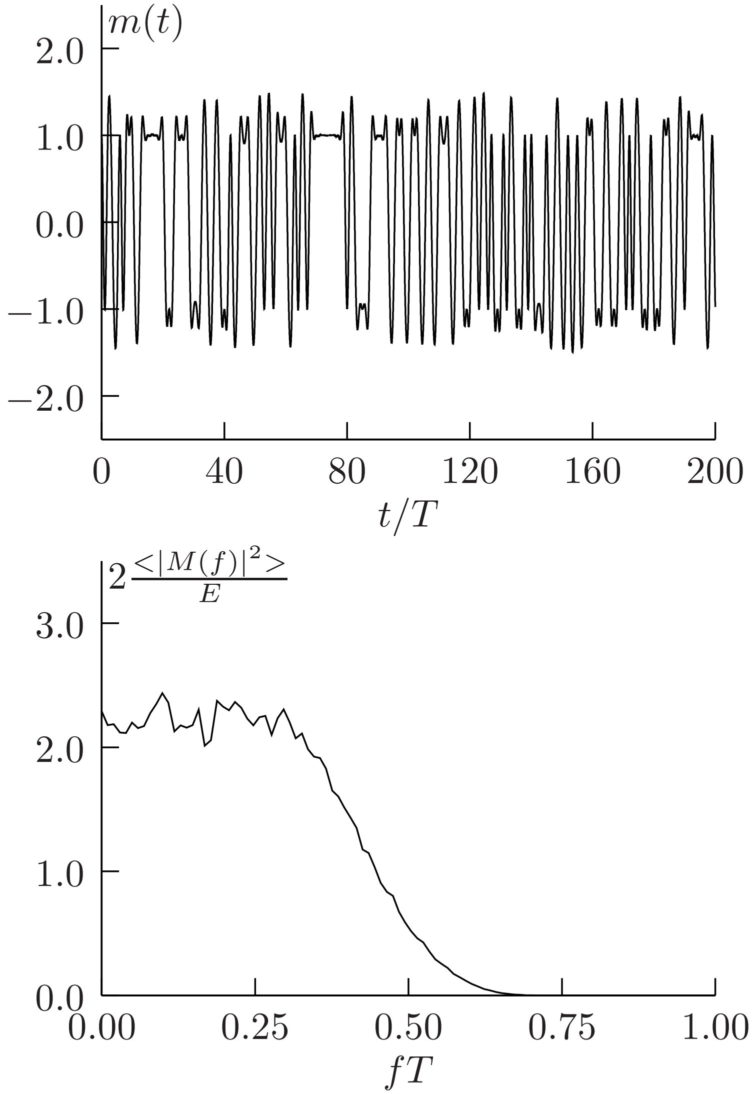

Figure 1.9: Top: A message signal produced using a random data sequence and raised-cosine pulses with $\beta = 0.5$. Bottom: Normalized average energy spectrum of $m(t)$ computed numerically using the following procedure: a message signal of length $32768T$ was generated using a random sequence of bits. The long message signal was divided into short segments of length approximately $100T$. The energy spectrum of each short segment was computed, and all spectra were averaged. The average spectrum was normalized so that the area under the spectrum is 1.0. Note that the shape of the energy spectrum exhibits the raised-cosine shape of the pulses. Since $\beta = 0.5$, the bandwidth of the spectrum is $WT = \frac{1}{2}(1 + 0.5) = 0.75$.

bits per second = pulses per second x bits per pulse

- Given a channel with bandwidth $W$ (Hz), maximum pulse rate is $2W$ (Nyquist).
- Maximum number of bits per pulse?
  In practice, the energy per pulse will be limited by hardware constraints. Thus, peak pulse amplitude (largest value of $|a_n|$) is limited.
- To increase bits per pulse when peak amplitude is limited, must decrease the spacing between amplitudes. If the difference between pulse amplitudes becomes smaller than rms noise, then the receiver can't tell the difference between amplitudes. So bits per pulse is limited by channel signal to noise ratio (SNR).
- If SNR is large, can use a large set of pulse amplitudes and hence many bits per pulse.

Summary - bits per pulse is limited by signal to noise ratio on the channel
The Shannon Channel Capacity theorem tells us what is possib

$$C = W \log_2(1 + SNR)$$

$C$ = channel capacity in bits per second
$W$ = channel bandwidth in Hz
$SNR$ = signal to noise power ratio

Apparently, for the signaling scheme that we have been discus
number of bits per pulse is:

$$\tfrac{1}{2} \log_2(1 + SNR)$$

e.g. 1MBit/s in a 20 kHz channel
SNR=2^(C/W)-1 =
2^(10^6/2(10^4))-1=2^50-1=10^15
(150 dB)

100kBit/s in same channel
SNR=2^5-1 = 31 (15 dB)

SNR=1 => 1/2 bit per pulse ?
Need to send two symbols to convey one bit (FEC).

Digital Television (DTV) message signal:

$$m(t) = \sum_n a_n p(t - nT)$$

$a_n \in (-3.5, -2.5, -1.5, -0.5, 0.5, 1.5, 2.5, 3.5)$

8 possible pulse amplitudes: $log_2(8) = 3$ bits/pulse

Signaling rate $T^{-1} = 10.762238$ Mpulses/sec, or 3 bits/pulse $\times 10.762238 \simeq 32.387$ Mbits/sec.

About 40 percent of the bits are used to provide forward error correction, so that actual data rate is approximately $0.60 \times 32.387 =$ 19.4 Mbits/sec.

Pulses, $p(t)$, are square-root raised-cosine with $\beta = 0.0575$ (5.75% excess bandwidth).

Pulse bandwidth (and message signal bandwidt
$W = \frac{1}{2T}(1 + \beta) = 5.69$ MHz.

Min SNR for 20 Mbit/s in 6 MHz channel is:
SNR=2^20/6-1=9 (10log10(9)=9.5 dB)

In practice, need about 16 dB.

# Modulation - overview

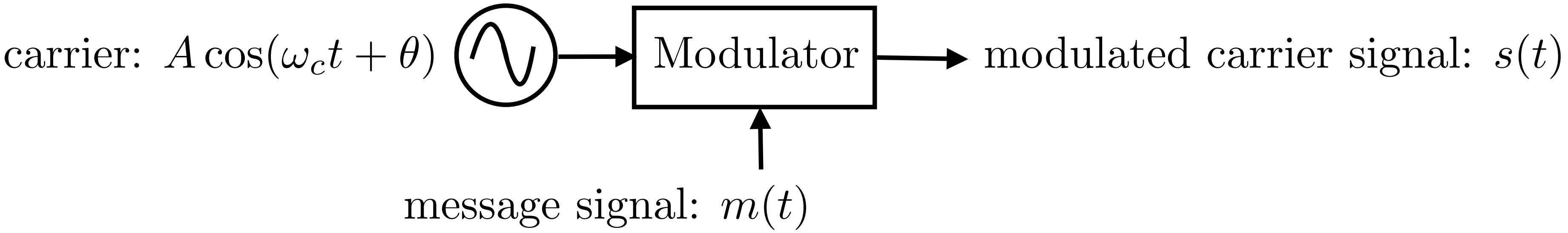

carrier: $A\cos(\omega_c t + \theta)$

Modulator

modulated carrier signal: $s(t)$

message signal: $m(t)$

1. Amplitude Modulation (linear):

amplitude, $A$, varies in response to $m(t)$, i.e. $A \rightarrow A(t) = Am(t) + B$

linear in the following sense: if $m_1(t)$ results in $s_1(t)$ and $m_2(t)$ results in $s_2(t)$, then $m_1(t) + m_2(t)$ results in $s_1(t) + s_2(t)$.

2. Angle Modulation (nonlinear):

phase, $\theta$, varies in response to $m(t)$, i.e. $\theta \rightarrow \theta(t) = k_p m(t)$ or $\frac{d\theta}{dt} = k_f m(t)$

nonlinear because $m_1(t) + m_2(t)$ does not yield $s_1(t) + s_2(t)$.

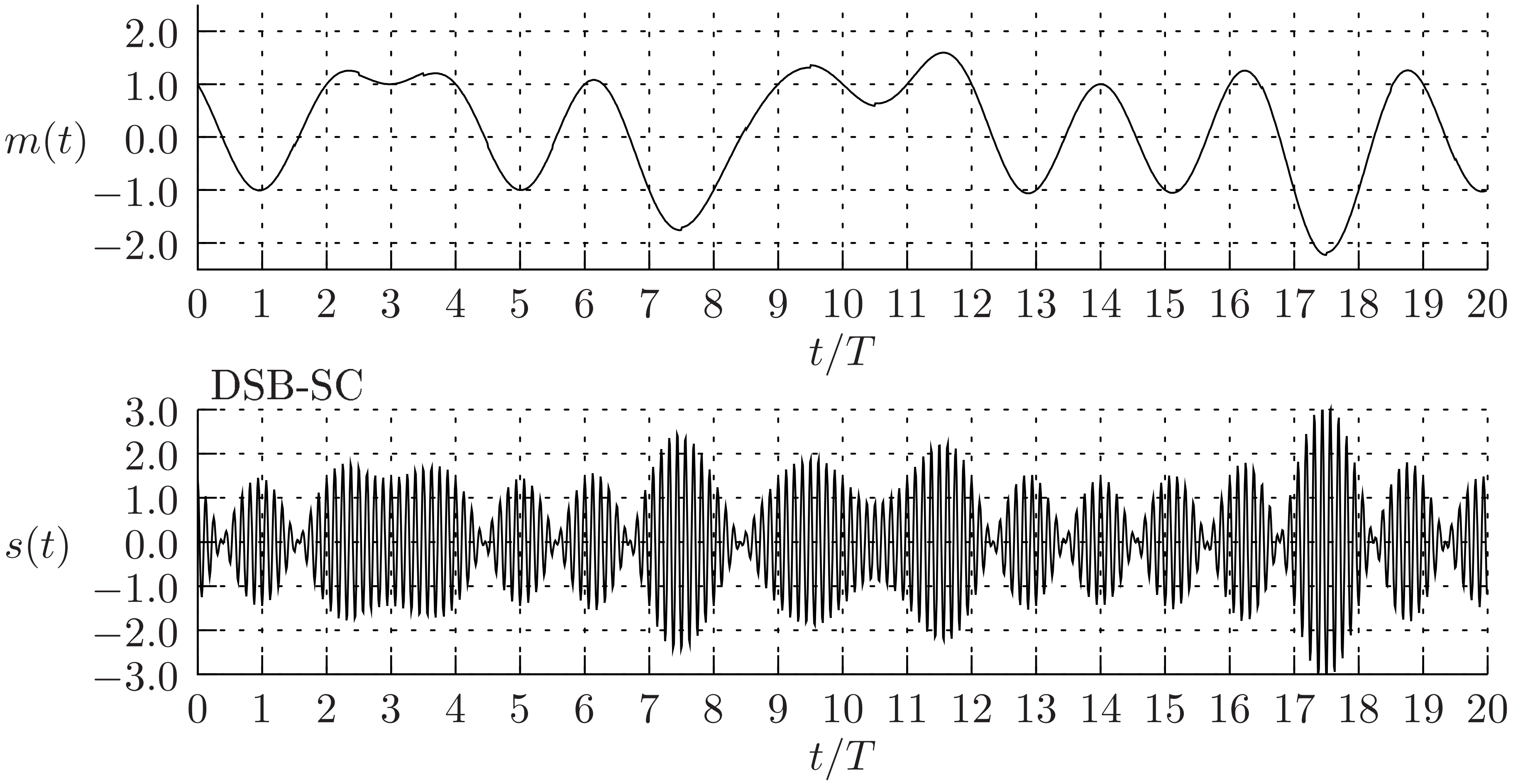

Figure 1.8: Top: message signal representing 20 information bits generated using raised-cosine pulses with $\beta = 0.1$. Bottom: DSB-SC signal, $s(t)$, normalized such that $< s^2(t) >= 1$.

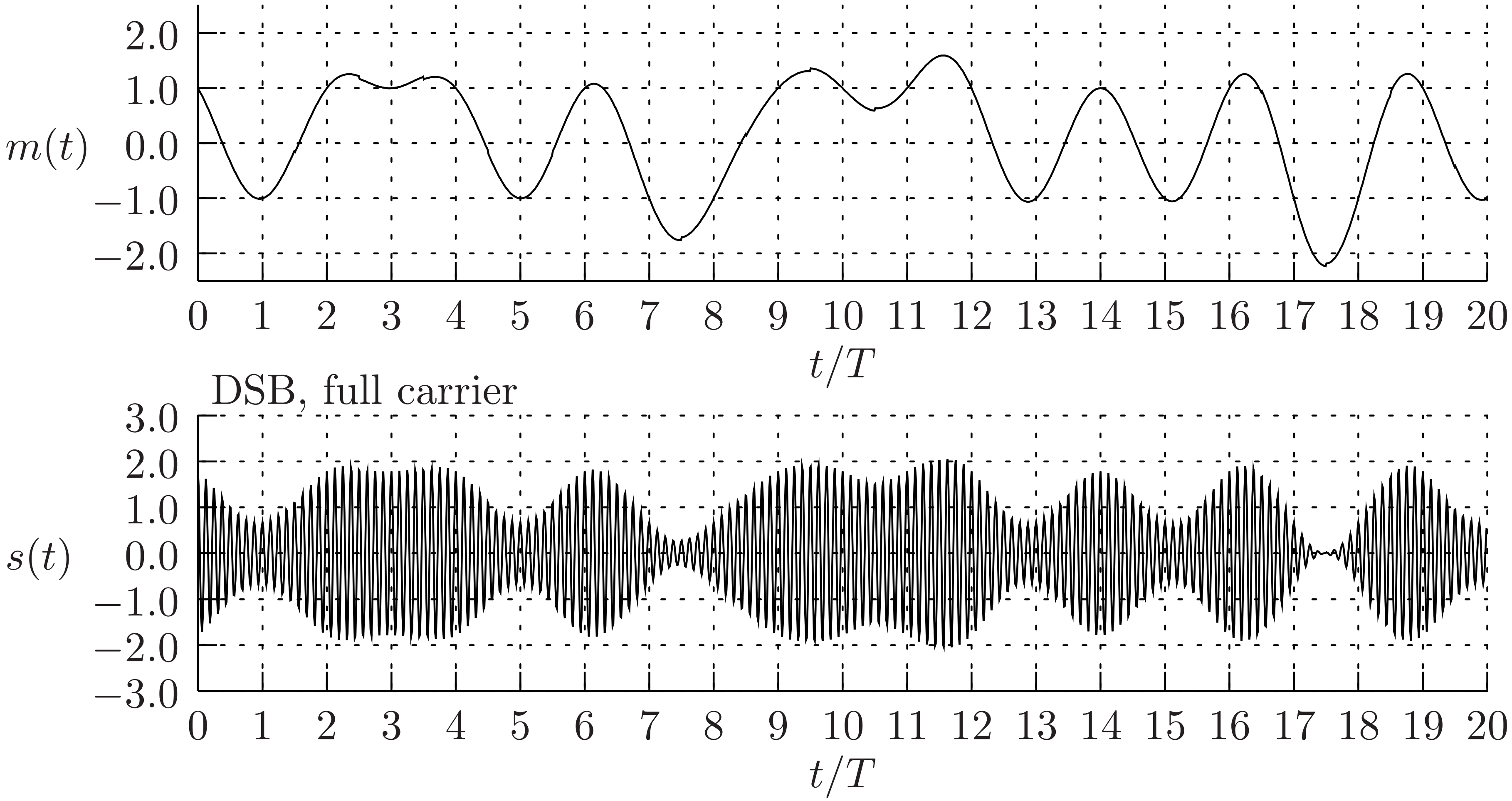

Figure 1.17: Top: message signal representing 20 information bits generated using raised-cosine pulses with $\beta = 0.1$. Bottom: DSB with full-carrier signal, $s(t)$, normalized such that $< s^2(t) >= 1$. Compare the bottom plot with the corresponding plot in Figure 1.9.

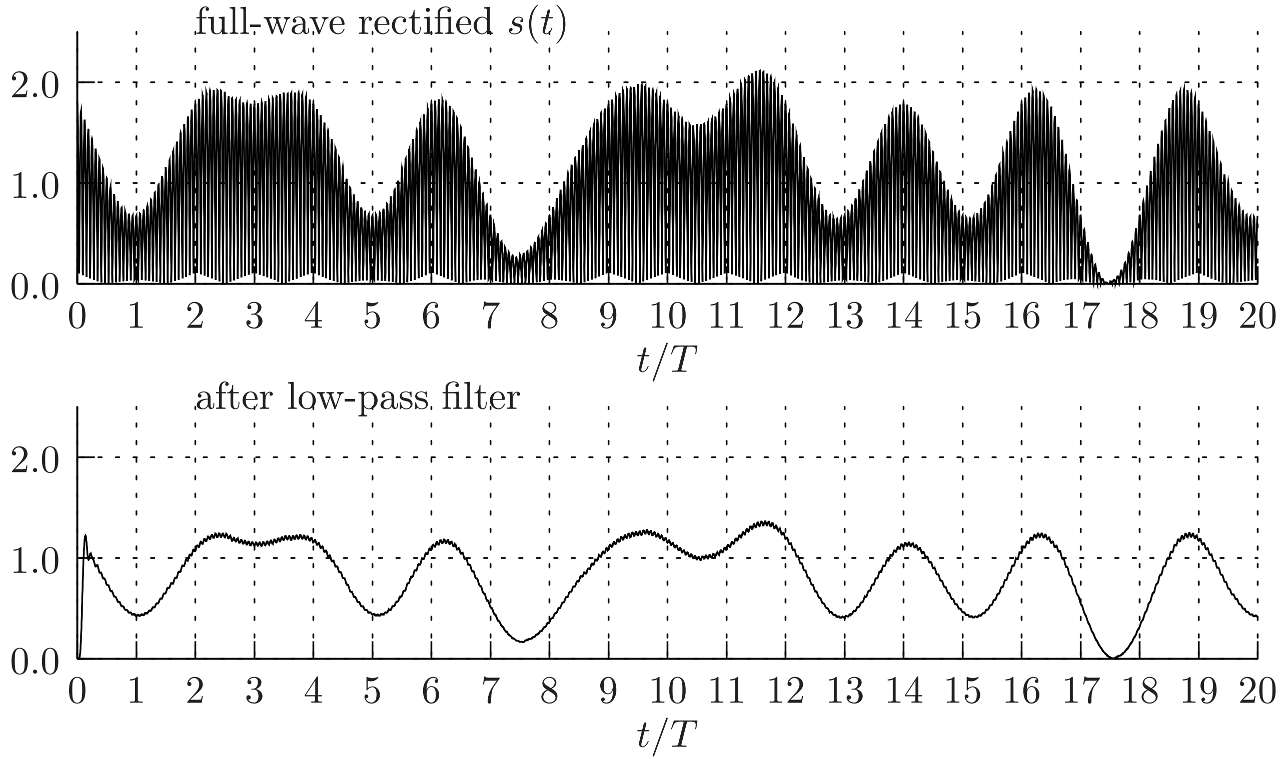

Figure 1.18: Upper plot shows $|s(t)|$, which is the result of passing $s(t)$ through a full-wave rectifier. The lower plot was obtained by passing the signal shown in the upper plot through a low-pass filter with cutoff frequency larger than the bandwidth of $m(t)$ (W) and smaller than $f_c - W$. The transient at the beginning of the lower plot is the start-up transient of the digital lowpass filter used to produce the simulated signal.

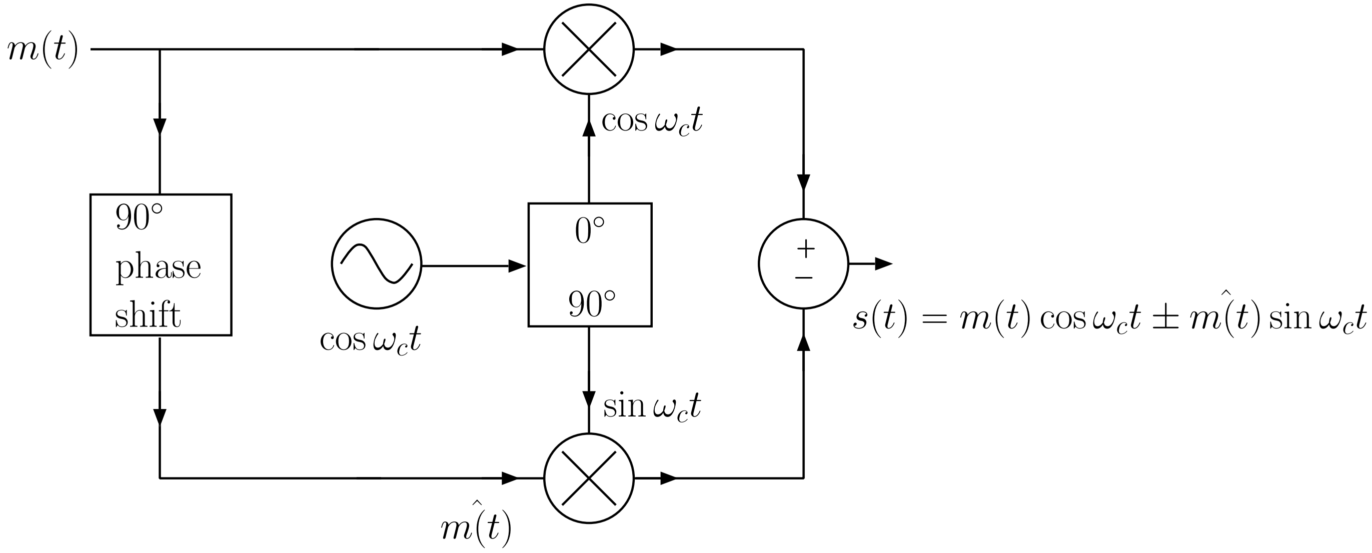
$m(t)$
90° phase shift
$\cos\omega_c t$
0°
90°
$\cos\omega_c t$
$\sin\omega_c t$
$\hat{m}(t)$
+
−
$s(t) = m(t)\cos\omega_c t \pm \hat{m}(t)\sin\omega_c t$

Figure 1.22: Phasing method for generation of an SSB signal.

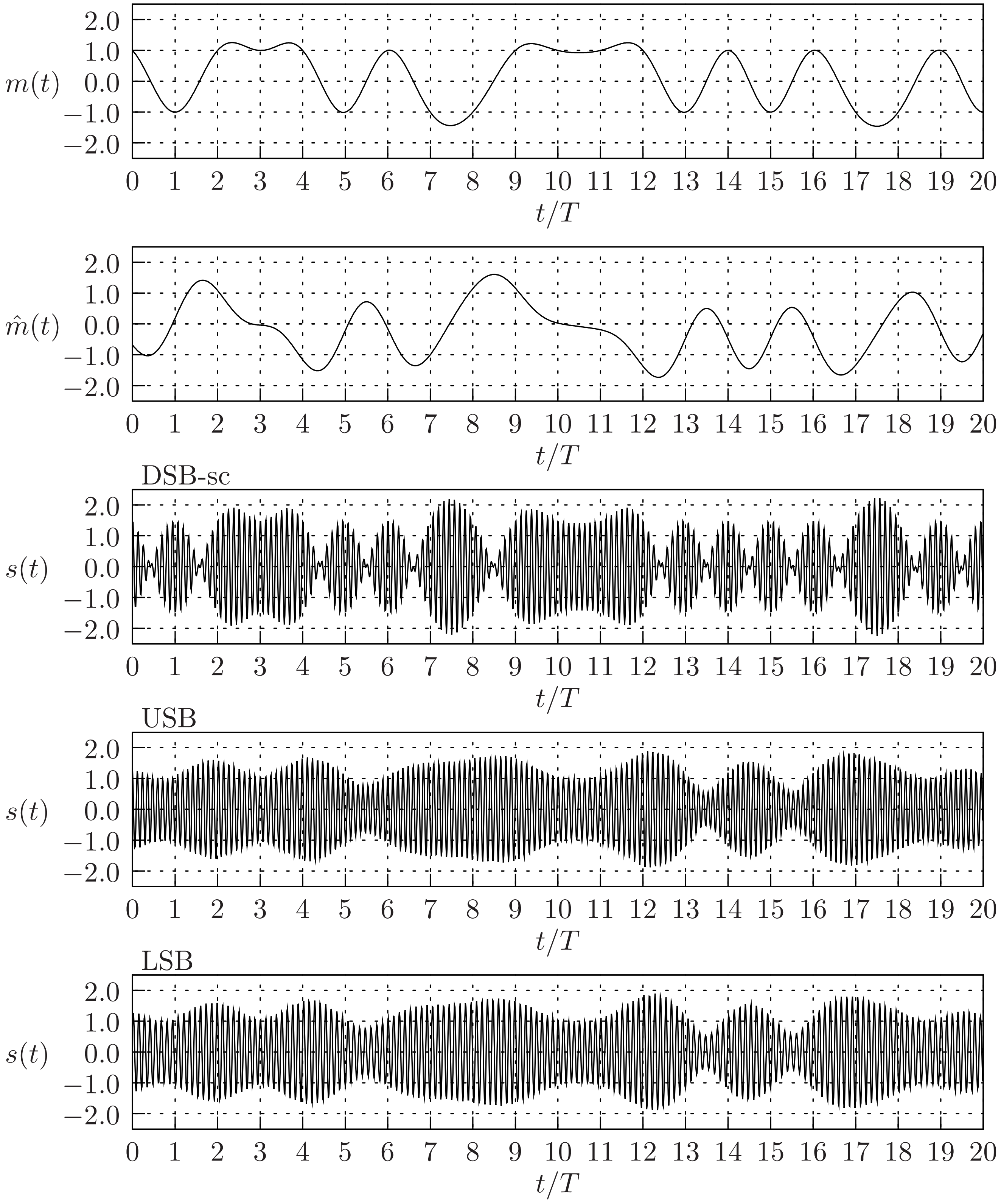
m(t)
m̂(t)
DSB-sc
USB
LSB
s(t)
2.0
1.0
0.0
−1.0
−2.0
0 1 2 3 4 5 6 7 8 9 10 11 12 13 14 15 16 17 18 19 20
t/T

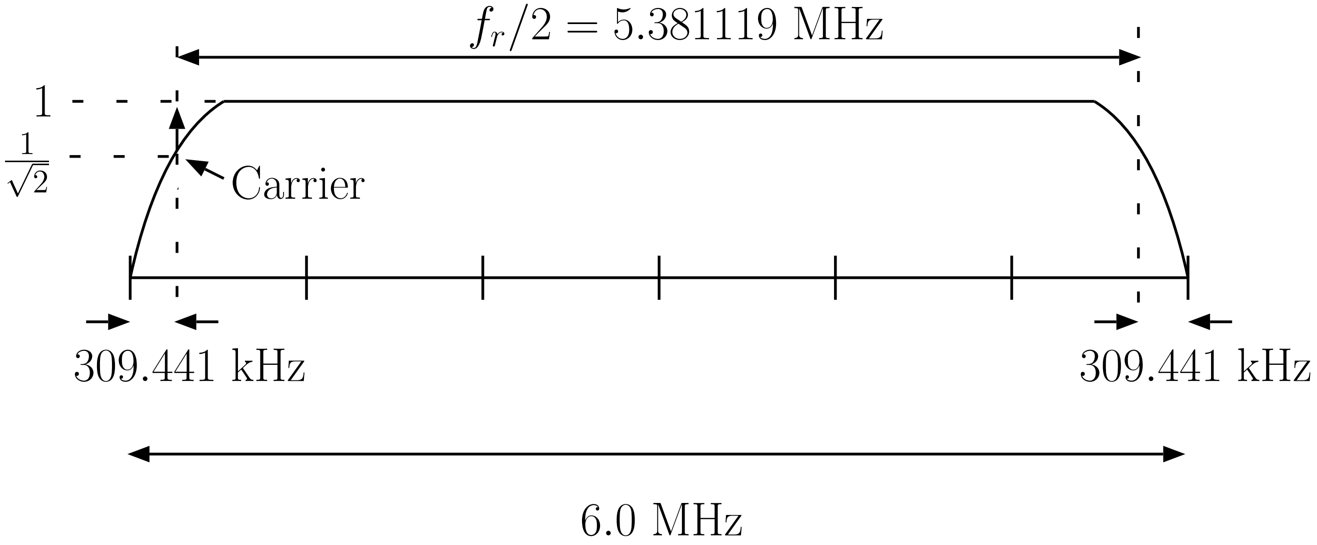

$f_r/2 = 5.381119$ MHz
1
$\frac{1}{\sqrt{2}}$
Carrier
309.441 kHz
309.441 kHz
6.0 MHz

Figure 1.26: The spectrum of a television signal as transmitted for digital television (DTV) using the ATSC (Advanced Television Systems Committee) 8VSB system.

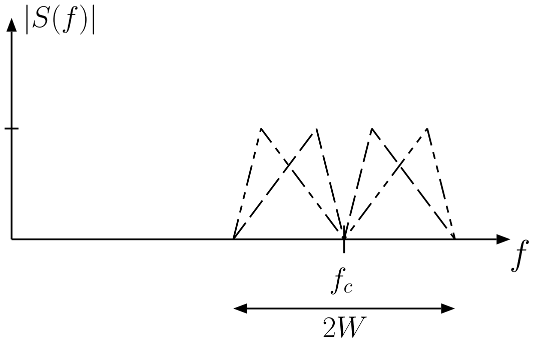

Figure 1.24: Two DSB-SC components with overlapping spectra.

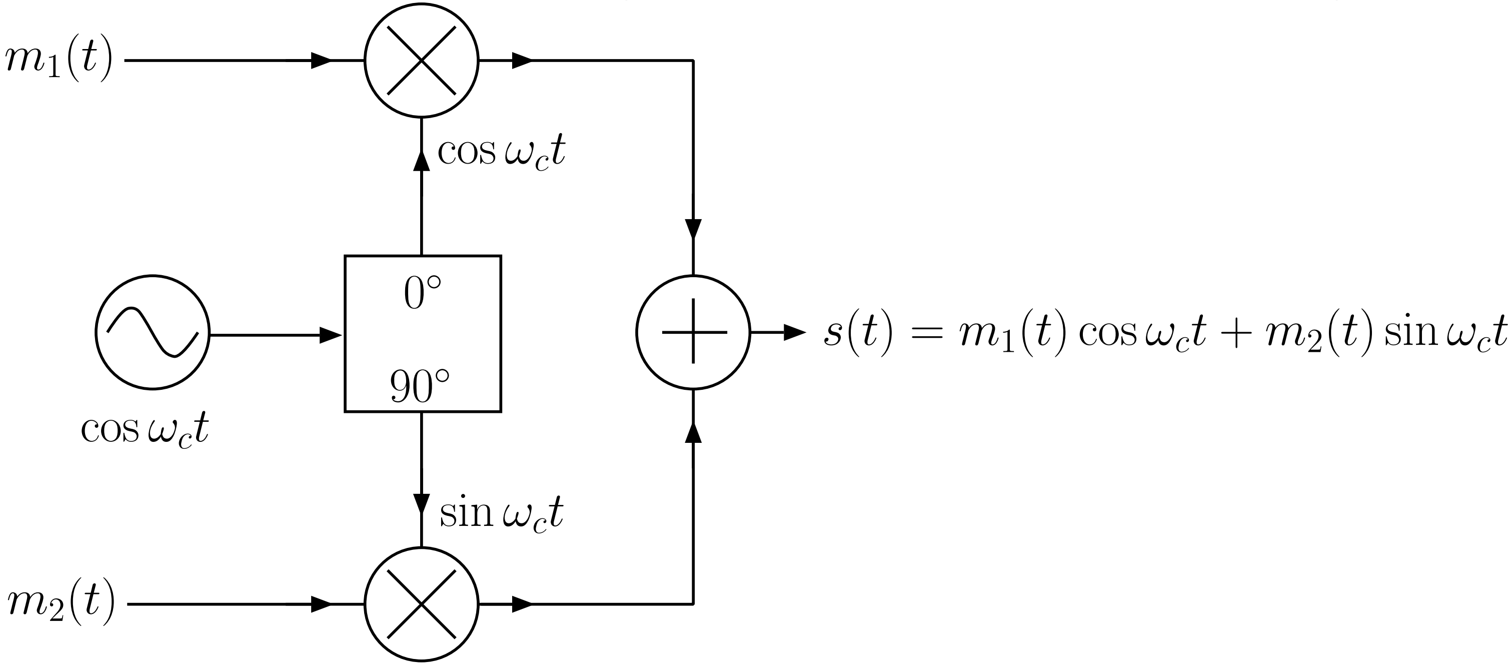
$m_1(t)$
$\cos\omega_c t$
0°
90°
$\cos\omega_c t$
$\sin\omega_c t$
$m_2(t)$
$s(t) = m_1(t)\cos\omega_c t + m_2(t)\sin\omega_c t$

Figure 1.23: Quadrature multiplexer/modulator.

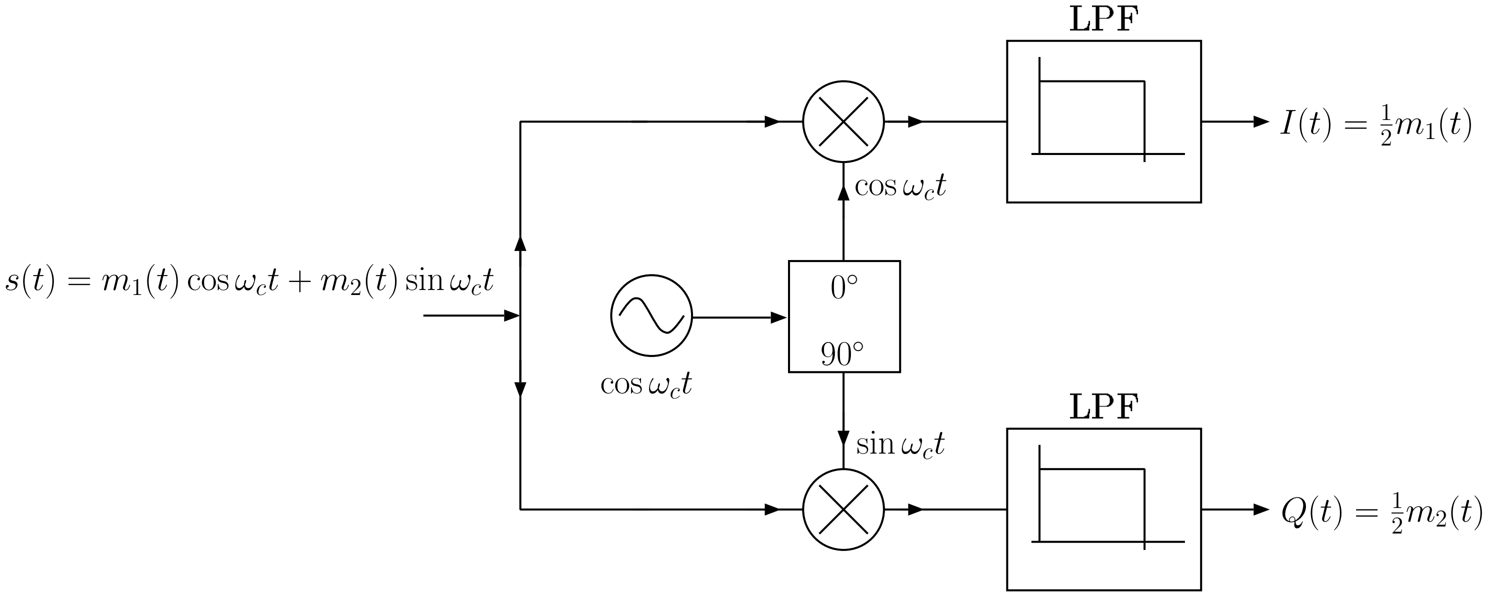
LPF
$I(t) = \frac{1}{2}m_1(t)$
$\cos\omega_c t$
$s(t) = m_1(t)\cos\omega_c t + m_2(t)\sin\omega_c t$
0°
90°
$\cos\omega_c t$
LPF
$\sin\omega_c t$
$Q(t) = \frac{1}{2}m_2(t)$

Figure 1.25: De-multiplexing of quadrature-multiplexed signals.

Summary of Amplitude (Linear) Modulation

DSB: $s(t) = (Am(t) + B)\cos(\omega_c t)$

$B = 0 \rightarrow$ Suppressed carrier (DSB-SC)
$Am(t) + B > 0 \ \forall\ t \rightarrow$ Full carrier

SSB: $s(t) = Am(t)\cos(\omega_c t) + A\hat{m}(t)\sin(\omega_c t);$

$\hat{m}(t) = \mathcal{F}^{-1}[-j\text{sgn}(\omega)M(\omega)],$
where $-j\text{sgn}(\omega)$ is the Hilbert Transform filter

VSB: $s(t) = Am(t)\cos(\omega_c t) + A\hat{m}(t)\sin(\omega_c t);$

$\hat{m}(t) = \mathcal{F}^{-1}[H(\omega)M(\omega)];$
where $H(\omega)$ is a modified Hibert Transform filter

Quadrature multiplexed signal:

$$s(t) = Am_1(t)\cos(\omega_c t) + Am_2(t)\sin(\omega_c t)$$

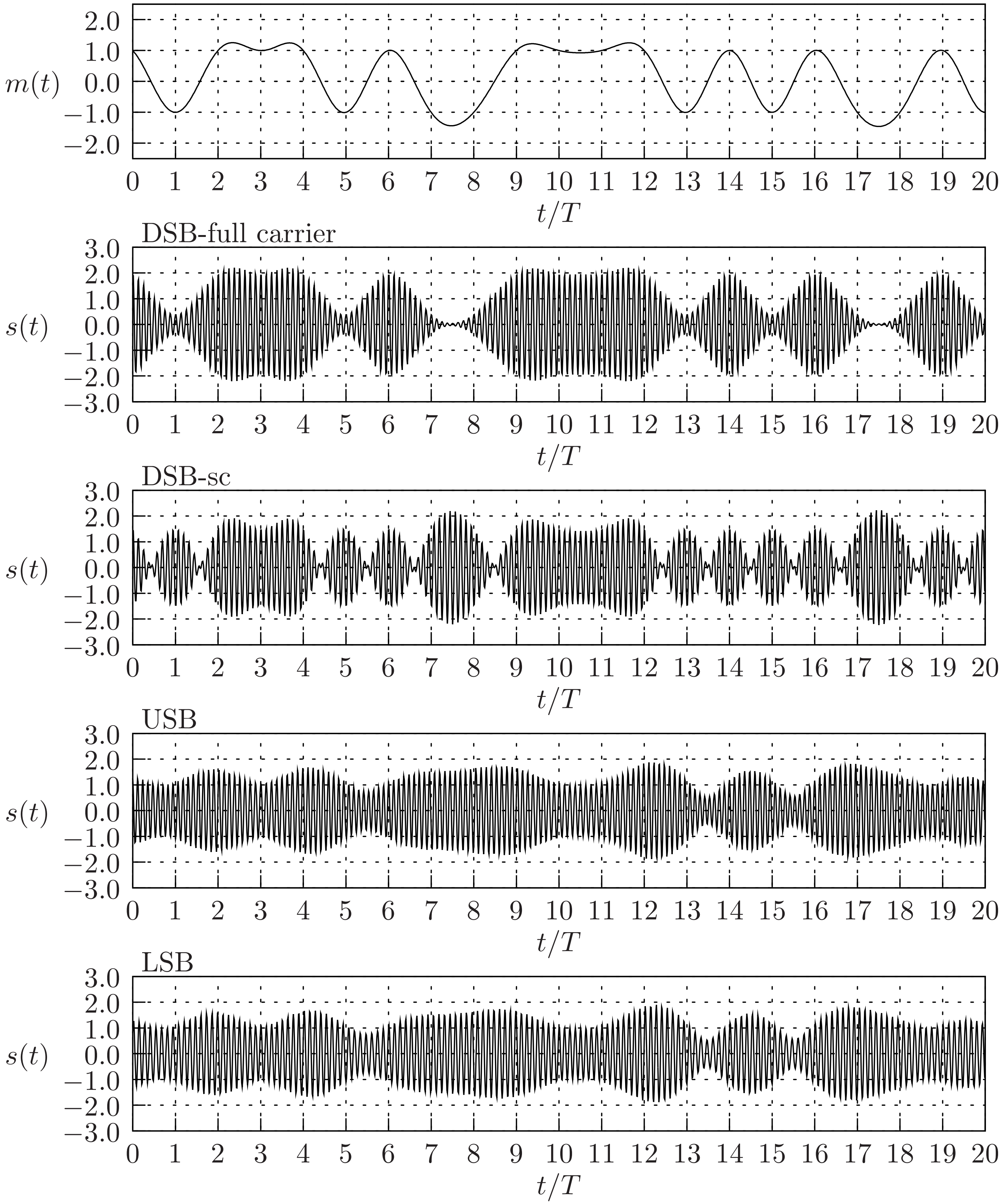
m(t)
2.0
1.0
0.0
−1.0
−2.0
0 1 2 3 4 5 6 7 8 9 10 11 12 13 14 15 16 17 18 19 20
t/T
DSB-full carrier
s(t)
3.0
2.0
1.0
0.0
−1.0
−2.0
−3.0
0 1 2 3 4 5 6 7 8 9 10 11 12 13 14 15 16 17 18 19 20
t/T
DSB-sc
s(t)
3.0
2.0
1.0
0.0
−1.0
−2.0
−3.0
0 1 2 3 4 5 6 7 8 9 10 11 12 13 14 15 16 17 18 19 20
t/T
USB
s(t)
3.0
2.0
1.0
0.0
−1.0
−2.0
−3.0
0 1 2 3 4 5 6 7 8 9 10 11 12 13 14 15 16 17 18 19 20
t/T
LSB
s(t)
3.0
2.0
1.0
0.0
−1.0
−2.0
−3.0
0 1 2 3 4 5 6 7 8 9 10 11 12 13 14 15 16 17 18 19 20
t/T

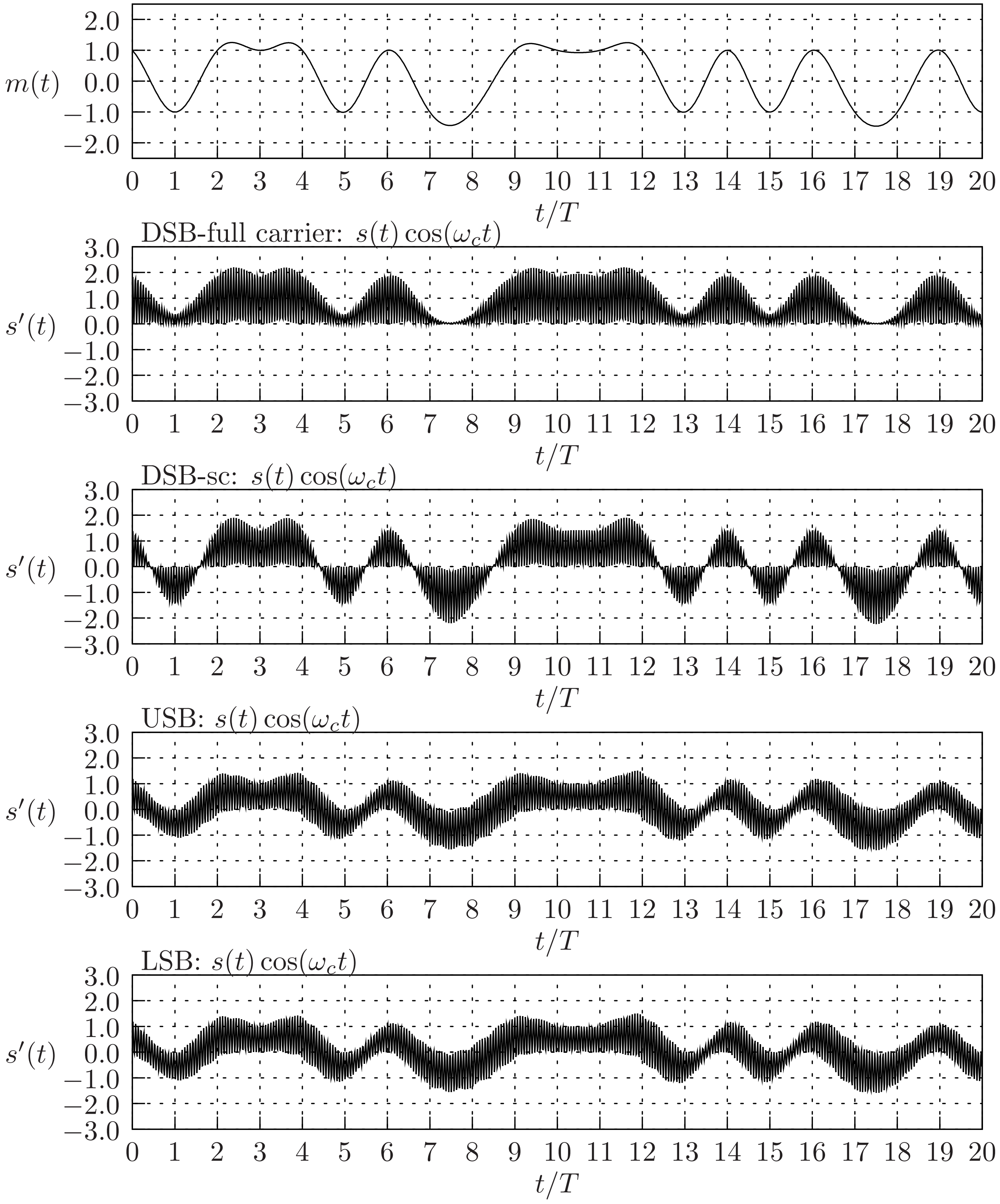
m(t)
2.0
1.0
0.0
−1.0
−2.0
0 1 2 3 4 5 6 7 8 9 10 11 12 13 14 15 16 17 18 19 20
t/T
DSB-full carrier: $s(t)\cos(\omega_c t)$
s′(t)
3.0
2.0
1.0
0.0
−1.0
−2.0
−3.0
0 1 2 3 4 5 6 7 8 9 10 11 12 13 14 15 16 17 18 19 20
t/T
DSB-sc: $s(t)\cos(\omega_c t)$
s′(t)
3.0
2.0
1.0
0.0
−1.0
−2.0
−3.0
0 1 2 3 4 5 6 7 8 9 10 11 12 13 14 15 16 17 18 19 20
t/T
USB: $s(t)\cos(\omega_c t)$
s′(t)
3.0
2.0
1.0
0.0
−1.0
−2.0
−3.0
0 1 2 3 4 5 6 7 8 9 10 11 12 13 14 15 16 17 18 19 20
t/T
LSB: $s(t)\cos(\omega_c t)$
s′(t)
3.0
2.0
1.0
0.0
−1.0
−2.0
−3.0
0 1 2 3 4 5 6 7 8 9 10 11 12 13 14 15 16 17 18 19 20
t/T

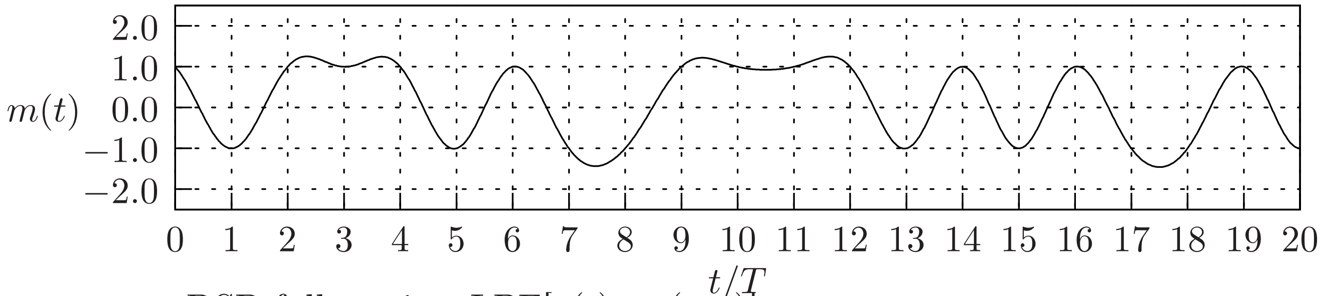

DSB-full carrier: LPF$[s(t)\cos(\omega_c t)]$

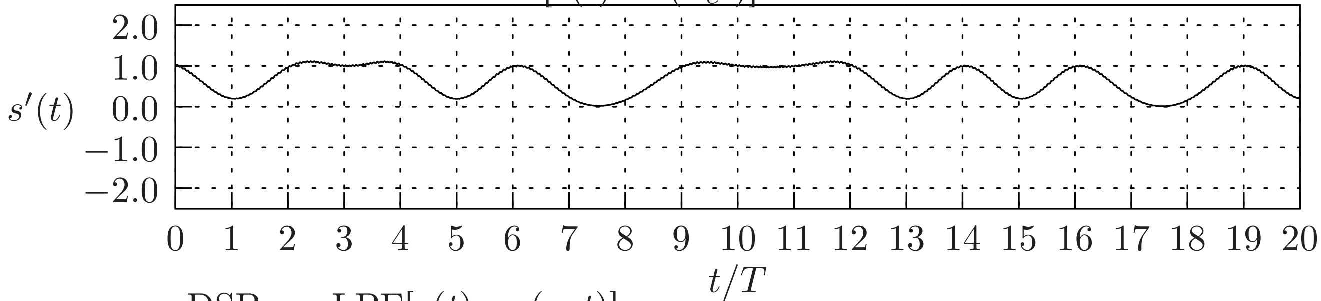

DSB-sc: LPF$[s(t)\cos(\omega_c t)]$

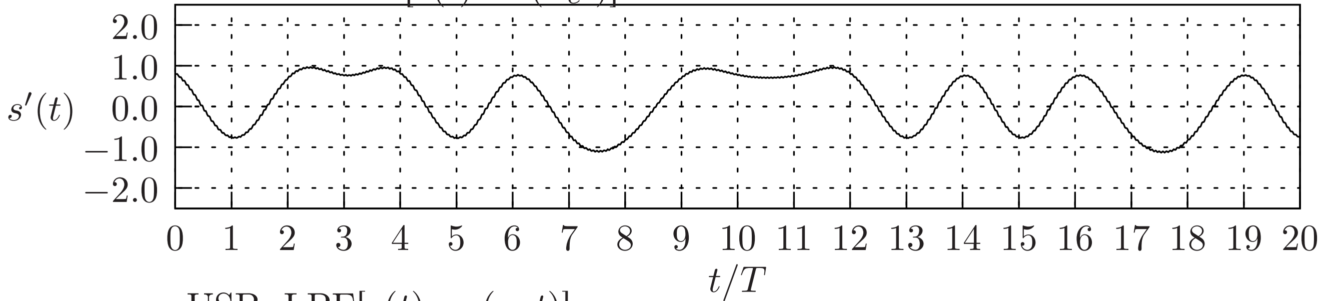

USB: LPF$[s(t)\cos(\omega_c t)]$

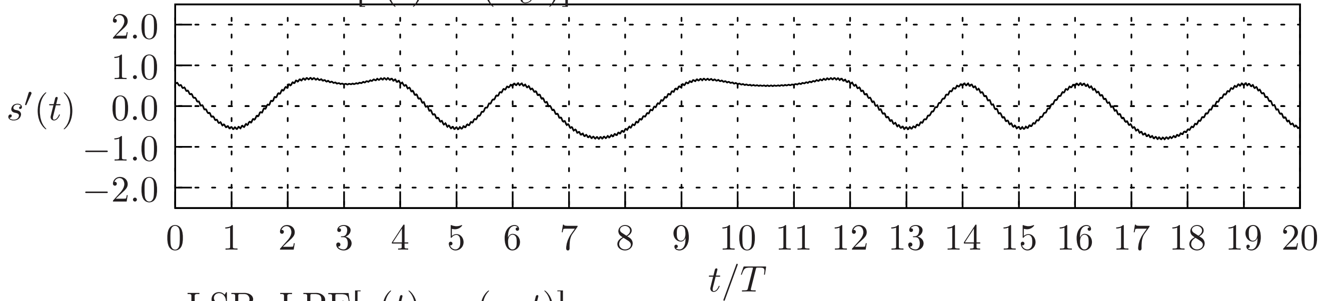

LSB: LPF$[s(t)\cos(\omega_c t)]$

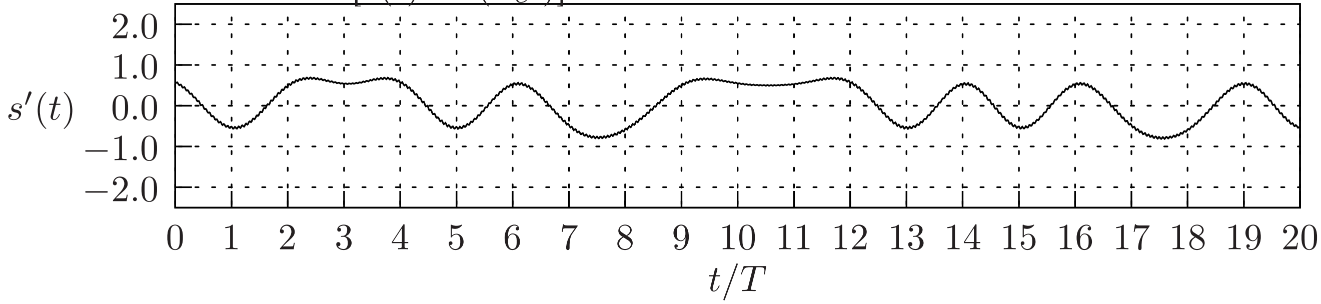

$$S(\omega) = \pi A_c \sum_{n=-\infty}^{\infty} \left[ J_n(\beta)\delta(\omega - \omega_c - n\omega_m) + J_n(\beta)\delta(\omega + \omega_c + n\omega_m) \right]$$

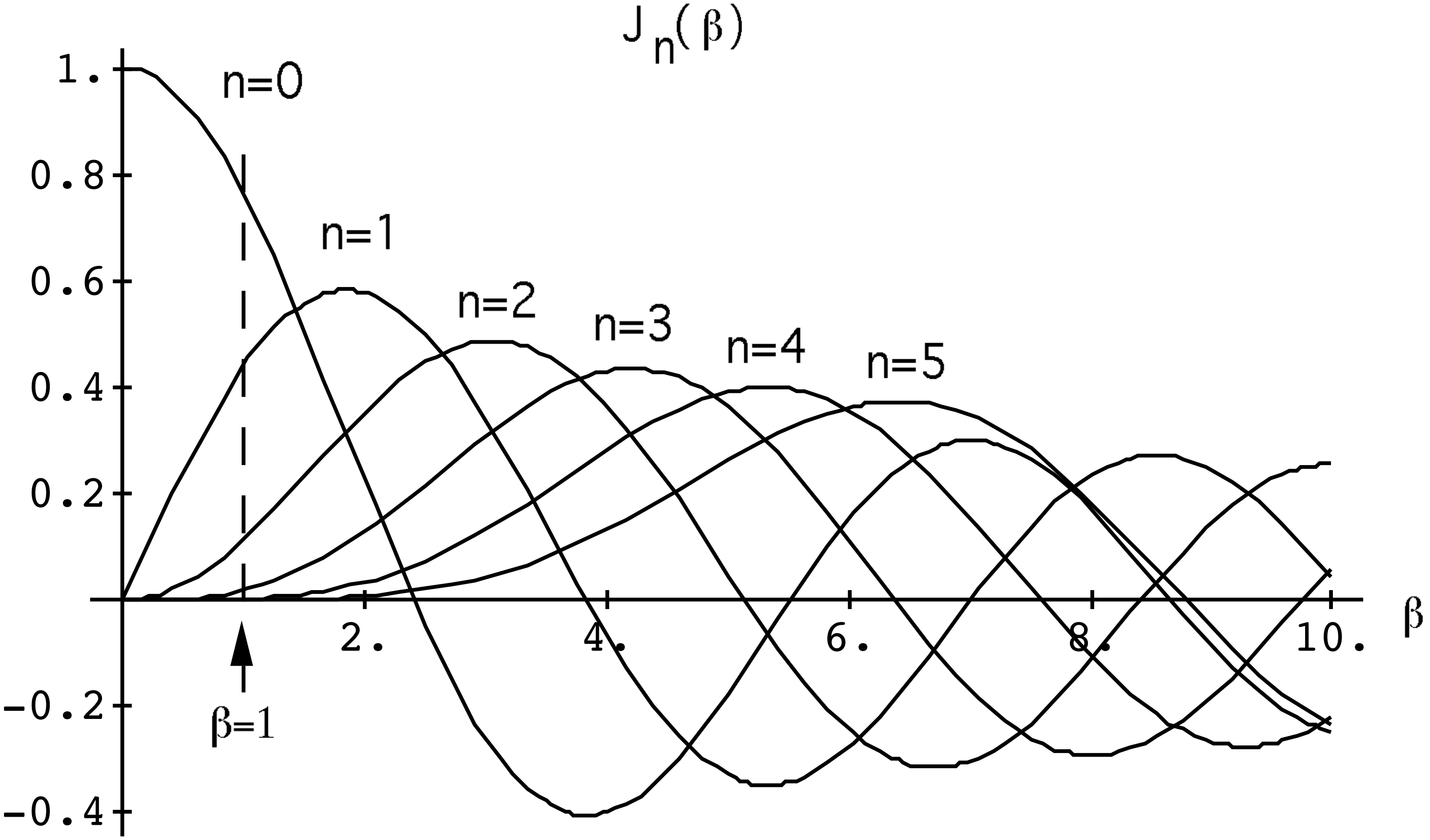

Figure 1.28: Bessel functions of order n for n=0,1,2,3,4,5.

$$J_{-n}(x) = (-1)^n J_n(x)$$

$$s(t) = A_c \cos(2\pi 20t + \sin(2\pi 2t))$$

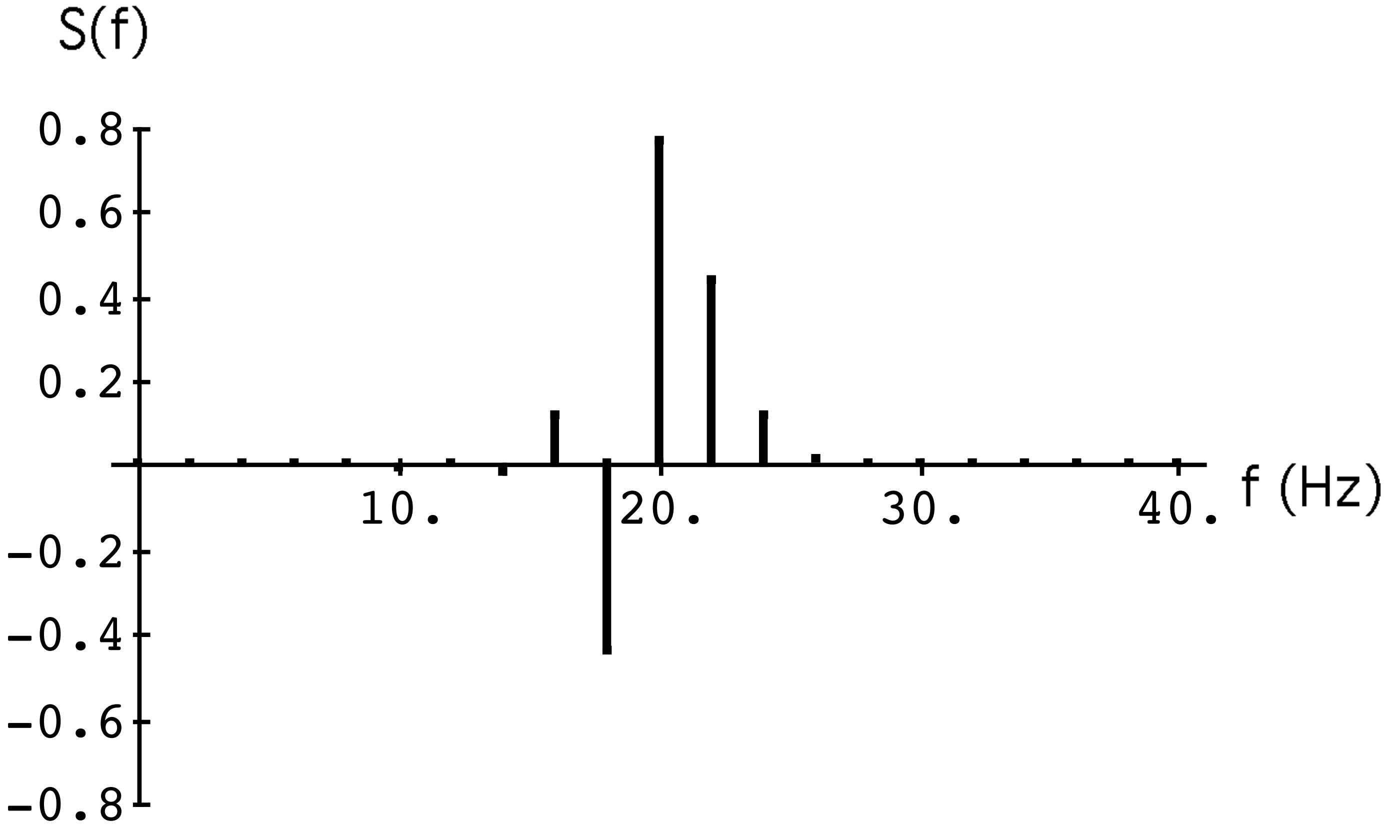

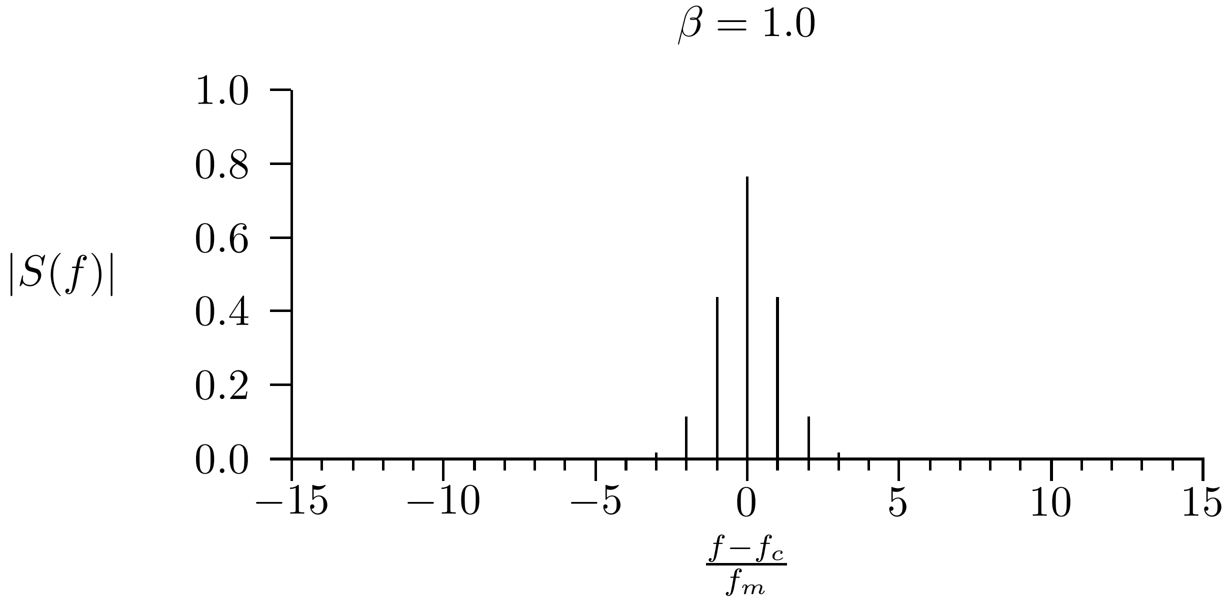
$\beta = 1.0$

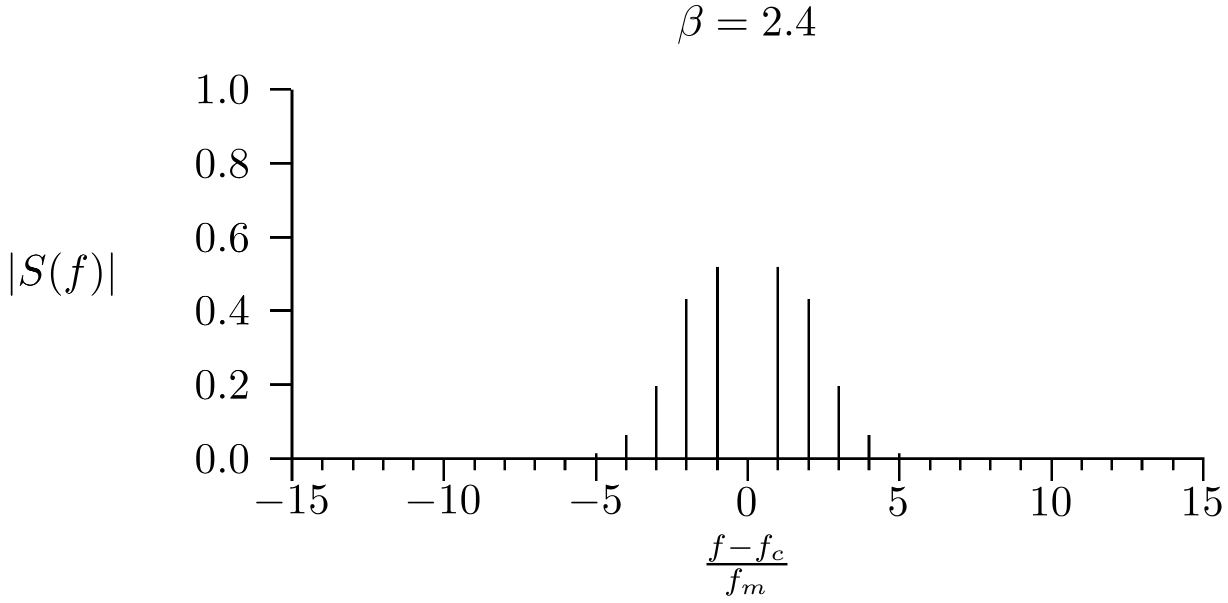
$\beta = 2.4$

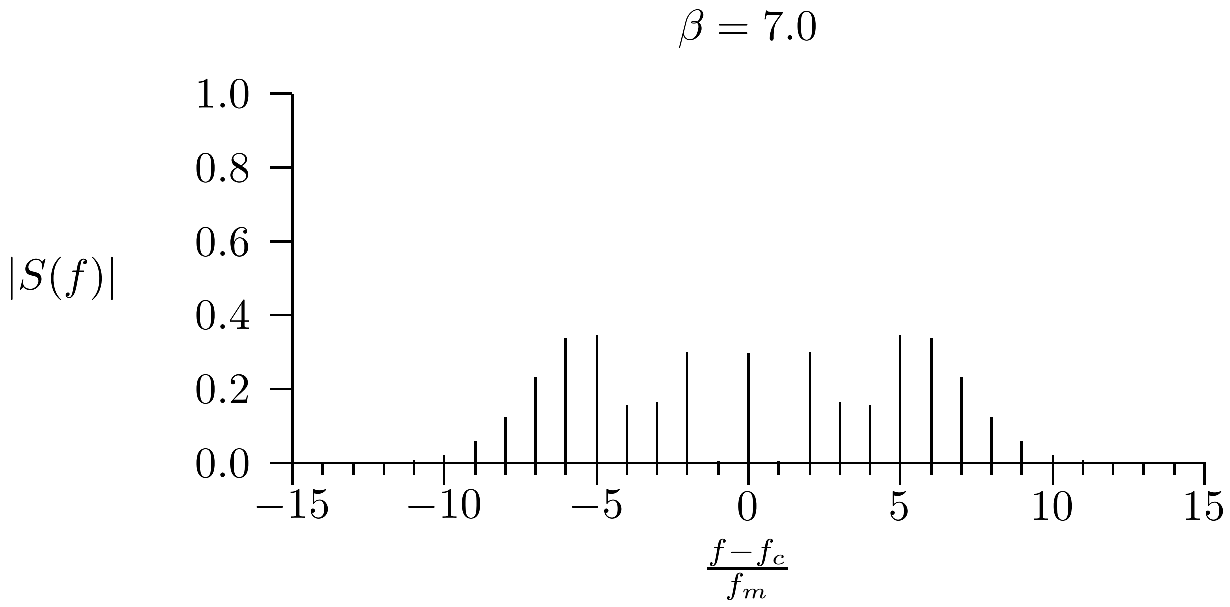

$\beta = 7.0$

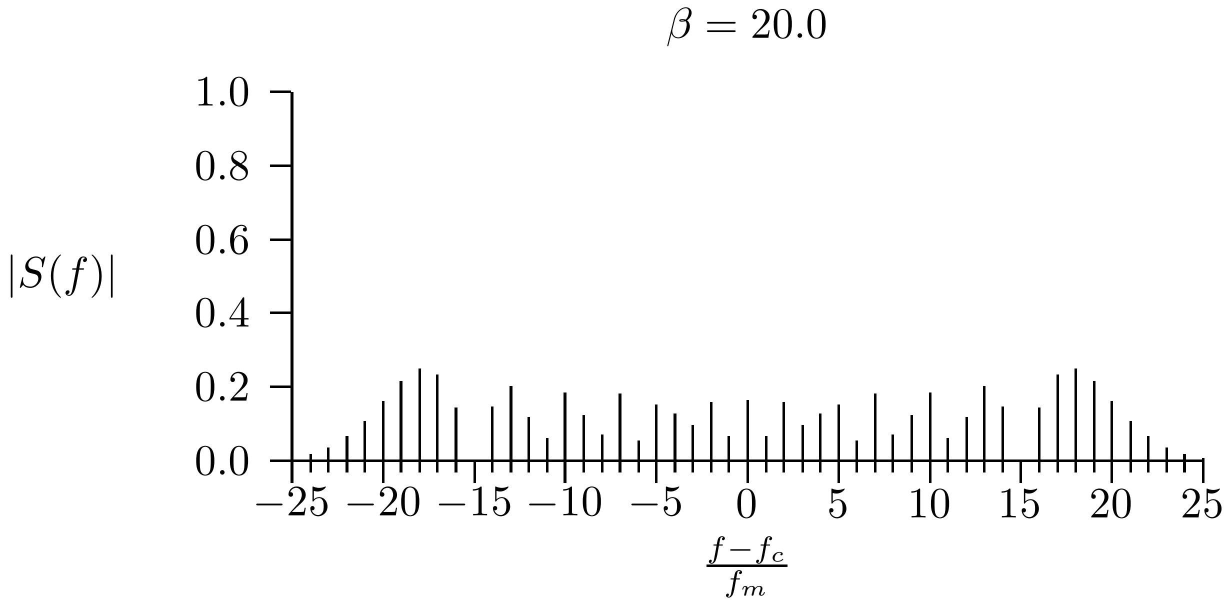

$\beta = 20.0$

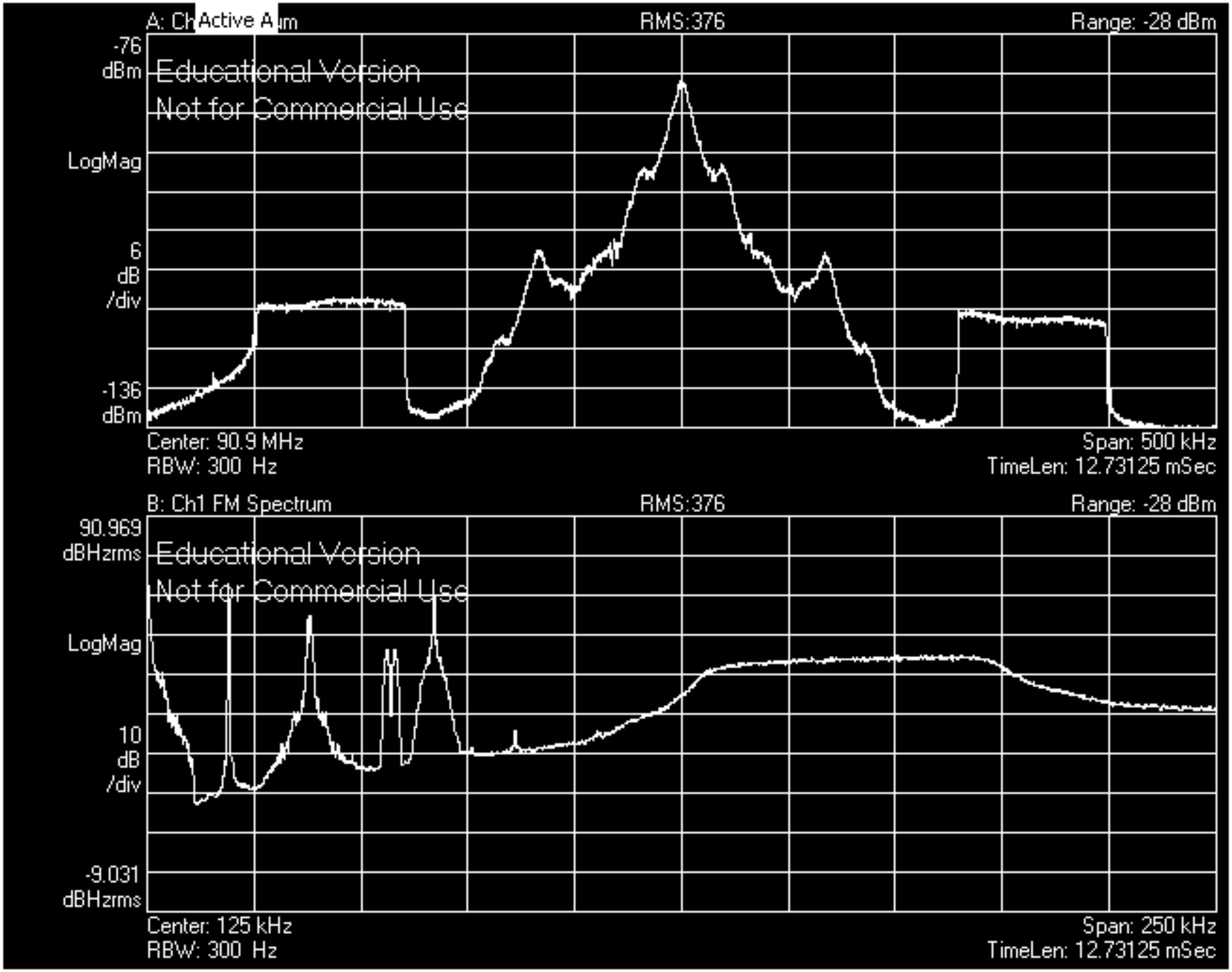
A: Ch Active A m
RMS:376
Range: -28 dBm
-76 dBm
Educational Version
Not for Commercial Use
LogMag
6 dB /div
-136 dBm
Center: 90.9 MHz
RBW: 300 Hz
Span: 500 kHz
TimeLen: 12.73125 mSec
B: Ch1 FM Spectrum
RMS:376
Range: -28 dBm
90.969 dBHzrms
Educational Version
Not for Commercial Use
LogMag
10 dB /div
-9.031 dBHzrms
Center: 125 kHz
RBW: 300 Hz
Span: 250 kHz
TimeLen: 12.73125 mSec

# Continuous phase Frequency-Shift-Keying (FSK) modulation:

$$s(t) = \cos(2\pi f_c t + 2\pi h \int_{-\infty}^{t} m(t')dt');$$

$$m(t) = \sum_n a_n p(t - nT)$$

$$p(t) \text{ is normalized so that } \int_0^T p(t)dt = 0.5$$

If $p(t)$ is a rectangular pulse, and if $a_n = [... - 1, 1, -1, 1, -1, 1, ...]$ then $m(t)$ will be a square wave with peak amplitude $\pm\frac{1}{2T}$.

The associated time-varying phase will be a triangle wave that ramps from 0 up to $\pi h$, then down to 0, etc.

The instantaneous frequency during the phase ramps will be constant. The frequency deviation will be:

$$\Delta f(t) = \pm\frac{h}{2T}$$

Bluetooth uses $\frac{1}{T} = 1$ Mbit/s and $h = 0.315$, so the peak frequency deviation is $\pm\frac{h}{2T} = \pm 157.5$ kHz.

To limit the bandwidth of the message signal, Bluetooth systems filter the rectangular pulses using a Gaussian filter with -3 dB bandwidth:

$$B = 0.5(\tfrac{1}{T}) = 500 \text{ kHz}.$$

This is usually described as a $BT = 0.5$ Gaussian-filtered pulse and Bluetooth is said to utilize Gaussian Frequency Shift Keying, or GFSK.

Simulation example

Two cases, continuous-phase frequency-shift keying with:

(a) rectangular pulses

(b) Gaussian-filtered pulses with $BT = 0.5$ (like Bluetooth pulse).

Carrier frequency: $f_c = 1500$ Hz
Modulation index: $h = 0.315$
Symbol rate: $1/T = 200\,\mathrm{s}^{-1}$

Peak frequency deviation: $\Delta f_{max} = \frac{h}{2T} = 0.315 * 100 \simeq 32$ Hz

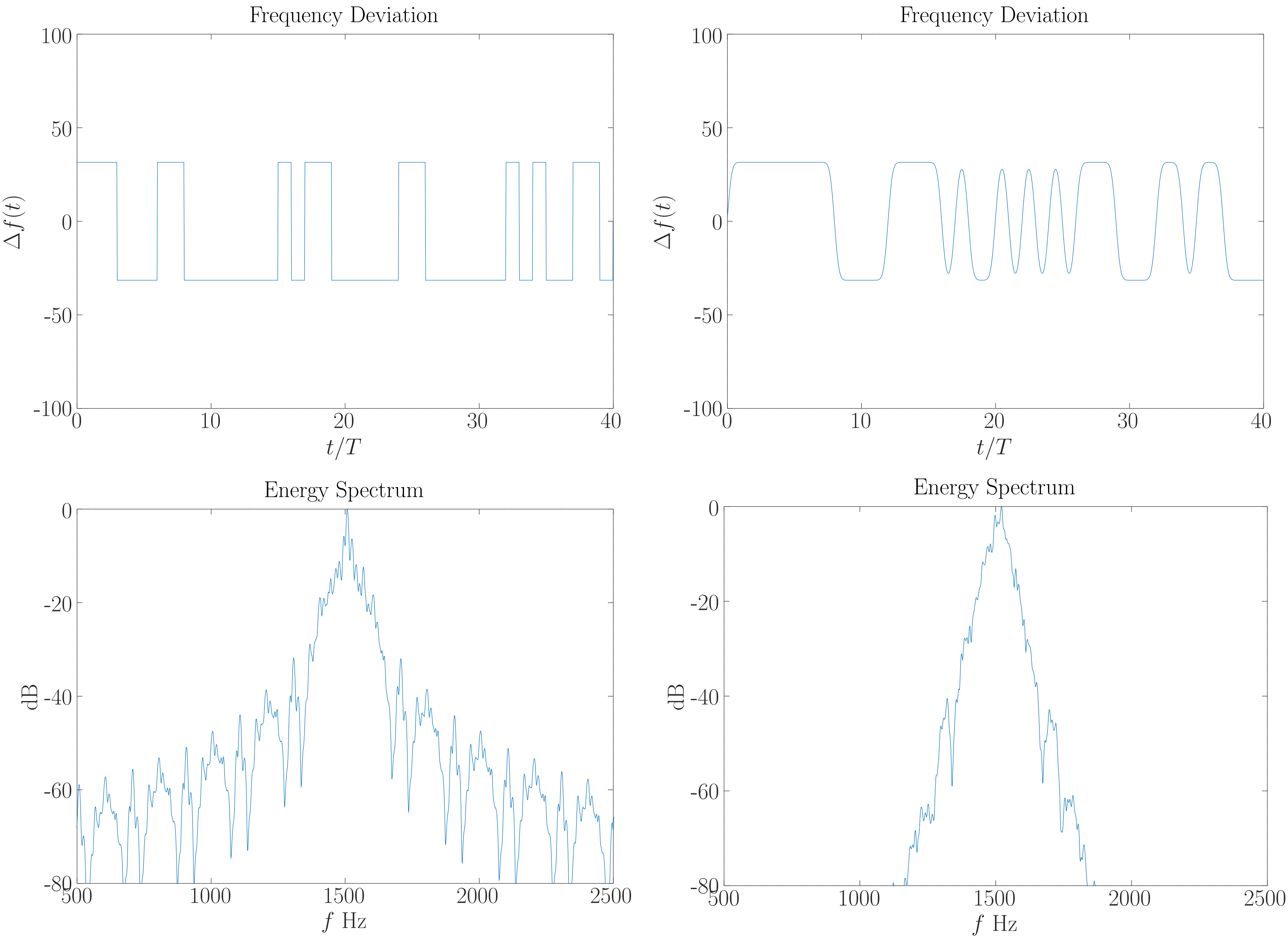
Frequency Deviation
Δf(t)
100
50
0
-50
-100
0
10
20
30
40
t/T
Frequency Deviation
Δf(t)
100
50
0
-50
-100
0
10
20
30
40
t/T
Energy Spectrum
dB
0
-20
-40
-60
-80
500
1000
1500
2000
2500
f Hz
Energy Spectrum
dB
0
-20
-40
-60
-80
500
1000
1500
2000
2500
f Hz

Carson's Rule says:

$$BW \simeq 2(\Delta f_{max} + W)$$

$$BW \simeq 2(\frac{h}{2T} + \frac{1}{2T})$$

$$BW \simeq \frac{1}{T}(1 + h)$$

e.g. for GFSK with $h = 0.315$ and $1/T = 200$ bit/s, Carson's rule predicts $BW \simeq 260$ Hz. In practice, the bandwidth that contains 99% of the signal power is closer to $\frac{1}{T} = 200$ Hz. (For Bluetooth, then, 99% bandwidth is $\simeq 1$ MHz.)

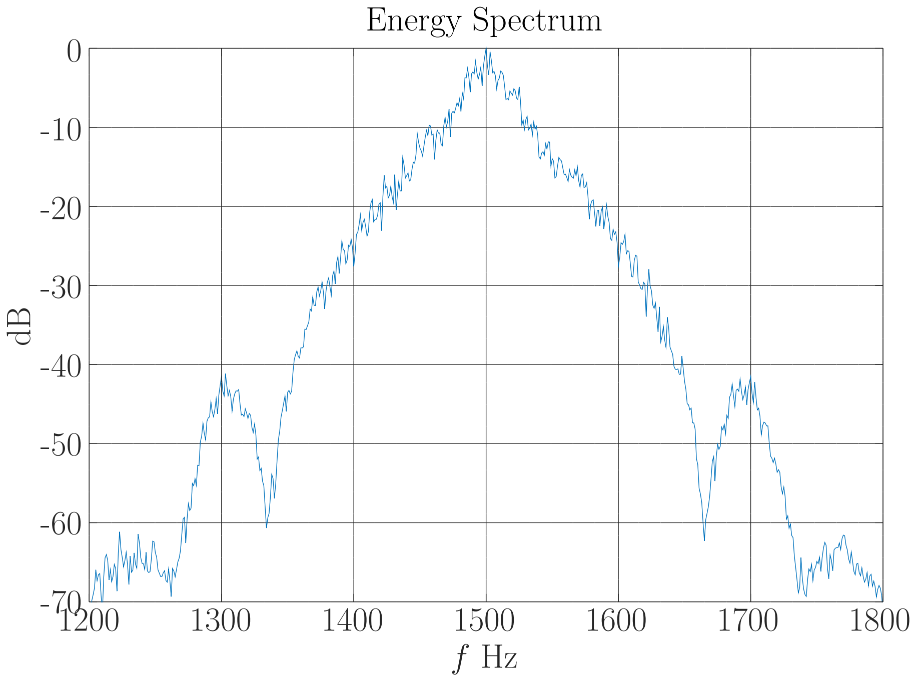

# Quadrature FM Demodulator

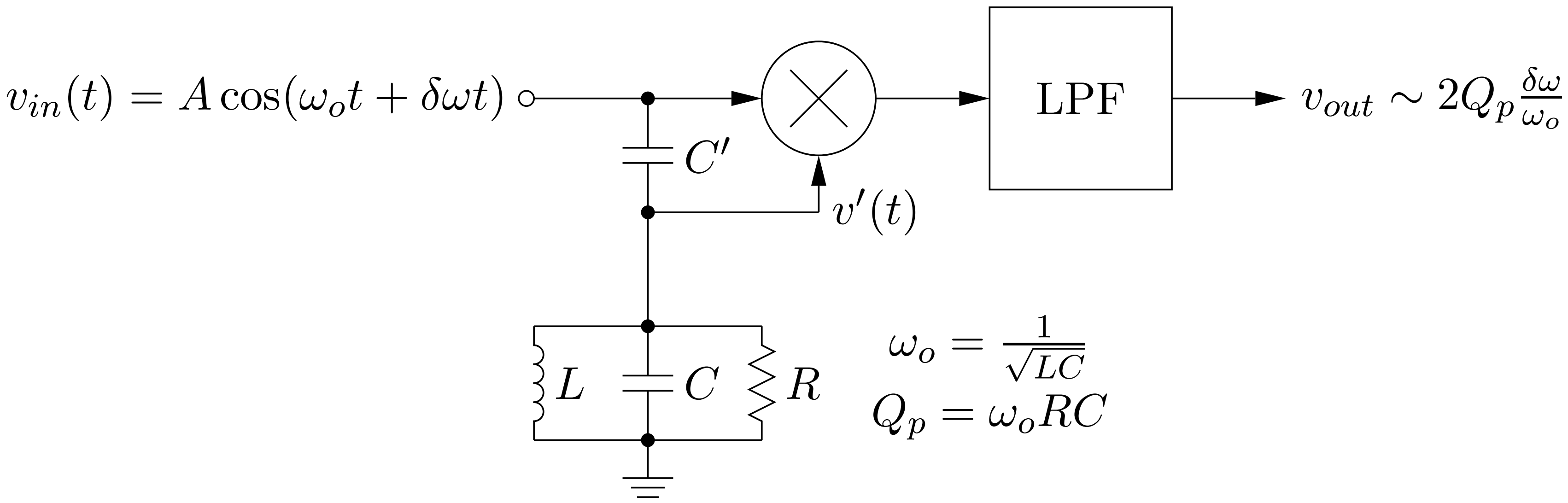
$v_{in}(t) = A\cos(\omega_o t + \delta\omega t)$
$C'$
$v'(t)$
LPF
$v_{out} \sim 2Q_p\frac{\delta\omega}{\omega_o}$
$L$
$C$
$R$

$$\omega_o = \frac{1}{\sqrt{LC}}$$
$$Q_p = \omega_o RC$$

- The demodulator operates with the RLC circuit tuned to resonance at the carrier frequency of $v_{in}$, $\omega_o$.

- The voltage divider consisting of $C'$ and the resonant RLC circuit converts small frequency deviations in $v_{in}$ to phase shifts of $v'$ relative to $v_{in}$.

- For small frequency deviations, $\delta\omega$, $v'$ is phase shifted by $\pi/2 - 2Q_p\frac{\delta\omega}{\omega_o}$.

- The multiplier and LPF act as a phase comparator, producing output proportional to $2Q_p\frac{\delta\omega}{\omega_o}$ for small frequency deviations, $\delta\omega$.

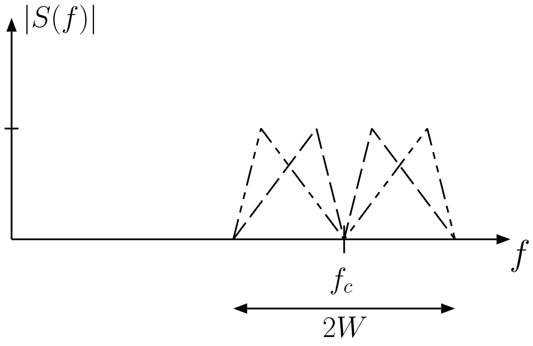

Figure 1.24: Two DSB-SC components with overlapping spectra.

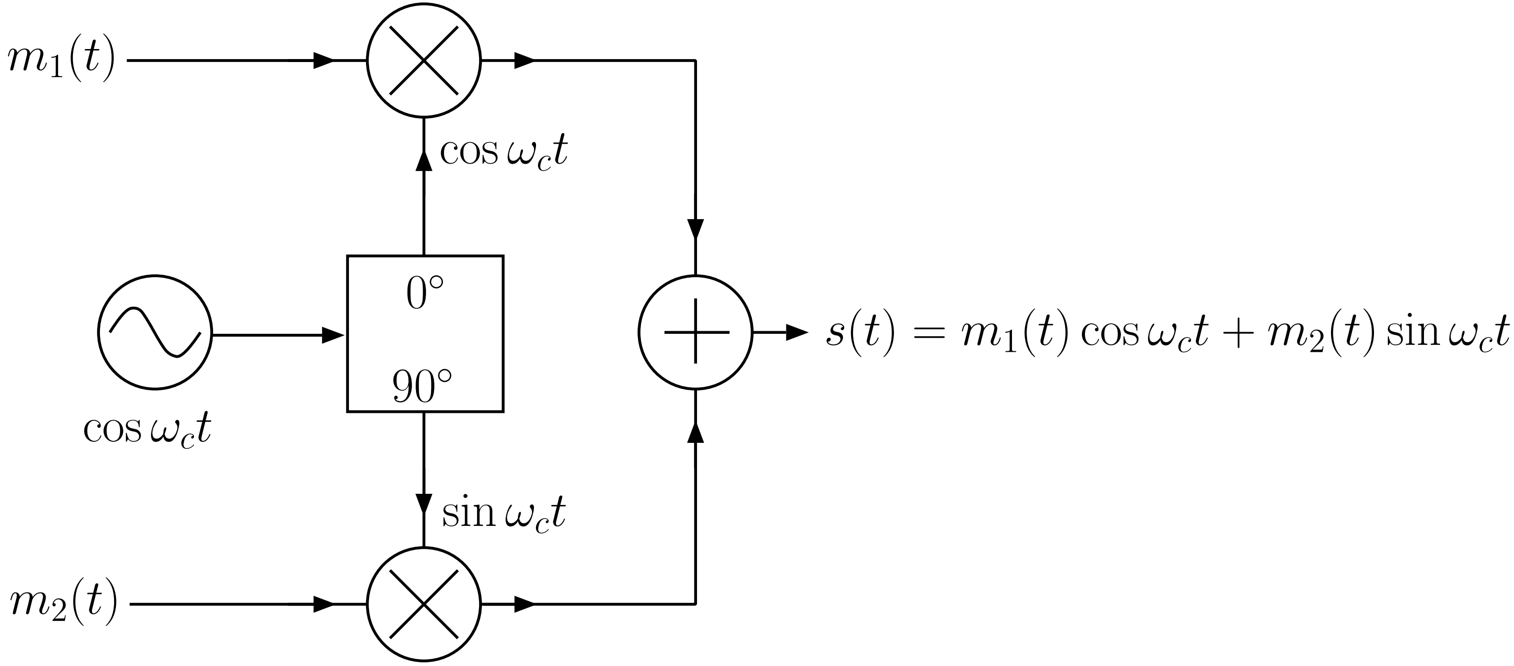

$m_1(t)$
$\cos\omega_c t$
0°
90°
$\cos\omega_c t$
$\sin\omega_c t$
$m_2(t)$
$s(t) = m_1(t)\cos\omega_c t + m_2(t)\sin\omega_c t$

Figure 1.23: Quadrature multiplexer/modulator.

The quadrature modulator can be used to generate any type of modulation.

Consider a signal that is both amplitude and angle modulated:

$$s(t) = A(t)\cos(\omega_c t + \theta(t))$$

Using a trigonometric identity, this can be written in terms of in-phase and quadrature components:

$$s(t) = A(t)\cos(\theta(t))\cos(\omega_c t) - A(t)\sin(\theta(t))\sin(\omega_c t)$$

$$s(t) = m_1(t)\cos(\omega_c t) + m_2(t)\sin(\omega_c t)$$

where

$$m_1(t) = A(t)\cos(\theta(t))$$

$$m_2(t) = -A(t)\sin(\theta(t))$$

Similarly, the quadrature demodulator can be used to demodulate any type of modulation. (Additional signal processing is required).

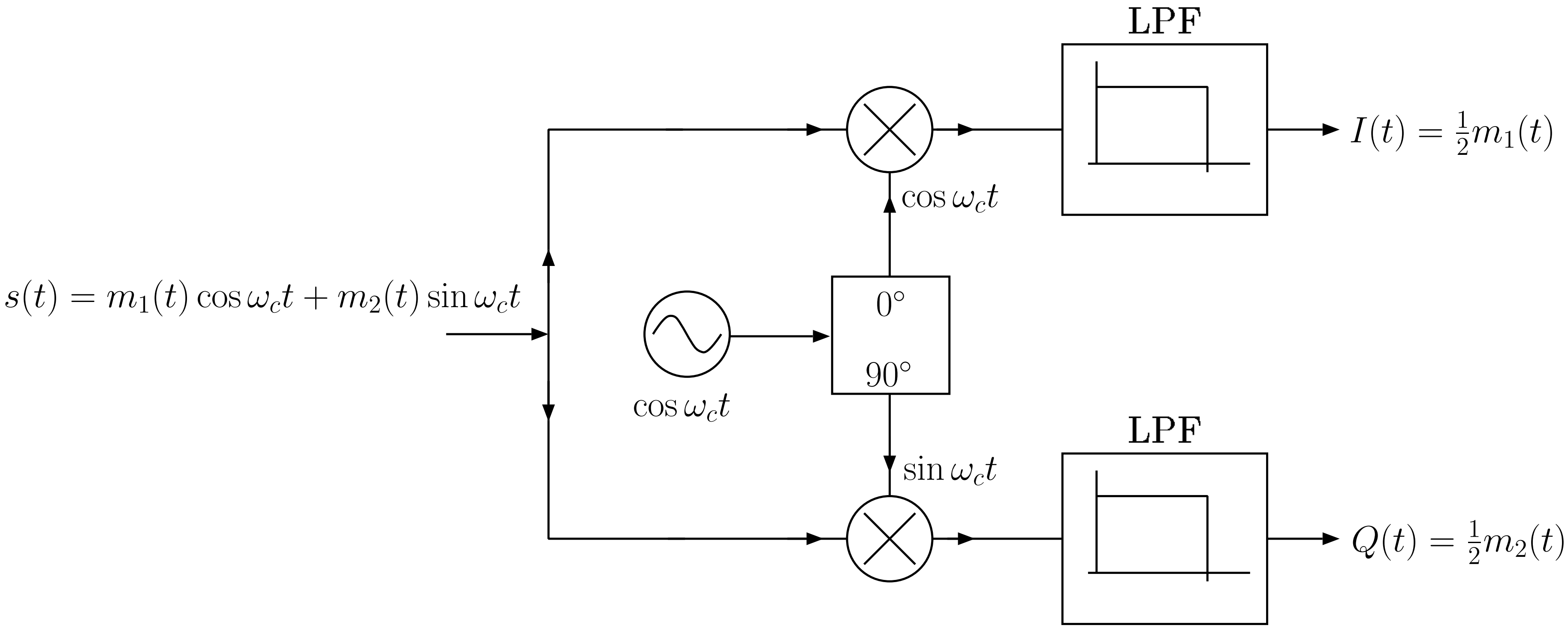
LPF
$I(t) = \frac{1}{2}m_1(t)$
$\cos\omega_c t$
$s(t) = m_1(t)\cos\omega_c t + m_2(t)\sin\omega_c t$
0°
90°
$\cos\omega_c t$
LPF
$\sin\omega_c t$
$Q(t) = \frac{1}{2}m_2(t)$

With perfect carrier recovery:

$$I(t) = \frac{1}{2}m_1(t) = \frac{1}{2}A(t)\cos(\theta(t))$$

$$Q(t) = \frac{1}{2}m_2(t) = -\frac{1}{2}A(t)\sin(\theta(t))$$

Outputs from quadrature demodulator are:

$$I(t) = \frac{1}{2}m_1(t) = \frac{1}{2}A(t)\cos(\theta(t))$$

$$Q(t) = \frac{1}{2}m_2(t) = -\frac{1}{2}A(t)\sin(\theta(t))$$

Can recover $A(t)$ and $\theta(t)$ unambiguously as long as $A(t) \geq 0$ (positive envelope):

$$A(t) = 2\sqrt{I^2(t) + Q^2(t)}$$

$$\theta(t) = -\arctan(\frac{Q(t)}{I(t)})$$

If the signal is frequency modulated, then instantaneous frequency is proportional to the message signal:

$$\frac{d\theta(t)}{dt} = \frac{-1}{I^2 + Q^2}(I\frac{dQ}{dt} - Q\frac{dI}{dt})$$

# Tuned Demodulator

$s_i(t) = A(1 + m(t))\cos(\omega_c t + \theta)$+noise

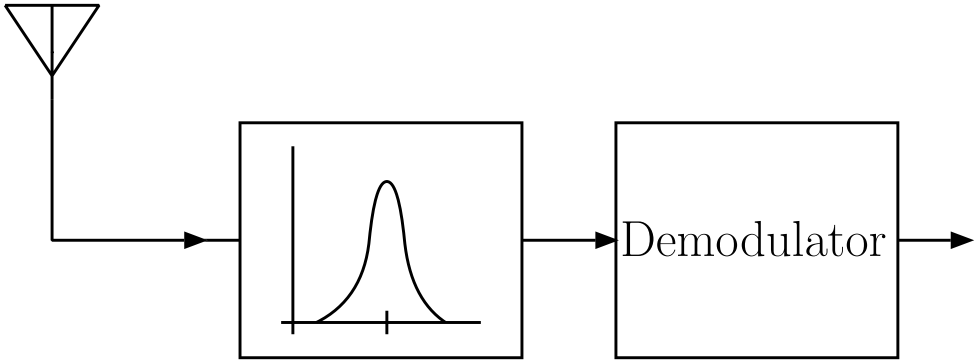

Demodulator

$s_o(t) = A(1 + m(t))$+noise

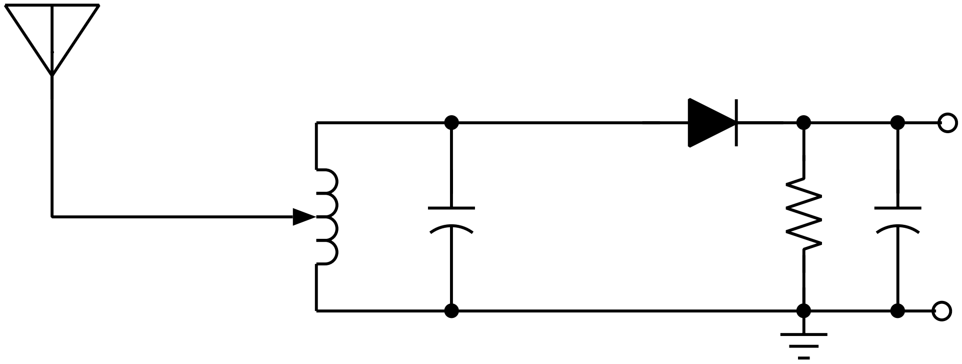

# Filter facts

- Physical limitations of filters play a dominant role in receiver design.

- Analog filters are based on resonators.
  - electromagnetic resonators: LC circuits, T-line stubs, waveguide/cavity, and combinations thereof.
  - electro-mechanical resonators use a transducer to couple electrical signals into and out of a mechanical resonator. Transduction occurs naturally in piezo-electric materials such as quartz and certain ceramics.

- Achieving a good shape factor (frequency response close to rectangular) requires many resonators.

- Tunable filters require tunable resonators and tunable coupling between resonators. Tuning only possible with electromagnetic resonators, and is only convenient with LC resonators. Not practical to tune filters with more than 2 or 3 resonators.

- Minimum fractional bandwidth of practically realizable tunable filters based on LC resonators is 1%, and shape factor will be poor (large). Hence, tunable filters are not suitable for channel selection.

- At low frequencies (< 100 MHz) can use electromechanical resonators to realize single-frequency filters with fractional bandwidth as small as 0.01%. At moderate frequencies (up to a few GHz) can use surface-acoustic-wave (SAW) filters to realize single-frequency filters with fractional bandwidth smaller than 1%.

|  | Carrier Frequency, $f_c$ | Channel Bandwidth, BW | Fractional Bandwidth, BW/$f_c$ |
|---|---|---|---|
| AM Broadcast | 1 MHz | 10 kHz | 0.01(1%) |
| FM Broadcast | 100 MHz | 200 kHz | 0.002 (0.2%) |
| DTV | 600 MHz | 6 MHz | 0.01 (1%) |
| WiFi 802.11n | 5 GHz | 40 MHz | 0.008 (0.8%) |
| Bluetooth | 2.4 GHz | 80 MHz (all channels) | 0.033 (3.3%) |
| 4G Cellphone uplink (typical) | 1.8 GHz | 5 MHz | 0.0028 (0.3%) |
| SDARS (Sirius/XM) | 2.326 GHz | 12.5 MHz | 0.0054 (0.5%) |

# Filters | Lumped Element Designs

Our custom package concepts provide additional shielding for better ultimate rejection

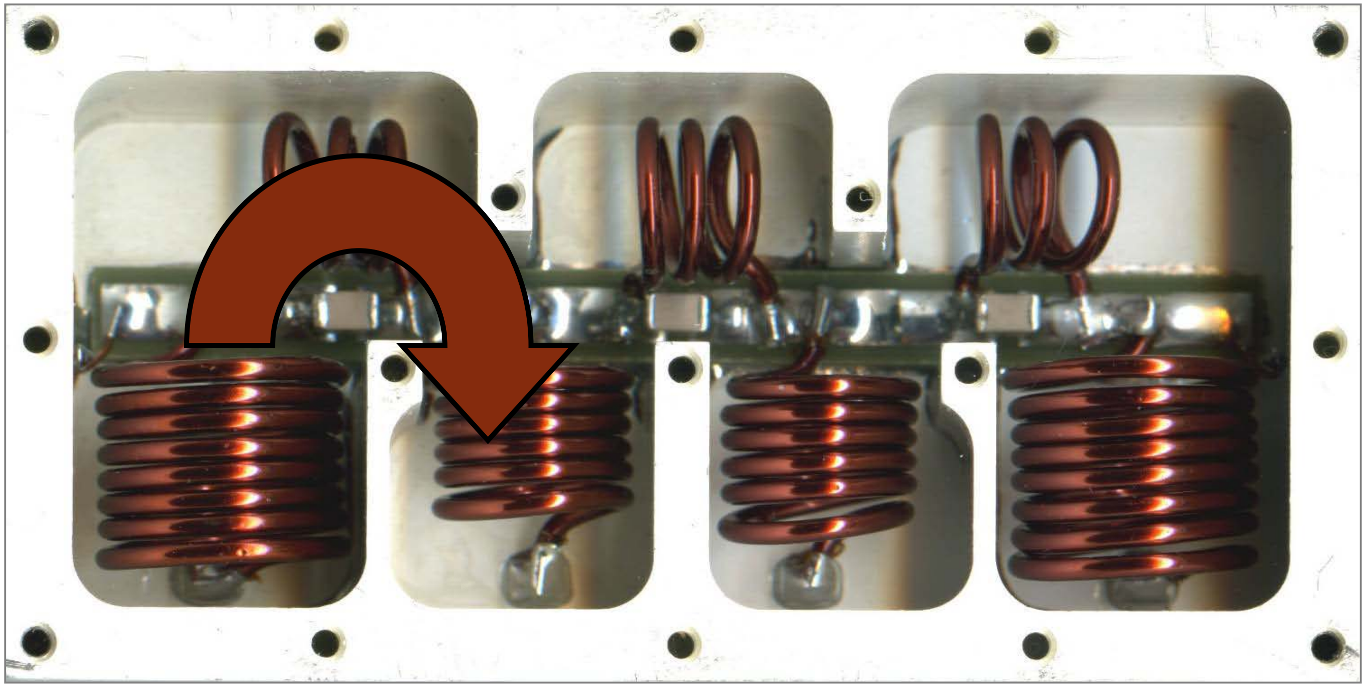

We can incorporate a unique low dielectric constant stabilizing structure to reduce overall sensitivity to shock and vibration

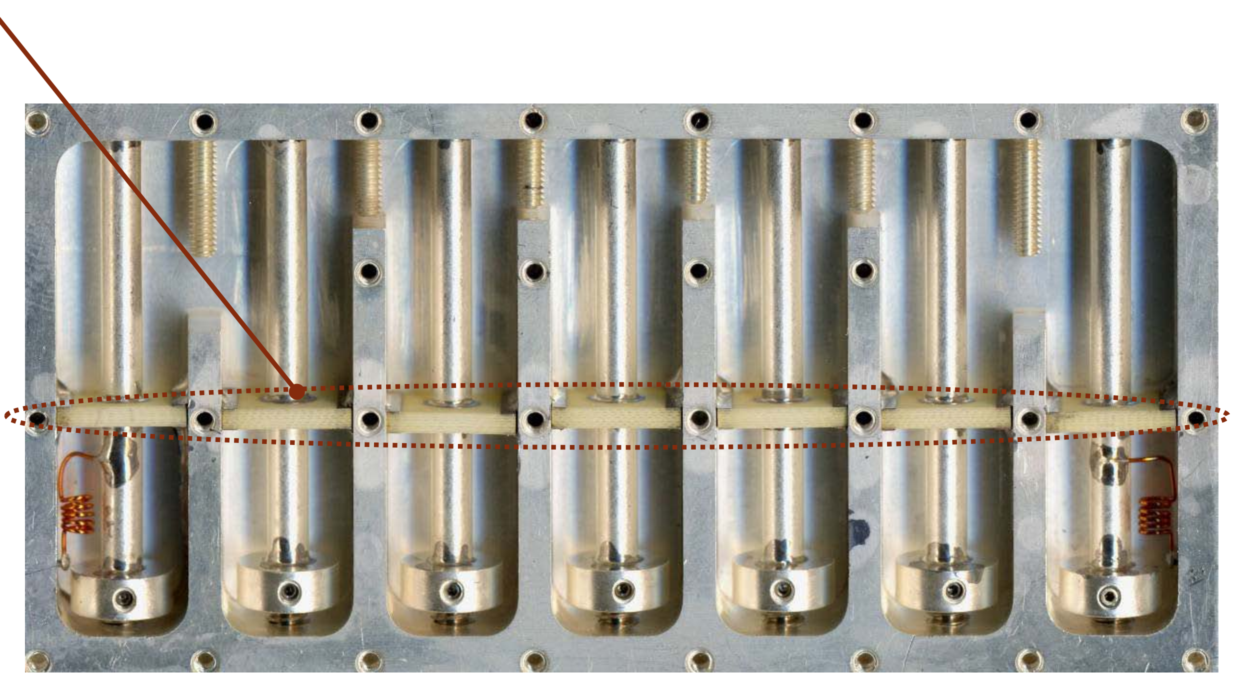

# Filters | Tubular Filters

## • Tubular Advantages

- *30 MHz to 5 GHz*
- *Broad stopbands*
- *Ideal for harmonic rejection*
- *Moderate bandwidths (2% to 50%)*
- *Chebyshev transfer functions*
- *High power handling capability*

## • Applications and Technology Trends

- *Mature technology - most current military applications are better served through LC or cavity filters*

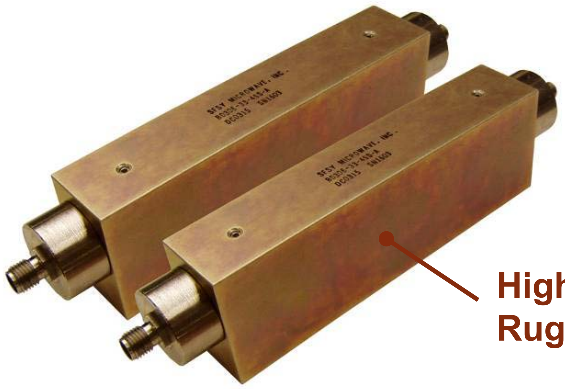

**High Power**
**Rugged Mounting**

**We have experience in high power tubular designs up to 5000 watts**

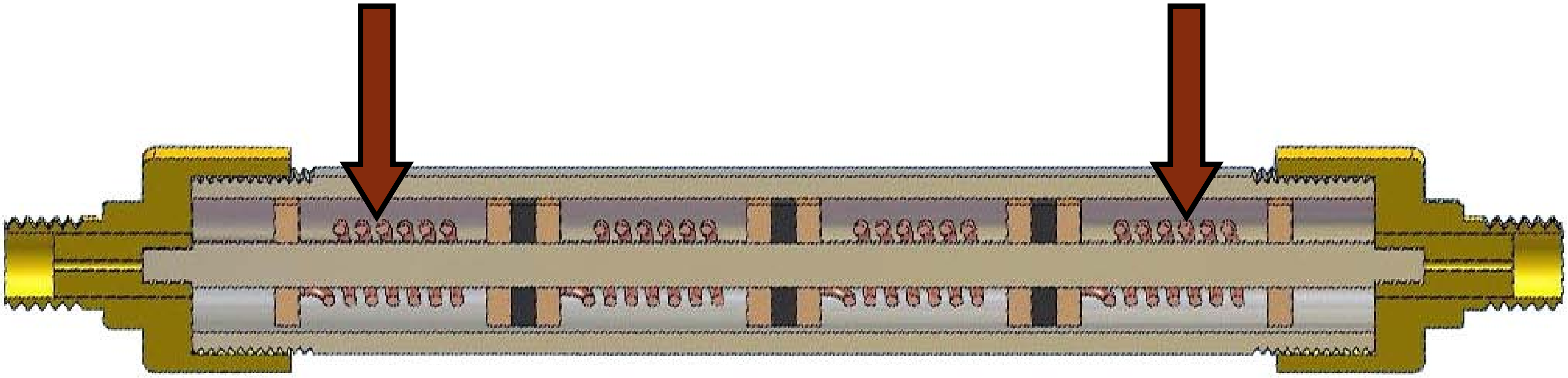

# Filters | Ceramic Filter Designs

## Alternative coupling structures offers design flexibility and superior performance

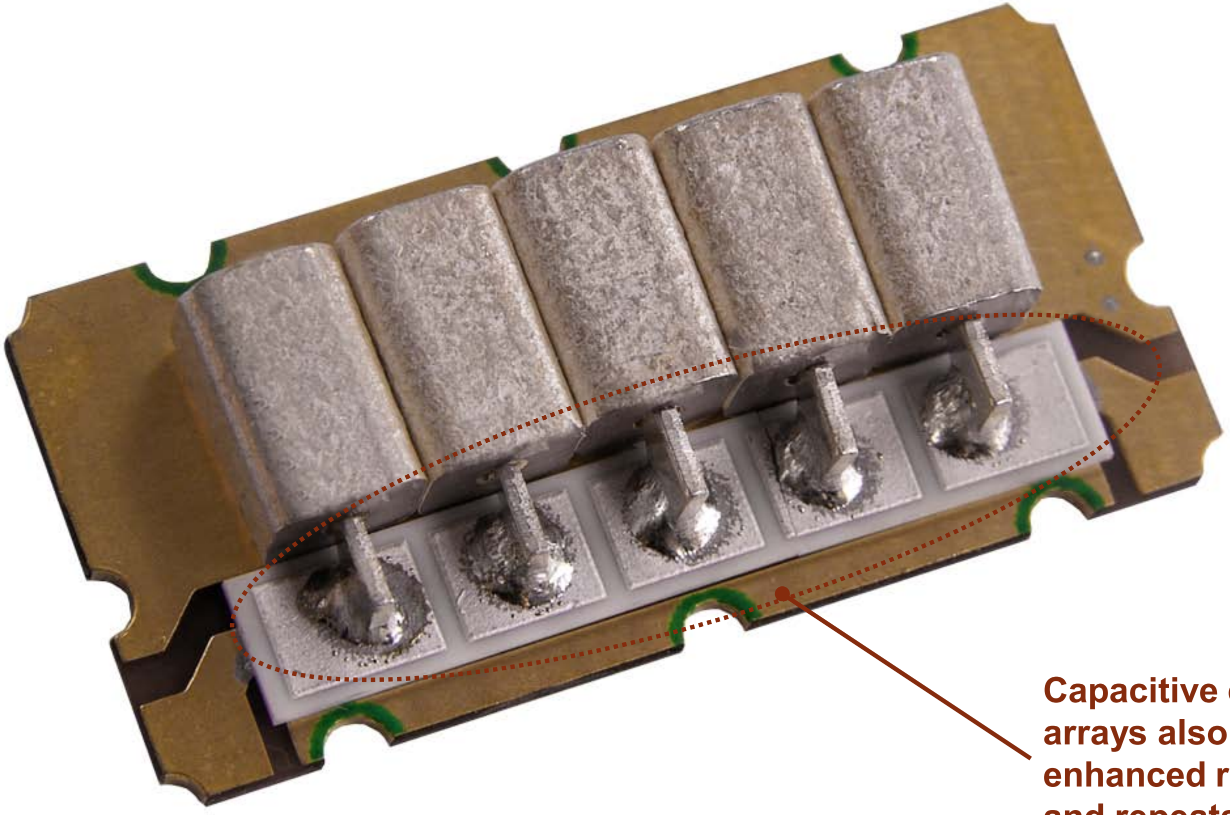

Capacitive coupling arrays also offer enhanced reliability and repeatability

Surface Acoustic Wave (SAW) filters are commonly used for frequencies in the range 50-2000 MHz.

Finger spacing, d, determines the wavelength that is:
(i) strongly excited by the input transducer and
(ii) produces a large response at the output transducer.

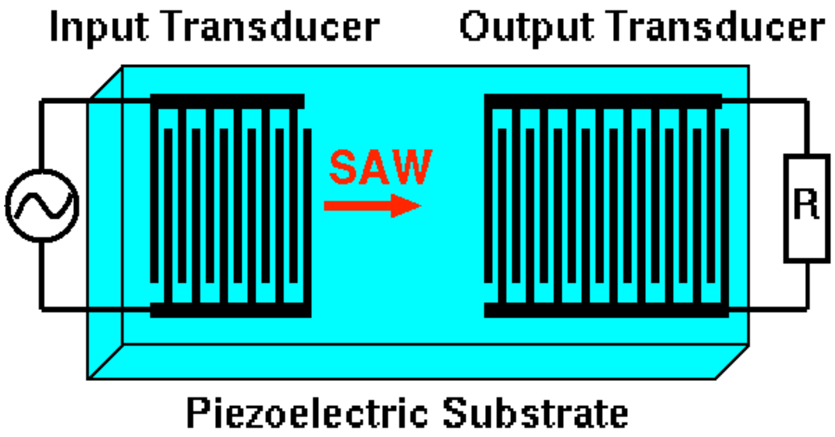
Input Transducer
Output Transducer
SAW
R
Piezoelectric Substrate

Figure taken from Wikipedia

# Regenerative amplifier -> demodulator

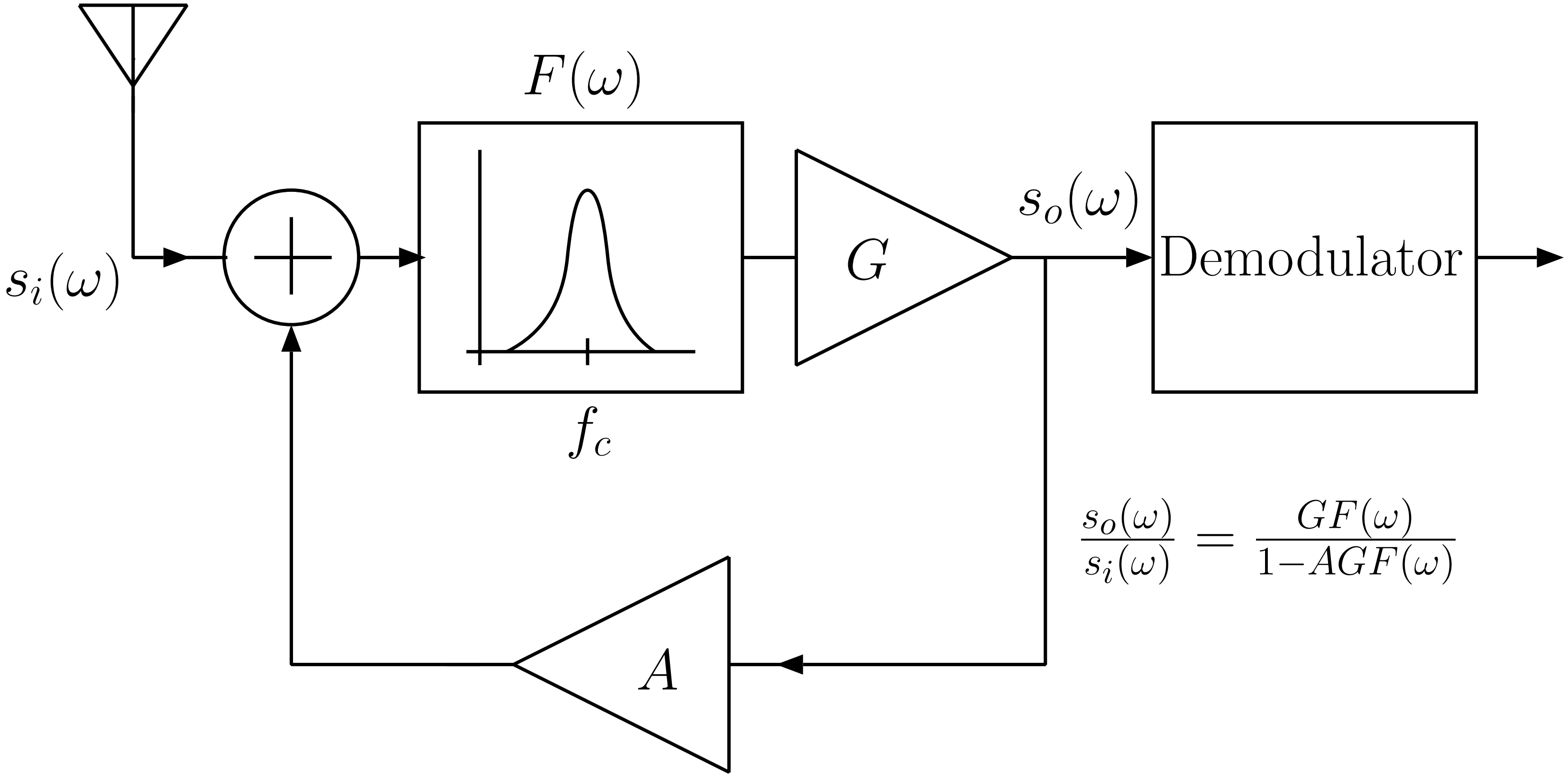
$F(\omega)$
$s_i(\omega)$
$f_c$
$G$
$s_o(\omega)$
Demodulator
$A$

$$\frac{s_o(\omega)}{s_i(\omega)} = \frac{GF(\omega)}{1-AGF(\omega)}$$

Invented by Edwin Armstrong (1912) while he was an undergraduate at Columbia

# Tuned-radio-frequency (TRF) receiver

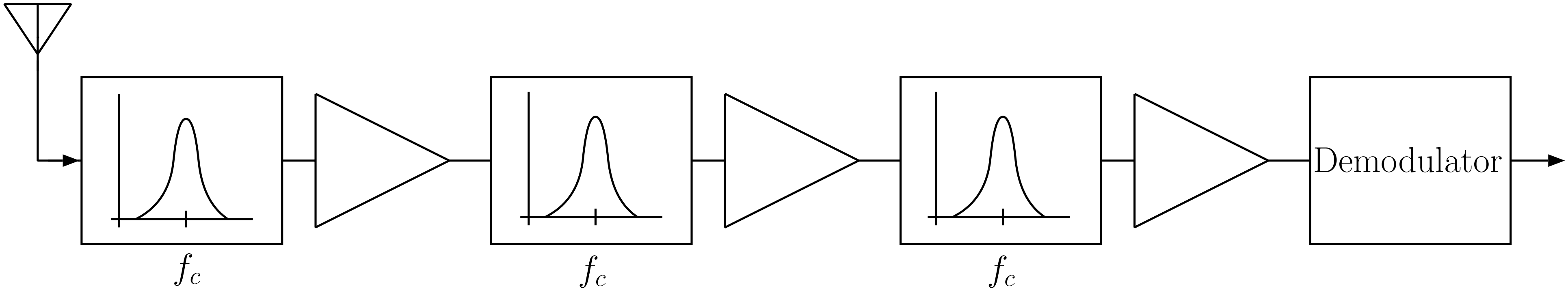
$f_c$
$f_c$
$f_c$
Demodulator

Each filter must be tuned to the same center frequency.

# Superheterodyne Receiver

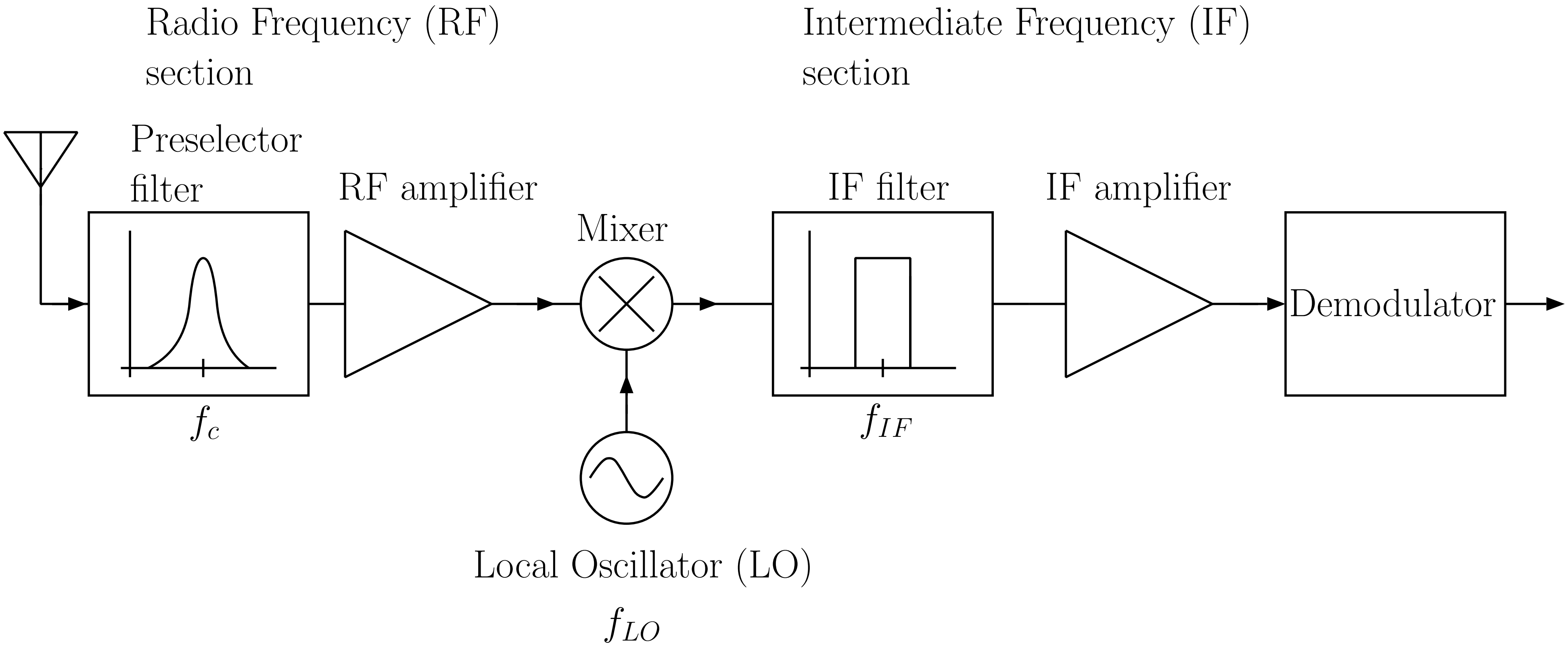
Radio Frequency (RF) section
Intermediate Frequency (IF) section
Preselector filter
RF amplifier
Mixer
IF filter
IF amplifier
Demodulator
$f_c$
$f_{IF}$
Local Oscillator (LO)
$f_{LO}$

Invented by Major Edwin Armstrong (1917) while he was in the Army Signal Corps

# Frequency translation is performed by the mixer/LO.

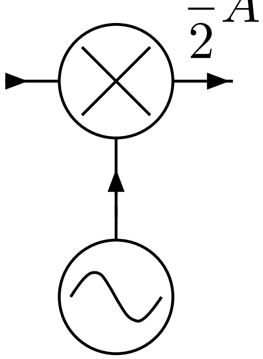

$$A(t)\cos(\omega_c t + \theta(t))$$

$$\frac{1}{2}A(t)\cos((\omega_c - \omega_{LO})t + \theta(t)) + \frac{1}{2}A(t)\cos((\omega_c + \omega_{LO})t + \theta(t))$$

$$\cos(\omega_{LO} t)$$

two output signals at carrier frequencies $|f_c \pm f_{LO}|$

modulation is preserved without distortion on both signals

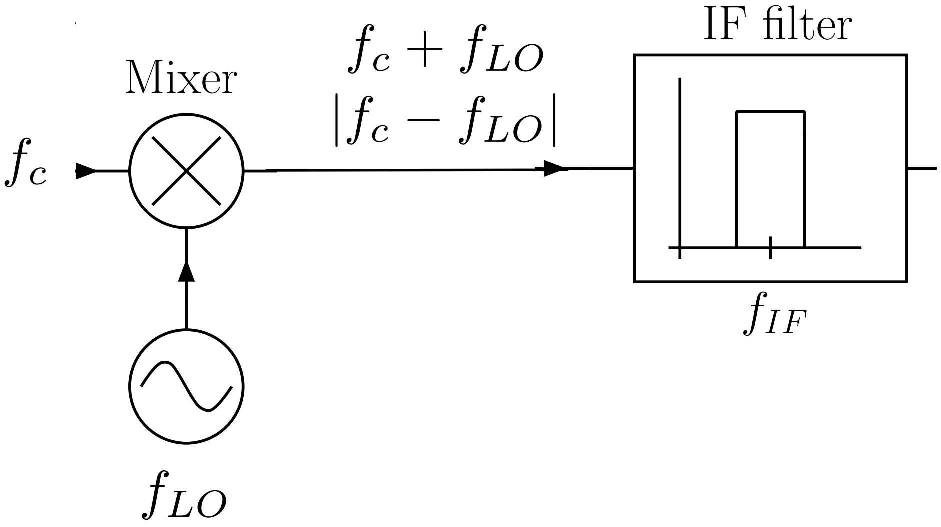
Mixer
$f_c$
$f_c + f_{LO}$
$|f_c - f_{LO}|$
IF filter
$f_{IF}$
$f_{LO}$

$f_{LO}$ is adjusted so that either

$$f_c + f_{LO} = f_{IF}$$

or

$$|f_c - f_{LO}| = f_{IF}$$

If $f_{IF} > f_c$ then the conversion is called "up-conversion".
If $f_{IF} < f_c$ then the conversion is called "down-conversion"

# "High LO" and "Low LO"

Given $f_c$ and $f_{IF}$, there are 2 choices for $f_{LO}$ which will convert (or "mix") $f_c \rightarrow f_{IF}$:

$$f_{LO} = |f_c - f_{IF}| \qquad \text{Low LO}$$
$$f_{LO} = f_c + f_{IF} \qquad \text{High LO}$$

# Image response

Given $f_{IF}$ and $f_{LO}$, there are 2 input frequencies that will be mixed to $f_{IF}$:

$$f_{c1} = f_{LO} + f_{IF}$$
$$f_{c2} = |f_{LO} - f_{IF}|$$

One of these is the desired carrier frequency. The other is called the "image frequency", $f_{IM}$.

The image response represents a potential source of interference. The purpose of the pre-selector filter is to reject signals at the image frequency.

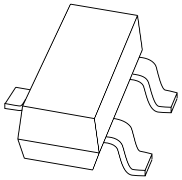

# BB207

## FM variable capacitance double diode

**Rev. 02 — 27 April 2004** **Product data sheet**

## 1. Product profile

### 1.1 General description

The BB207 is a variable capacitance double diode with a common cathode, fabricated in silicon planar technology, and encapsulated in the SOT23 small plastic SMD package.

### 1.2 Features

- Excellent linearity
- $C_{d(1V)}$: 81 pF; $C_{d(7.5V)}$: 27.6 pF
- $C_{d(1V)}$ to $C_{d(7.5V)}$ ratio: min. 2.6
- Very low series resistance
- Small plastic SMD package.

### 1.3 Applications

- Electronic tuning in FM-radio.

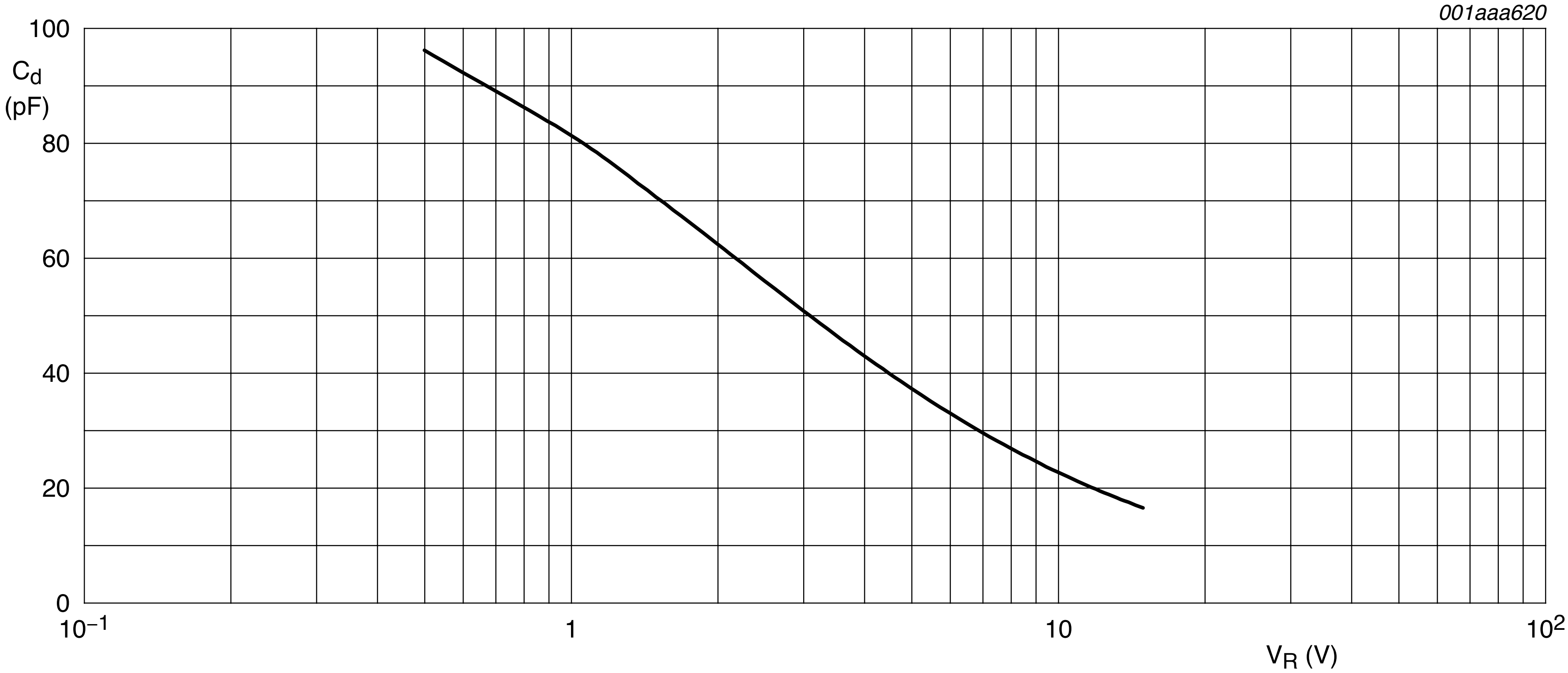

f = 1 MHz; $T_j$ = 25 °C.

**Fig 1. Diode capacitance as a function of reverse voltage; typical values.**

# Introducing the Spectre ELITE Radar Detector Detector

Spectre ELITE

## Next generation technology in radar detector detection

Federal law prohibits drivers of commercial motor vehicles from using radar detectors. In fact, Federal Motor Carrier Safety Administration Regulation 392.71 prohibits these drivers from even possessing a radar detector. Plus, radar detectors are illegal in all vehicles in Washington, D.C., Virginia, and on all U.S. military installations.

**Selectable Filter Switch**

ON
FILTER
OFF
MUTE
LOW

**The Spectre ELITE features electronic circuit design enhancements and a new selectable filter switch for easier target acquisition and greater range.**

And although many radar detector manufacturers may say that their devices are undetectable, the Spectre ELITE detects hundreds of radar detector models in use all over the U.S. That's because all radar detectors, including those that feature "cloaking" or "Spectre Alert," operate - and are detected - in the same way.

The Spectre ELITE detects radar detectors by sensing electromagnetic "leakage" from a component common to every radar detector, the local oscillator. Some manufacturers try to evade detection by suppressing local oscillator leakage with shielding; others try to adjust the leakage to a frequency that the ELITE isn't designed to detect, while others turn off the local oscillator when they detect the Spectre. In most cases, the ELITE can detect these "stealthy" detectors before they can detect the ELITE and shut down.

# Four types of single-conversion superhets

| | | | | | | |
|---|---|---|---|---|---|---|
| (1) | **Up - conversion:** | | $\mathbf{f_{IF} > f_{cmax} > f_{cmin}}$ | | | |
| High LO | (1a) | $\mathbf{f_{LO} = f_{IF} + f_c}$ | $f_{IM} = f_c + 2f_{IF}$ | $\lvert f_{IM} - f_c \rvert = 2f_{IF}$ | | |
| Low LO | (1b) | $\mathbf{f_{LO} = f_{IF} - f_c}$ | $f_{IM} = 2f_{IF} - f_c$ | $\lvert f_{IM} - f_c \rvert = 2f_{LO}$ | | |
| (2) | **Down - conversion:** | | $\mathbf{f_{IF} < f_{cmin} < f_{cmax}}$ | | | |
| High LO | (2a) | $\mathbf{f_{LO} = f_{IF} + f_c}$ | $f_{IM} = f_c + 2f_{IF}$ | $\lvert f_{IM} - f_c \rvert = 2f_{IF}$ | | |
| Low LO | (2b) | $\mathbf{f_{LO} = f_c - f_{IF}}$ | $f_{IM} = \lvert f_c - 2f_{IF} \rvert$ | $\lvert f_{IM} - f_c \rvert = 2f_{IF}$ | if | $f_c > 2f_{IF}$ |
| | | | | $\lvert f_{IM} - f_c \rvert = 2f_{LO}$ | if | $f_c < 2f_{IF}$ |

Note: In cases (1a) and (1b) (i.e. upconversion) $f_{IM} > f_{cmax}$. This means that images are always above the highest carrier frequency of interest and therefore outside the band of interest. A fixed preselector filter can be used to pass the entire band of interest while still rejecting images.

A single frequency conversion is not always enough.

For example, suppose we want to receive signals with $f_c \simeq 5$ GHz and $BW = 5$ kHz.

The bandwidth of the IF filter should be 5 kHz, so fractional bandwidth of IF filter is $\frac{5e3}{f_{IF}}$.

To reject the 1/2-IF response, preselector bandwidth must be smaller than $f_{IF}$, so fractional preselector bandwidth is $\frac{f_{IF}}{5e9}$.

Suppose we want both fractional bandwidths $> 0.01$:

$$\frac{5e3}{f_{IF}} > 0.01 \rightarrow f_{IF} < 5e5$$

$$\frac{f_{IF}}{5e9} > 0.01 \rightarrow f_{IF} > 5e7$$

Can't satisfy both constraints. Need to use more than one conversion or image-reject mixer.

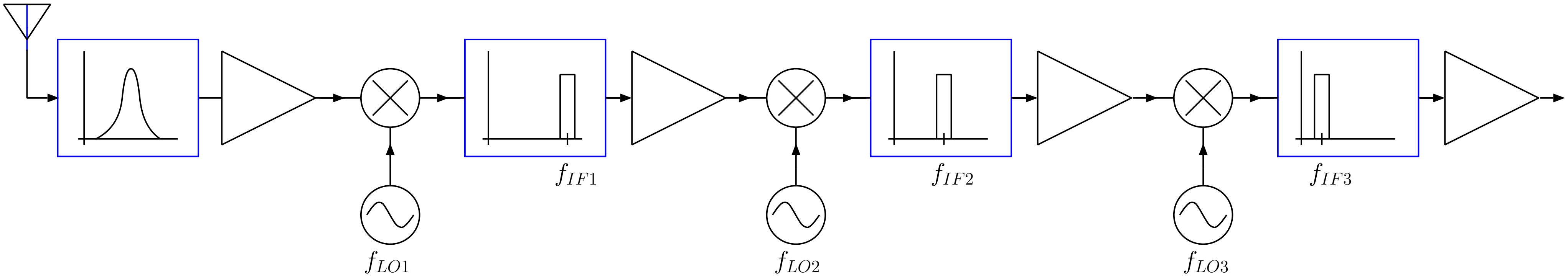
$f_{IF1}$
$f_{LO1}$
$f_{IF2}$
$f_{LO2}$
$f_{IF3}$
$f_{LO3}$

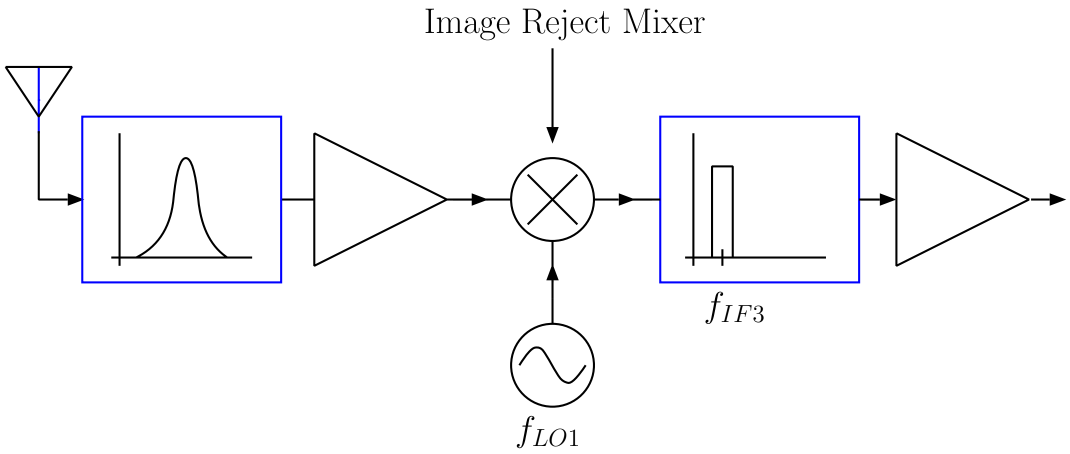
Image Reject Mixer
$f_{IF3}$
$f_{LO1}$

# Image-reject mixer

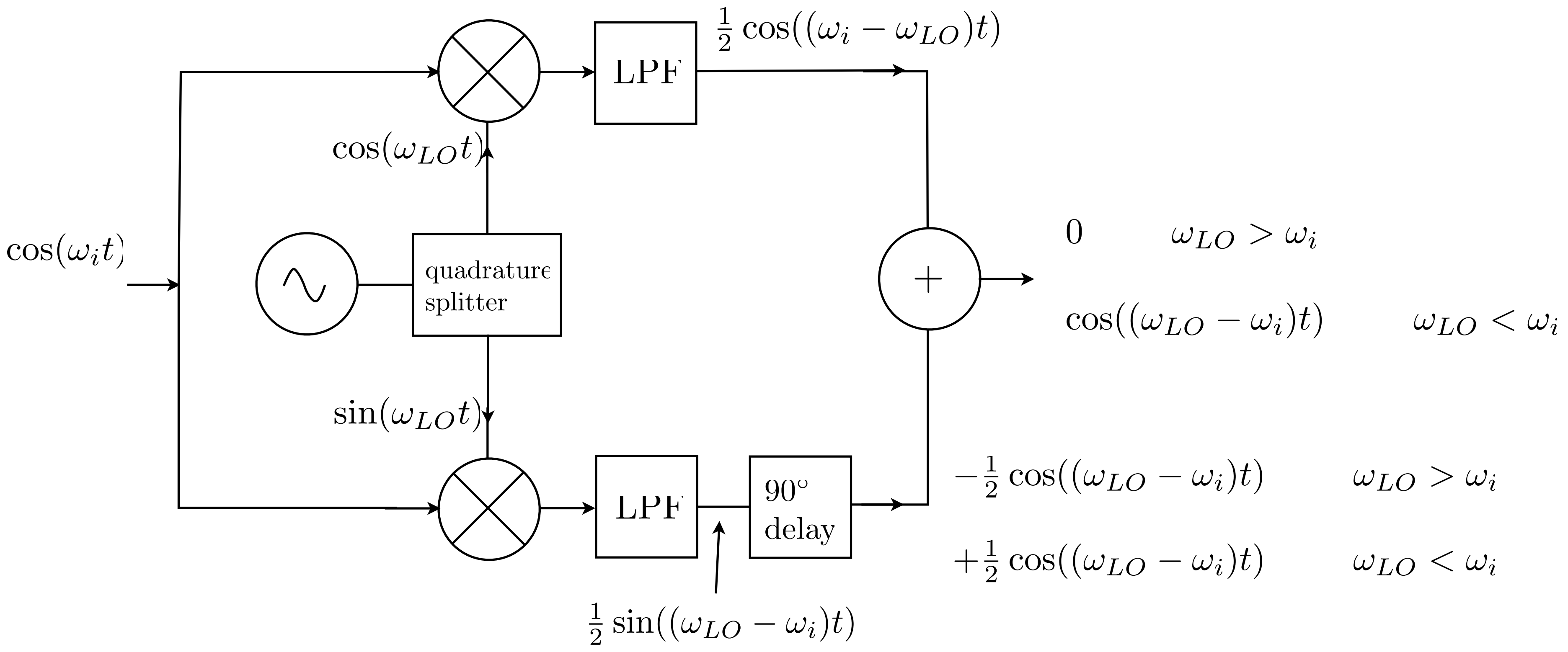

$\frac{1}{2}\cos((\omega_i - \omega_{LO})t)$

LPF

$\cos(\omega_{LO} t)$

$\cos(\omega_i t)$

quadrature splitter

$+$

$0 \qquad \omega_{LO} > \omega_i$

$\cos((\omega_{LO} - \omega_i)t) \qquad \omega_{LO} < \omega_i$

$\sin(\omega_{LO} t)$

LPF

$90^\circ$ delay

$-\frac{1}{2}\cos((\omega_{LO} - \omega_i)t) \qquad \omega_{LO} > \omega_i$

$+\frac{1}{2}\cos((\omega_{LO} - \omega_i)t) \qquad \omega_{LO} < \omega_i$

$\frac{1}{2}\sin((\omega_{LO} - \omega_i)t)$

An input signal with frequency smaller than the LO produces no output, and an input signal with frequency greater than $f_{LO}$ produces output at the difference frequency $|f_i - f_{LO}|$.

This configuration is an "image-reject" mixer for downconversion and low-LO.

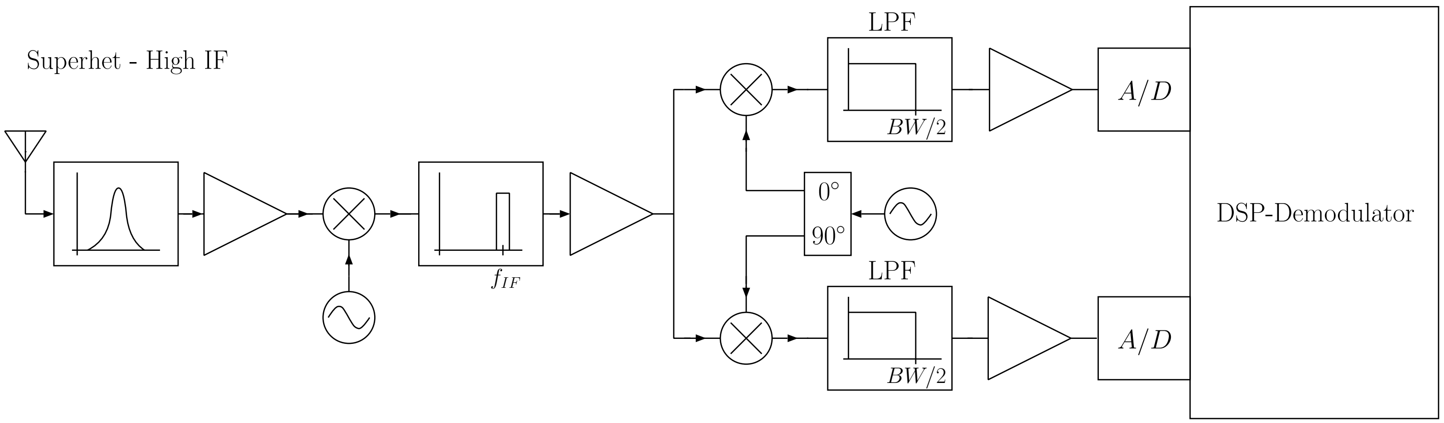
Superhet - High IF
$f_{IF}$
LPF
$BW/2$
0°
90°
LPF
$BW/2$
$A/D$
$A/D$
DSP-Demodulator

(a)

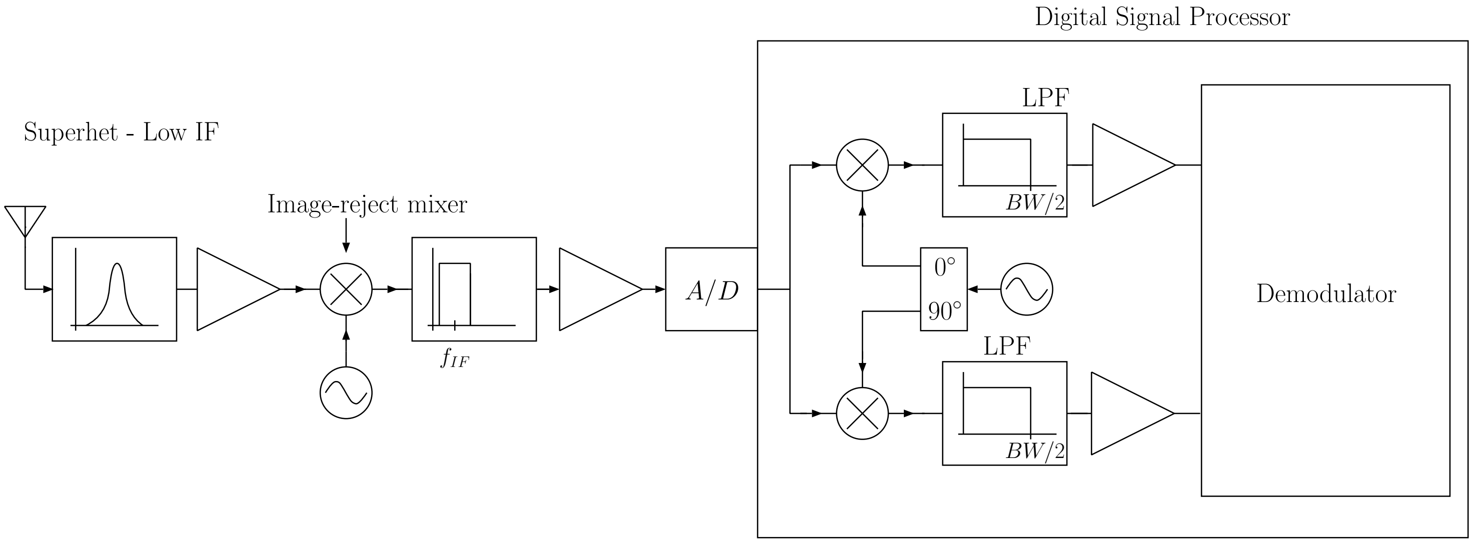
Digital Signal Processor
Superhet - Low IF
Image-reject mixer
$f_{IF}$
$A/D$
LPF
$BW/2$
0°
90°
LPF
$BW/2$
Demodulator

(b)

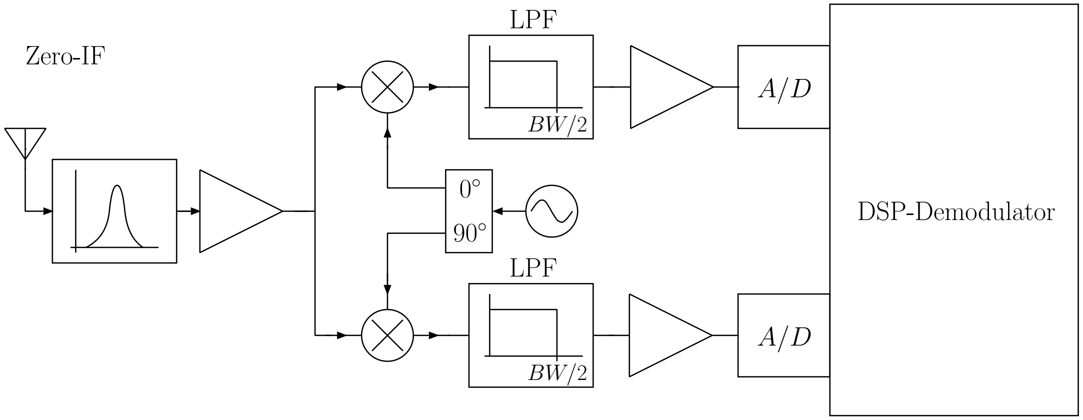
Zero-IF
LPF
$BW/2$
0°
90°
LPF
$BW/2$
$A/D$
$A/D$
DSP-Demodulator

(c)

# High IF, Low IF, and "zero IF"

## Superhet with High IF

- Quadrature demod circuitry operates at relatively low frequency
- A/D converters operate at low frequency/sampling-rate

## Superhet with Low-IF

- Only 1 A/D converter
- Quadrature demod is done in DSP - perfect I/Q channel balance.
- May need "image-reject" mixer to attenuate the image response.

## Zero-IF (direct conversion)

- Fewest components
- Quadrature demod operates at carrier frequency (need high frequency quadrature splitter and 2 high frequency mixers)
- LO leakage causes DC offsets in I/Q channels. I and Q channel output spectrum has a (possibly large) "spike" at DC. Can saturate DC-coupled amplifiers - must be removed. Desired signal's DC component will also be removed.
- Phase noise from LO is a problem. High gain at baseband means that down-converted phase noise is more troublesome than in topologies with less gain.

19-2135; Rev 1; 8/02

MAXIM

# 315MHz Low-Power, +3V Superheterodyne Receiver

## General Description

The MAX1470 is a fully integrated low-power CMOS superheterodyne receiver for use with amplitude-shift-keyed (ASK) data in the 315MHz band. With few required external components, and a low-current power-down mode, it is ideal for cost- and power-sensitive applications in the automotive and consumer markets. The chip consists of a 315MHz low-noise amplifier (LNA), an image rejection mixer, a fully integrated 315MHz phase-lock-loop (PLL), a 10.7MHz IF limiting amplifier stage with received-signal-strength indicator (RSSI) and an ASK demodulator, and analog baseband data-recovery circuitry.

The MAX1470 is available in a 28-pin TSSOP package.

## Applications

Remote Keyless Entry
Garage Door Openers
Remote Controls
Wireless Sensors
Wireless Computer Peripherals
Security Systems
Toys
Video Game Controllers
Medical Systems

## Features

- **Operates from a Single +3.0V to +3.6V Supply**
- **Built-In 53dB RF Image Rejection**
- **-115dBm Receive Sensitivity***
- **250µs Startup Time**
- **Low 5.5mA Operating Supply Current**
- **1.25µA Low-Current Power-Down Mode for Efficient Power Cycling**
- **250MHz to 500MHz Operating Band (Image Rejection Optimized at 315MHz)**
- **Integrated PLL with On-Board Voltage-Controlled Oscillator (VCO) and Loop Filter**
- **Selectable IF Bandwidth Through External Filter**
- **Complete Receive System from RF to Digital Data Out**

**See Note 2, AC Electrical Characteristics.*

## Ordering Information

| PART | TEMP RANGE | PIN-PACKAGE |
|---|---|---|
| MAX1470EUI | -40°C to +85°C | 28 TSSOP |

***Typical Application Circuit appears at end of data sheet.***
***Pin Configuration appears at end of data sheet.***

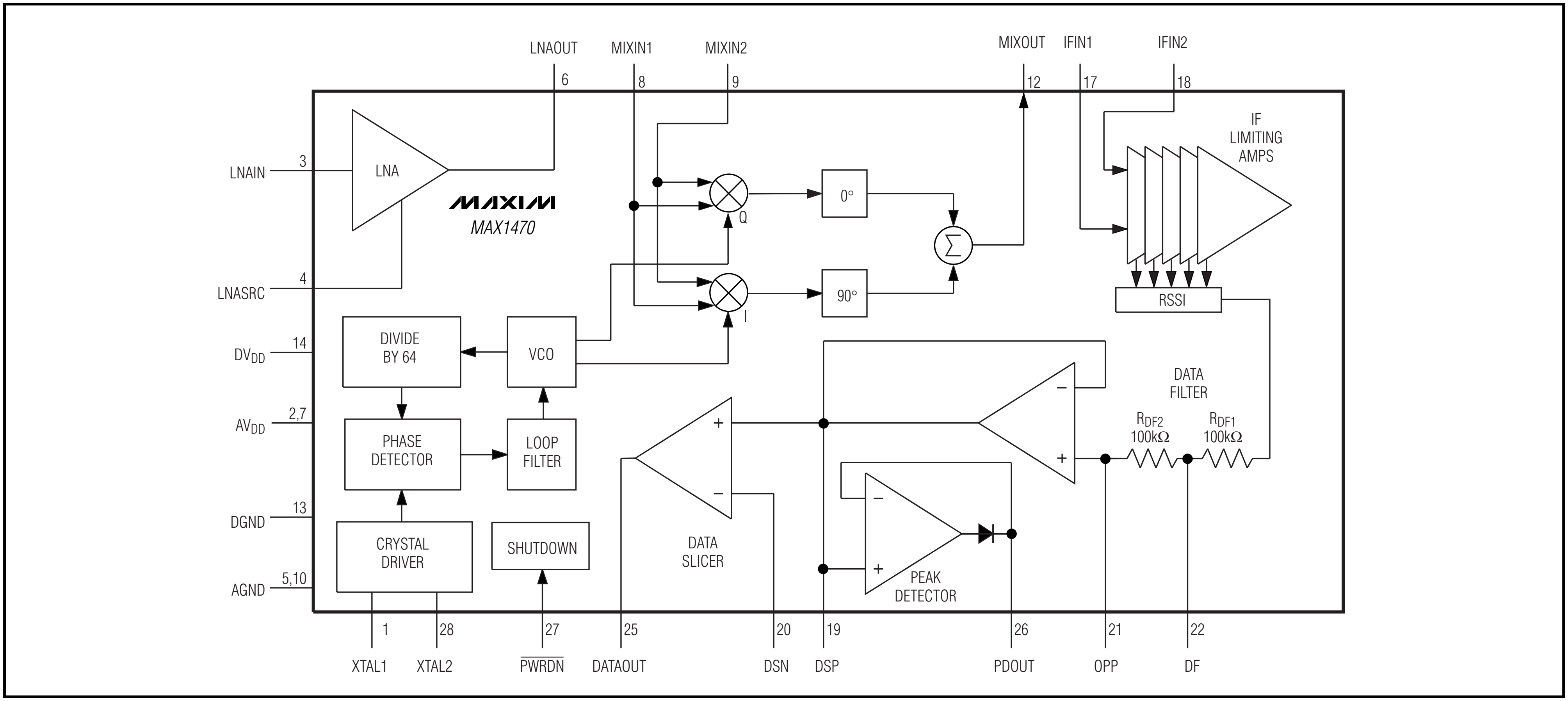
LNAOUT
MIXIN1
MIXIN2
MIXOUT
IFIN1
IFIN2
6
8
9
12
17
18
LNAIN
3
LNA
MAXIM
MAX1470
Q
I
0°
90°
Σ
IF
LIMITING
AMPS
RSSI
LNASRC
4
$DV_{DD}$
14
DIVIDE
BY 64
VCO
$AV_{DD}$
2,7
PHASE
DETECTOR
LOOP
FILTER
DATA
FILTER
$R_{DF2}$
100kΩ
$R_{DF1}$
100kΩ
DGND
13
AGND
5,10
CRYSTAL
DRIVER
SHUTDOWN
DATA
SLICER
PEAK
DETECTOR
+
−
1
28
27
25
20
19
26
21
22
XTAL1
XTAL2
$\overline{PWRDN}$
DATAOUT
DSN
DSP
PDOUT
OPP
DF

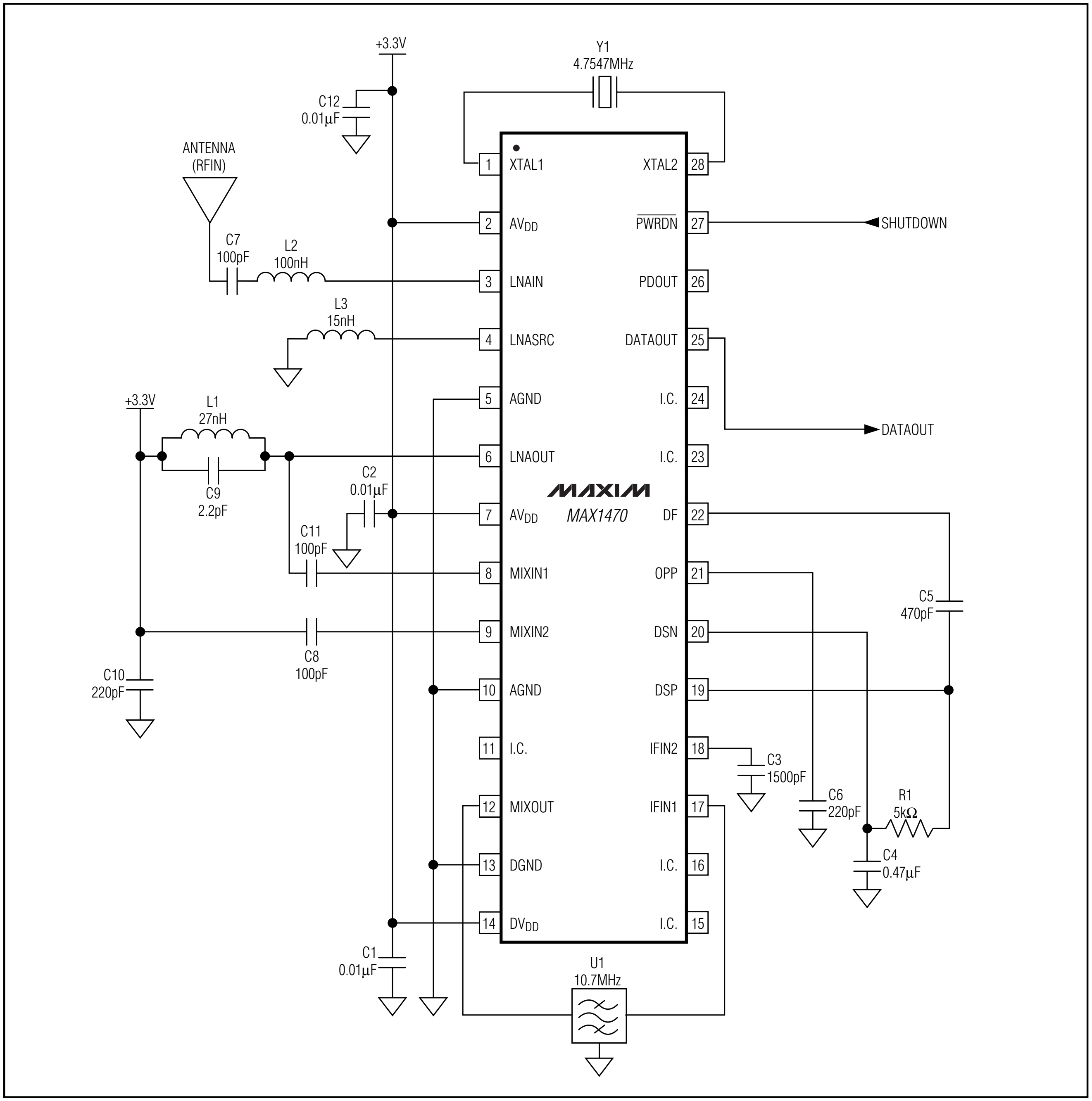
+3.3V
C12
0.01µF
Y1
4.7547MHz
ANTENNA
(RFIN)
C7
100pF
L2
100nH
L3
15nH
+3.3V
L1
27nH
C9
2.2pF
C2
0.01µF
C11
100pF
C8
100pF
C10
220pF
C1
0.01µF
U1
10.7MHz
MAXIM
MAX1470
1 XTAL1
2 AVDD
3 LNAIN
4 LNASRC
5 AGND
6 LNAOUT
7 AVDD
8 MIXIN1
9 MIXIN2
10 AGND
11 I.C.
12 MIXOUT
13 DGND
14 DVDD
28 XTAL2
27 PWRDN
26 PDOUT
25 DATAOUT
24 I.C.
23 I.C.
22 DF
21 OPP
20 DSN
19 DSP
18 IFIN2
17 IFIN1
16 I.C.
15 I.C.
SHUTDOWN
DATAOUT
C5
470pF
C3
1500pF
C6
220pF
R1
5kΩ
C4
0.47µF

### ***Mixer***

A unique feature of the MAX1470 is the integrated image rejection of the mixer. This device was designed to eliminate the need for a costly front-end SAW filter for many applications. The advantage of not using a SAW filter is increased sensitivity, simplified antenna matching, less board space, and lower cost.

The mixer cell is a pair of double-balanced mixers that perform an IQ downconversion of the 315MHz RF input to the 10.7MHz IF with low-side injection (i.e., $f_{LO} = f_{RF} - f_{IF}$). The image rejection circuit then combines these signals to achieve ~50dB of image rejection over the full temperature range. Low-side injection is required due to the on-chip image-rejection architecture. The IF output is driven by a source-follower, biased to create a driving impedance of 330Ω to interface with an off-chip 330Ω ceramic IF filter. The voltage conversion gain driving a 330Ω load is approximately 13dB.

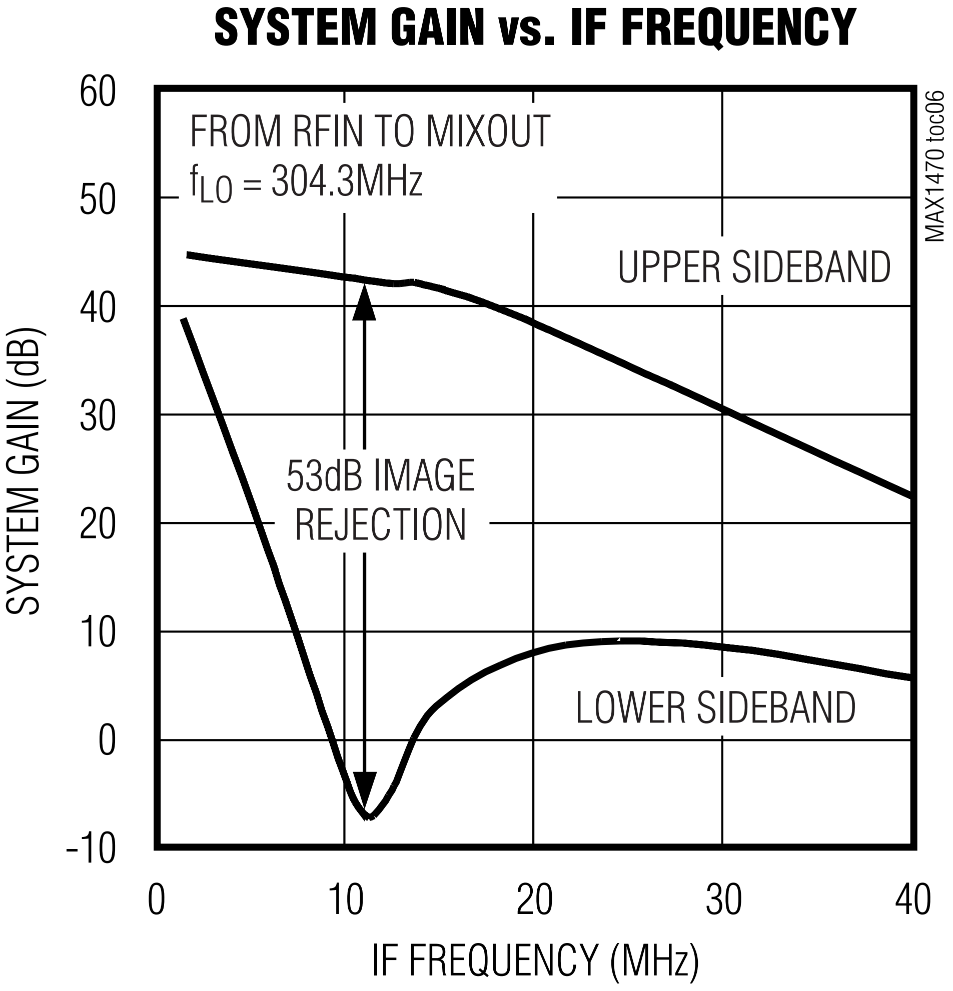

19-3123; Rev 1a; 9/04

EVALUATION KIT
AVAILABLE

# Complete SDARS Receiver

## General Description

The MAX2140 complete receiver is designed for satellite digital audio radio services (SDARS). The device includes a fully monolithic VCO and only needs a SAW at the IF and a crystal to generate the reference frequency.

To form a complete SDARS radio, the MAX2140 requires only a low-noise amplifier (LNA), which can be controlled by a baseband controller. The small number of external components needed makes the MAX2140-based platform the lowest cost and the smallest solution for SDARS.

The receiver includes a self-contained RF AGC loop and baseband-controlled IF AGC loop, effectively providing a total dynamic range of over 92dB.

Channel selectivity is ensured by the SAW filter and by on-chip monolithic lowpass filters.

The fractional-N PLL allows a very small frequency step, making possible the implementation of an AFC loop. Additionally, the reference is provided by an external XTAL and on-chip oscillator. A reference buffer output is also provided.

A 2-wire interface ($I^2C$™ bus compatible) programs the circuit for a wide variety of conditions, providing features such as:

- Programmable gains
- Lowpass filters tuning
- Individual functional block shutdown

The MAX2140 minimizes the requirement on the baseband controller. No compensation or calibration procedures are required. The device is available in a 7mm × 7mm 44-pin thin QFN package.

## Applications

Satellite Digital Audio Radio Services (SDARS)

2.4GHz ISM Radios

*$I^2C$ is a trademark of Philips Corp.*

*Purchase of $I^2C$ components from Maxim Integrated Products, Inc., or one of its sublicensed Associated Companies, conveys a license under the Philips $I^2C$ Patent Rights to use these components in an $I^2C$ system, provided that the system conforms to the $I^2C$ Standard Specification as defined by Philips.*

## Features

- ♦ **Integrated Receiver, Requires Only One SAW Filter**
- ♦ **Self-Contained RF AGC Loop**
- ♦ **Differential I/Q Interface**
- ♦ **Complete Integrated Frequency Generation**
- ♦ **Bias Supply for External LNAs**
- ♦ **Overcurrent Protection**
- ♦ **Low-Power Standby Mode**
- ♦ **Very Small 44-Pin Thin QFN Package**

## Ordering Information

| PART | TEMP RANGE | PIN-PACKAGE |
|---|---|---|
| MAX2140ETH | -40°C to +85°C | 44 Thin QFN-EP* |

**EP = Exposed paddle.*

## Block Diagram/Pin Configuration

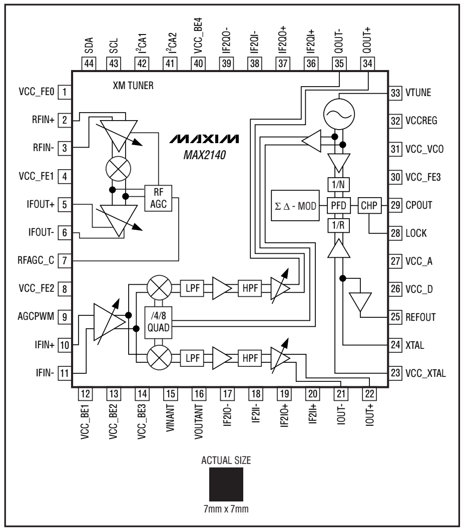
SDA 44
SCL 43
$I^2CA1$ 42
$I^2CA2$ 41
VCC_BE4 40
IF2QO- 39
IF2QI- 38
IF2QO+ 37
IF2QI+ 36
QOUT- 35
QOUT+ 34
XM TUNER
VCC_FE0 1
RFIN+ 2
RFIN- 3
VCC_FE1 4
IFOUT+ 5
IFOUT- 6
RFAGC_C 7
VCC_FE2 8
AGCPWM 9
IFIN+ 10
IFIN- 11
RF AGC
MAXIM
MAX2140
Σ Δ - MOD
1/N
PFD
1/R
CHP
LPF
HPF
/4/8 QUAD
LPF
HPF
33 VTUNE
32 VCCREG
31 VCC_VCO
30 VCC_FE3
29 CPOUT
28 LOCK
27 VCC_A
26 VCC_D
25 REFOUT
24 XTAL
23 VCC_XTAL
12 VCC_BE1
13 VCC_BE2
14 VCC_BE3
15 VINANT
16 VOUTANT
17 IF2IO-
18 IF2II-
19 IF2IO+
20 IF2II+
21 IOUT-
22 IOUT+
ACTUAL SIZE
7mm x 7mm

**For pricing, delivery, and ordering information, please contact Maxim/Dallas Direct! at 1-888-629-4642, or visit Maxim's website at www.maxim-ic.com.**

19-3123; Rev 3; 10/05

EVALUATION KIT
AVAILABLE

MAXIM

# Complete SDARS Receiver

## General Description

The MAX2140 complete receiver is designed for satellite digital audio radio services (SDARS). The device includes a fully monolithic VCO and only needs a SAW at the IF and a crystal to generate the reference frequency.

To form a complete SDARS radio, the MAX2140 requires only a low-noise amplifier (LNA), which can be controlled by a baseband controller. The small number of external components needed makes the MAX2140-based platform the lowest cost and the smallest solution for SDARS.

The receiver includes a self-contained RF AGC loop and baseband-controlled IF AGC loop, effectively providing a total dynamic range of over 92dB.

Channel selectivity is ensured by the SAW filter and by on-chip monolithic lowpass filters.

The fractional-N PLL allows a very small frequency step, making possible the implementation of an AFC loop. Additionally, the reference is provided by an external XTAL and on-chip oscillator. A reference buffer output is also provided.

## Features

- ♦ **Integrated Receiver, Requires Only One SAW Filter**
- ♦ **Self-Contained RF AGC Loop**
- ♦ **Differential I/Q Interface**
- ♦ **Complete Integrated Frequency Generation**
- ♦ **Bias Supply for External LNAs**
- ♦ **Overcurrent Protection**
- ♦ **Low-Power Standby Mode**
- ♦ **Very Small 44-Pin Thin QFN Package**

## Ordering Information

| PART | TEMP RANGE | PIN-PACKAGE |
|---|---|---|
| MAX2140ETH | -40°C to +85°C | 44 Thin QFN-EP* |
| MAX2140ETH+ | -40°C to +85°C | 44 Thin QFN-EP* |

## Block Diagram/Pin Configuration

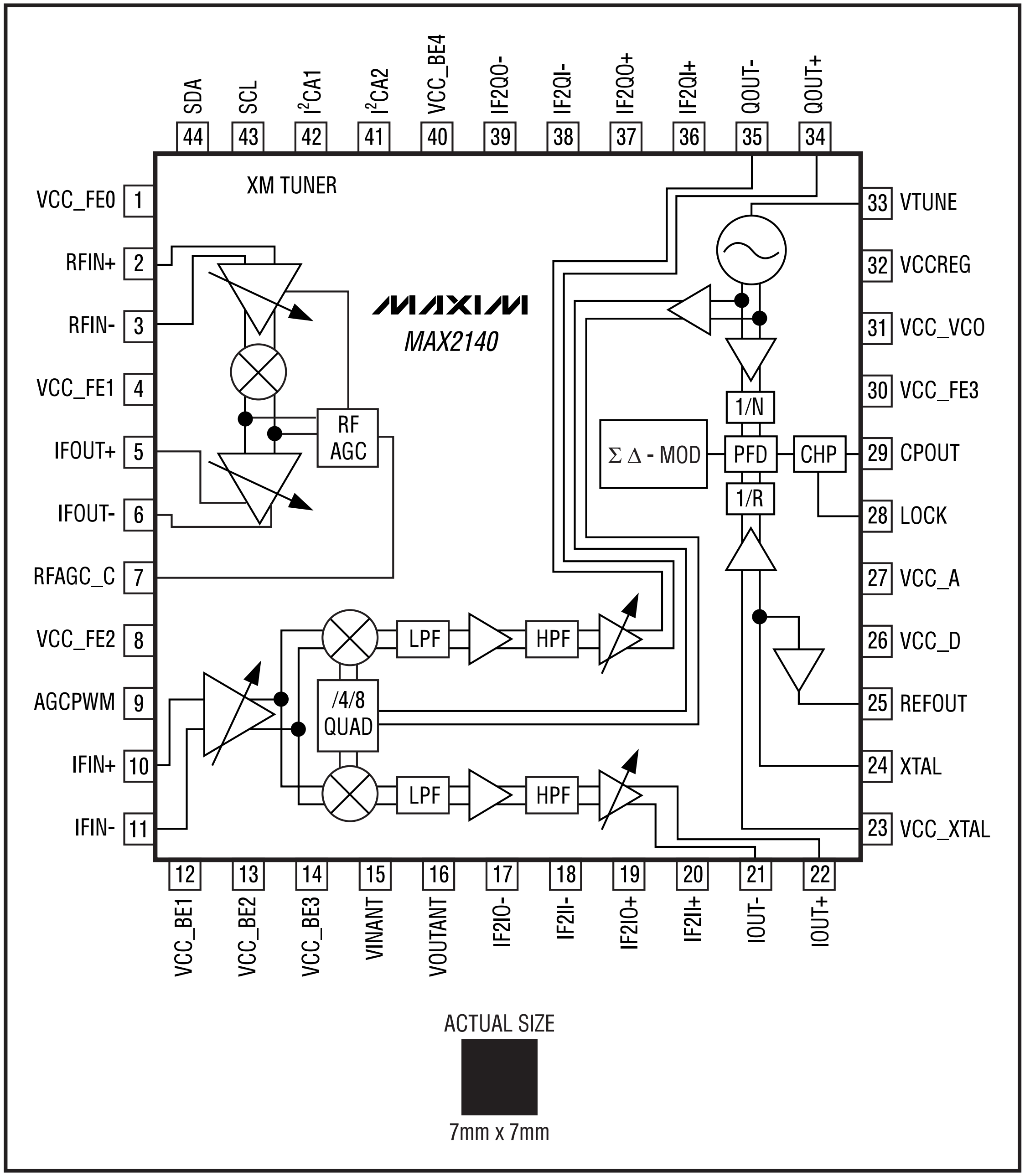
SDA 44
SCL 43
I2CA1 42
I2CA2 41
VCC_BE4 40
IF2QO- 39
IF2QI- 38
IF2QO+ 37
IF2QI+ 36
QOUT- 35
QOUT+ 34
VCC_FE0 1
RFIN+ 2
RFIN- 3
VCC_FE1 4
IFOUT+ 5
IFOUT- 6
RFAGC_C 7
VCC_FE2 8
AGCPWM 9
IFIN+ 10
IFIN- 11
VTUNE 33
VCCREG 32
VCC_VCO 31
VCC_FE3 30
CPOUT 29
LOCK 28
VCC_A 27
VCC_D 26
REFOUT 25
XTAL 24
VCC_XTAL 23
12 VCC_BE1
13 VCC_BE2
14 VCC_BE3
15 VINANT
16 VOUTANT
17 IF2IO-
18 IF2II-
19 IF2IO+
20 IF2II+
21 IOUT-
22 IOUT+
XM TUNER
MAXIM
MAX2140
RF AGC
/4/8 QUAD
LPF
HPF
LPF
HPF
Σ Δ - MOD
PFD
CHP
1/N
1/R
ACTUAL SIZE
7mm x 7mm

## Detailed Description

### Front End

The front end of the MAX2140, which downconverts the RF signal to IF, is defined from the differential RF inputs (pins RFIN+ and RFIN-) to the output (pins IFOUT+ and IFOUT-) to the SAW filter.

The front end includes a self-contained analog RF AGC loop. The engagement threshold of the loop can be programmed from -35dBm to -15dBm referred to the RF input in 1dB steps using the RF4–RF0 programming bits. The time constant of the loop is set externally by the capacitor connected to RFAGC_C.

The image reject first mixer ensures a good image and half IF rejection.

The front-end gain can be reduced by programming bits PM3–PM0 over a 22dB range, with a step of 2dB. This allows the selections of SAW filters with different insertion loss.

The IF output is nominally 900Ω differentially and requires pullup inductors to $V_{CC}$, which can be used as part of the matching network to the SAW filter impedance.

### Back End

The back end, which downconverts the IF signal to quadrature baseband, is defined from the SAW filter inputs (pins IFIN+ and IFIN-) to the baseband outputs (pins IOUT+, IOUT-, QOUT+, QOUT-).

The back end contains an IF AGC loop, which is closed by the baseband controller. The IF AGC control voltage is applied at the AGCPWM pin. The gain can be reduced over 53dB (typ) and exhibits a log-linear characteristic.

The back end also contains individual lowpass filters on each channel. The lowpass-filter bandwidth is the useful SDARS downconverted bandwidth (6.25MHz). The lowpass-filter performance is factory trimmed. The bit IOT switches between the factory-trimmed set and the control through the $I^2C$-compatible bus using bits B4–B1. Even when using the factory-trimmed set, the user can still slightly modify the cutoff frequency (by ±250kHz) by varying bits LP1/LP0.

Highpass filters are also inserted in the back-end signal paths. Their purpose is to remove the DC offset. They are designed for a low corner frequency so as not to degrade the SDARS content. Their exact cutoff frequency is set by the external capacitors connected between IF2 access pins, given by the following equation:

$$f_{cutoff} = 1/(2 \times \pi \times R \times C) \text{ [Hz]}$$

where R = 8000Ω, C = external capacitor to be connected.

Finally, the HPF bit allows an increase to the back-end gain by 4dB at the slight expense of a degraded in-band linearity.

### Frequency Generation

An on-chip VCO and a low-step fractional-N PLL ensure the necessary frequency generation. The 1st mixer's LO is at the VCO frequency itself, while the 2nd mixer's LO is the VCO frequency divided by 4 or by 8 (bit D48). Hence, the two possible IF frequencies for SDARS are 467MHz and 259MHz. Typical applications are based on 259MHz IF frequency.

The reference divider path in the PLL can either use an external crystal and the on-chip crystal oscillator or an external TCXO that can overdrive the on-chip crystal oscillator. A reference division ratio of 1 or 2 is set by the REF bit. The crystal oscillator (or TCXO) signal is available at pin REFOUT. The output is either at the same frequency as the reference signal, or divided by two, based on the setting of bit RFD.

The VCO main division ratio is set by bits N6–N0 (for the integer part) and bits F19–F00 (for the fractional part). The minimum step is below 30Hz, small enough for effective AFC to be implemented by the baseband.

The charge-pump (pin CPOUT) is to be connected to the VCO tuning input (pin VTUNE) through an appropriate loop filter.

### Overcurrent Protection

This DC function allows external circuitry consuming up to 150mA and connected to the pin VOUTANT to sink current from a $V_{CC}$ line (pin VINANT) through overcurrent-protection circuitry.

When no overcurrent is present, a low dropout voltage exists between pins VINANT and VOUTANT. In overcurrent conditions (including short-circuit from VOUTANT to GND), the current is limited to approximately 300mA and bit ACP in the READ byte status goes high.

This circuit also senses if the current drawn at the pin VOUTANT is typically larger than 20mA, in which case the bit AND from the READ byte status goes high (the purpose is to inform the baseband controller if there is any device drawing current from VOUTANT).

## AC ELECTRICAL CHARACTERISTICS

(MAX2140 EV kit, current drawn at VOUTANT, $I_{VOUTANT}$ = 150mA max, $V_{CC}$ = 3.1V to 3.6V, VINANT = 3.1V to 5.3V, $f_{RF}$ = 2320MHz to 2345MHz, $f_{LO}$ = 2076MHz, $T_A$ = -40°C to +85°C. Typical values are at $V_{CC}$ = VINANT = 3.3V, $f_{RF}$ = 2338MHz, $T_A$ = +25°C, unless otherwise noted.) (Note 2)

Interstage (IF) 259MHz SAW filter specification: insertion loss = 19dB max, 9.3MHz to 12MHz from center attenuation = 24dB min, beyond 12MHz from center attenuation = 40dB min.

| PARAMETER | SYMBOL | CONDITIONS | MIN | TYP | MAX | UNITS |
|---|---|---|---|---|---|---|
| **GENERAL RECEIVER** | | | | | | |
| Minimum Input RF Power to Produce 20m$V_{P-P}$ (Differential) at I and Q Baseband Outputs | $P_{MIN}$ | IF AGC is set at maximum gain, bit HPF = 0 (Note 4) | | -91 | -84 | dBm |
| Maximum Input RF Power to Produce 400m$V_{P-P}$ (Differential) at I and Q Baseband Outputs | $P_{MAX}$ | RF AGC threshold: RF_AGC_TRIP = -17dBm; IF AGC is set at minimum gain, bit HPF = 0 | | +3 | | dBm |
| LO to RF Input Leakage | $P_{LK\_H}$ | LO-related spurious > 2GHz | | -66 | | dBm |
| | $P_{LK\_L}$ | LO-related spurious < 2GHz | | -38 | | |
| Noise Figure (Notes 3, 5) | NF | RF AGC is at maximum gain, IF AGC is at reference gain | | 8.5 | 10.4 | dB |
| In-Band Input IP3 (Notes 5, 6) | I_IIP3 | RF AGC is at maximum gain, IF AGC is at reference gain | | -32 | | dBm |
| Out-of-Band Input IP3 (Notes 5, 7) | O_IIP3 | RF AGC is at maximum gain, IF AGC is at reference gain | | -9 | | dBm |
| In-Band Input IP2 (Notes 5, 6) | I_IIP2 | RF AGC is at maximum gain, IF AGC is at reference gain | | +1 | | dBm |
| Out-of-Band Input IP2 (Notes 5, 7) | O_IIP2 | RF AGC is at maximum gain, IF AGC is at reference gain | | +38 | | dBm |
| Opposite Sideband Rejection | OSR | Baseband frequencies = 100kHz (Note 4) | 32 | 39 | | dB |
| Image Rejection | IRej | At $f_{LO}$ - $f_{IF}$ | | 54 | | dB |
| Half IF Rejection | HRej | At $f_{LO}$ + 0.5 x $f_{IF}$ | | 53 | | dB |
| **RF AGC LOOP** | | | | | | |
| LNA Gain Reduction | RFAGC_ Range | (Note 4) | 30 | 42 | | dB |
| Minimum RF AGC Trip Point | RFAGC_mi | Bits RF4/3/2/1/0 = 00000 (BIN) | | -35 | | dBm |
| RF AGC Trip Point | RFAGC_int | Bits RF4/3/2/1/0 = 00010 (BIN) (Note 4) | -37 | -33 | -29 | dBm |
| Maximum RF AGC Trip Point | RFAGC_m | Bits RF4/3/2/1/0 = 10100 (BIN) | | -15 | | dBm |
| **FRONT-END (FE) PROGRAMMABLE GAIN** | | | | | | |
| FE Programmable Gain Range | FE_Rge | (Note 4) | 19 | 22 | 26 | dB |
| FE Programmable Gain Step | FE_Step | | | 2 | | dB |
| **IF FILTER INTERFACE** | | | | | | |
| IF Output Differential Admittance | Yout, IF | Between pins IFOUT+, IFOUT-, $f_{IF}$ = 259MHz and 467MHz | | 1/900 + j0 | | S |
| Input Differential Impedance Presented by the IC to the IF Filter Output | Zin, IF | Between pins IFOUT+, IFOUT-, $f_{IF}$ = 259MHz and 467MHz | | 150 + j0 | | Ω |

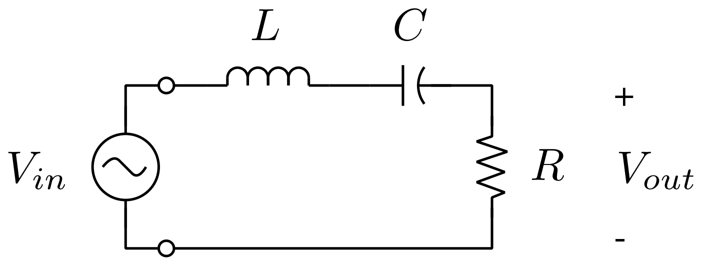

Figure 4.1: Series RLC circuit as a filter.

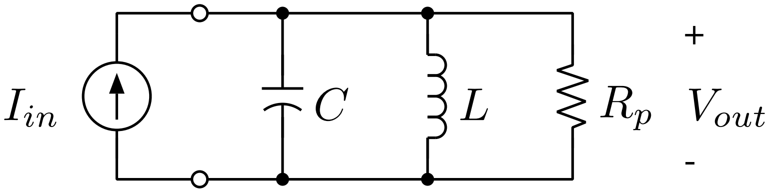

Figure 4.6: Parallel RLC as a filter

$$H(s) = \frac{V_{out}(s)}{V_{in}(s)} = \frac{R}{R + sL \, + \frac{1}{sC}}$$

$$H(j\omega) = \frac{1}{1 + jQ_s\left(\frac{\omega}{\omega_o} - \frac{\omega_o}{\omega}\right)}$$

$$\omega_o = \frac{1}{\sqrt{LC}}$$

$$Q_s = \frac{\omega_o L}{R} = \frac{1}{R}\sqrt{\frac{L}{C}}$$

$$Z(s) \quad = \quad \frac{V_{out}(s)}{I_{in}(s)} \quad = \quad \left[\frac{1}{R_p} + \frac{1}{sL} + sC\right]^{-1}$$

$$Z(j\omega) = \frac{R_p}{1 + jQ_p\left(\frac{\omega}{\omega_o} - \frac{\omega_o}{\omega}\right)}$$

$$\omega_o \quad = \quad \frac{1}{\sqrt{LC}}$$

$$Q_p \quad = \quad \frac{R_p}{\omega_0 L}$$

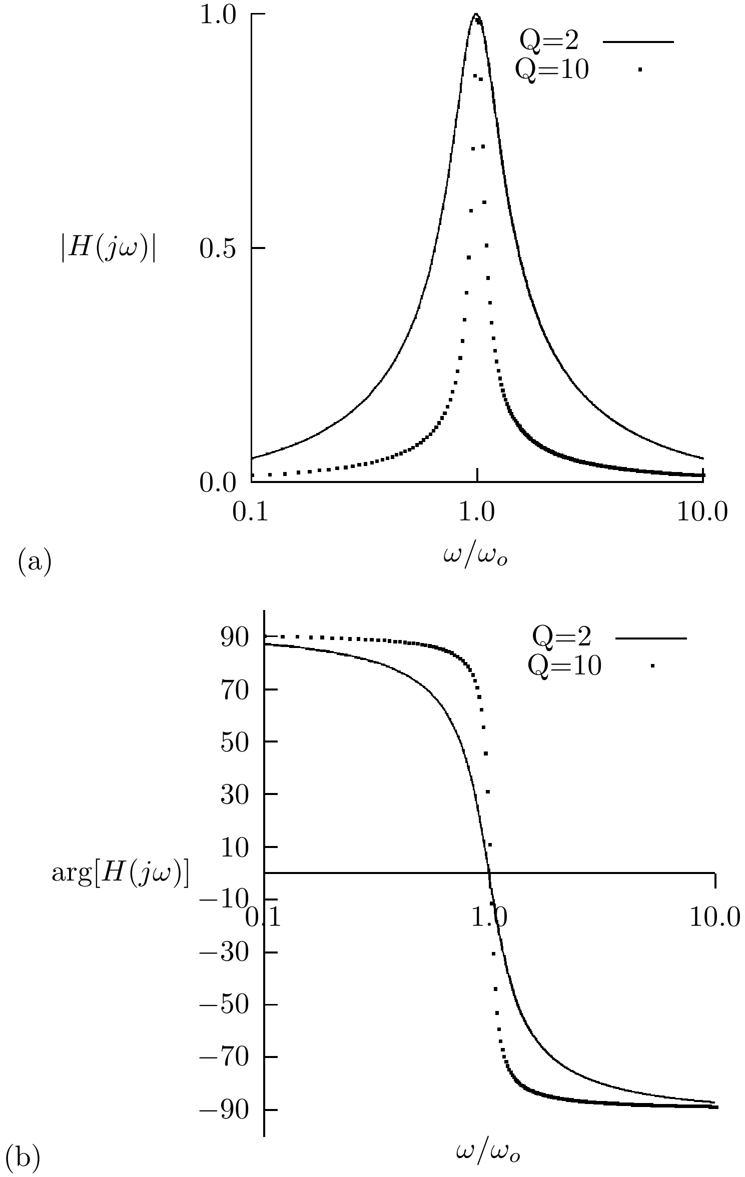

Figure 4.3: (a) Magnitude and (b) phase of the voltage transfer function for Q=2 (solid) and Q=10 (dotted) vs. $\omega/\omega_o$ with a logarithmic frequency axis.

# Quadrature FM Demodulator

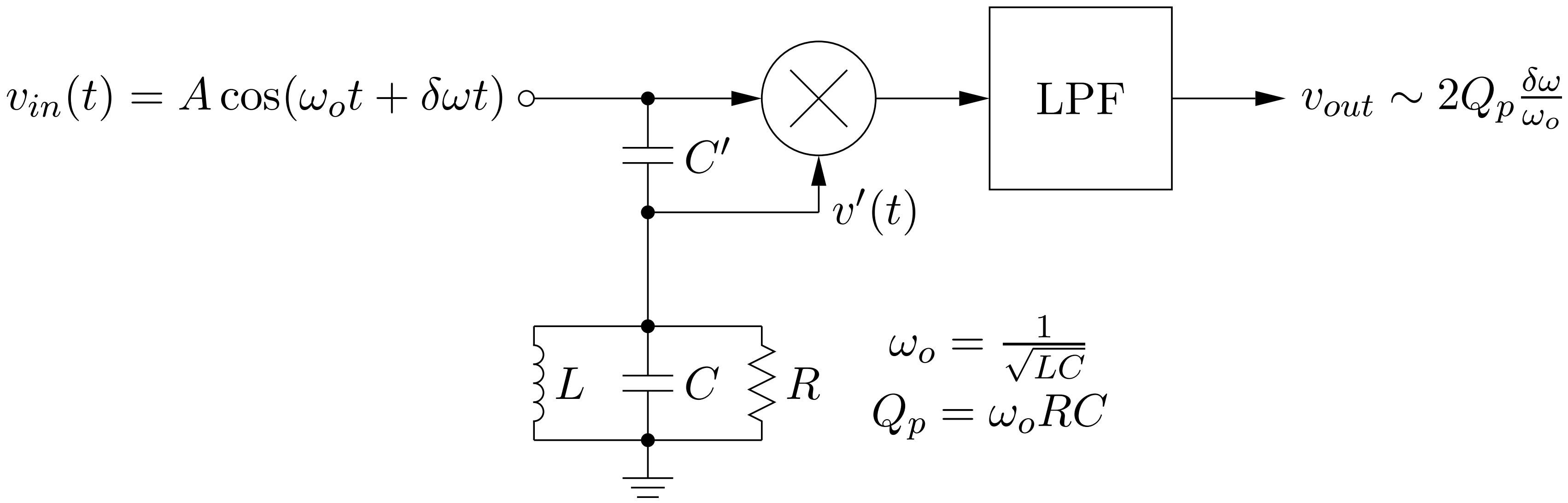
$v_{in}(t) = A\cos(\omega_o t + \delta\omega t)$
$C'$
$v'(t)$
LPF
$v_{out} \sim 2Q_p\frac{\delta\omega}{\omega_o}$
$L$
$C$
$R$
$\omega_o = \frac{1}{\sqrt{LC}}$
$Q_p = \omega_o RC$

- The demodulator operates with the RLC circuit tuned to resonance at the carrier frequency of $v_{in}$, $\omega_o$.

- The voltage divider consisting of $C'$ and the resonant RLC circuit converts small frequency deviations in $v_{in}$ to phase shifts of $v'$ relative to $v_{in}$.

- For small frequency deviations, $\delta\omega$, $v'$ is phase shifted by $\pi/2 - 2Q_p\frac{\delta\omega}{\omega_o}$.

- The multiplier and LPF act as a phase comparator, producing output proportional to $2Q_p\frac{\delta\omega}{\omega_o}$ for small frequency deviations, $\delta\omega$.

# Quadrature FM Demodulator

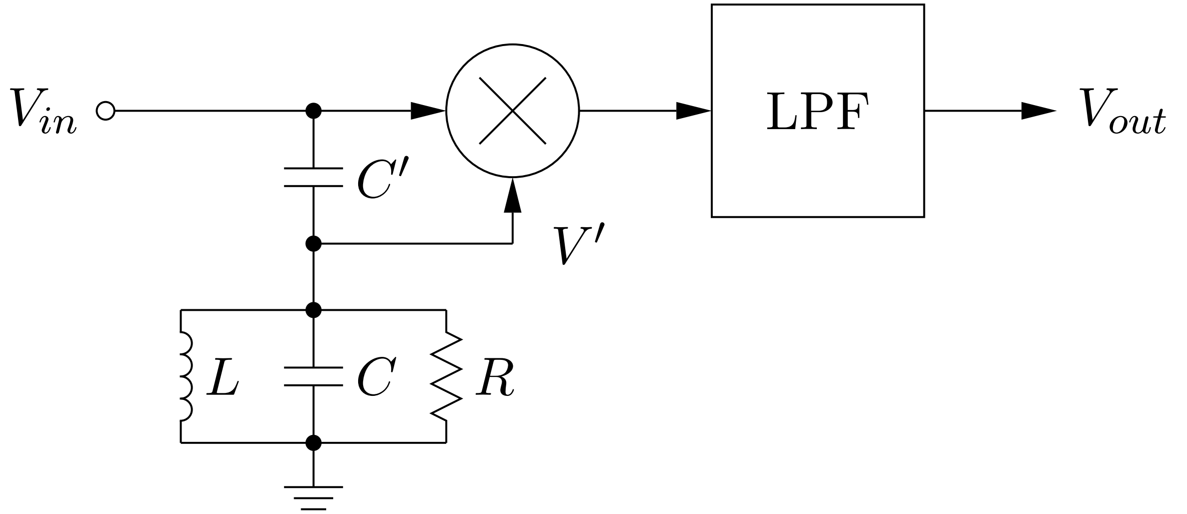

Using upper-case symbols $V_{in}$, $V'$ for phasors:

$$V' = \frac{Z_p}{Z_p + \frac{1}{j\omega C'}} V_{in}; \qquad Z_p = j\omega L || \frac{1}{j\omega C} || R$$

If $C'$ is small, such that $\frac{1}{\omega C'} \gg |Z_p|$, then $V' \simeq j\omega C' Z_p V_{in}$.

Let $\theta'$, $\theta_p$, and $\theta_{in}$ represent the phase angles of $V'$, $Z_p$, and $V_{in}$, respectively. Then:

$$\theta' = \frac{\pi}{2} + \theta_p + \theta_{in}$$

Phase difference between $V_{in}$ and $V'$ is $\frac{\pi}{2} + \theta_p$ where $\theta_p$ is the phase angle of $Z_p$.

Impedance of a parallel RLC circuit is:

$$Z_p(\omega) = \frac{R}{1+jQ_p(\frac{\omega}{\omega_o}-\frac{\omega_o}{\omega})} = |Z_p(\omega)|e^{j\theta_p(\omega)}$$

$$\theta_p(\omega) = -\tan^{-1} Q_p(\frac{\omega}{\omega_o} - \frac{\omega_o}{\omega})$$

Let $\omega = \omega_o + \delta\omega$. If $\delta\omega \ll \omega_o$, then

$$\theta_p(\omega) \simeq -2Q_p \frac{\delta\omega}{\omega_o}$$

For small frequency deviations away from resonance the phase of $Z_p$ is proportional to the frequency deviation, $\delta\omega$.

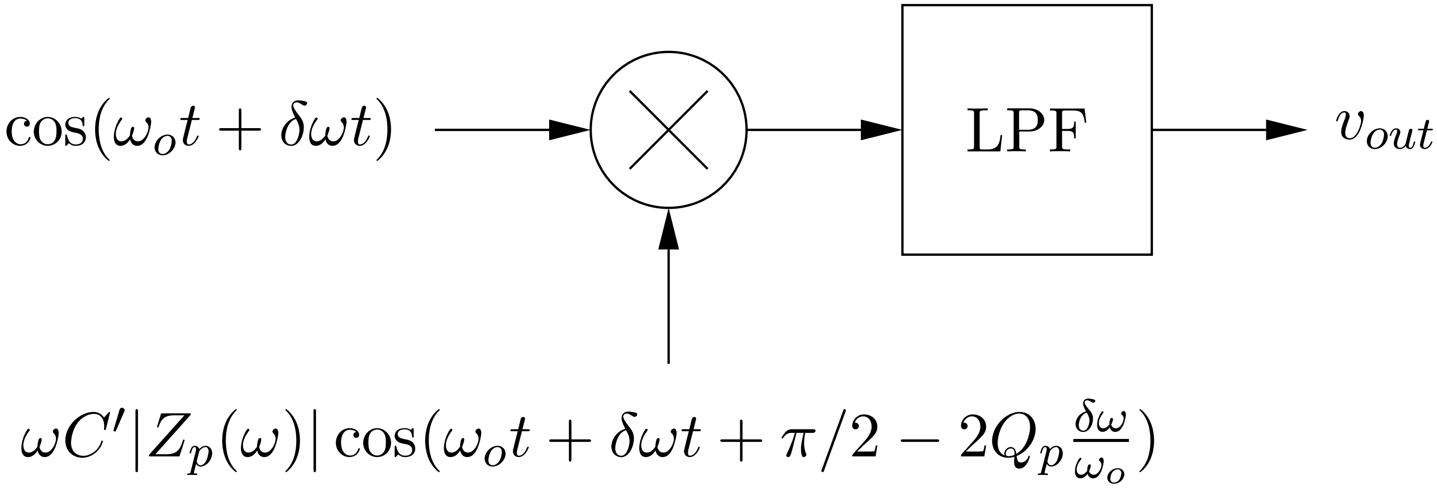
$\cos(\omega_o t + \delta\omega t)$
LPF
$v_{out}$
$\omega C'|Z_p(\omega)|\cos(\omega_o t + \delta\omega t + \pi/2 - 2Q_p\frac{\delta\omega}{\omega_o})$

The multiplier is usually configured such that the lower input is "saturated", in which case the output does not depend on the magnitude of the lower input.

The lowpass filter rejects the double-frequency term in the mixer output, leaving the cosine of the phase difference. The output is:

$$v_{out} \sim \cos(\tfrac{\pi}{2} - 2Q_p\tfrac{\delta\omega}{\omega_o}) = \sin(2Q_p\tfrac{\delta\omega}{\omega_o})$$

If $2Q_p\frac{\delta\omega}{\omega_o} \ll 1$, then $v_{out} \sim 2Q_p\frac{\delta\omega}{\omega_o}$.

Summary:

- For small frequency deviations $(\delta\omega)$ away from $\omega_o$, $v_{out} \sim 2Q_p \frac{\delta\omega}{\omega_o}$.

- For large frequency deviations, the output is a nonlinear function of deviation. See section 4.5 of the course notes for details.

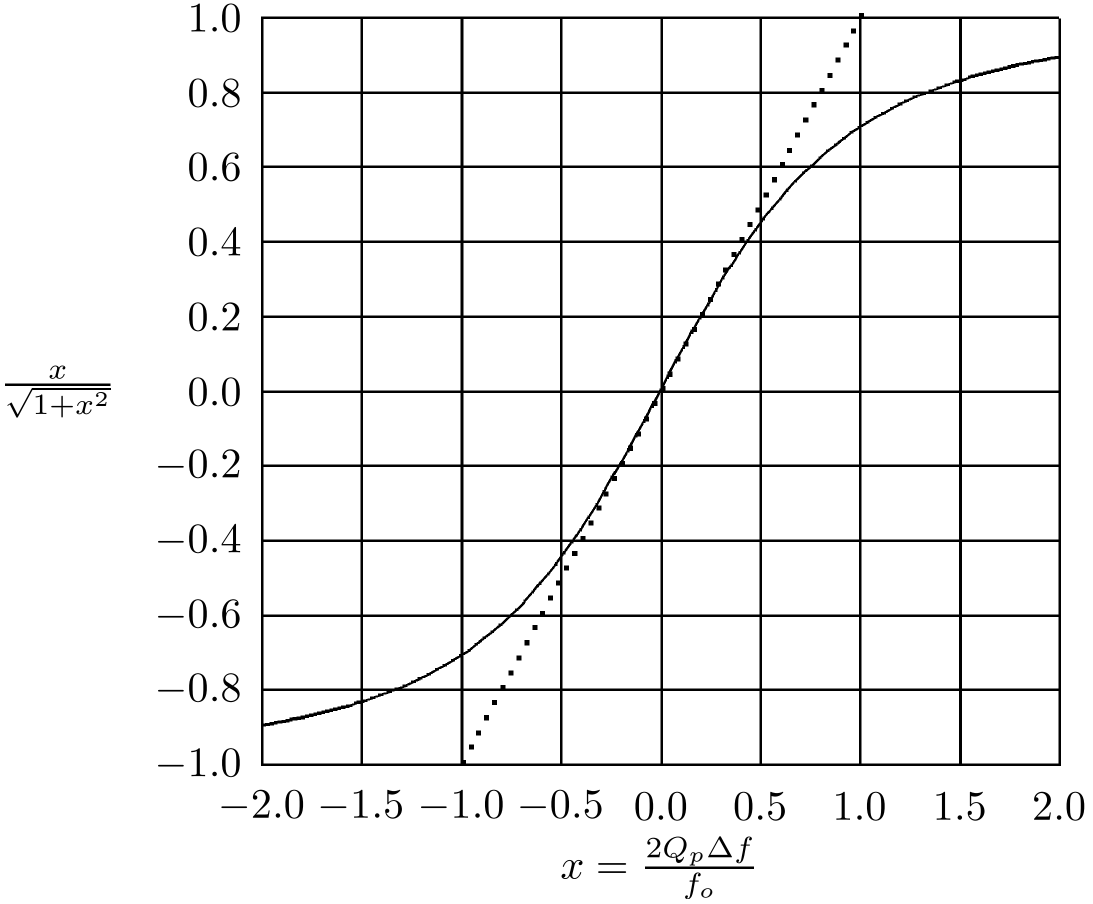

Figure 4.23: Output voltage verses normalized frequency deviation for a quadrature demodulator employing a saturated input for $v'$. The dotted line shows an ideal linear response with the same slope as the actual response at $x = 0$.

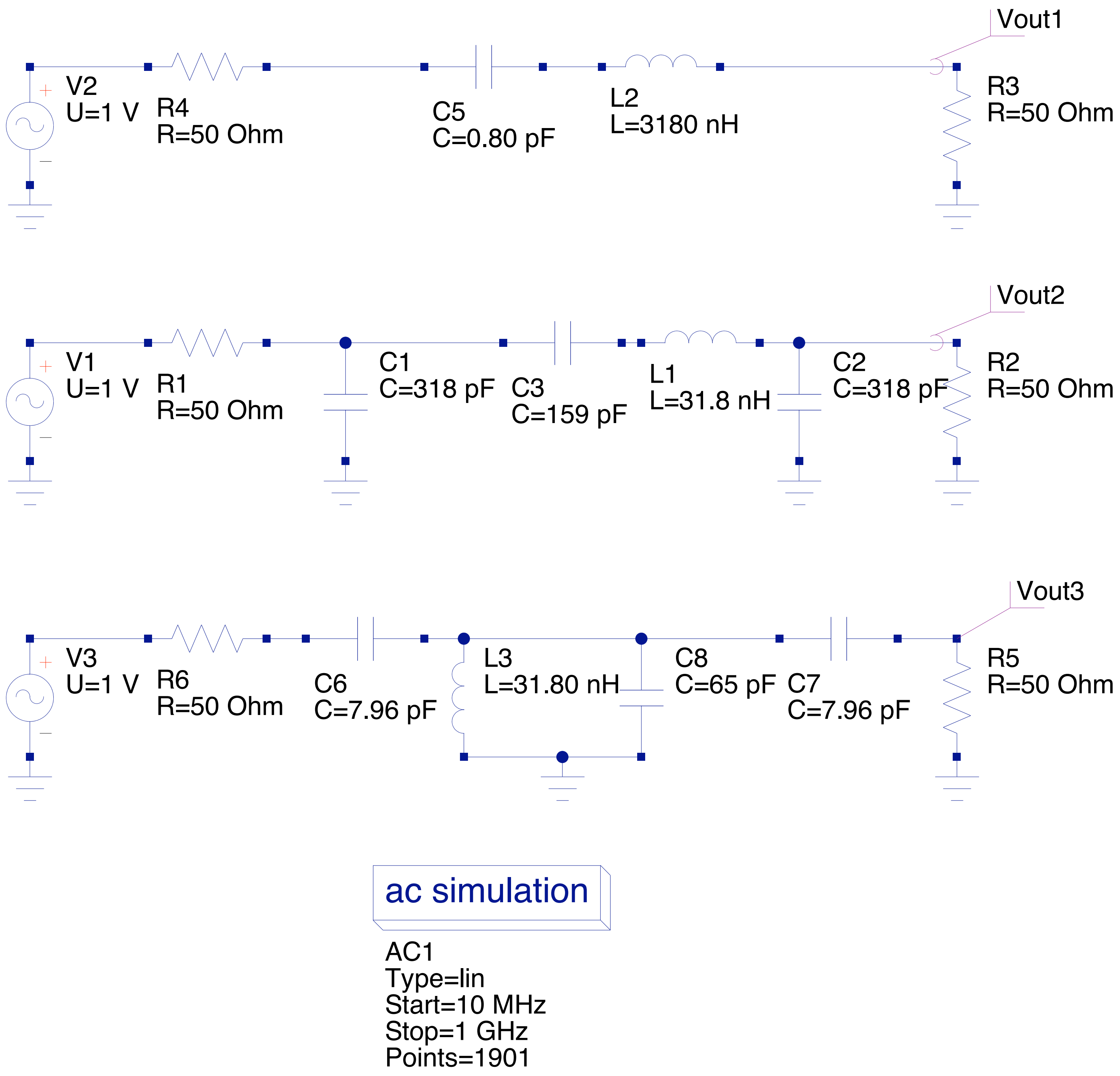
Vout1
V2
U=1 V
R4
R=50 Ohm
C5
C=0.80 pF
L2
L=3180 nH
R3
R=50 Ohm
Vout2
V1
U=1 V
R1
R=50 Ohm
C1
C=318 pF
C3
C=159 pF
L1
L=31.8 nH
C2
C=318 pF
R2
R=50 Ohm
Vout3
V3
U=1 V
R6
R=50 Ohm
C6
C=7.96 pF
L3
L=31.80 nH
C8
C=65 pF
C7
C=7.96 pF
R5
R=50 Ohm
ac simulation
AC1
Type=lin
Start=10 MHz
Stop=1 GHz
Points=1901

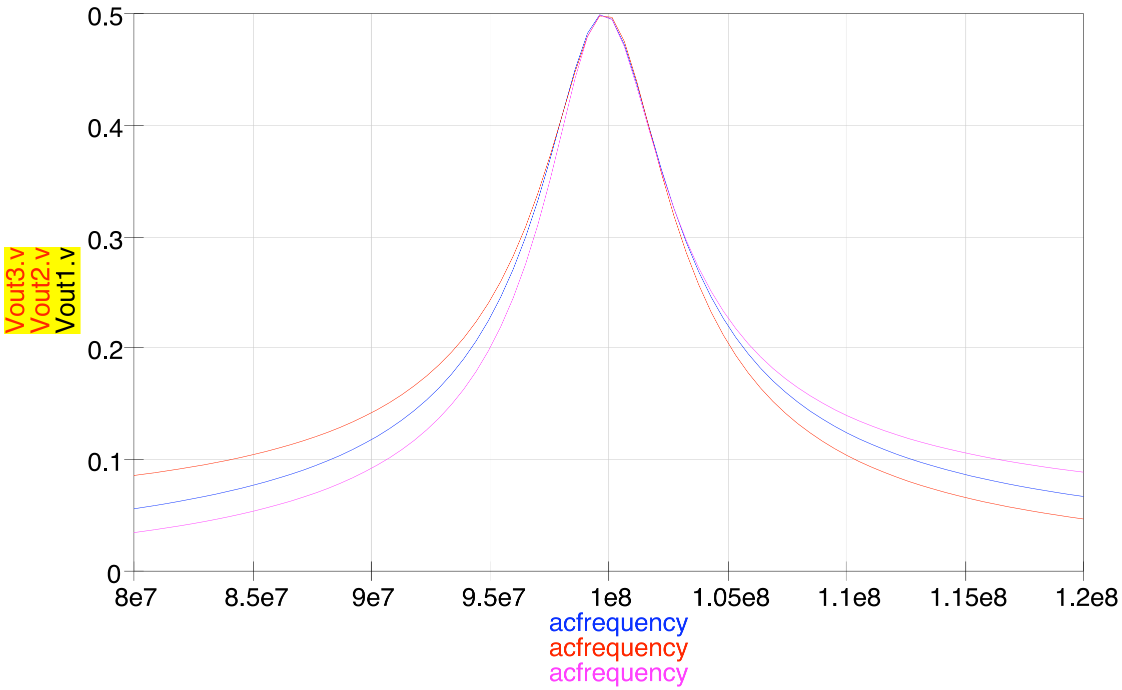
Vout3.v
Vout2.v
Vout1.v
0.5
0.4
0.3
0.2
0.1
0
8e7
8.5e7
9e7
9.5e7
1e8
1.05e8
1.1e8
1.15e8
1.2e8
acfrequency
acfrequency
acfrequency

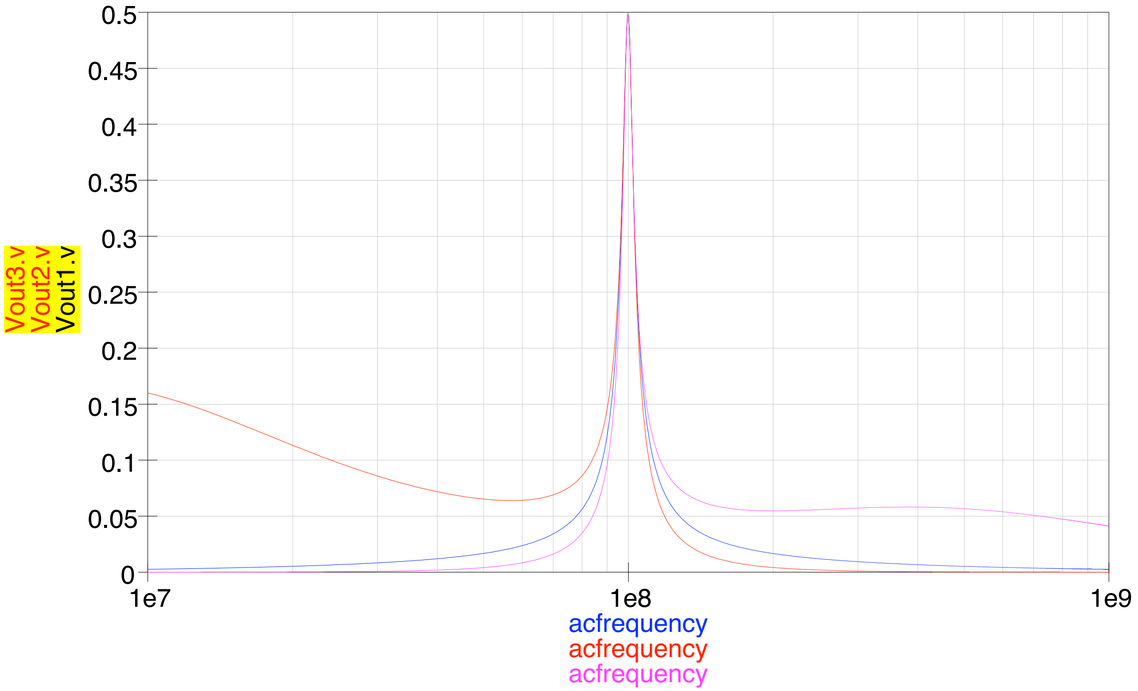
Vout3.v
Vout2.v
Vout1.v
0.5
0.45
0.4
0.35
0.3
0.25
0.2
0.15
0.1
0.05
0
1e7
1e8
1e9
acfrequency
acfrequency
acfrequency

# Optimum Frequencies for Amidon Toroidal Inductor Cores

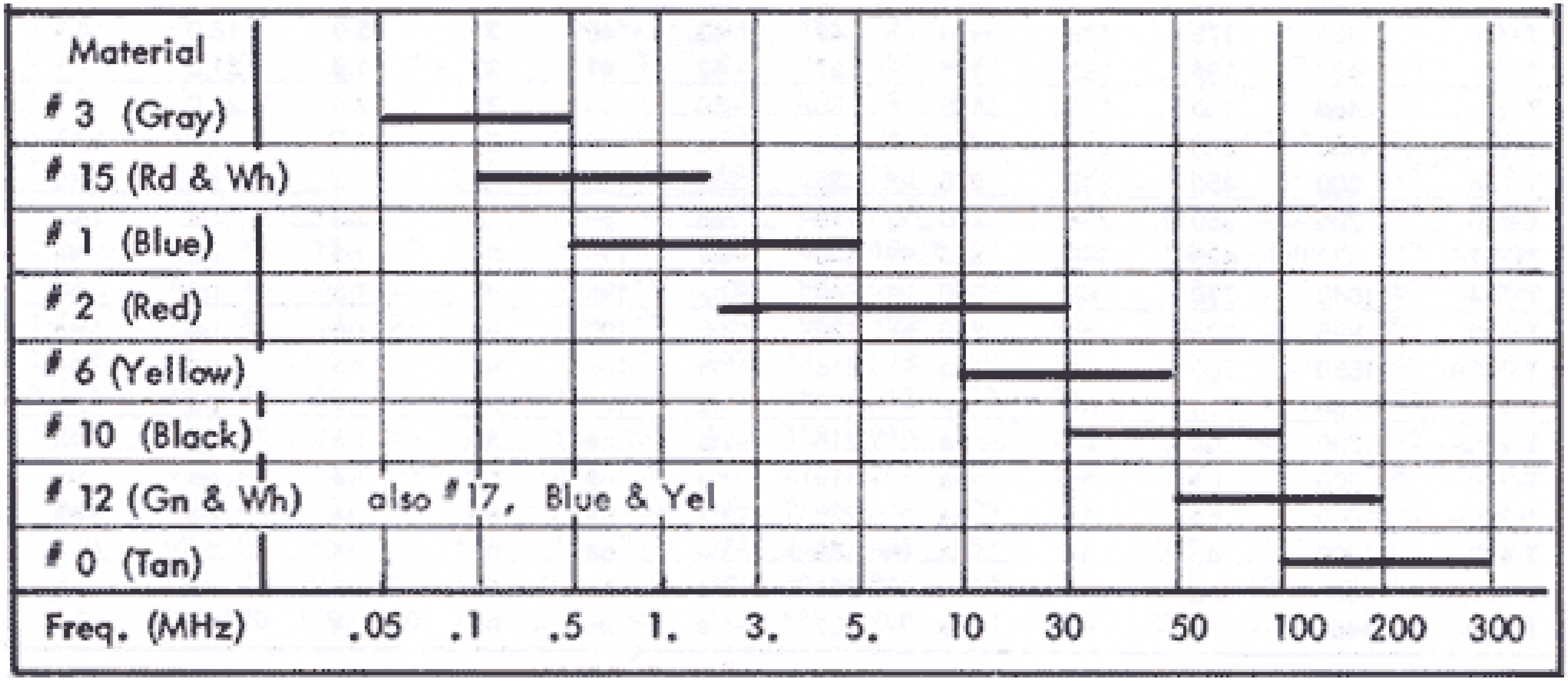

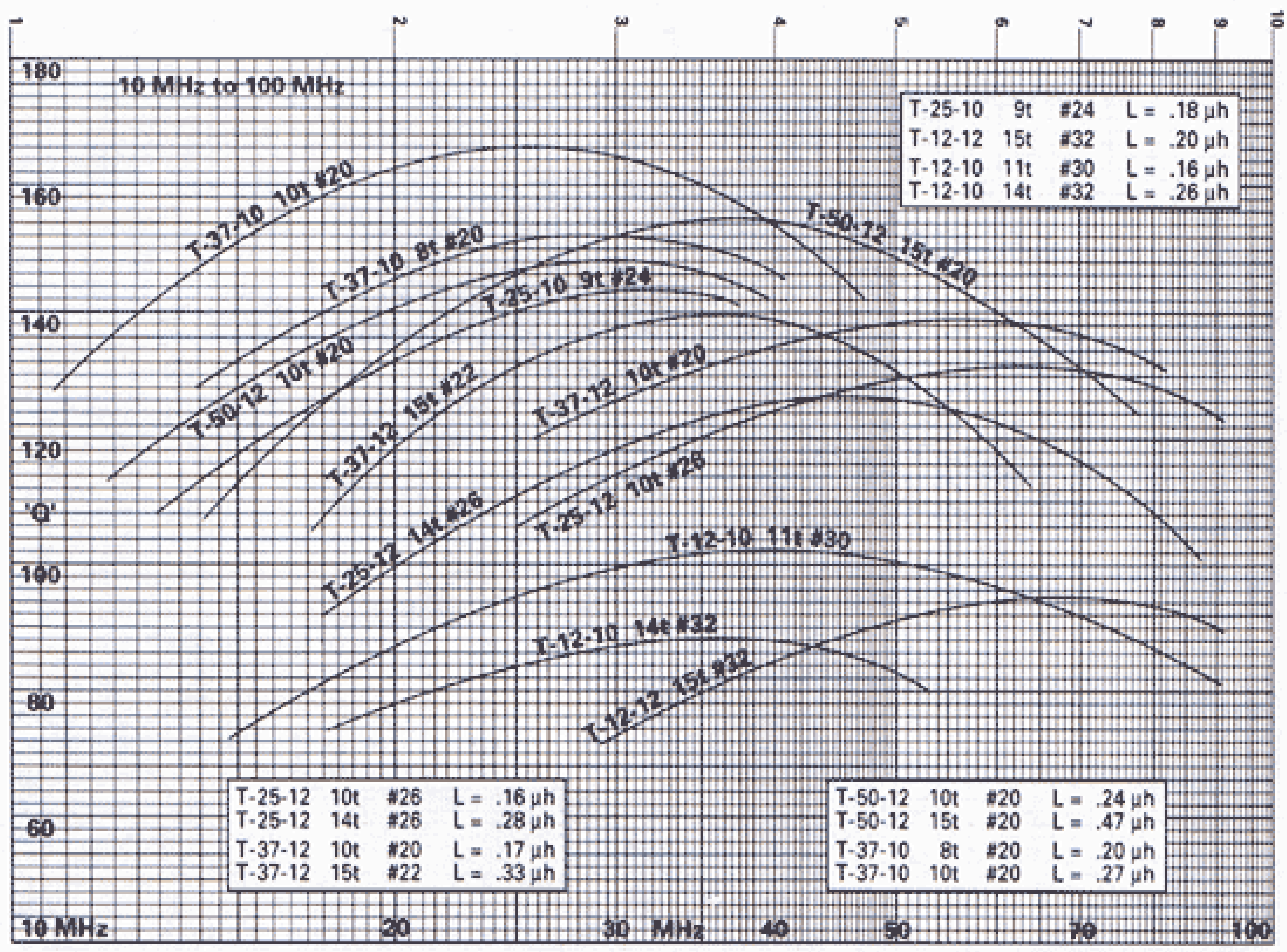

1
2
3
4
5
6
7
8
9
10
180
160
140
120
'Q'
100
80
60
10 MHz to 100 MHz
10 MHz
20
30 MHz
40
50
70
100
T-37-10 10t #20
T-37-10 8t #20
T-25-10 9t #24
T-50-12 15t #20
T-50-12 10t #20
T-37-12 15t #22
T-37-12 10t #20
T-25-12 14t #26
T-25-12 10t #28
T-12-10 11t #30
T-12-10 14t #32
T-12-12 15t #32
T-25-10 9t #24 L = .18 µh
T-12-12 15t #32 L = .20 µh
T-12-10 11t #30 L = .16 µh
T-12-10 14t #32 L = .26 µh
T-25-12 10t #26 L = .16 µh
T-25-12 14t #26 L = .28 µh
T-37-12 10t #20 L = .17 µh
T-37-12 15t #22 L = .33 µh
T-50-12 10t #20 L = .24 µh
T-50-12 15t #20 L = .47 µh
T-37-10 8t #20 L = .20 µh
T-37-10 10t #20 L = .27 µh

# Q versus Frequency
# 0805CS Surface Mount Inductors

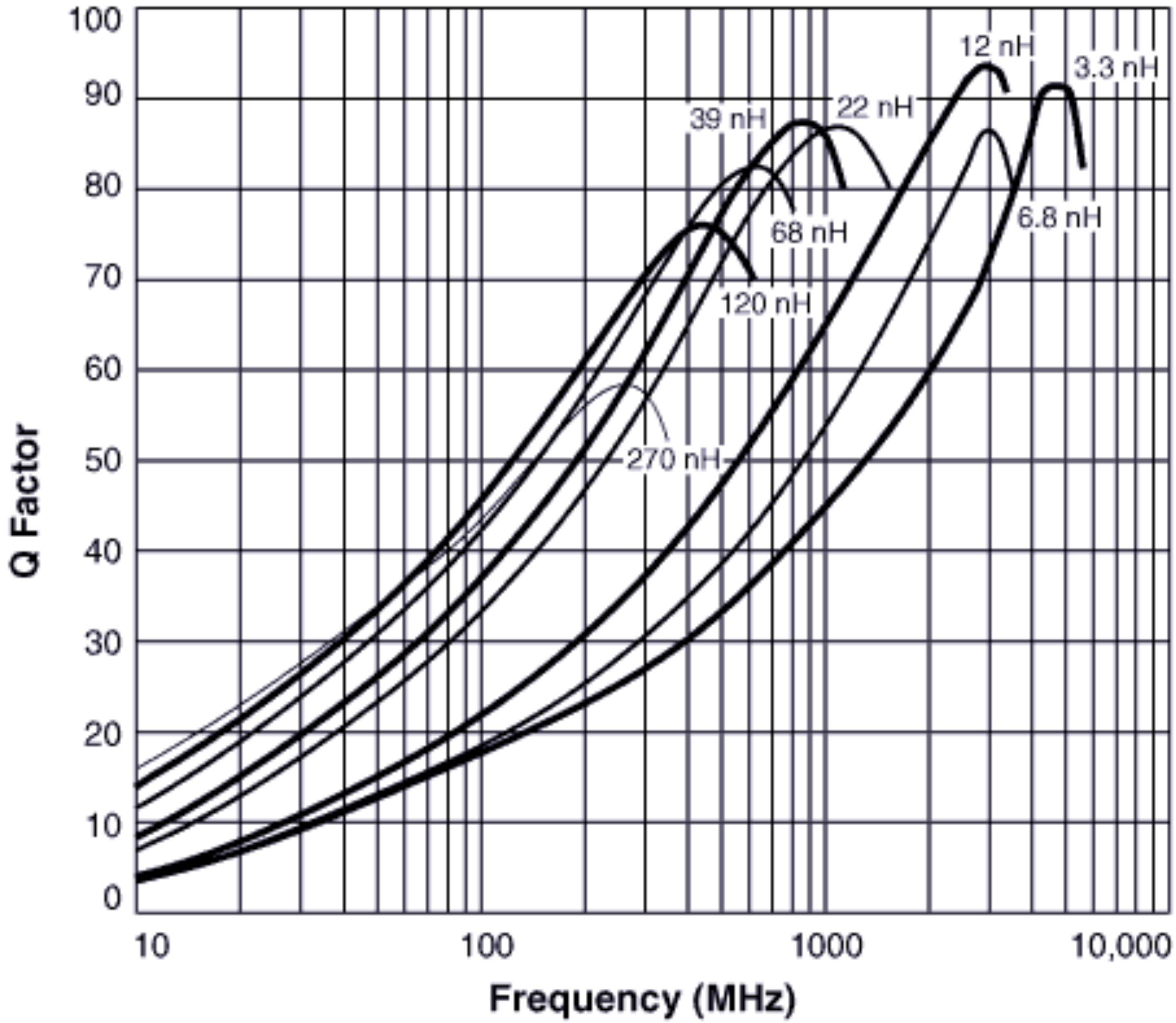

Copyright © 2000, Coilcraft, Inc.
Updated: August 14, 2003

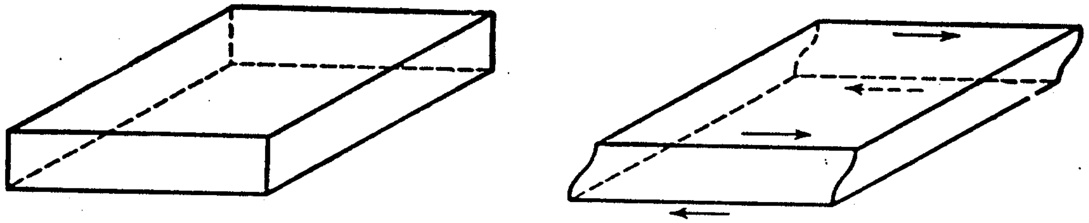

(a) Undistorted plate

(b) Distortion for fundamental mode

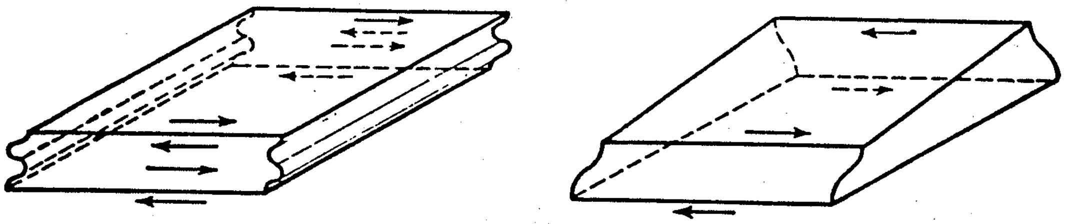

(c) Distortion for third harmonic mode

(d) Distortion for another type of higher mode

FIG. 8-10.—Motions associated with fundamental and higher modes of vibrations of the high-frequency shear type. For the sake of clarity, the extent of motion is great exaggerated. The arrows indicate the direction of motion.

## Crystal ‘cut’

*Figure 1 shows many of the ‘cut’ orientations, which may be made from a single Z plate quartz crystal, related to the X, Y and Z axis.*

Fig.3 Cut orientations from a single Z plate crystal

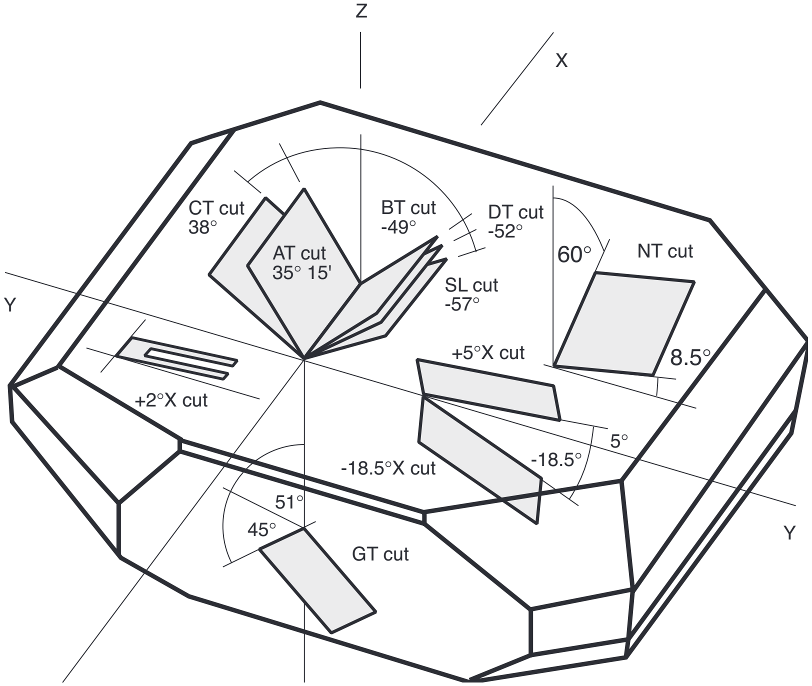
Z
X
Y
Y
CT cut
38°
AT cut
35° 15'
BT cut
-49°
DT cut
-52°
SL cut
-57°
60°
NT cut
8.5°
+5°X cut
+2°X cut
5°
-18.5°
-18.5°X cut
51°
45°
GT cut

*Fig. 1 Cut orientations from a Z plate quartz crystal*

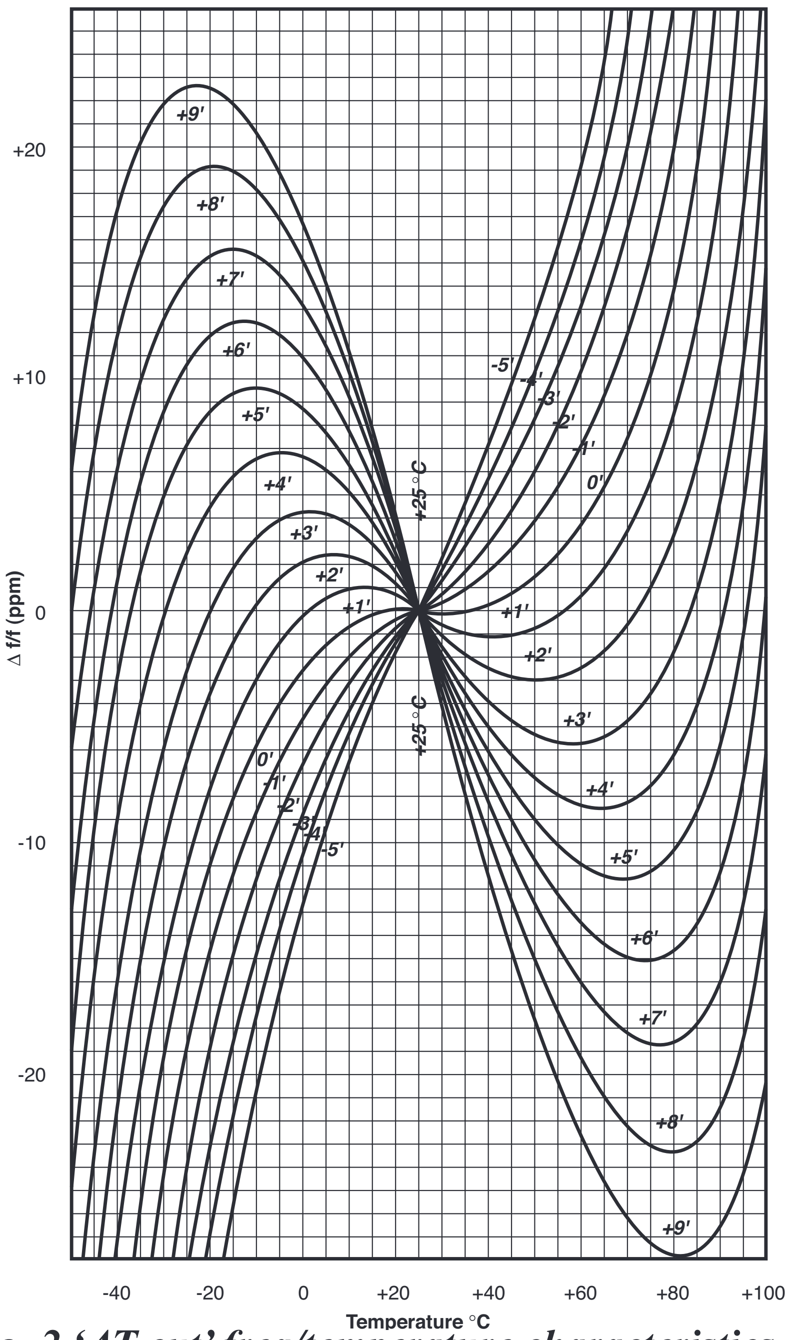

Fig. 2 'AT cut' freq/temperature characteristics

## ■ Features

- ● RoHS compliant and lead-free product
- ● 1.2 mm height. Ideal for space constraint applications such as PCMCIA
- ● Ceramic package with seam sealed kovar lid.
- ● The whole package is grounded via the topmetal lid and the two bottom pads .

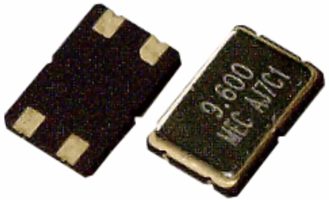

RoHS Compliance

### General Specifications

| Item / Type | **MQ** series ( 7.0 * 5.0 * 1.2 mm ) |
|---|---|
| Frequency Range & Crystal Cut | 6.000 ~ 50.000 MHz , AT-cut , Fundamental Mode ( see Table 1 )<br>30.000 ~ 125.000 MHz , AT-cut , 3rd overtone ( see Table 1 ) |
| Load Capacitance | Series Resonance or Parallel ( 8 to 32 pF typical ) |
| Drive Level | 10μ W ( 100μ W max. ) |
| Frequency Tolerance | ± 5 ppm , ± 10 ppm , ± 20 ppm or ± 30 ppm at 25°C |
| Frequency Stability | See Table 2 |
| Aging | △F / F : ±3 ppm / year ( max. ) |
| Storage Temperature Range | - 50°C to 105°C |

Table 1
Series Resistance ( max. )

| Freq.(MHz) | Osc. Mode | E.S.R. | Freq.(MHz) | Osc. Mode | E.S.R. |
|---|---|---|---|---|---|
| 6.0 ~ 8.0 | AT , Fund. | 80 Ω | 30.0~ 40.0 | AT , 3rd | 100 Ω |
| 8.0 ~ 11.0 | AT , Fund. | 60 Ω | 40.1~ 50.0 | AT , 3rd | 80 Ω |
| 11.1~ 14.0 | AT , Fund. | 50 Ω | 50.1~125.0 | AT , 3rd | 90 Ω |
| 14.1~ 50.0 | AT , Fund. | 40 Ω | | | |

Table 2
Frequency stability Vs Operating temperature range

| Temp. (ºC) \ ppm | | ± 5 | ± 10 | ± 15 | ± 20 | ± 25 | ± 30 |
|---|---|---|---|---|---|---|---|
| X | -10 to 60°C | ○ | ○ | ○ | ○ | ○ | ○ |
| Y | -20 to 70°C | ▲ | ○ | ○ | ○ | ○ | ○ |
| I | -40 to 85°C | | | ○ | ○ | ○ | ○ |

○ : available ; ▲: contact Mercury

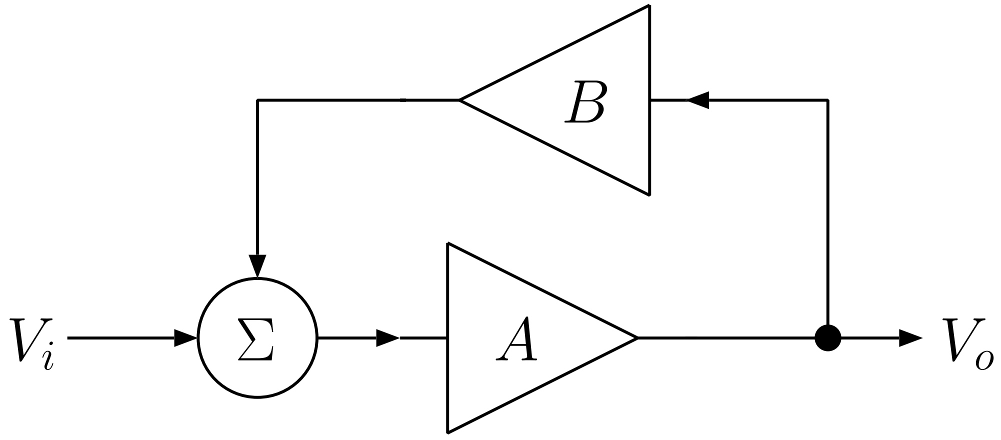

The voltage transfer function for this system is

$$\frac{V_o}{V_i} = \frac{A(s)}{1 - A(s)B(s)}$$

where the quantity $A(s)B(s)$ is called the open loop gain of the system. Define

$$A_{lo} = A(s)B(s)$$

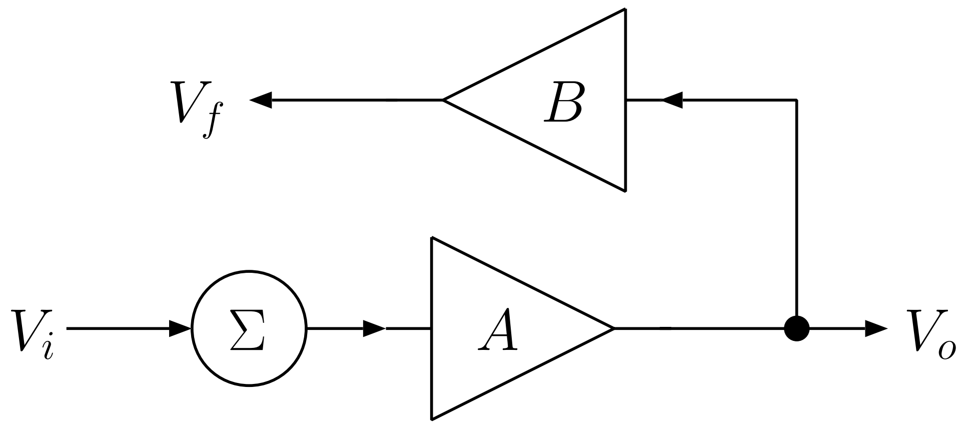

Loop gain is calculated by opening the feedback loop and taking the output at the point where the loop was opened, i.e.

$$A_{lo} = \frac{V_f}{V_i}.$$

Roots of the equation

$$1 - A_{lo}(s) = 0$$

are the pole locations.

When poles of the transfer function are on the $j\omega$ axis the system supports steady-state oscillation (neither decaying or growing).

A pole is on the $j\omega$ axis if the following equation is satisfied for some real value of frequency, denoted by $\omega_o$:

$$A_{lo}(j\omega_o) = 1.$$

If $A_{lo}(j\omega_o) = 1$ can be satisfied for some real $\omega_o$, then the system supports steady-state oscillation at frequency $\omega_o$.

$A_{lo}$ is a complex quantity, so two conditions must be satisfied for steady-state oscillation to occur. They are called the *Barkhausen Criteria* for oscillation:

$$\arg[A_{lo}(\omega_o)] = 2n\pi, \text{for } n \text{ an integer}$$

$$|A_{lo}(\omega_o)| = 1$$

Practical oscillator circuits are designed so that poles are actually in the RHP. The circuit is then unstable, and any small perturbation will result in an oscillation that grows exponentially, i.e. like $e^{\alpha t}$, $\alpha > 0$.

Thermal noise, or the transient caused by turning on the supply voltage provides the initial excitation that excites the growing oscillation.

When the oscillation amplitude is sufficiently large, nonlinear saturation of the amplifier (often a single transistor) effectively reduces the loop gain, moving the pole onto the $j\omega$ axis, and oscillation is limited at a finite value.

Initial oscillation will start and grow if

$$\arg[A_{lo}(\omega_o)] = 2n\pi, \text{for } n \text{ an integer}$$

and

$$|A_{lo}(\omega_o)| > 1$$

Summary of procedure for loop gain design of oscillator circuits.

1. Identify feedback loop. Break the loop and terminate with the impedance that the feedback output normally sees when the loop is closed. Solve for loop gain function, $A_{lo}(s)$.

2. Solve $\arg[A_{lo}(\omega)] = 2n\pi$ to determine the potential frequency (or frequencies) of oscillation, $\omega_o$. This will yield an expression for $\omega_o$ in terms of circuit parameters. Choose the parameters so that $\omega_o$ is the desired value.

3. Set $|A_{lo}(\omega_o)| = 1$. This will yield an expression for the minimum gain required for the amplifier. For example, when the amplifier is a single transistor, this will yield an expression for $g_{m,ss}$, which is the transconductance required for steady-state oscillation. Bias the transistor so that the actual transconductance is larger than $g_{m,ss}$ to ensure $|A_{lo}(\omega_o)| > 1$.

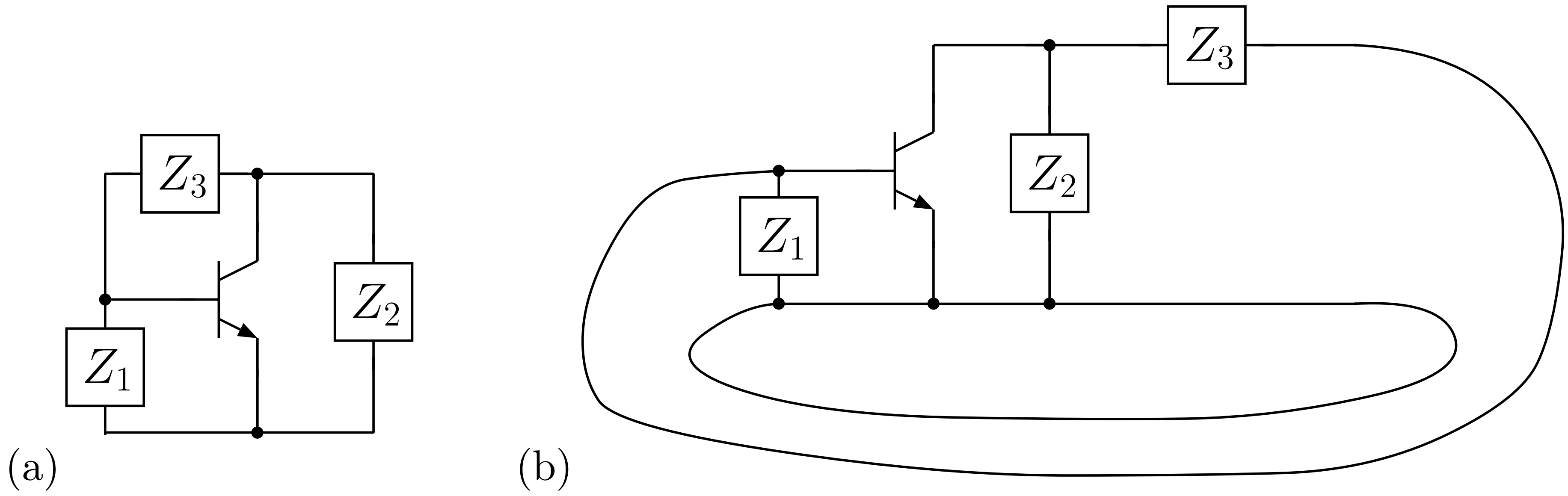
$Z_3$
$Z_1$
$Z_2$
(a)
$Z_3$
$Z_1$
$Z_2$
(b)

Figure 5.3: (a) Topology of one class of oscillator circuits. (b) Same as (a), redrawn to show the feedback path from output to input through $Z_3$.

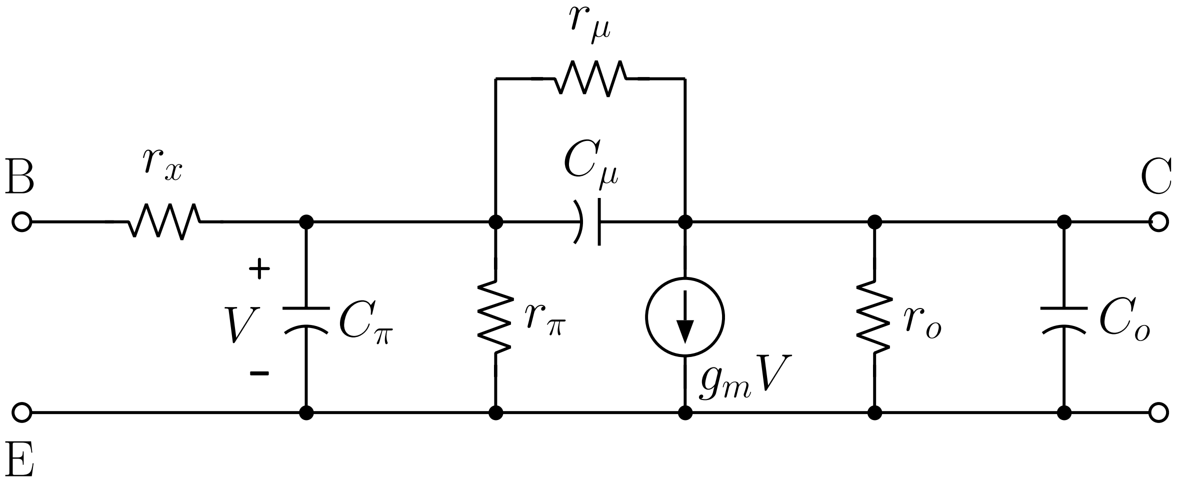
$r_\mu$
B
$r_x$
$C_\mu$
C
+
$V$
–
$C_\pi$
$r_\pi$
$g_mV$
$r_o$
$C_o$
E

Figure A.2: Hybrid-pi small-signal model for BJT

$$r_\pi \simeq \frac{.025\beta}{I_{CQ}} \qquad g_m \simeq 40I_{CQ}$$

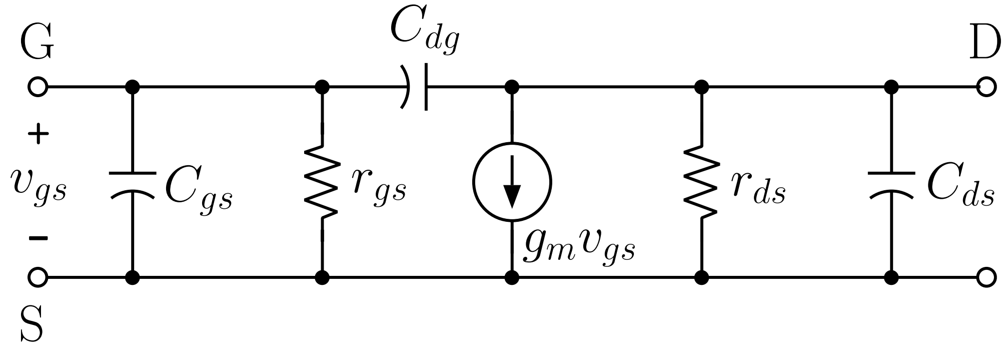
G
$C_{dg}$
D
+
$v_{gs}$
–
$C_{gs}$
$r_{gs}$
$g_m v_{gs}$
$r_{ds}$
$C_{ds}$
S

Figure A.3: Hybrid-pi equivalent circuit for the FET

$$g_m = \frac{2}{|V_P|}\sqrt{I_{DSS}I_D}.$$

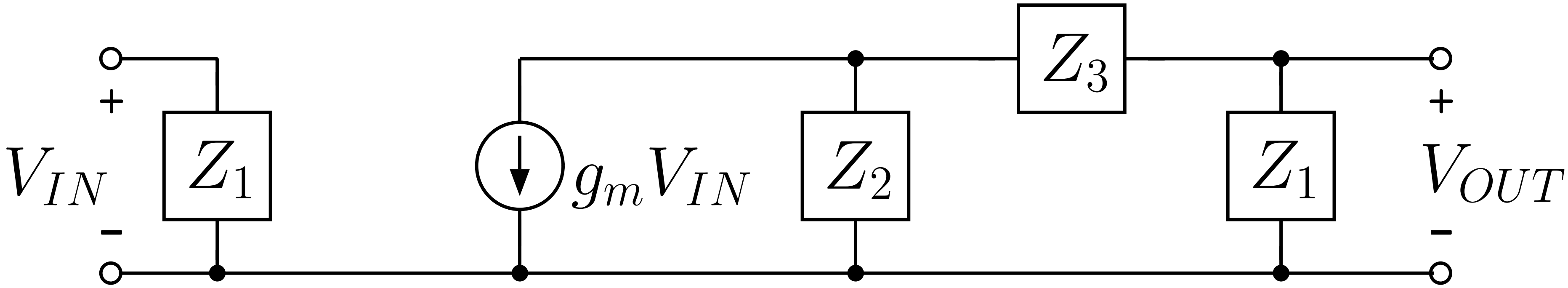
$V_{IN}$
+
−
$Z_1$
$g_m V_{IN}$
$Z_2$
$Z_3$
$Z_1$
$V_{OUT}$
+
−

Figure 5.5: Feedback loop terminated with $Z_1$

$$A_{lo} = \frac{V_{OUT}}{V_{IN}} = -g_m Z_2 || (Z_1 + Z_3) \frac{Z_1}{Z_1+Z_3} = \frac{-g_m Z_1 Z_2}{Z_1+Z_2+Z_3}$$

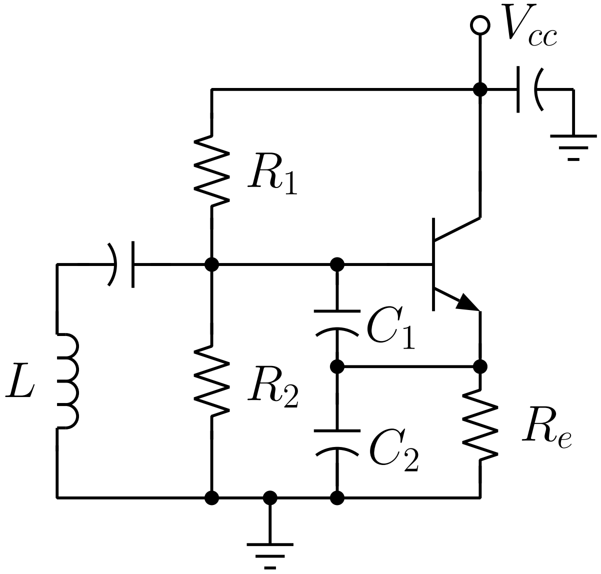
$V_{cc}$
$R_1$
$C_1$
$L$
$R_2$
$R_e$
$C_2$

(a)

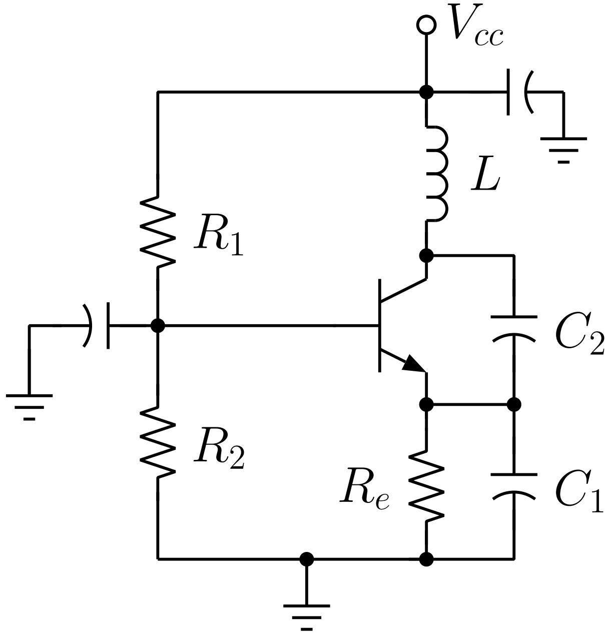
$V_{cc}$
$L$
$R_1$
$C_2$
$R_2$
$R_e$
$C_1$

(b)

# Double-balanced mixer and oscillator

# SA612A

## DESCRIPTION

The SA612A is a low-power VHF monolithic double-balanced mixer with on-board oscillator and voltage regulator. It is intended for low cost, low power communication systems with signal frequencies to 500MHz and local oscillator frequencies as high as 200MHz. The mixer is a "Gilbert cell" multiplier configuration which provides gain of 14dB or more at 45MHz.

The oscillator can be configured for a crystal, a tuned tank operation, or as a buffer for an external L.O. Noise figure at 45MHz is typically below 6dB and makes the device well suited for high performance cordless phone/cellular radio. The low power consumption makes the SA612A excellent for battery operated equipment. Networking and other communications products can benefit from very low radiated energy levels within systems. The SA612A is available in an 8-lead dual in-line plastic package and an 8-lead SO (surface mounted miniature package).

## FEATURES

- Low current consumption
- Low cost
- Operation to 500MHz
- Low radiated energy
- Low external parts count; suitable for crystal/ceramic filter
- Excellent sensitivity, gain, and noise figure

## PIN CONFIGURATION

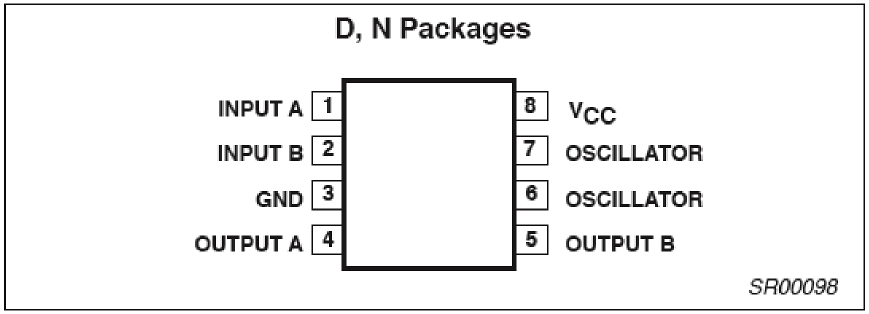

Figure 1. Pin Configuration

## APPLICATIONS

- Cordless telephone
- Portable radio
- VHF transceivers
- RF data links
- Sonabuoys
- Communications receivers
- Broadband LANs
- HF and VHF frequency conversion
- Cellular radio mixer/oscillator

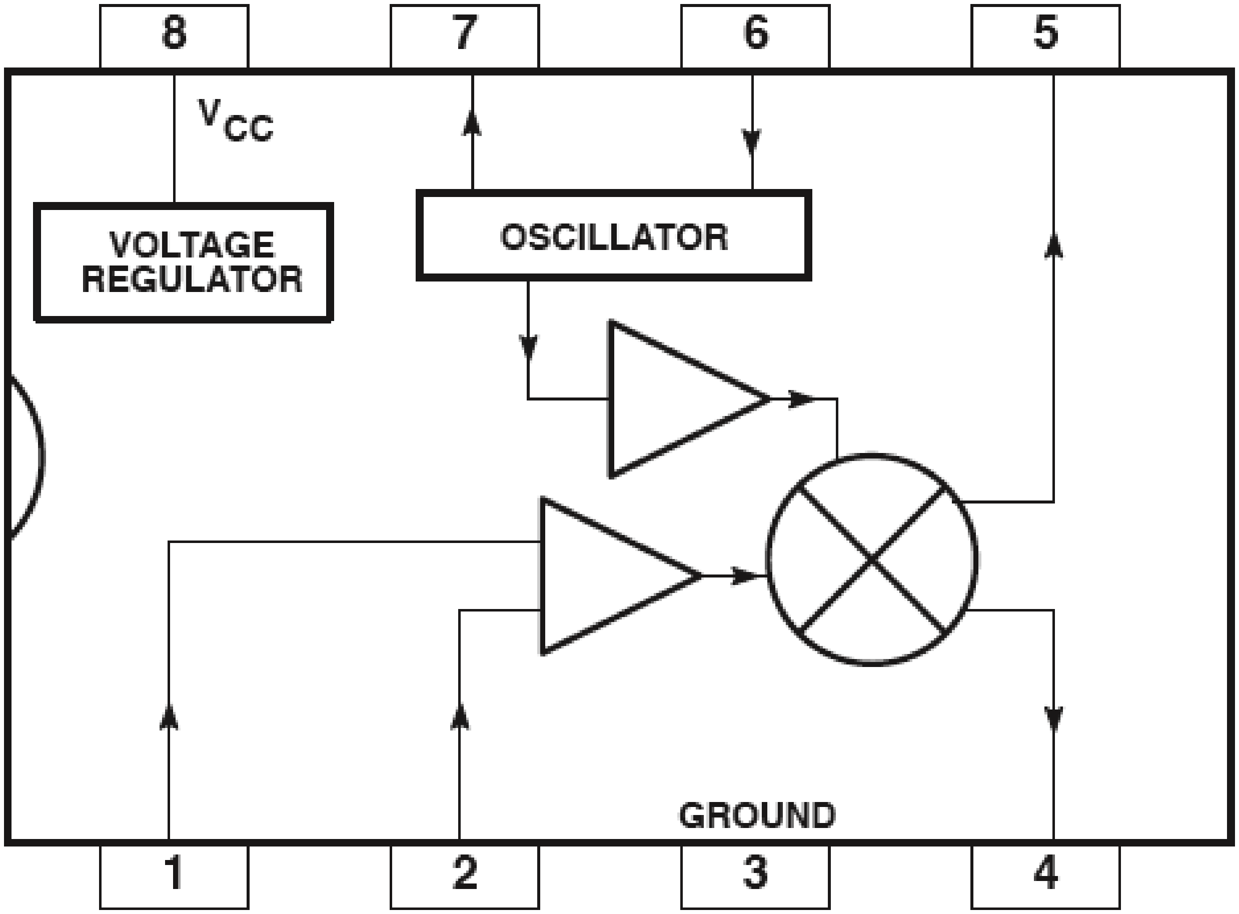
8
7
6
5
VCC
VOLTAGE REGULATOR
OSCILLATOR
GROUND
1
2
3
4

Figure 2. Block Diagram

## TEST CONFIGURATION

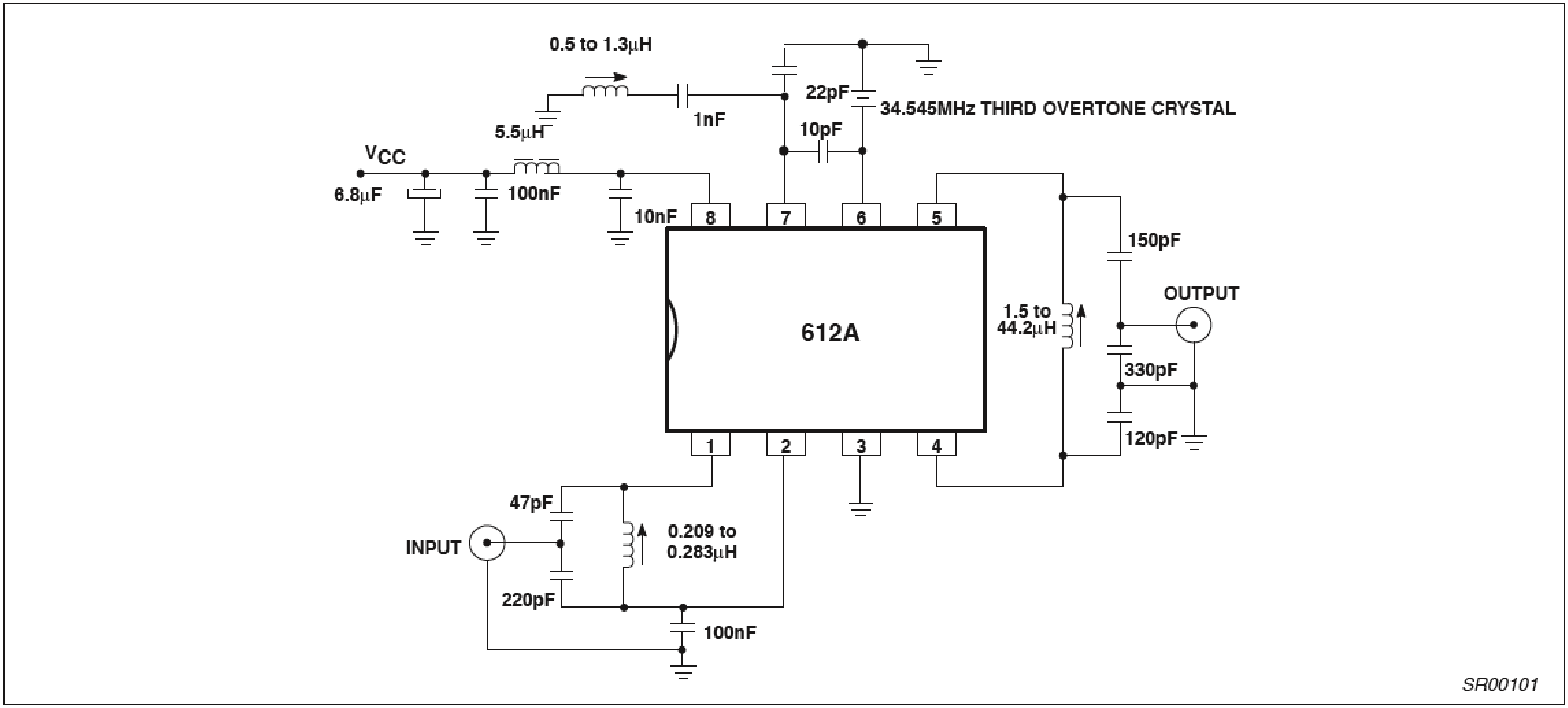
0.5 to 1.3µH
5.5µH
1nF
22pF
34.545MHz THIRD OVERTONE CRYSTAL
10pF
VCC
6.8µF
100nF
10nF
8
7
6
5
150pF
OUTPUT
1.5 to
44.2µH
612A
330pF
120pF
1
2
3
4
47pF
INPUT
0.209 to
0.283µH
220pF
100nF
SR00101

Figure 3. Test Configuration

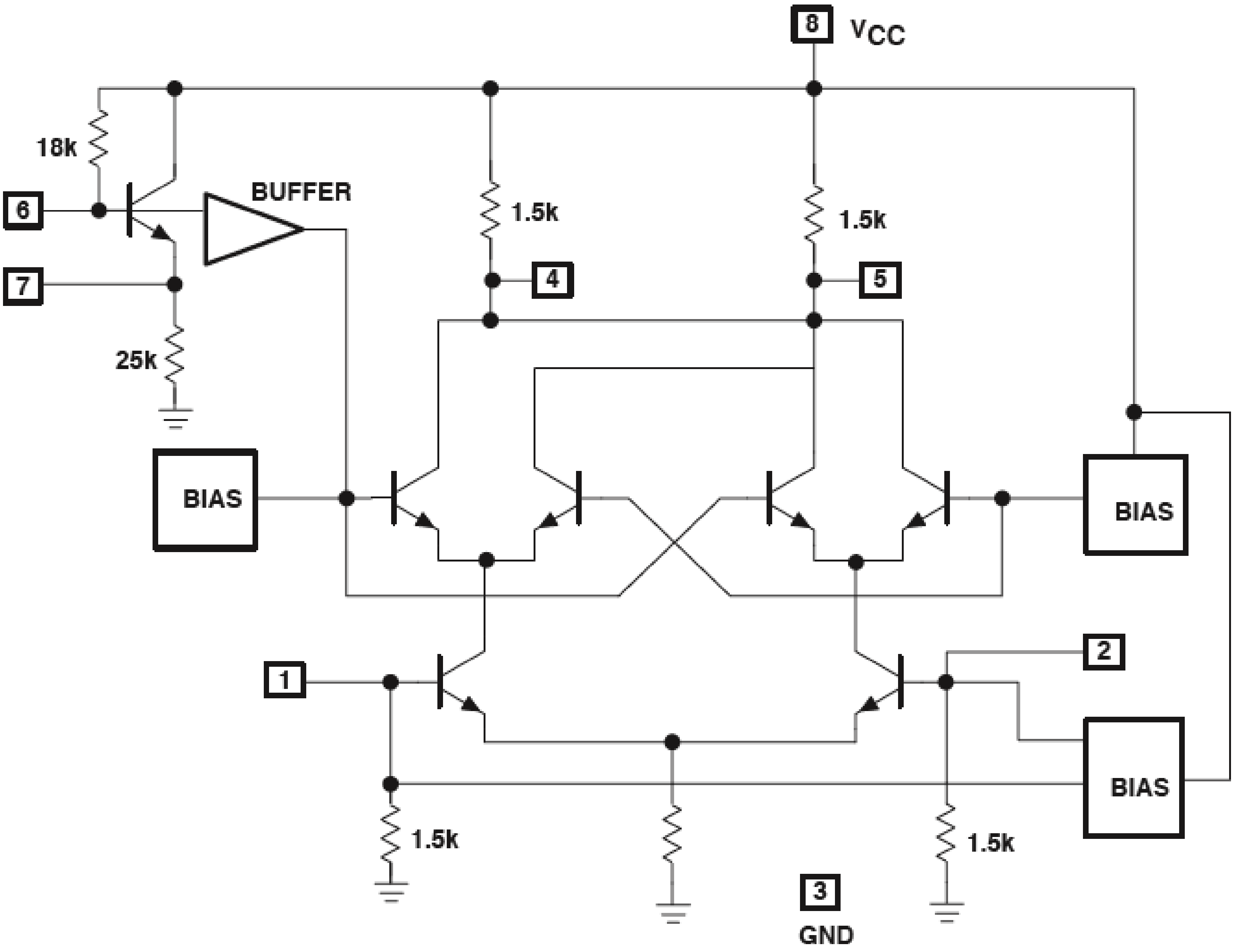
8
VCC
18k
6
BUFFER
1.5k
1.5k
4
5
7
25k
BIAS
BIAS
1
2
BIAS
1.5k
1.5k
3
GND

Figure 4. Equivalent Circuit

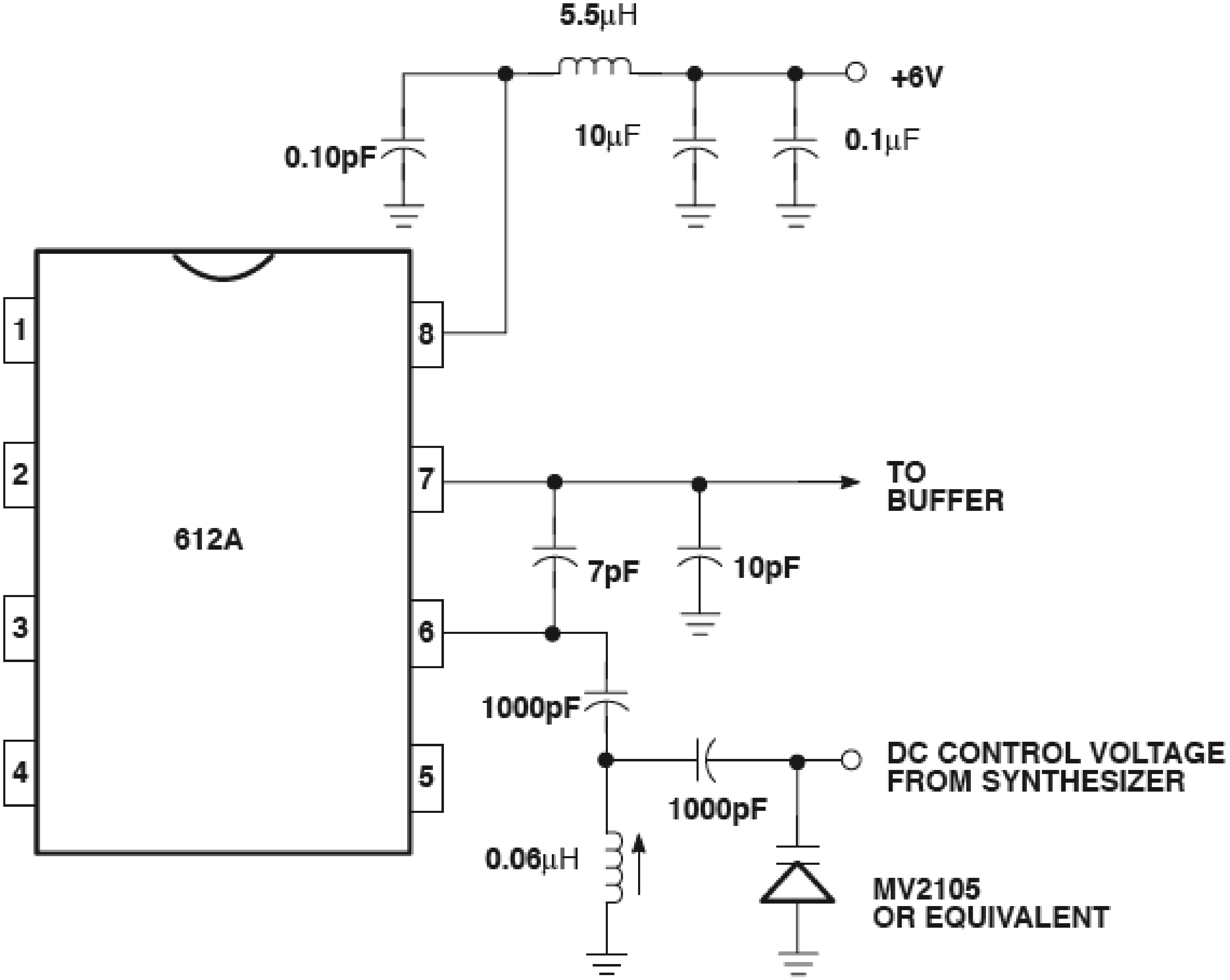
5.5µH
+6V
0.10pF
10µF
0.1µF
1
2
3
4
8
7
6
5
612A
TO
BUFFER
7pF
10pF
1000pF
DC CONTROL VOLTAGE
FROM SYNTHESIZER
1000pF
0.06µH
MV2105
OR EQUIVALENT

Order this document by MC3363/D

MOTOROLA

# Low Power Dual Conversion FM Receiver

The MC3363 is a single chip narrowband VHF FM radio receiver. It is a dual conversion receiver with RF amplifier transistor, oscillators, mixers, quadrature detector, meter drive/carrier detect and mute circuitry. The MC3363 also has a buffered first local oscillator output for use with frequency synthesizers, and a data slicing comparator for FSK detection.

- Wide Input Bandwidth – 200 MHz Using Internal Local Oscillator
  – 450 MHz Using External Local Oscillator
- RF Amplifier Transistor
- Muting Operational Amplifier
- Complete Dual Conversion
- Low Voltage: $V_{CC}$ = 2.0 V to 6.0 Vdc
- Low Drain Current: $I_{CC}$ = 3.6 mA (Typical) at $V_{CC}$ = 3.0 V, Excluding RF Amplifier Transistor
- Excellent Sensitivity: Input 0.3 μV (Typical) for 12 dB SINAD Using Internal RF Amplifier Transistor
- Data Shaping Comparator
- Received Signal Strength Indicator (RSSI) with 60 dB Dynamic Range
- Low Number of External Parts Required
- Manufactured in Motorola's MOSAIC® Process Technology

# MC3363

## LOW POWER DUAL CONVERSION FM RECEIVER

**SEMICONDUCTOR TECHNICAL DATA**

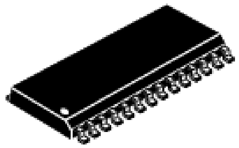

**DW SUFFIX**
PLASTIC PACKAGE
CASE 751F
(SO-28L)

**ORDERING INFORMATION**

| Device | Operating Temperature Range | Package |
|---|---|---|
| MC3363DW | $T_A$ = – 40 to +85°C | SO–28L |

## Figure 2. Test Circuit

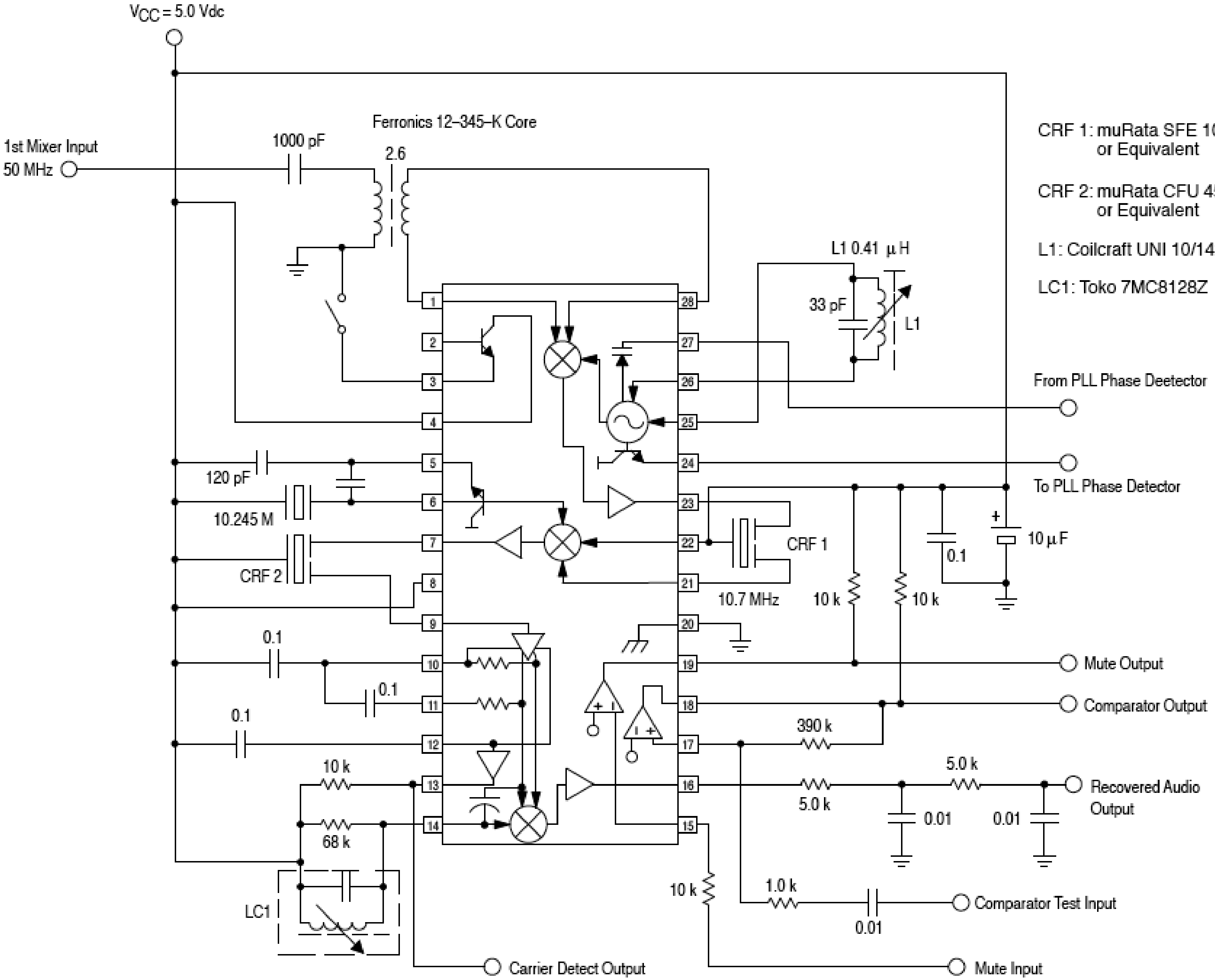
$V_{CC}$ = 5.0 Vdc
1st Mixer Input
50 MHz
1000 pF
Ferronics 12–345–K Core
2.6
120 pF
10.245 M
CRF 2
0.1
0.1
0.1
10 k
68 k
LC1
Carrier Detect Output
L1 0.41 µH
33 pF
L1
From PLL Phase Deetector
To PLL Phase Detector
CRF 1
10.7 MHz
0.1
10 µF
10 k
10 k
Mute Output
Comparator Output
390 k
5.0 k
5.0 k
0.01
0.01
Recovered Audio Output
10 k
1.0 k
0.01
Comparator Test Input
Mute Input
1
2
3
4
5
6
7
8
9
10
11
12
13
14
15
16
17
18
19
20
21
22
23
24
25
26
27
28

CRF 1: muRata SFE 10.7 mA
or Equivalent

CRF 2: muRata CFU 455D
or Equivalent

L1: Coilcraft UNI 10/142 10–1/2 Turns

LC1: Toko 7MC8128Z

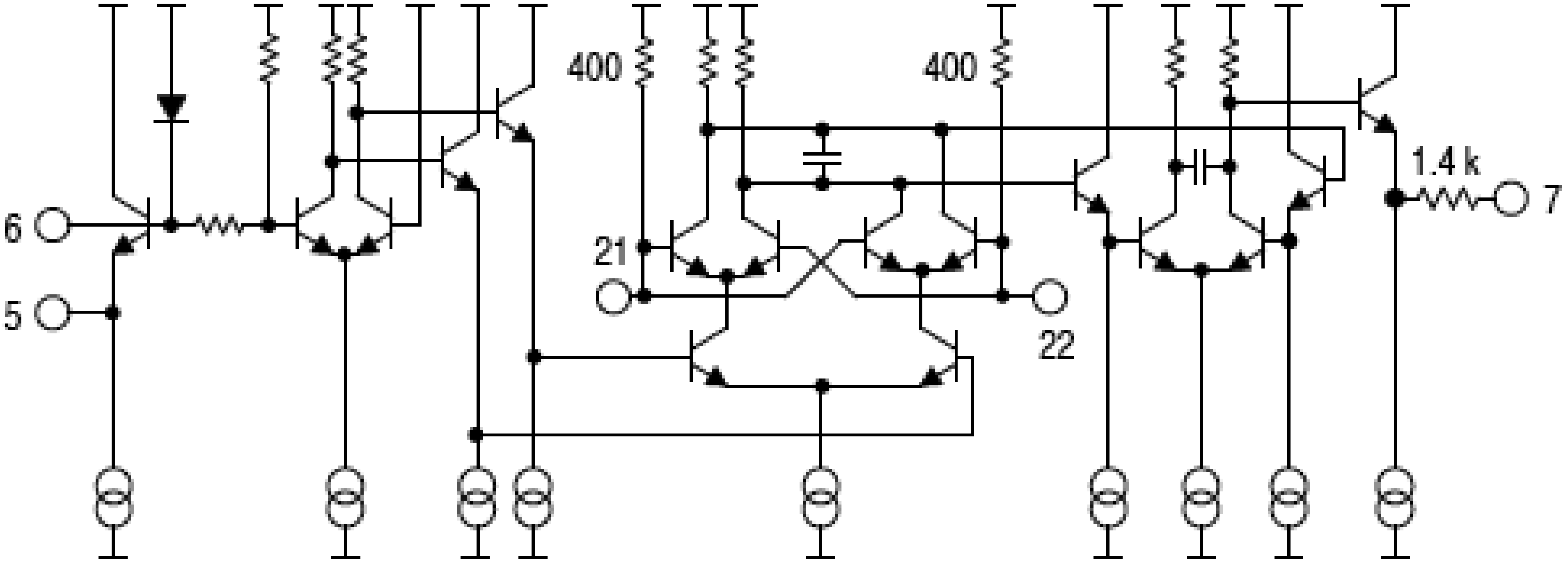
1.4 k

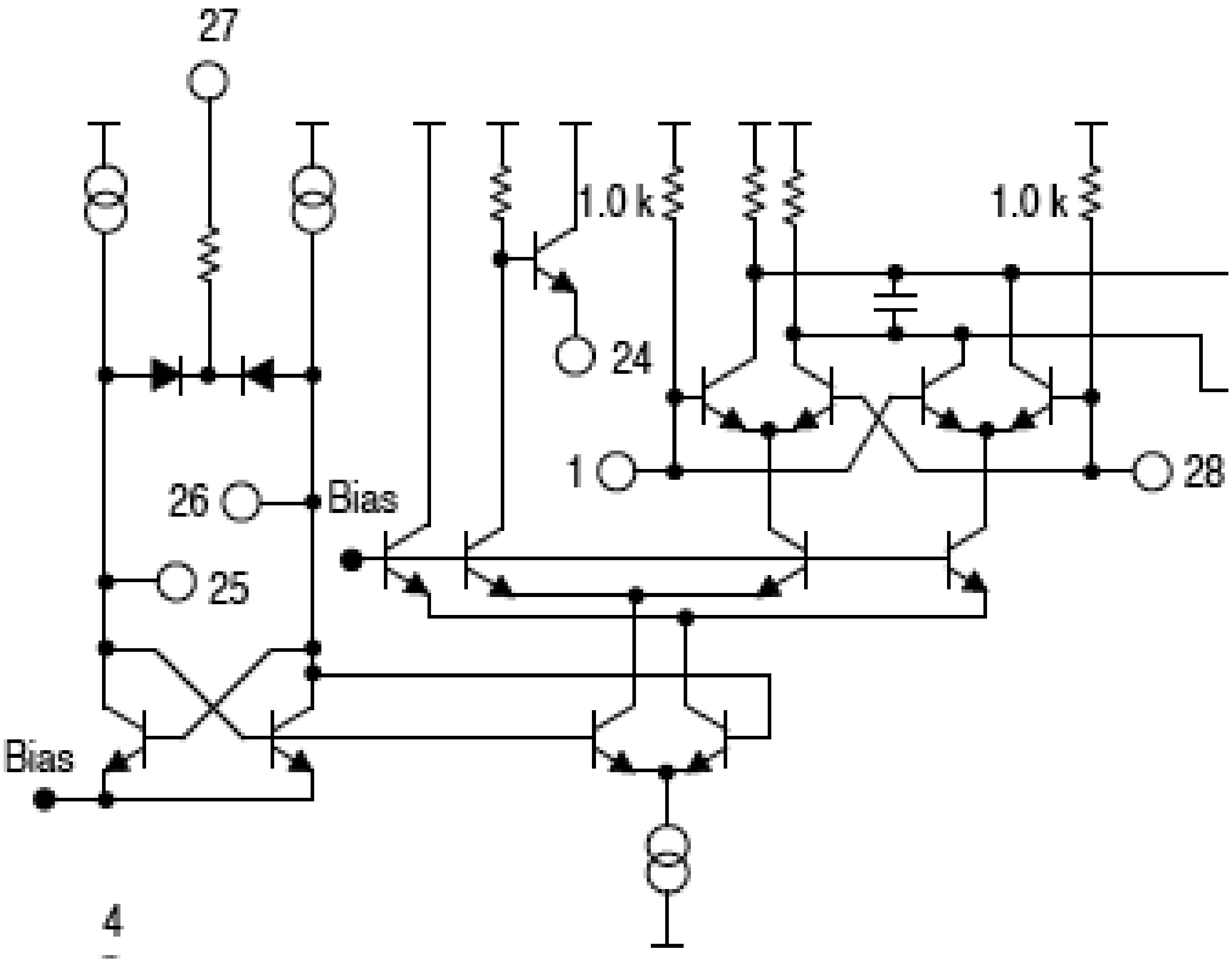
1.0 k
1.0 k
Bias
Bias

MOTOROLA

# FM Communications Receivers

# MC13135
# MC13136

## DUAL CONVERSION NARROWBAND FM RECEIVERS

The MC13135/MC13136 are the second generation of single chip, dual conversion FM communications receivers developed by Motorola. Major improvements in signal handling, RSSI and first oscillator operation have been made. In addition, recovered audio distortion and audio drive have improved. Using Motorola's MOSAIC™ 1.5 process, these receivers offer low noise, high gain and stability over a wide operating voltage range.

Both the MC13135 and MC13136 include a Colpitts oscillator, VCO tuning diode, low noise first and second mixer and LO, high gain limiting IF, and RSSI. The MC13135 is designed for use with an LC quadrature detector and has an uncommitted op amp that can be used either for an RSSI buffer or as a data comparator. The MC13136 can be used with either a ceramic discriminator or an LC quad coil and the op amp is internally connected for a voltage buffered RSSI output.

These devices can be used as stand–alone VHF receivers or as the lower IF of a triple conversion system. Applications include cordless telephones, short range data links, walkie–talkies, low cost land mobile, amateur radio receivers, baby monitors and scanners.

- Complete Dual Conversion FM Receiver – Antenna to Audio Output
- Input Frequency Range – 200 MHz
- Voltage Buffered RSSI with 70 dB of Usable Range
- Low Voltage Operation – 2.0 to 6.0 Vdc (2 Cell NiCad Supply)
- Low Current Drain – 3.5 mA Typ
- Low Impedance Audio Output < 25 Ω
- VHF Colpitts First LO for Crystal or VCO Operation
- Isolated Tuning Diode
- Buffered First LO Output to Drive CMOS PLL Synthesizer

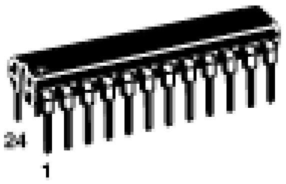

**P SUFFIX**
PLASTIC PACKAGE
CASE 724

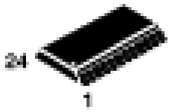

**DW SUFFIX**
PLASTIC PACKAGE
CASE 751E
(SO–24L)

### ORDERING INFORMATION

| Device | Operating Temperature Range | Package |
|---|---|---|
| MC13135P | $T_A = -40°$ to $+85°C$ | Plastic DIP |
| MC13135DW | | SO–24L |
| MC13136P | | Plastic DIP |
| MC13136DW | | SO–24L |

## PIN CONNECTIONS

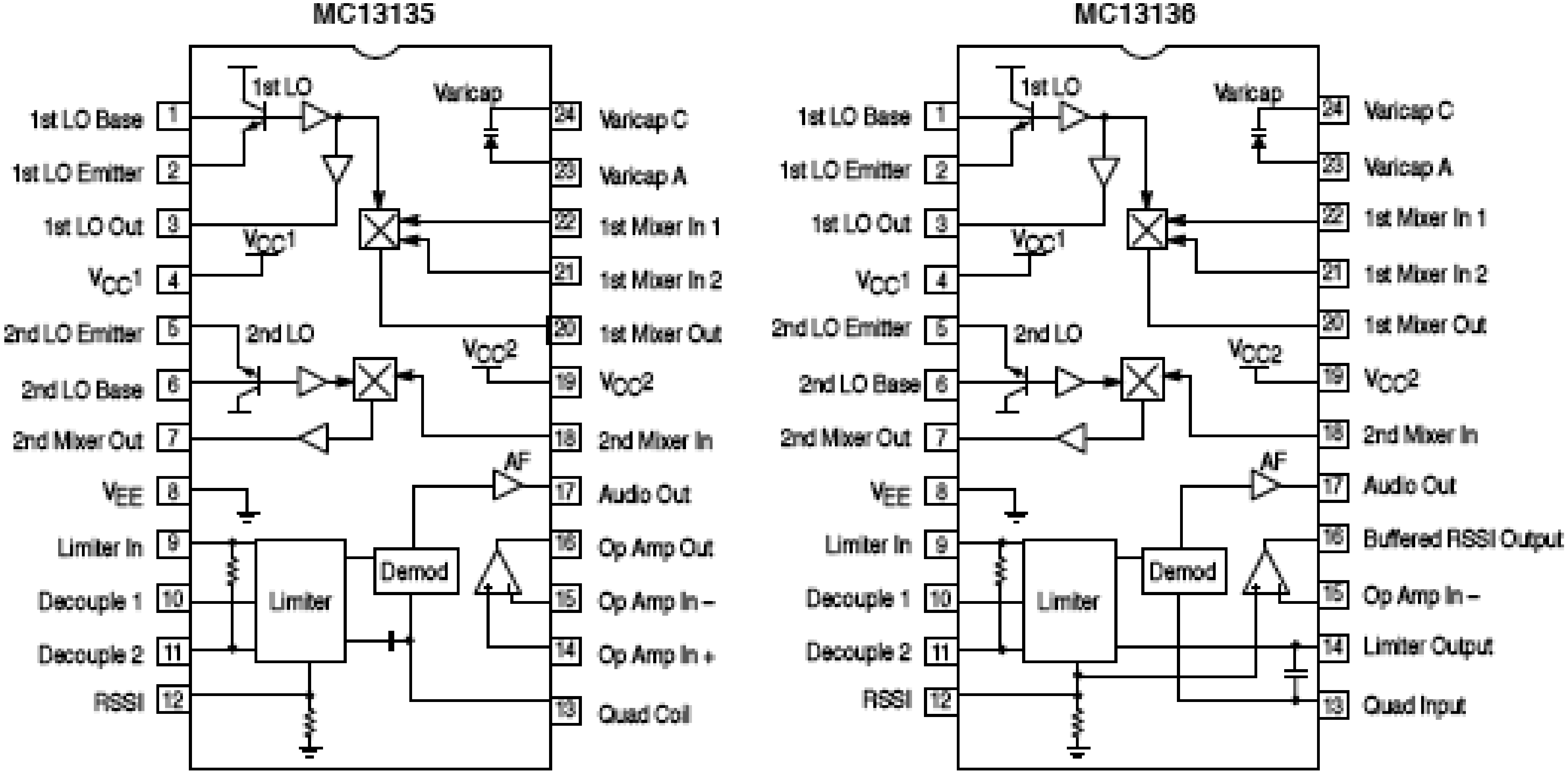
MC13135
1 1st LO Base
2 1st LO Emitter
3 1st LO Out
4 VCC1
5 2nd LO Emitter
6 2nd LO Base
7 2nd Mixer Out
8 VEE
9 Limiter In
10 Decouple 1
11 Decouple 2
12 RSSI
24 Varicap C
23 Varicap A
22 1st Mixer In 1
21 1st Mixer In 2
20 1st Mixer Out
19 VCC2
18 2nd Mixer In
17 Audio Out
16 Op Amp Out
15 Op Amp In –
14 Op Amp In +
13 Quad Coil
1st LO
Varicap
VCC1
2nd LO
VCC2
AF
Limiter
Demod
MC13136
1 1st LO Base
2 1st LO Emitter
3 1st LO Out
4 VCC1
5 2nd LO Emitter
6 2nd LO Base
7 2nd Mixer Out
8 VEE
9 Limiter In
10 Decouple 1
11 Decouple 2
12 RSSI
24 Varicap C
23 Varicap A
22 1st Mixer In 1
21 1st Mixer In 2
20 1st Mixer Out
19 VCC2
18 2nd Mixer In
17 Audio Out
16 Buffered RSSI Output
15 Op Amp In –
14 Limiter Output
13 Quad Input
1st LO
Varicap
VCC1
2nd LO
VCC2
AF
Limiter
Demod

Each device contains 142 active transistors.

© Motorola, Inc. 1996

Figure 1a. MC13135 Test Circuit

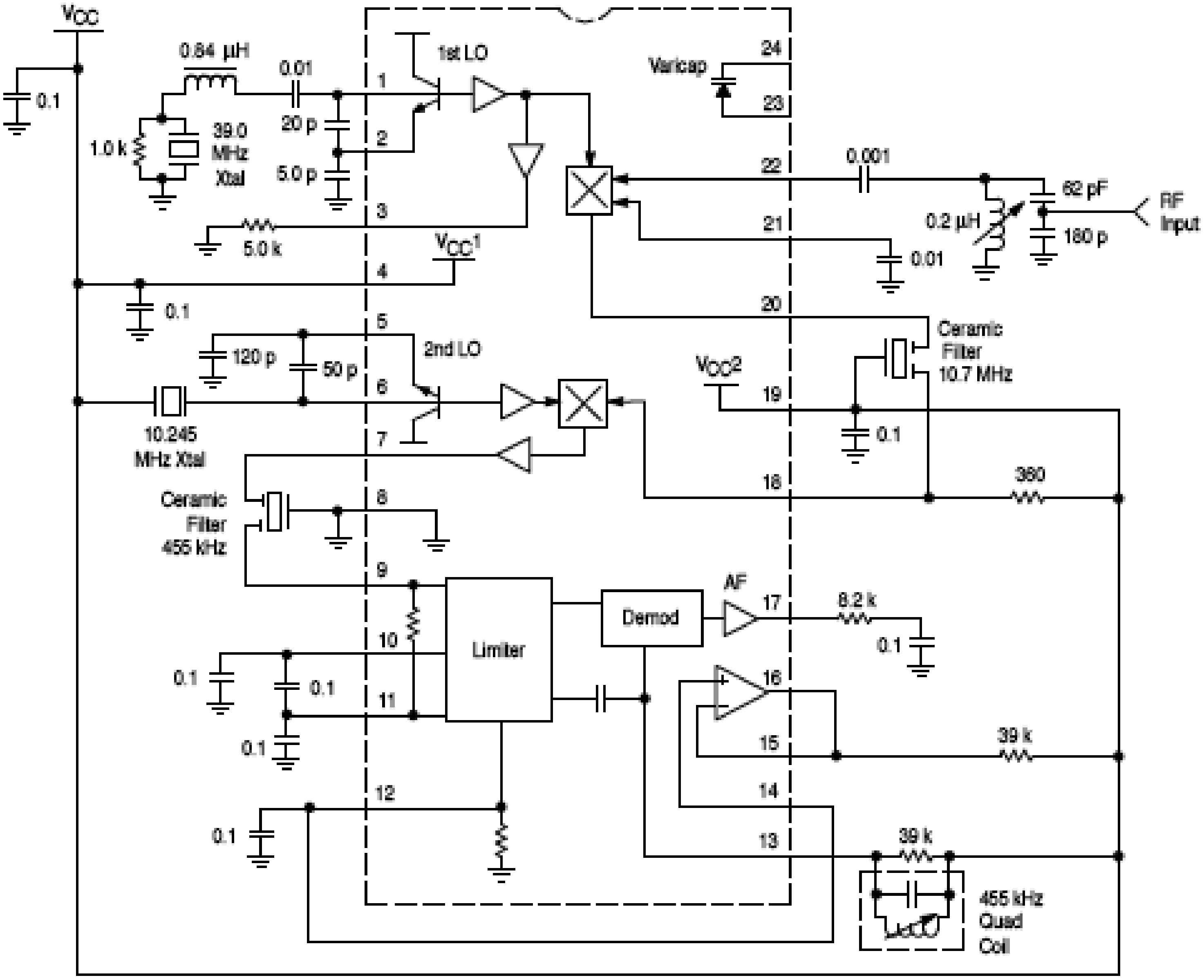
$V_{CC}$
0.1
0.84 µH
0.01
1st LO
Varicap
24
23
1
2
20 p
1.0 k
39.0 MHz Xtal
5.0 p
22
0.001
62 pF
RF Input
0.2 µH
180 p
3
5.0 k
$V_{CC}1$
21
0.01
4
0.1
20
5
2nd LO
120 p
50 p
Ceramic Filter 10.7 MHz
$V_{CC}2$
6
19
10.245 MHz Xtal
0.1
7
18
360
Ceramic Filter 455 kHz
8
9
AF
Limiter
Demod
17
8.2 k
0.1
10
0.1
0.1
11
16
0.1
15
39 k
12
14
0.1
13
39 k
455 kHz Quad Coil

Figure 1b. MC13136 Quad Detector Test Circuit

# From: Analog Circuit Design: Art, Science, and Personalities

**Max Wien, Mr. Hewlett, and a Rainy Sunday Afternoon**

**Figure 7-3.** Hewlett's Figure 3 detailed the oscillator circuit. Note Wien network and lamp (Courtesy Stanford University Archives.)

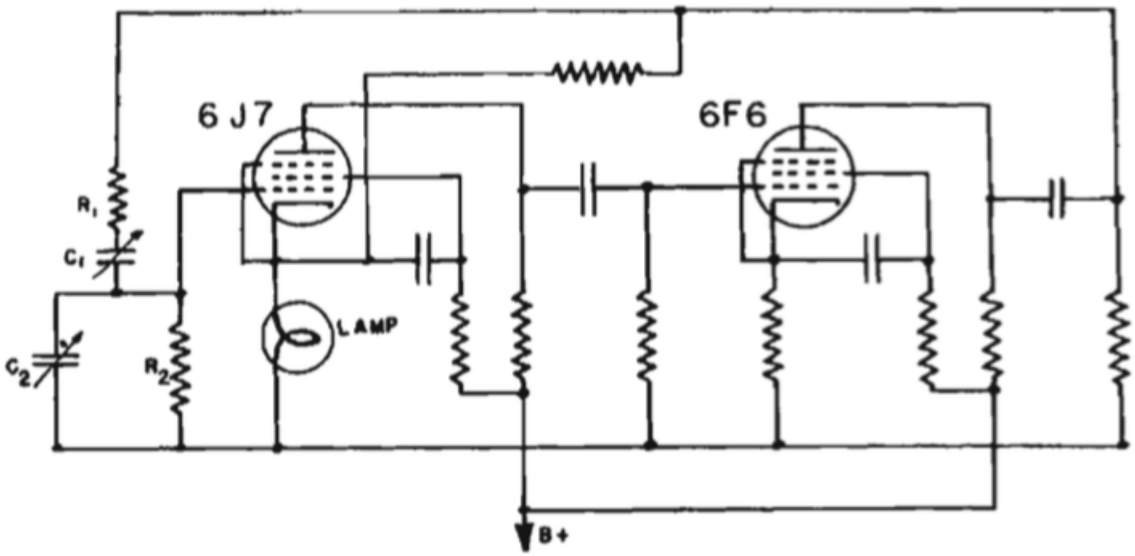
6 J7
6F6
R1
C1
C2
R2
LAMP
B+

This circuit, from Hewlett's 1939 MS thesis, formed the basis of HP's Model 200A Audio Oscillator. (patented 1942)

**Jim Williams**

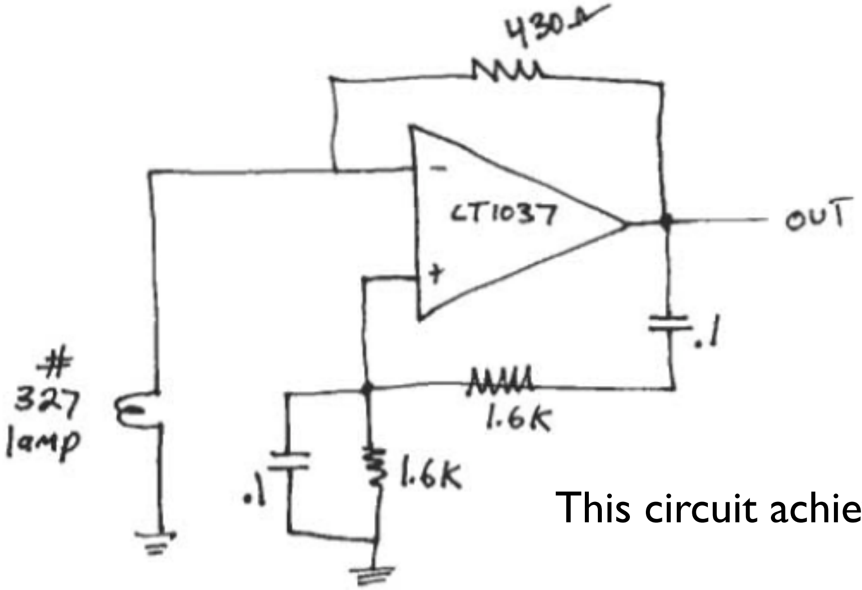
430Ω
−
+
LT1037
OUT
.1
#
327
lamp
1.6K
.1
1.6K

**Figure 7-5.** My version of Hewlett's circuit. Distortion was much better, but I was fifty years too late.

This circuit achieved 0.0025% THD.

the collector current at a nearly constant value. Suppose that the time-varying component of the base-emitter voltage is sinusoidal, i.e.,

$$V_{be} = V_{DC} \; + \; v_1 cos\omega t \tag{A.13}$$

and let $x = v_1 q/kT = v_1/25\text{mV}$ (at room temperature). Then

$$I_C = I_S \exp[V_{DC} q/kT] \exp[\, x \, cos\omega t] \tag{A.14}$$

The term $\exp[\, x \cos \omega t]$ is a non-sinusoidal periodic function of time and can be expanded in a Fourier series. The series is

$$\exp[\, x \, \cos \, \omega t] = I_o(x) \; + \; 2 \, \sum_{n=1}^{\infty} I_n(x) \cos(n\omega t) \tag{A.15}$$

where the coefficients $I_n(x)$ are values of the modified Bessel function of the first kind. Using this relationship, the collector current waveform can be written as

$$I_C = I_{DCo} \, [I_o(x) + 2 \sum_{n=1} I_n(x) \; \cos(n\omega t)] \tag{A.16}$$

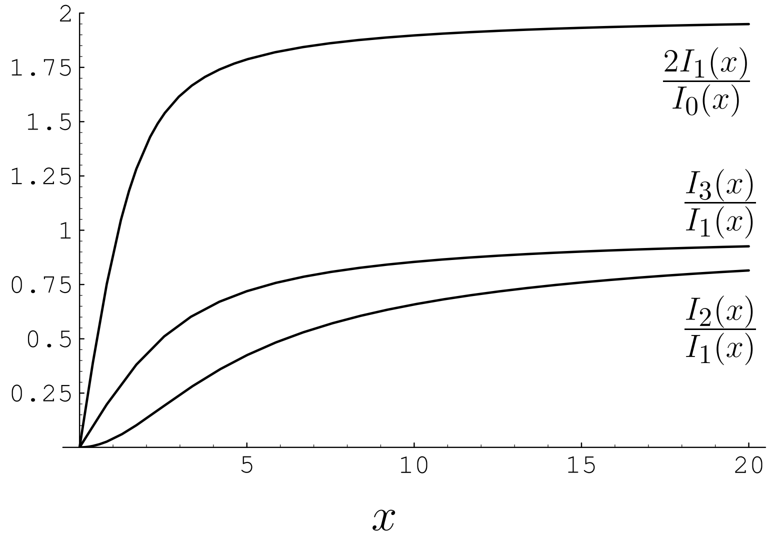

Figure A.5: $2I_1(x)/I_o(x)$ is the relative amplitude of the fundamental component of the collector current. The other curves show the ratio of second and third harmonic amplitudes to the fundamental amplitude.

small-signal transconductance can be obtained in the limit as x approaches 0, i.e.,

$$g_m = \lim_{x \to 0} I_{DC} \frac{2\, I_1(x)}{v_1 I_0(x)} = \frac{I_{DC}}{kT/q} \tag{A.19}$$

At room temperature $kT/q = 25\,\mathrm{mV}$, so

$$g_m = \frac{I_{DC}}{25\,\mathrm{mV}} \approx 40 I_{DC} \tag{A.20}$$

The large signal transconductance is

$$G_m(x) = I_{DC} \frac{2\, I_1(x)}{v_1 I_0(x)} = I_{DC} \frac{q}{kT} \frac{2\, I_1(x)}{x\, I_0(x)} = g_m \frac{2}{x} \frac{I_1(x)}{I_0(x)} \tag{A.21}$$

The ratio of the large signal to small-signal transconductance is shown in Figure A.6. This

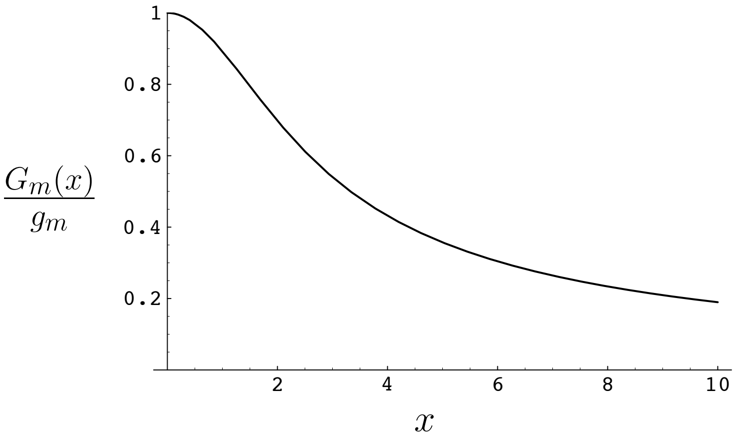

Figure A.6: Ratio of large signal to small-signal transconductance

Small-signal loop gain = 2.5

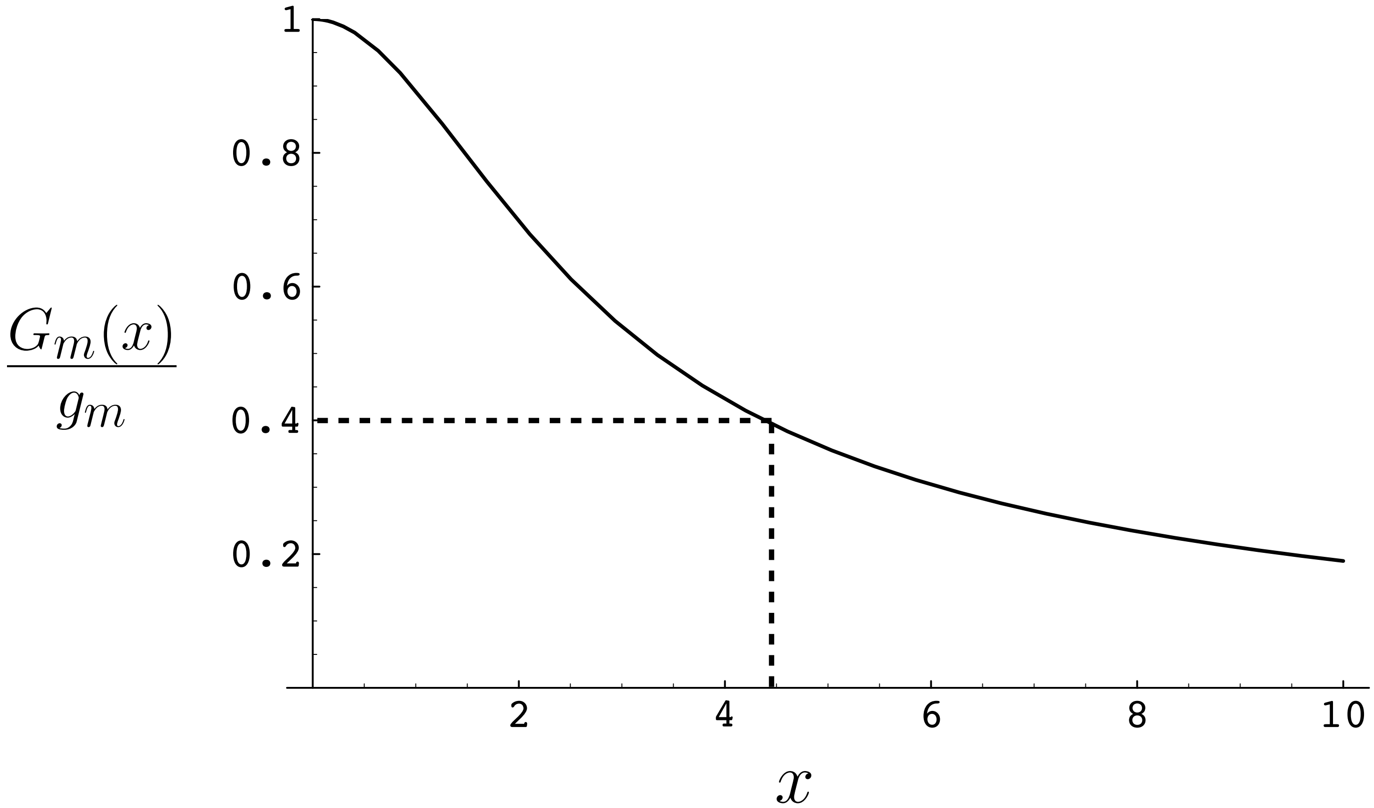

Base-emitter voltage, x=Vbe/(25 mV), grows until transconductance is reduced by the factor 1/2.5=0.4, which occurs with x=4.5. Hence, steady-state base-emitter voltage amplitude is 4.5*25 mV, or about 112 mV.

| Case | $C_1$ | $C_2$ | $g_{m,ss}$ | $g_m/g_{m,ss}$ |
|---|---|---|---|---|
| 1 | 2500 pF | 20.4 pF | 45.3 mS | 0.88 |
| 2 | 1000 pF | 20.6 pF | 18.1 mS | 2.2 |
| 3 | 500 pF | 21.1 pF | 9.42 mS | 4.4 |
| 4 | 200 pF | 22.5 pF | 3.77 mS | 11.0 |
| 5 | 100 pF | 25.4 pF | 1.83 mS | 21.8 |
| 6 | 22.5 pF | 200 pF | 2.23 mS | 17.9 |

the period 0.9-1.0 $\mu$s after the initial transient. For the cases where oscillation occurs, the expanded plots show the current and voltage waveforms when the circuit is undergoing steady-state oscillation.

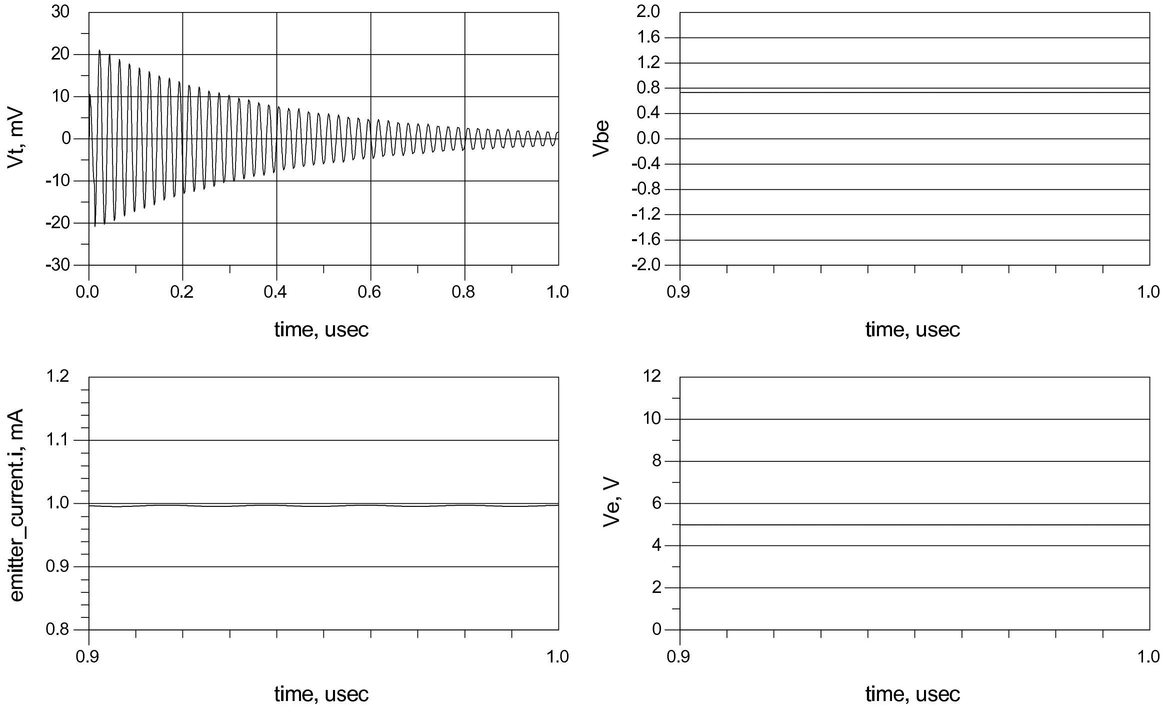

Figure 5.12: Case 1 - loop gain is 0.88, which is less than one, so oscillation does not start.

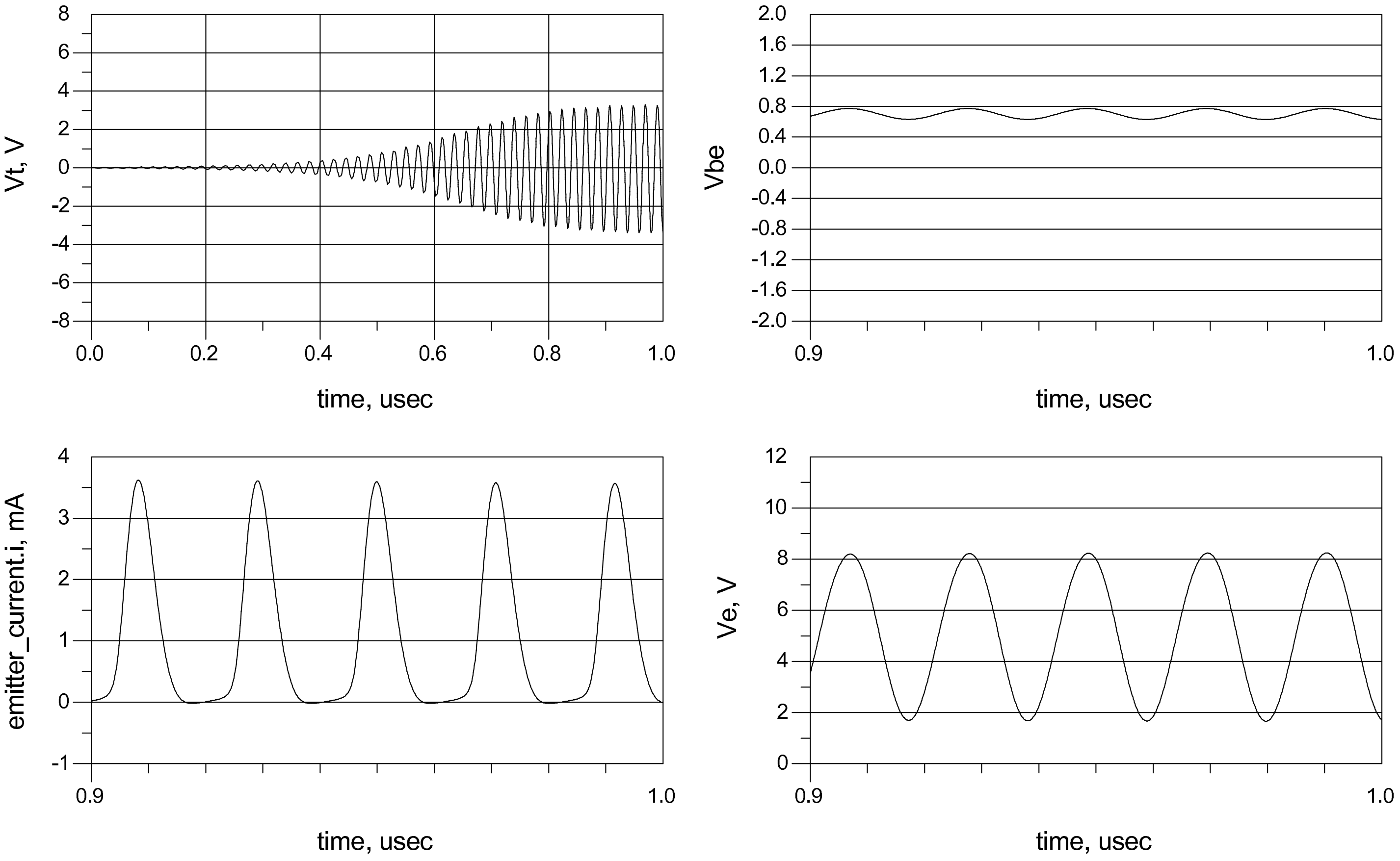

Figure 5.13: Case 2 - $g_m/g_{m,ss} = 2.2$.

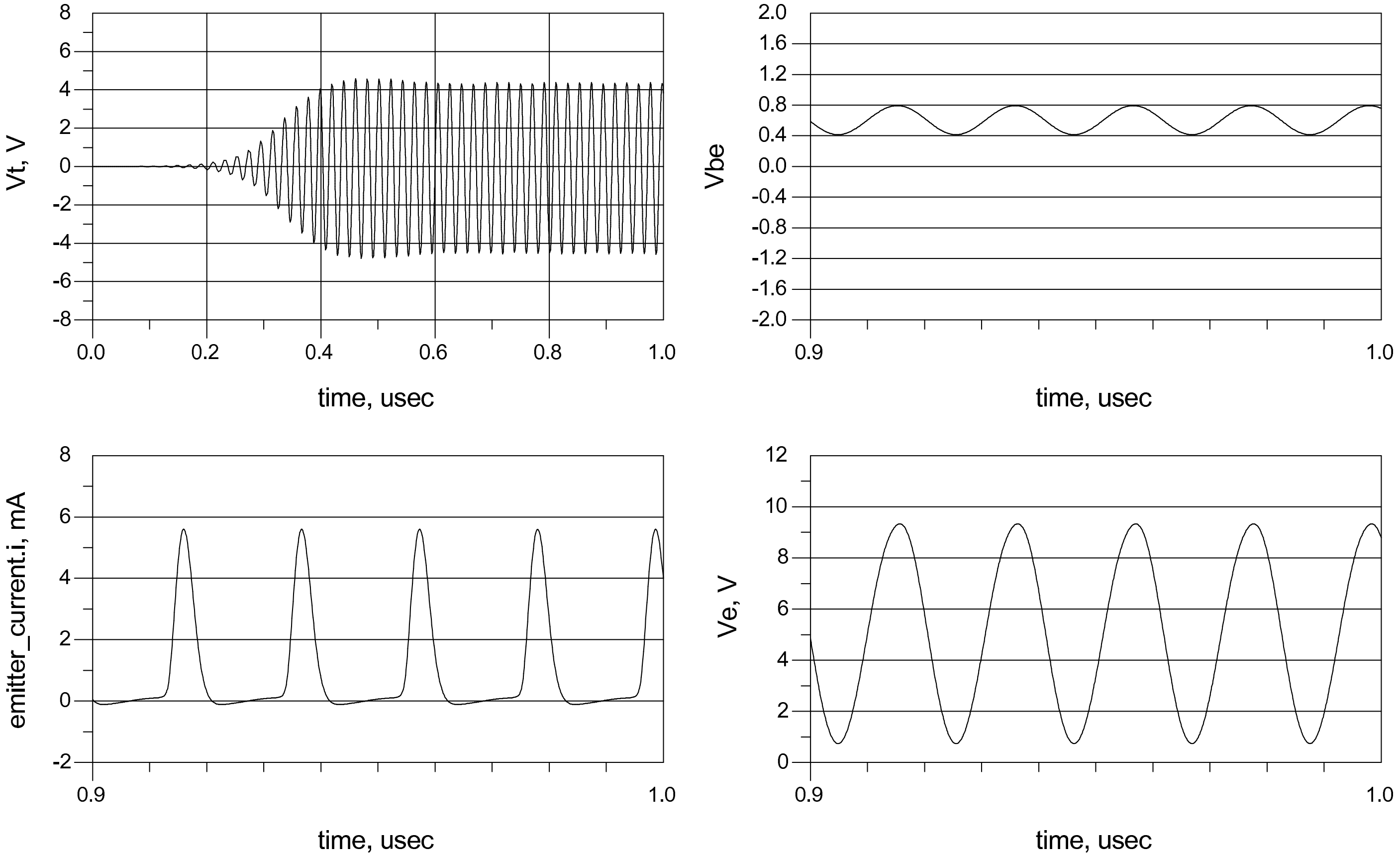

Figure 5.14: Case 3 - $g_m/g_{m,ss} = 4.4$.

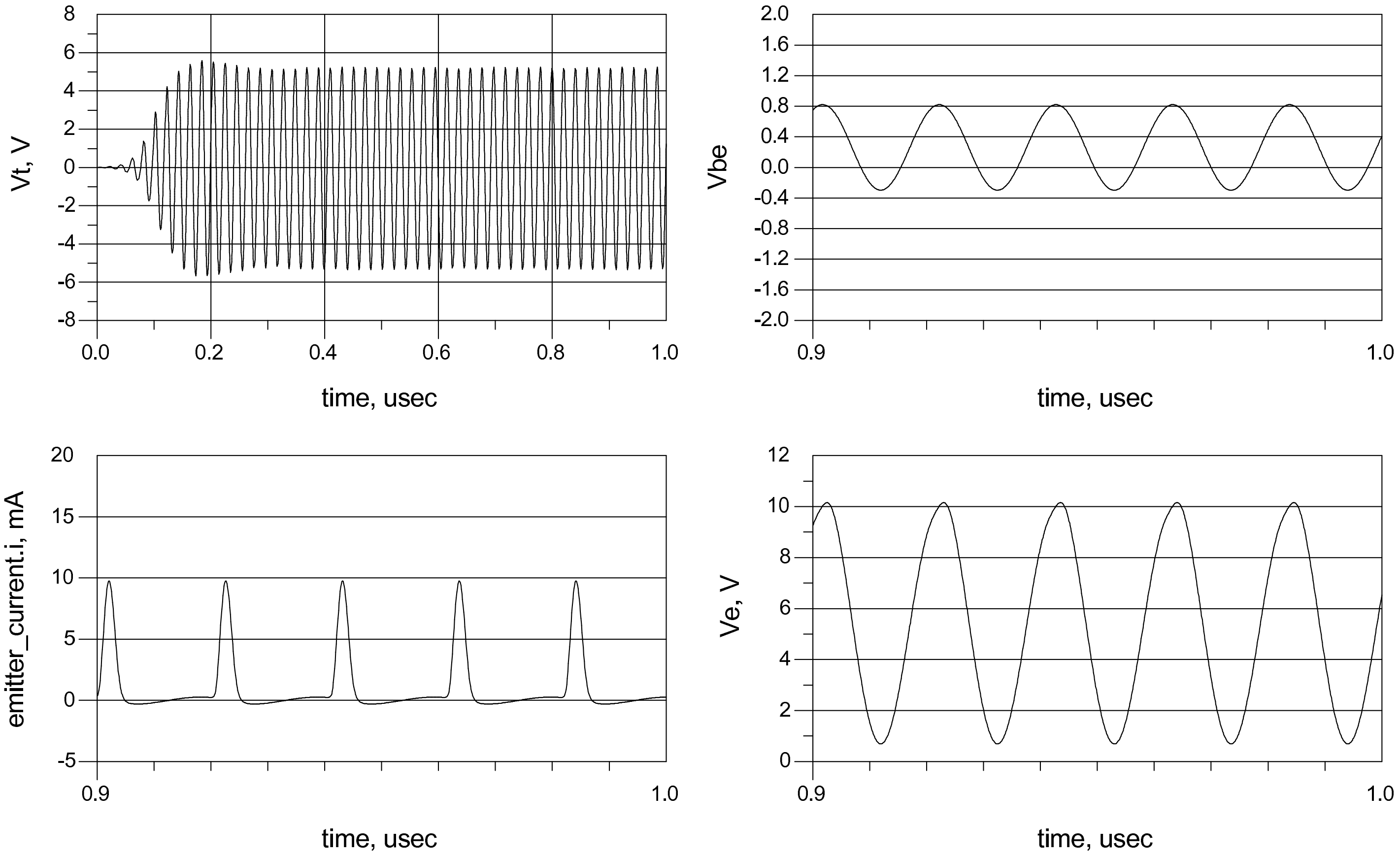

Figure 5.15: Case 4 - $g_m/g_{m,ss} = 11.0$.

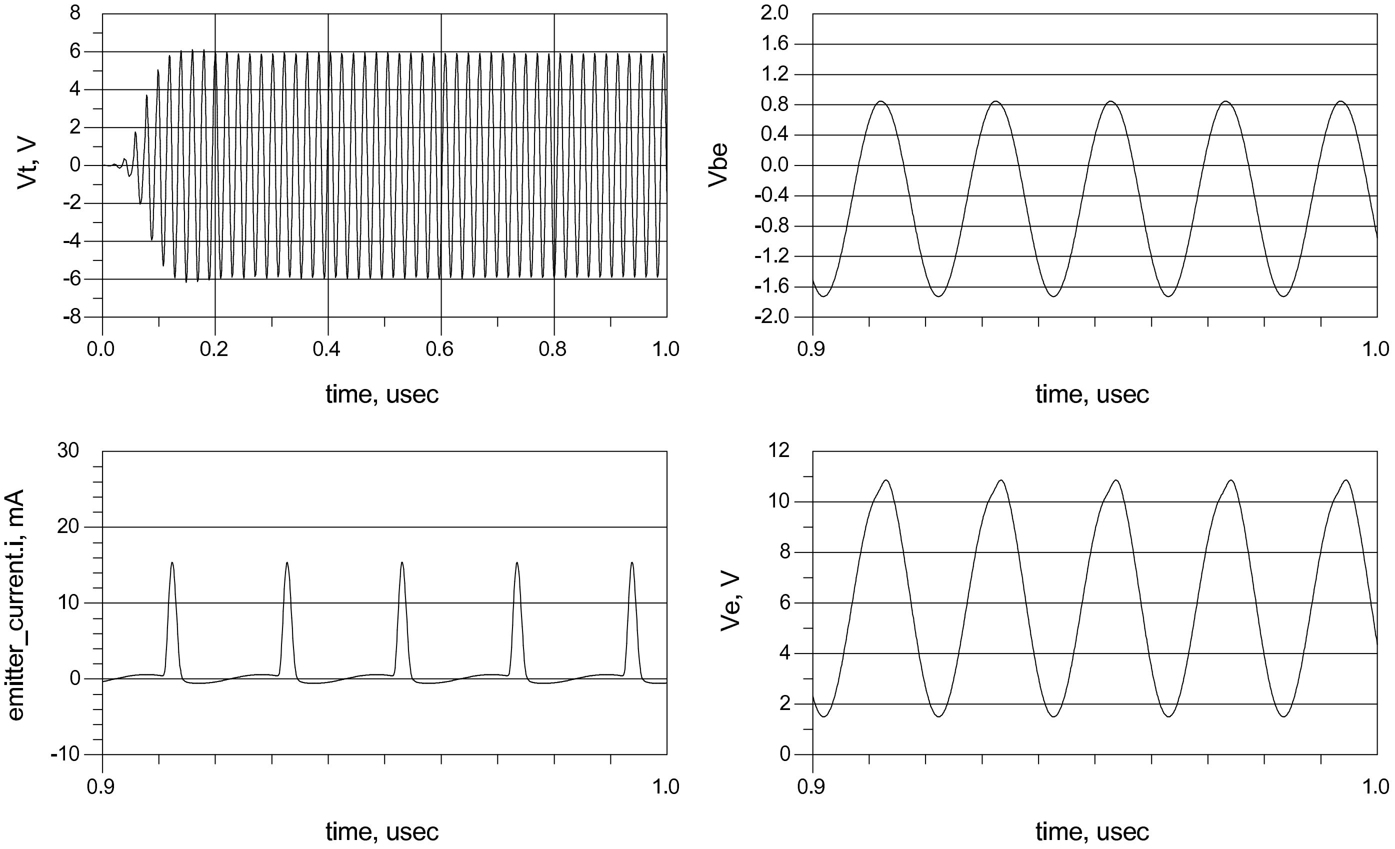

Figure 5.16: Case 5 - $g_m/g_{m,ss} = 21.8$.

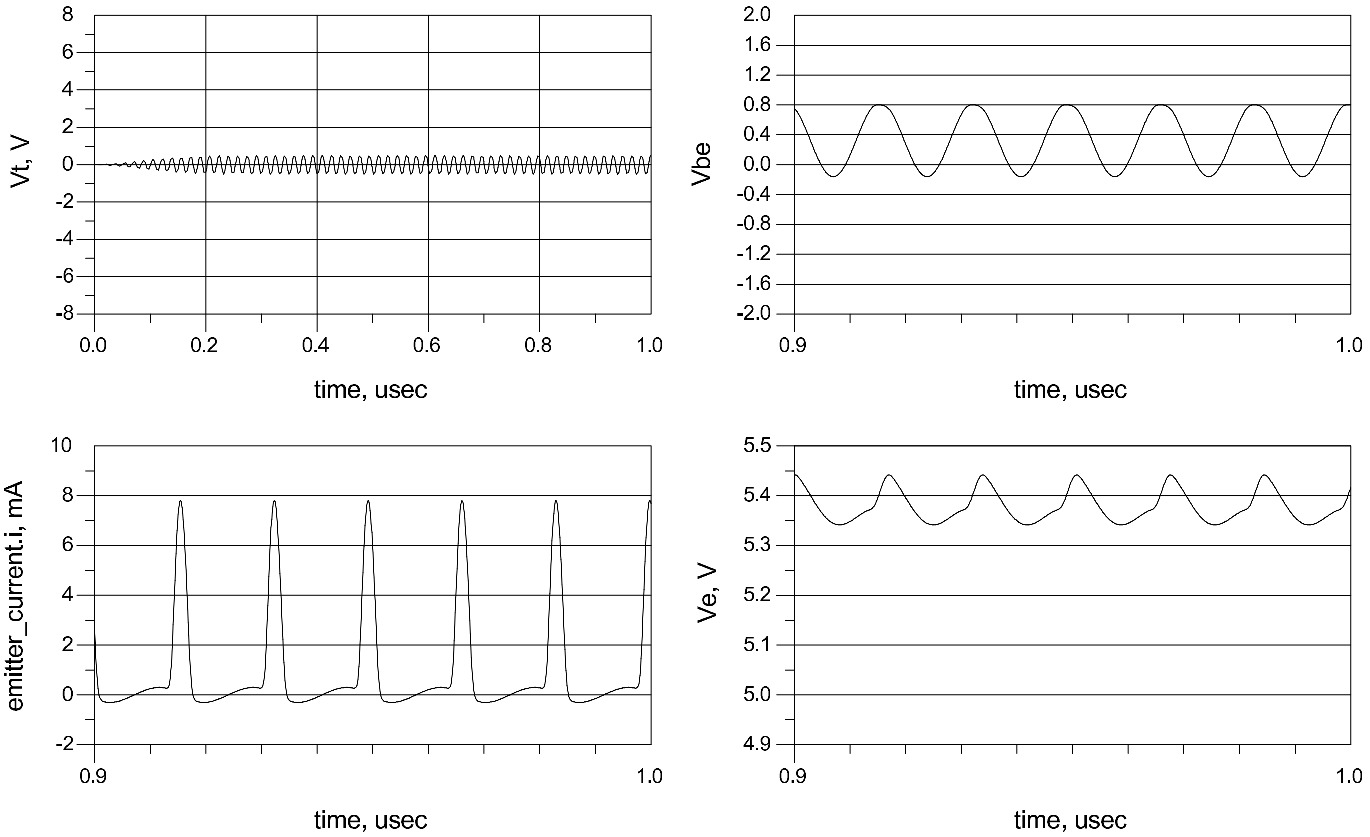

Figure 5.17: Case 6 - $g_m/g_{m,ss} = 17.9$.

Table 5.3: Comparison between predicted and simulated $|V_{be}|$ and $|V_e|/|V_{be}|$ ratio.

| Case | $g_m/g_{m,ss}$ | $\lvert V_{be}\rvert$ pred. | $\lvert V_{be}\rvert$ sim. | $\lvert V_e\rvert$ sim. | $C_1/C_2$ | $\lvert V_e\rvert/\lvert V_{be}\rvert$ |
|---|---|---|---|---|---|---|
| 1 | 0.88 | - | - | - | 122.5 | - |
| 2 | 2.2 | 94 mV | 71 mV | 3.27 V | 48.5 | 46.1 |
| 3 | 4.4 | 207 mV | 185 mV | 4.30 V | 23.7 | 23.2 |
| 4 | 11.0 | 537 mV | 554 mV | 4.70 V | 8.9 | 8.5 |
| 5 | 21.8 | 1.08 V | 1.29 V | 5.40 V | 3.9 | 4.2 |
| 6 | 17.9 | 882 mV | 483 mV | * | 0.11 | * |

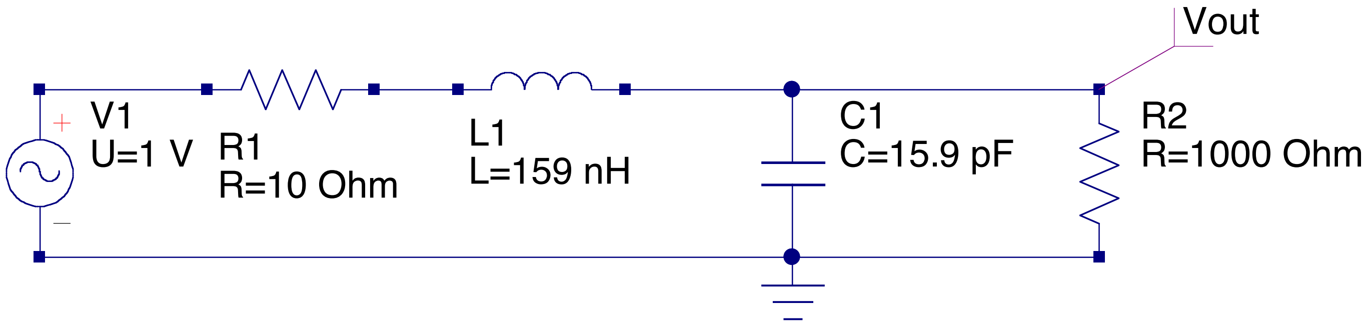
Vout
V1
U=1 V
R1
R=10 Ohm
L1
L=159 nH
C1
C=15.9 pF
R2
R=1000 Ohm

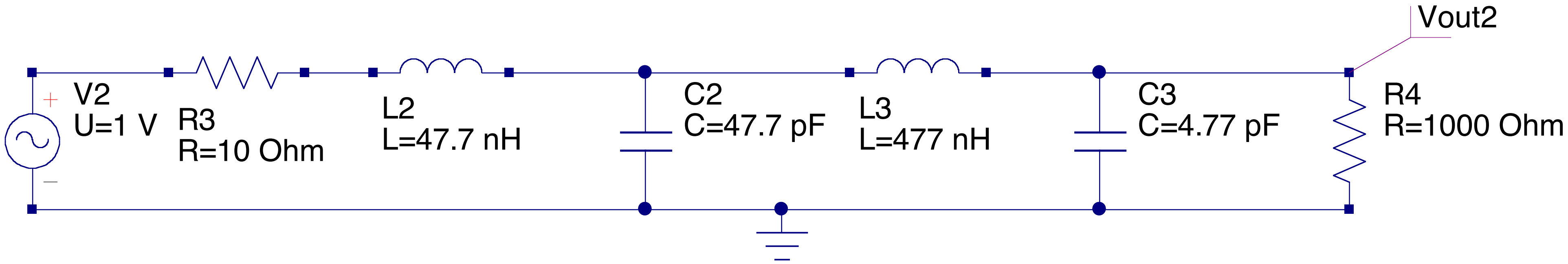
Vout2
V2
U=1 V
R3
R=10 Ohm
L2
L=47.7 nH
C2
C=47.7 pF
L3
L=477 nH
C3
C=4.77 pF
R4
R=1000 Ohm

ac simulation

AC1
Type=lin
Start=10 MHz
Stop=200 MHz
Points=101

Equation

Eqn1
Pavs=1/80

Equation

Eqn2
Gt=0.5*abs(Vout.v)^2/1000/Pavs

Equation

Eqn3
Gt2=0.5*abs(Vout2.v)^2/1000/Pavs

Equation

Eqn4
dBGt=dB(Gt)

Equation

Eqn5
dBGt2=dB(Gt2)

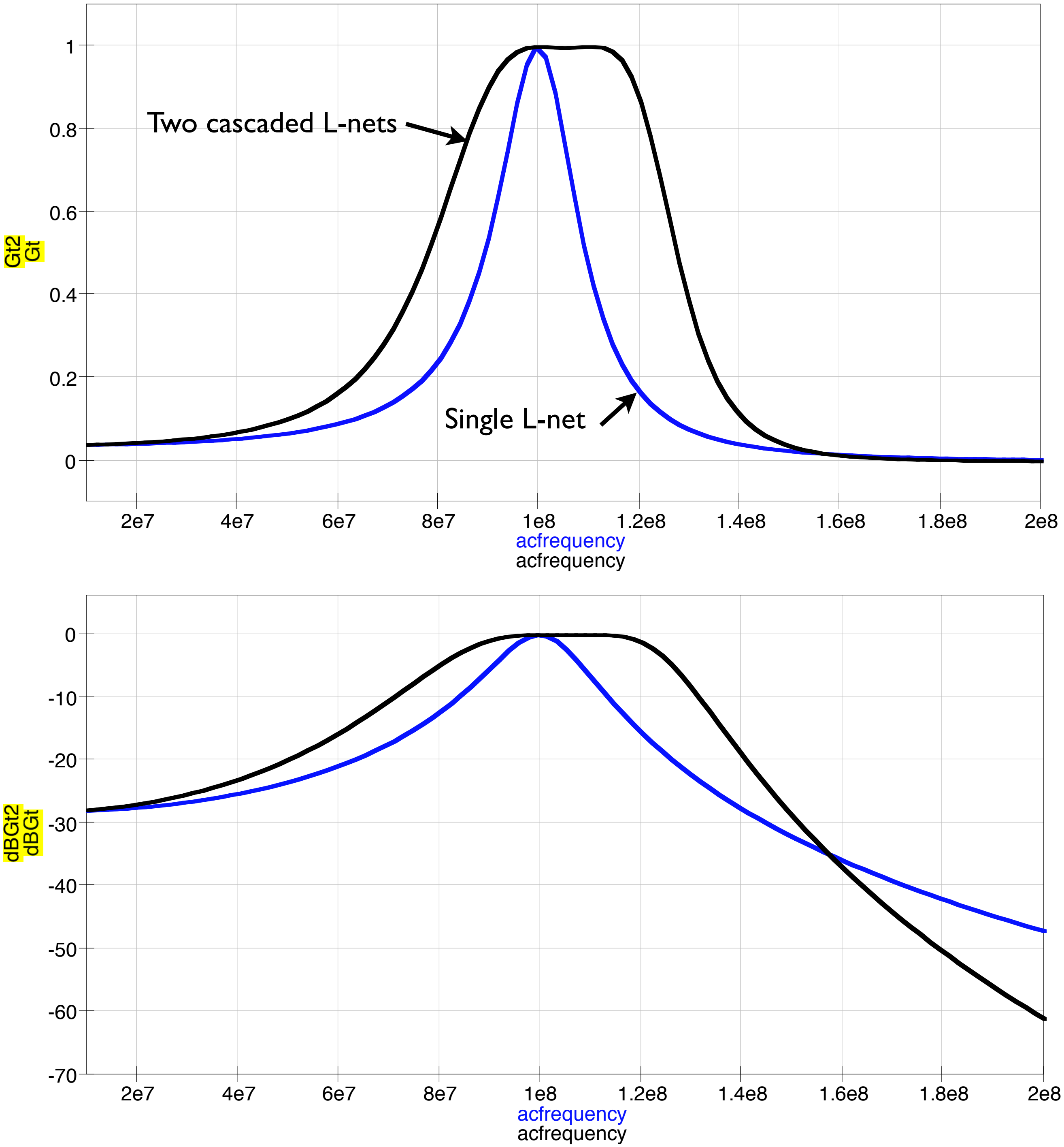

Two cascaded L-nets

Single L-net

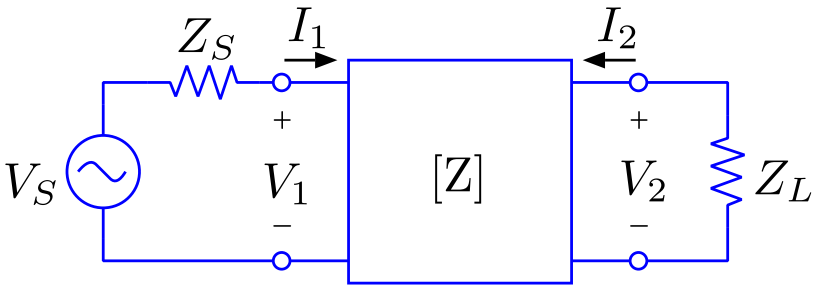

Figure 7.9: A system consisting of source, 2-port, and a load.

$$V_1 = Z_{11}I_1 + Z_{12}I_2$$
$$V_2 = Z_{21}I_1 + Z_{22}I_2$$

$$Z_{IN} = \frac{V_1}{I_1} = Z_{11} - \frac{Z_{12}Z_{21}}{Z_L + Z_{22}} \qquad Z_{OUT} = \frac{V_2}{I_2}|_{V_S=0} = Z_{22} - \frac{Z_{12}Z_{21}}{Z_S + Z_{11}}$$

$$A_V = \frac{V_2}{V_1} = \frac{Z_{21}Z_L}{Z_{11}Z_L + Z_{11}Z_{22} - Z_{12}Z_{21}}$$

Consider the two-winding transformer shown in Figure 7.11.

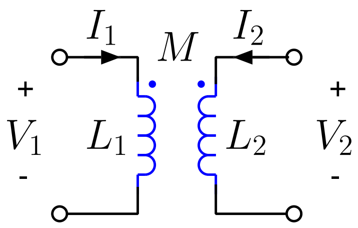

Figure 7.11: 2-winding transformer.

Ignoring losses, the equations that describe this device are

$$V_1 = j\omega L_1 I_1 + j\omega M I_2 \tag{7.59}$$

$$V_2 = j\omega M I_1 + j\omega L_2 I_2 \tag{7.60}$$

where $L_1$ and $L_2$ are the self inductances of the transformer windings and M is the mutual inductance. The "dot" convention is such that if current flows into the dotted terminals, the magnetic fluxes linking the two coils will reinforce each other. With this convention, M will be a positive number. The 2-winding transformer is completely described by its open-circuit impedance matrix,

$$[Z] = \begin{bmatrix} j\omega L_1 & j\omega M \\ j\omega M & j\omega L_2 \end{bmatrix}.$$

Since the circuit operation of the transformer is completely described by this impedance matrix, any network having the same defining equations can be substituted for the transformer. One useful equivalent circuit is shown in Figure 7.12.

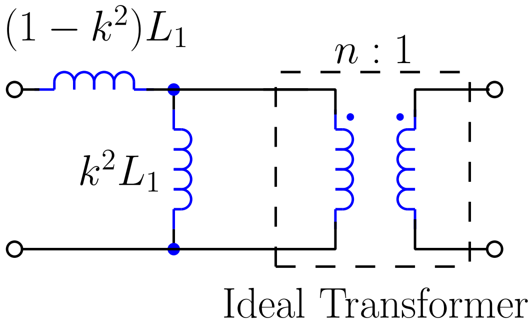

$$k = \frac{M}{\sqrt{L_1 L_2}}$$

$$n = k\sqrt{\frac{L_1}{L_2}}$$

Figure 7.12: Equivalent circuit for a two-winding transformer

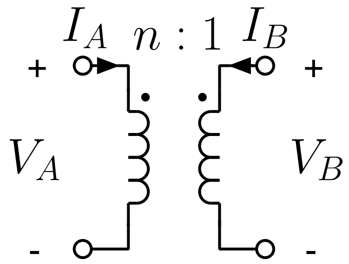

$$V_B = \frac{V_A}{n}$$

$$I_B = -nI_A$$

Figure 7.13: Terminal relations for the ideal transformer

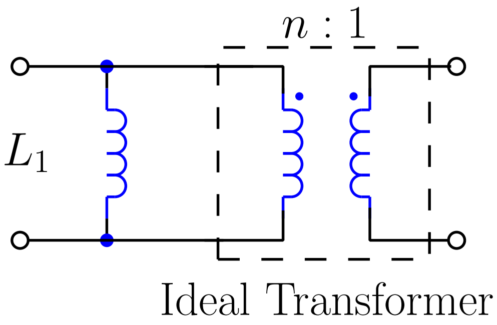

$n:1$
$L_1$
Ideal Transformer

Figure 7.14: Equivalent circuit when k approaches 1. In this case, the effective turns ratio is, approximately, $n = \sqrt{L_1/L_2}$.

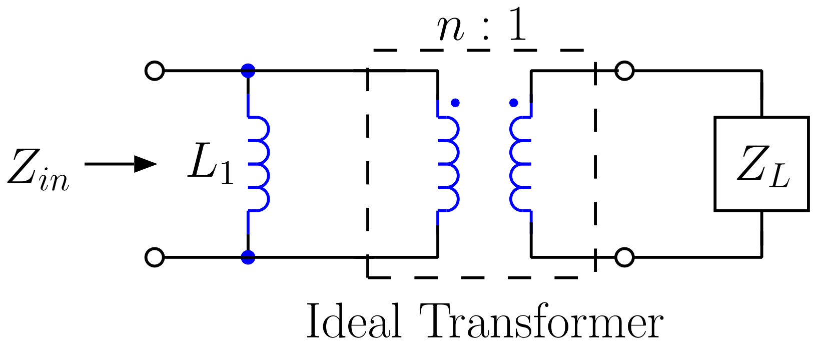

Figure 7.15: Tightly-coupled transformer used as impedance transformer

$$[Z] \simeq \begin{bmatrix} j\omega L_1 & j\omega L_1/n \\ j\omega L_1/n & j\omega L_1/n^2 \end{bmatrix}.$$

$$Z_{IN} = Z_{11} - \frac{Z_{12}Z_{21}}{Z_{22}+Z_L} = j\omega L_1 - \frac{(j\omega L_1/n)^2}{j\omega L_1/n^2 + Z_L} = \frac{j\omega L_1 Z_L n^2}{j\omega L_1 + Z_L n^2}$$

The tightly-coupled transformer will behave essentially like an ideal transformer if $\omega L_1 \gg |Z_L n^2|$ or, since $n^2 = L_1/L_2$, if $\omega L_2 \gg |Z_L|$. In this case

$$Z_{IN} \approx n^2 Z_L.$$

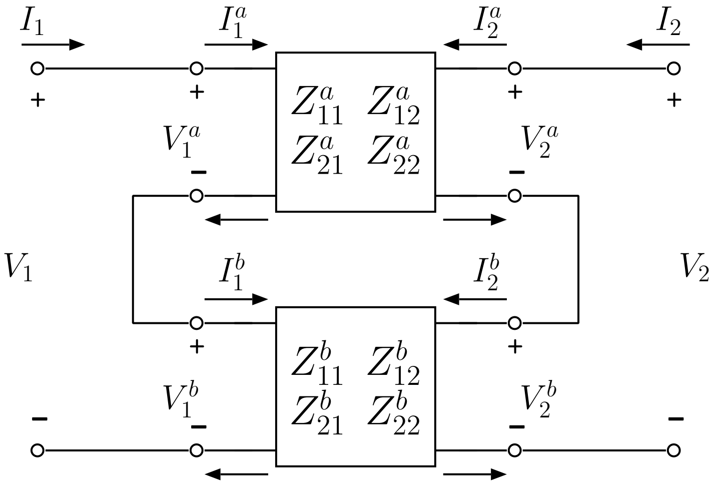
$I_1$
$I_1^a$
$I_2^a$
$I_2$
$Z_{11}^a$ $Z_{12}^a$
$Z_{21}^a$ $Z_{22}^a$
$V_1^a$
$V_2^a$
$V_1$
$V_2$
$I_1^b$
$I_2^b$
$Z_{11}^b$ $Z_{12}^b$
$Z_{21}^b$ $Z_{22}^b$
$V_1^b$
$V_2^b$
+
−

Figure 7.5: Two 2-ports interconnected such that the input and output ports are in series.

The series connection results in the relationships:

$$I_1 = I_1^a = I_1^b, \;\; I_2 = I_2^a = I_2^b$$

$$V_1 = V_1^a + V_1^b, \;\; V_2 = V_2^a + V_2^b.$$

In vector notation the voltage and current vectors must satisfy

$$\mathbf{I} = \mathbf{I}^a = \mathbf{I}^b \tag{7.24}$$

$$\mathbf{V} = \mathbf{V}^a + \mathbf{V}^b. \tag{7.25}$$

The voltage and current vectors for the individual 2-ports must satisfy:

$$\mathbf{V}^a = \mathbf{Z}^a\mathbf{I}^a \tag{7.26}$$

$$\mathbf{V}^b = \mathbf{Z}^b\mathbf{I}^b \tag{7.27}$$

Equations 7.24, 7.26, and 7.27 can be used in equation 7.26 to show:

$$\mathbf{V} = \{\mathbf{Z}^a + \mathbf{Z}^b\}\mathbf{I}. \tag{7.28}$$

Thus, the Z-parameter matrix for the series combination of 2-ports is the sum of the constituent Z-parameter matrices.

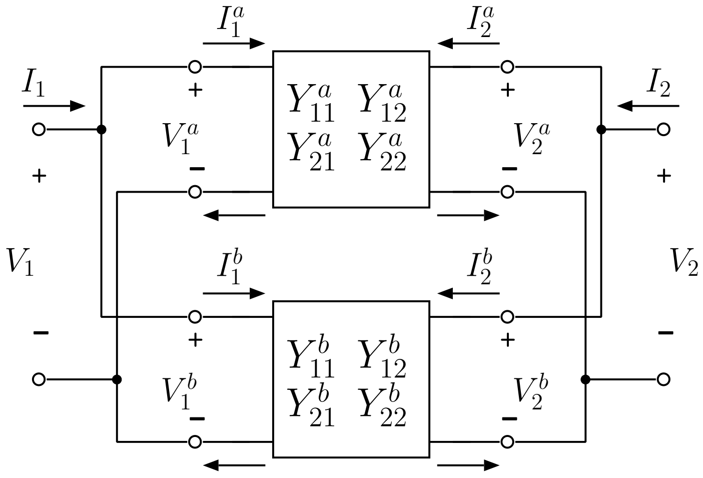

Figure 7.4: Two 2-ports interconnected such that the input and output ports are in parallel.

The parallel connection results in the following relationships:

$$V_1 = V_1^a = V_1^b, \;\; V_2 = V_2^a = V_2^b \tag{7.17}$$

$$I_1 = I_1^a + I_1^b, \;\; I_2 = I_2^a + I_2^b. \tag{7.18}$$

equations 7.17 and 7.18 can be written as:

$$\mathbf{V} = \mathbf{V}^a = \mathbf{V}^b \tag{7.19}$$

$$\mathbf{I} = \mathbf{I}^a + \mathbf{I}^b. \tag{7.20}$$

The voltage and current vectors associated with the individual 2-ports must satisfy

$$\mathbf{I}^a = \mathbf{Y}^a\mathbf{V}^a \tag{7.21}$$

$$\mathbf{I}^b = \mathbf{Y}^b\mathbf{V}^b. \tag{7.22}$$

Equations 7.19, 7.21, and 7.22 can be used in equation 7.20 to show that

$$\mathbf{I} = \{\mathbf{Y}^a + \mathbf{Y}^b\}\mathbf{V}. \tag{7.23}$$

Thus, the Y-parameter matrix for the parallel combination of 2-ports is the sum of the constituent Y-parameter matrices.

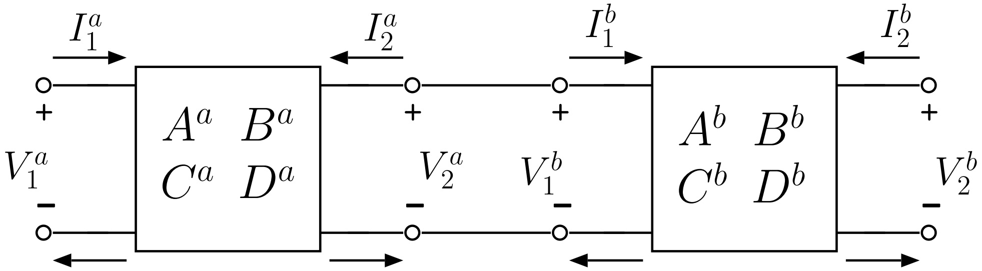

Figure 7.6: Two 2-ports in cascade.

The cascade connection results in the following relationships:

$$V_2^a = V_1^b, \;\; I_2^a = -I_1^b \tag{7.29}$$

Define the input vector $\mathbf{IN} = \begin{bmatrix} V_1 \\ I_1 \end{bmatrix}$, output vector $\mathbf{OUT} = \begin{bmatrix} V_2 \\ -I_2 \end{bmatrix}$, and chain parameter matrix $\mathbf{ABCD} = \begin{bmatrix} A & B \\ C & D \end{bmatrix}$. Then the relationships given in equation 7.29 can be written as:

$$\mathbf{OUT}^a = \mathbf{IN}^b \tag{7.30}$$

The following equations are satisfied by the individual 2-ports:

$$\mathbf{IN}^a = \mathbf{ABCD}^a\mathbf{OUT}^a \tag{7.31}$$

$$\mathbf{IN}^b = \mathbf{ABCD}^b\mathbf{OUT}^b \tag{7.32}$$

Using equation 7.32 in equation 7.30, and then using the result in equation 7.31 we find

$$\mathbf{IN}^a = \mathbf{ABCD}^a\mathbf{ABCD}^b\mathbf{OUT}^b. \tag{7.33}$$

### 7.7.1 Converting to Y-parameters

$$\begin{bmatrix} Y_{11} & Y_{12} \\ Y_{21} & Y_{22} \end{bmatrix} = \begin{bmatrix} \frac{Z_{22}}{D_Z} & -\frac{Z_{12}}{D_Z} \\ \\ -\frac{Z_{21}}{D_Z} & \frac{Z_{11}}{D_Z} \end{bmatrix} = \begin{bmatrix} \frac{1}{h_{11}} & -\frac{h_{12}}{h_{11}} \\ \\ \frac{h_{21}}{h_{11}} & \frac{D_h}{h_{11}} \end{bmatrix} = \begin{bmatrix} \frac{D}{B} & -\frac{D_{ABCD}}{B} \\ \\ -\frac{1}{B} & \frac{A}{B} \end{bmatrix}$$

### 7.7.2 Converting to Z-parameters

$$\begin{bmatrix} Z_{11} & Z_{12} \\ Z_{21} & Z_{22} \end{bmatrix} = \begin{bmatrix} \frac{Y_{22}}{D_Y} & -\frac{Y_{12}}{D_Y} \\ \\ -\frac{Y_{21}}{D_Y} & \frac{Y_{11}}{D_Y} \end{bmatrix} = \begin{bmatrix} \frac{D_h}{h_{22}} & \frac{h_{12}}{h_{22}} \\ \\ -\frac{h_{21}}{h_{22}} & \frac{1}{h_{22}} \end{bmatrix} = \begin{bmatrix} \frac{A}{C} & \frac{D_{ABCD}}{C} \\ \\ \frac{1}{C} & \frac{D}{C} \end{bmatrix}$$

### 7.7.3 Converting to h-parameters

$$\begin{bmatrix} h_{11} & h_{12} \\ h_{21} & h_{22} \end{bmatrix} = \begin{bmatrix} \frac{D_Z}{Z_{22}} & \frac{Z_{12}}{Z_{22}} \\ \\ -\frac{Z_{21}}{Z_{22}} & \frac{1}{Z_{22}} \end{bmatrix} = \begin{bmatrix} \frac{1}{Y_{11}} & -\frac{Y_{12}}{Y_{11}} \\ \\ \frac{Y_{21}}{Y_{11}} & \frac{D_Y}{Y_{11}} \end{bmatrix} = \begin{bmatrix} \frac{B}{D} & \frac{D_{ABCD}}{D} \\ \\ -\frac{1}{D} & \frac{C}{D} \end{bmatrix}$$

### 7.7.4 Converting to ABCD-parameters

$$\begin{bmatrix} A & B \\ C & D \end{bmatrix} = \begin{bmatrix} \frac{Z_{11}}{Z_{21}} & \frac{D_Z}{Z_{21}} \\ \\ \frac{1}{Z_{21}} & \frac{Z_{22}}{Z_{21}} \end{bmatrix} = \begin{bmatrix} -\frac{Y_{22}}{Y_{21}} & -\frac{1}{Y_{21}} \\ \\ -\frac{D_Y}{Y_{21}} & -\frac{Y_{11}}{Y_{21}} \end{bmatrix} = \begin{bmatrix} -\frac{D_h}{h_{21}} & -\frac{h_{11}}{h_{21}} \\ \\ -\frac{h_{22}}{h_{21}} & -\frac{1}{h_{21}} \end{bmatrix}$$

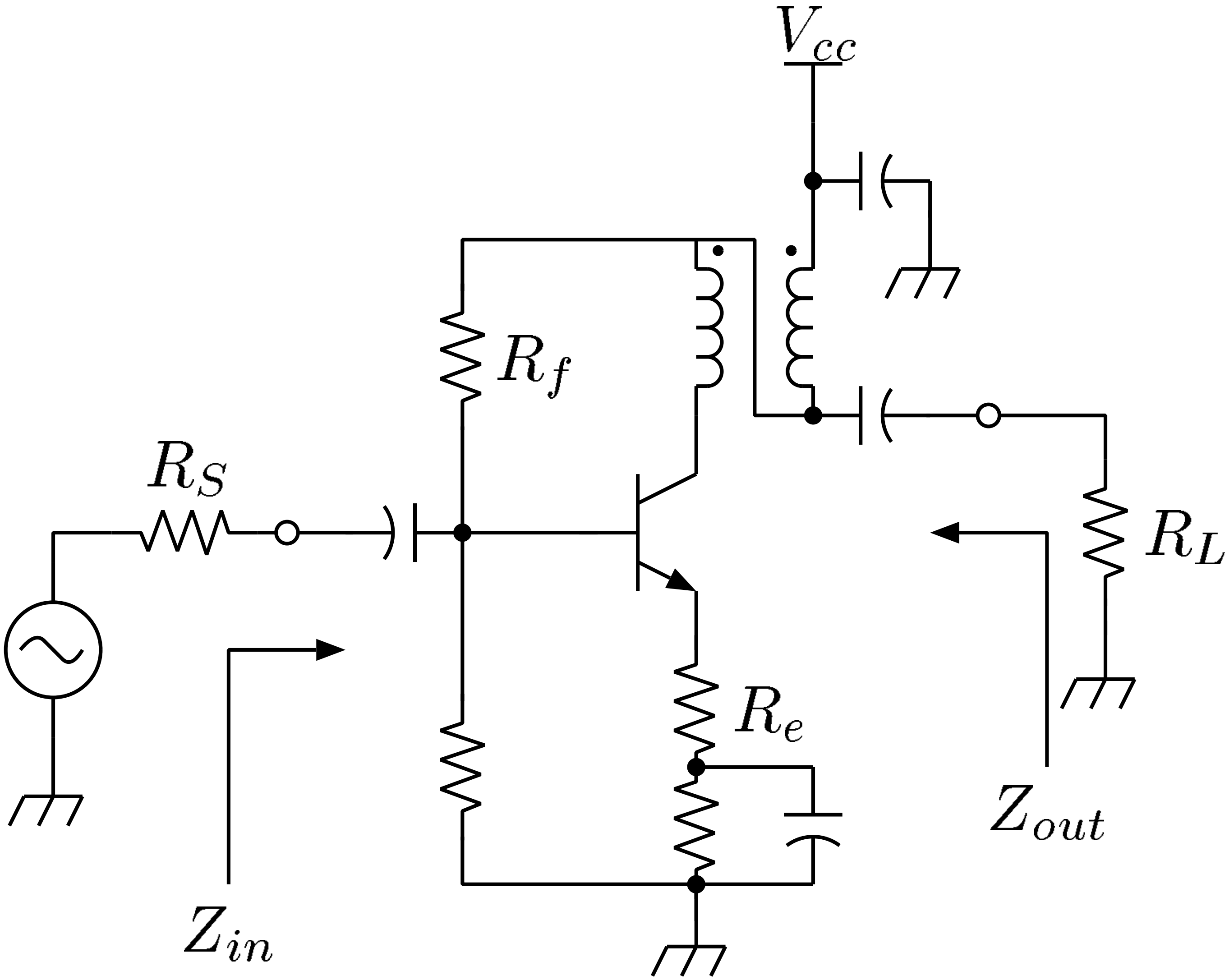
$V_{cc}$
$R_f$
$R_S$
$R_L$
$R_e$
$Z_{out}$
$Z_{in}$

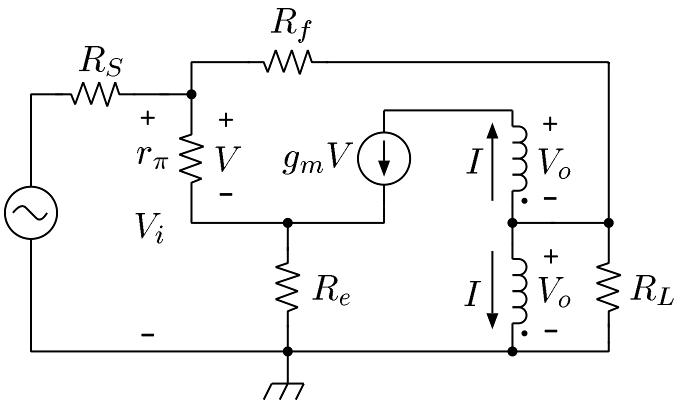
$R_f$
$R_S$
+
$r_\pi$
+
$V$
−
$g_mV$
$I$
+
$V_o$
−
$V_i$
$R_e$
$I$
+
$V_o$
−
$R_L$
−

Figure 7.22: Small signal model of amplifier with series and shunt feedback and 4:1 output transformer.

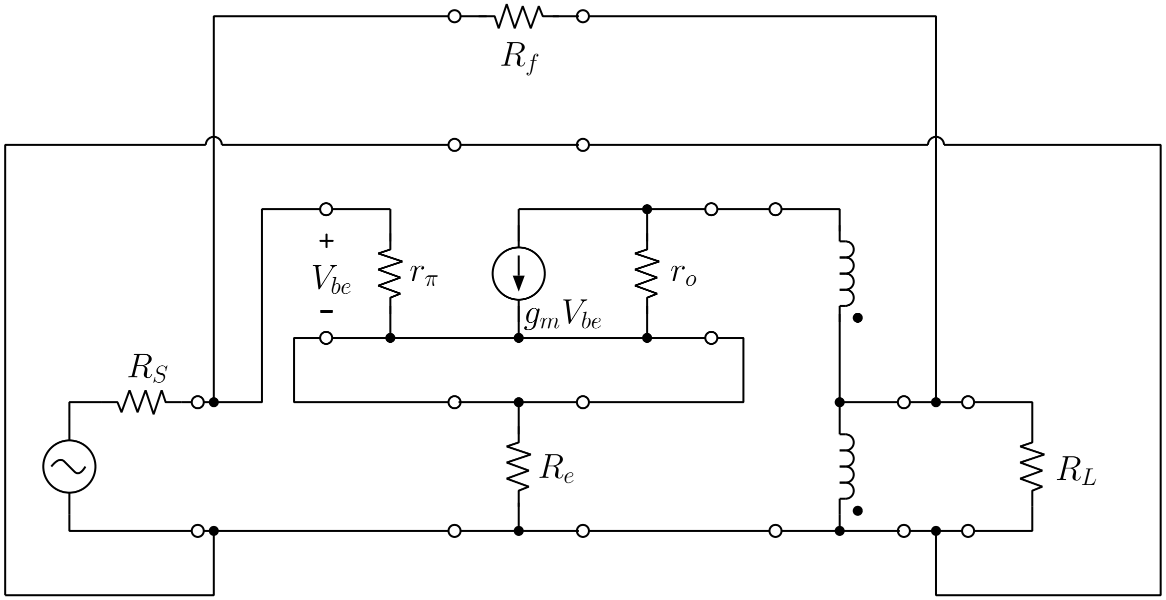
$R_f$
+
$V_{be}$
−
$r_\pi$
$g_mV_{be}$
$r_o$
$R_S$
$R_e$
$R_L$

Figure 7.23: Feedback amplifier drawn as a set of interconnected 2-ports.

## 8.4 Summary of useful S-parameter formulas

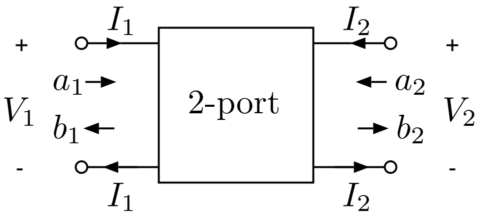

Relationship between impedance $Z_X$ ($X$ can be *in*, *out*, $S$, $L$) and reflection coefficient $\Gamma_X$ :

$$\Gamma_X = \frac{Z_X - Z_o}{Z_X + Z_o} \quad Z_X = Z_o \frac{1 + \Gamma_X}{1 - \Gamma_X}$$

Input reflection coefficient with arbitrary $Z_L$ :

$$\Gamma_{in} = S_{11} + \frac{S_{12}S_{21}\Gamma_L}{1 - S_{22}\Gamma_L}$$

Output reflection coefficient with arbitrary $Z_S$ :

$$\Gamma_{out} = S_{22} + \frac{S_{12}S_{21}\Gamma_S}{1 - S_{11}\Gamma_S}$$

Voltage gain with arbitrary $Z_L$ (voltage gain does not depend on $Z_S$):

$$A_V = \frac{V_2}{V_1} = \frac{S_{21}(1 + \Gamma_L)}{(1 + S_{11})(1 - S_{22}\Gamma_L) + S_{12}S_{21}\Gamma_L}$$

Current gain with arbitrary $Z_L$ (current gain does not depend on $Z_S$):

$$A_I = \frac{I_2}{I_1} = \frac{S_{21}(\Gamma_L - 1)}{(1 - S_{11})(1 - S_{22}\Gamma_L) - S_{12}S_{21}\Gamma_L}$$

Definitions of some commonly used quantities:

$$\begin{aligned}
D &= S_{11}S_{22} - S_{12}S_{21} \\
K &= \tfrac{1-|S_{11}|^2-|S_{22}|^2+|D|^2}{2|S_{12}S_{21}|} \\
B_1 &= 1 + |S_{11}|^2 - |D|^2 - |S_{22}|^2 \\
C_1 &= S_{11} - DS_{22}^* \\
B_2 &= 1 + |S_{22}|^2 - |D|^2 - |S_{11}|^2 \\
C_2 &= S_{22} - DS_{11}^*
\end{aligned}$$

A 2-port is unconditionally stable if:

$$K > 1 \text{ and } 1 - |S_{11}|^2 > |S_{12}S_{21}|$$

or, if:

$$K > 1 \text{ and } 1 - |S_{22}|^2 > |S_{12}S_{21}|$$

or, if:

$$K > 1 \text{ and } B_1 > 0$$

or, if:

$$K > 1 \text{ and } B_2 > 0$$

or, if:

$$K > 1 \text{ and } |D| < 1$$

or, if:

$$\mu_{ES} = \frac{1 - |S_{11}|^2}{|S_{22} - S_{11}^* D| + |S_{12}S_{21}|} > 1$$

or, if:

$$\mu'_{ES} = \frac{1 - |S_{22}|^2}{|S_{11} - S_{22}^* D| + |S_{12}S_{21}|} > 1$$

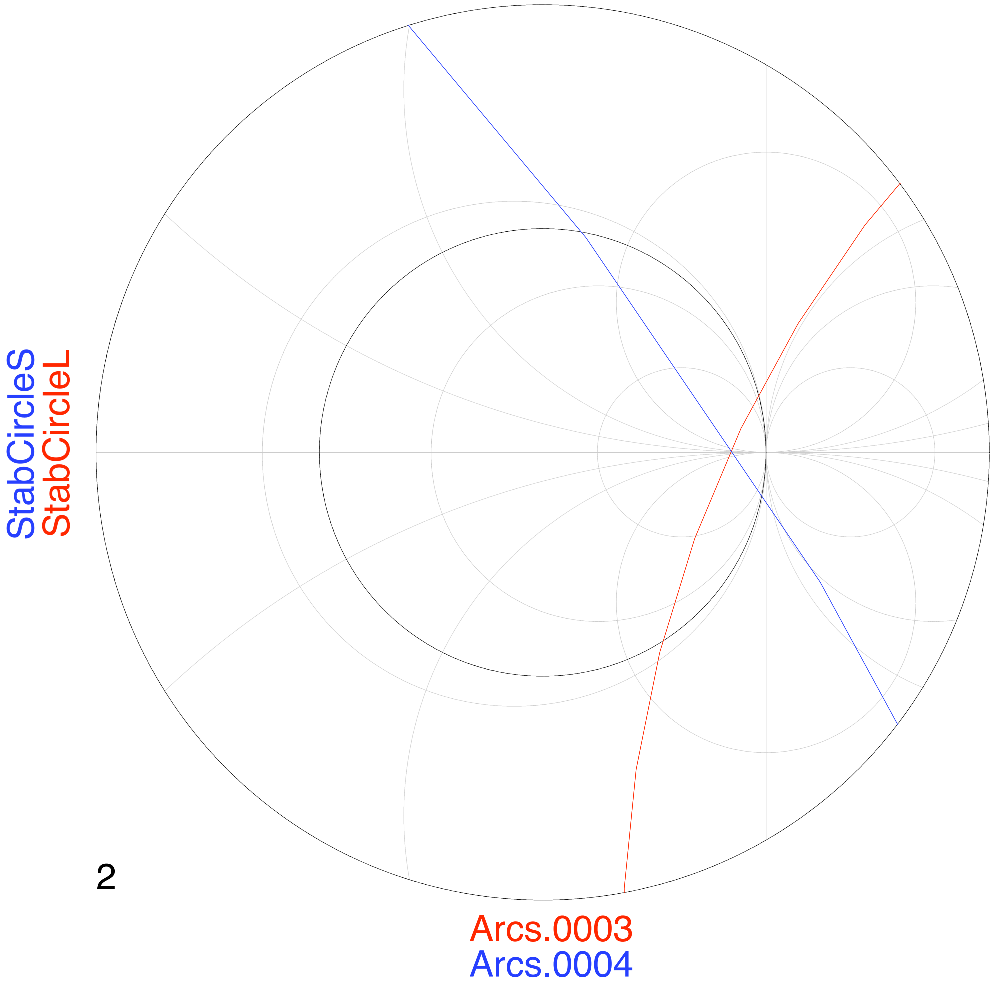
StabCircleS
StabCircleL
2
Arcs.0003
Arcs.0004

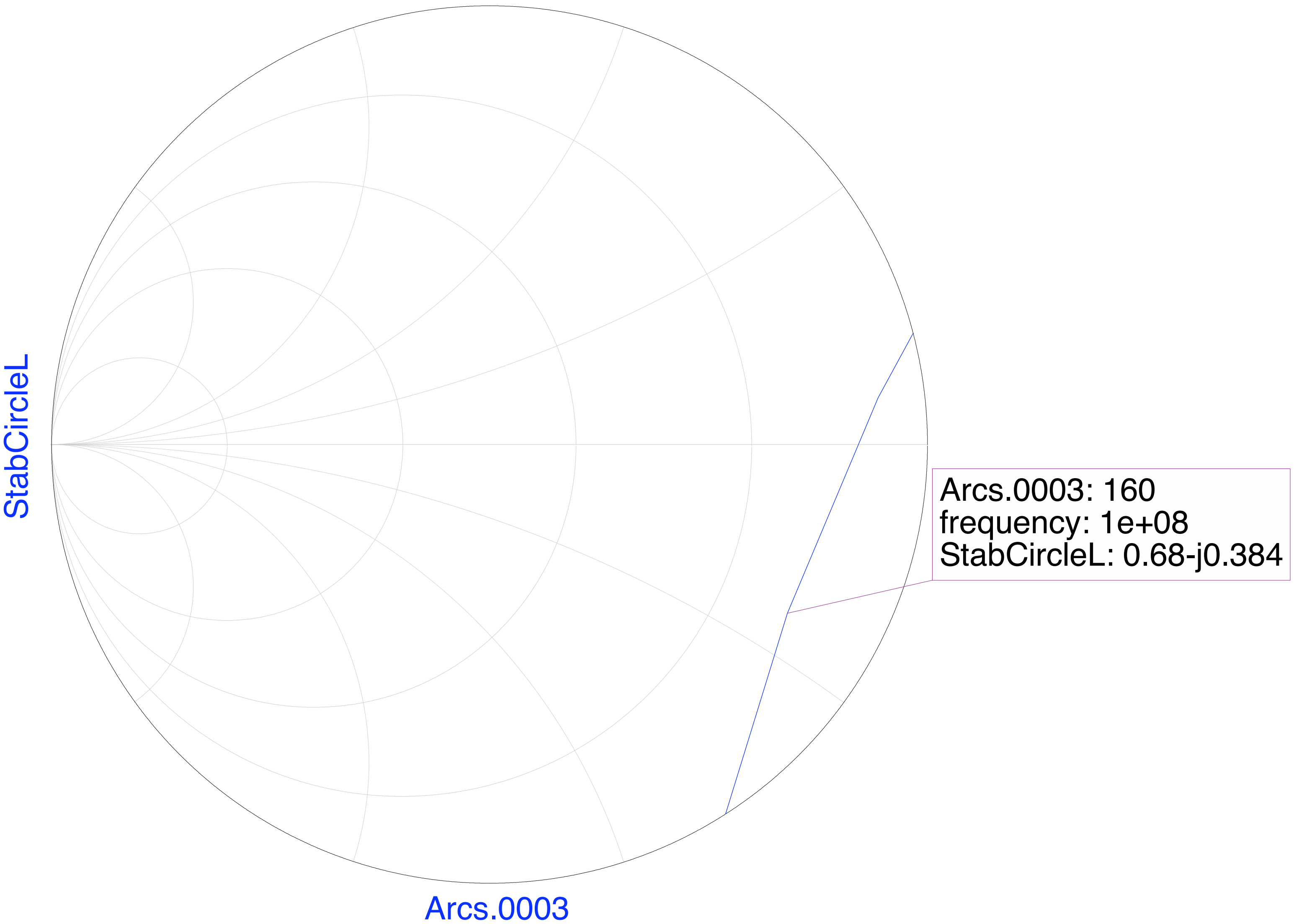
StabCircleL
Arcs.0003: 160
frequency: 1e+08
StabCircleL: 0.68-j0.384
Arcs.0003

## Amplifier with Gain = 20
## Minimum Parts

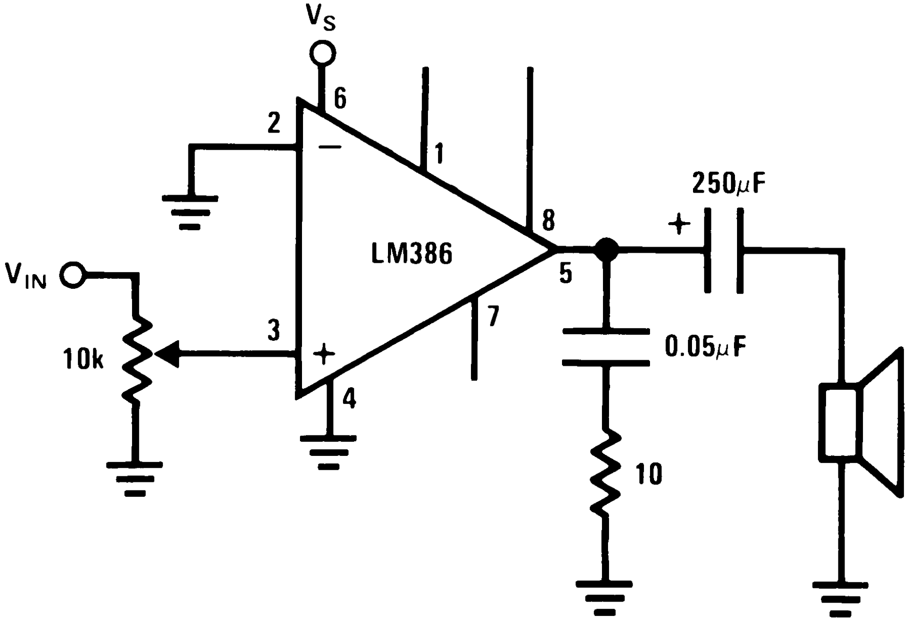
$V_S$
6
2
1
8
LM386
5
7
3
4
$V_{IN}$
10k
250μF
0.05μF
10

DS006976-3

JULY, 1928 PHYSICAL REVIEW VOLUME 32

# THERMAL AGITATION OF ELECTRICITY IN CONDUCTORS

BY J. B. JOHNSON

## ABSTRACT

*Statistical fluctuation of electric charge* exists in all conductors, producing random variation of potential between the ends of the conductor. The effect of these fluctuations has been measured by a vacuum tube amplifier and thermocouple, and can be expressed by the formula $\bar{I}^2=(2kT/\pi)\int_0^\infty R(\omega)|Y(\omega)|^2d\omega$. $I$ is the observed current in the thermocouple, $k$ is Boltzmann's gas constant, $T$ is the absolute temperature of the conductor, $R(\omega)$ is the *real* component of impedance of the conductor, $Y(\omega)$ is the transfer impedance of the amplifier, and $\omega/2\pi=f$ represents frequency. *The value of Boltzmann's constant* obtained from the measurements lie near the accepted value of this constant. *The technical aspects of the disturbance* are discussed. In an amplifier having a range of 5000 cycles and the input resistance $R$ the power equivalent of the effect is $\overline{V}^2/R=0.8\times10^{-16}$ watt, with corresponding power for other ranges of frequency. The least contribution of *tube noise* is equivalent to that of a resistance $R_c=1.5\times10^5 i_p/\mu$, where $i_p$ is the space current in milliamperes and $\mu$ is the effective amplification of the tube.

IN TWO short notes[1] a phenomenon has been described which is the result of spontaneous motion of the electricity in a conducting body. The electric charges in a conductor are found to be in a state of thermal agitation, in thermodynamic equilibrium with the heat motion of the atoms of the conductor. The manifestation of the phenomenon is a fluctuation of potential difference between the terminals of the conductor which can be measured by suitable instruments.

The effect is one of the causes of that disturbance which is called "tube noise" in vacuum tube amplifiers.[2] Indeed, it is often by far the larger part of the "noise" of a good amplifier. When such an amplifier terminates in a telephone receiver, and has a high resistance connected between the grid and

JULY, 1928 PHYSICAL REVIEW VOLUME 32

# THERMAL AGITATION OF ELECTRIC CHARGE IN CONDUCTORS*

BY H. NYQUIST

## ABSTRACT

*The electromotive force due to thermal agitation in conductors* is calculated by means of principles in thermodynamics and statistical mechanics. The results obtained agree with results obtained experimentally.

DR. J. B. JOHNSON[1] has reported the discovery and measurement of an electromotive force in conductors which is related in a simple manner to the temperature of the conductor and which is attributed by him to the thermal agitation of the carriers of electricity in the conductors. The work to be resported in the present paper was undertaken after Johnson's results were available to the writer and consists of a theoretical deduction of the electromotive force in question from thermodynamics and statistical mechanics.[2]

Consider two conductors each of resistance $R$ and of the same uniform temperature $T$ connected in the manner indicated in Fig. 1. The electromotive force due to thermal agitation in conductor I causes a current to be set up in the circuit whose value is obtained by dividing the electromotive force by $2R$. This current causes a heating or absorption of power in conductor II, the absorbed power being equal to the product of $R$ and the square of the current. In other words power is transferred from conductor I to conductor II. In

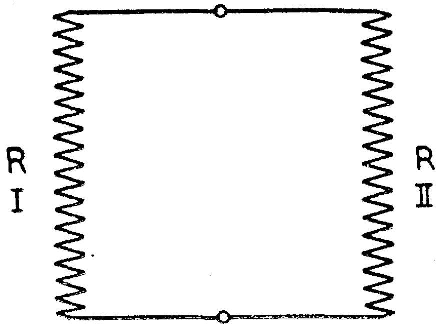

Fig. 1.

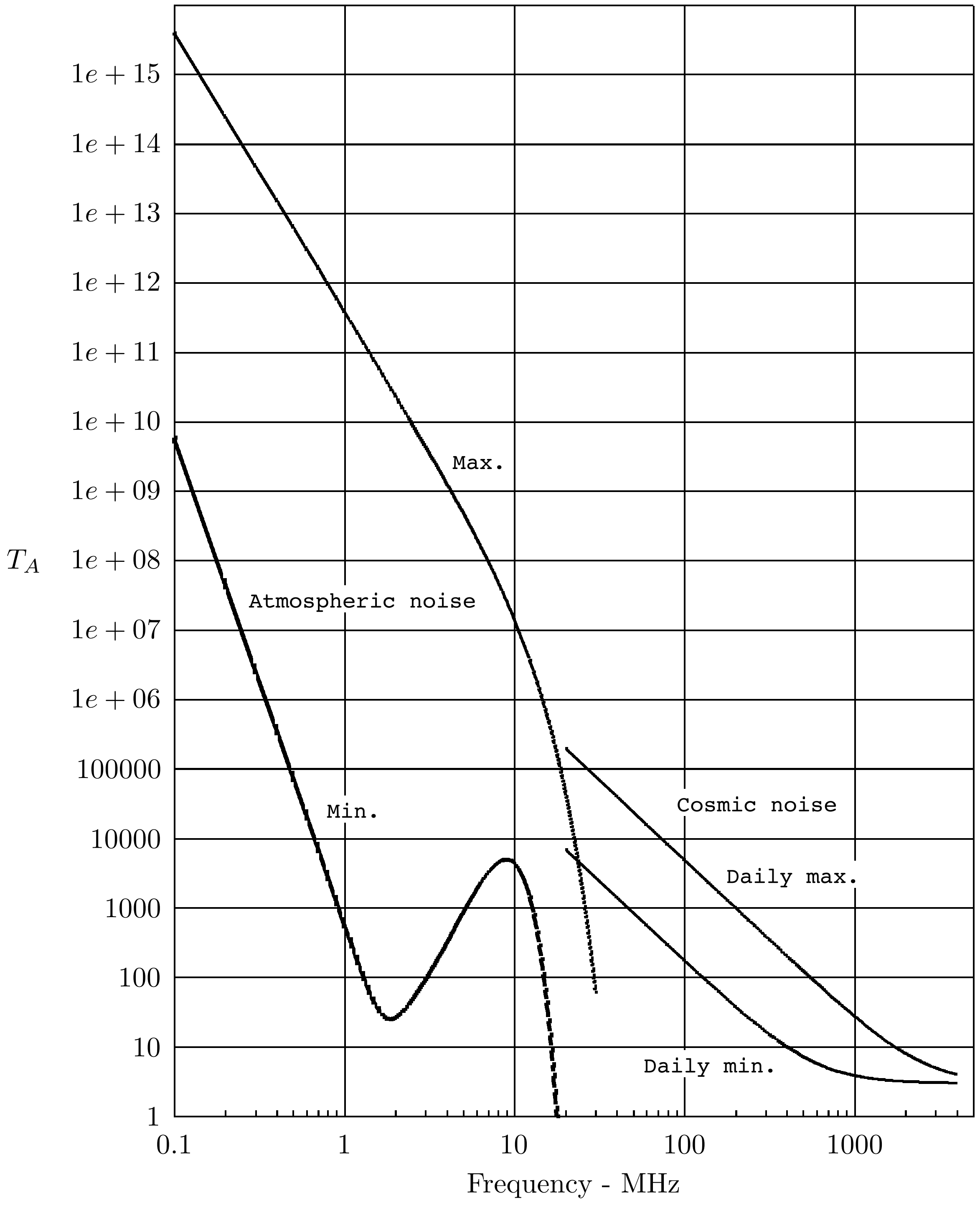
$T_A$
1e + 15
1e + 14
1e + 13
1e + 12
1e + 11
1e + 10
1e + 09
1e + 08
1e + 07
1e + 06
100000
10000
1000
100
10
1
0.1
1
10
100
1000
Frequency - MHz
Max.
Atmospheric noise
Min.
Cosmic noise
Daily max.
Daily min.

# www.setileague.org

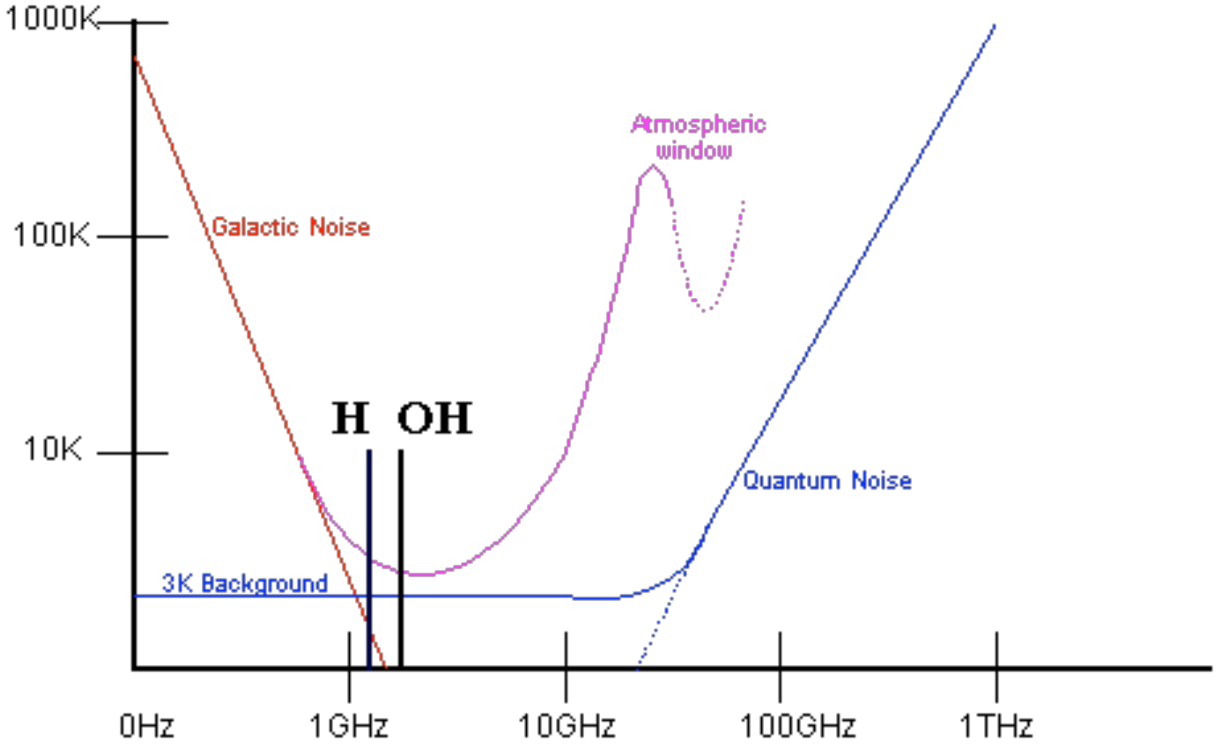

Toward the bottom of the microwave window, radiation from the precession of interstellar hydrogen is clearly heard in our receivers at a frequency of 1420.40575 MHz (corresponding to a wavelength around 21 cm). The Hydrogen Line, first detected by Ewen and Purcell at Harvard University in 1951, provided us with our first direct evidence that space is anything but an empty void...

Just a little way up the spectrum, near 1660 MHz (a wavelength of 18 cm), a team of scientists at MIT Lincoln Labs detected in the 1960s a cluster of radiation lines from interstellar hydroxyl ions (OH). Like the Hydrogen Line, the Hydroxyl Lines occur near the very quietest part of the radio spectrum. They too should be known to other civilizations which have studied the cosmos at radio frequencies.

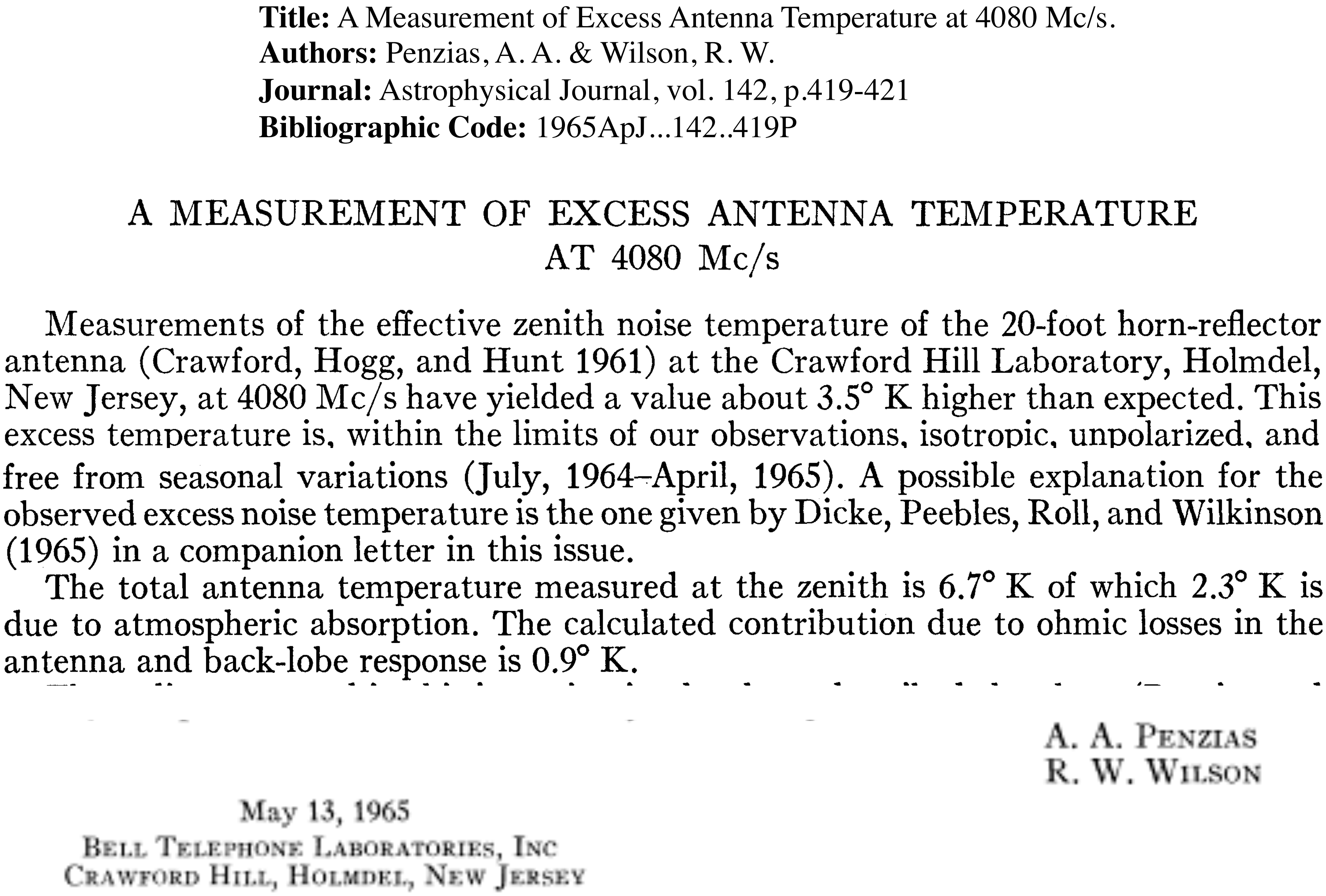

**Title:** A Measurement of Excess Antenna Temperature at 4080 Mc/s.
**Authors:** Penzias, A. A. & Wilson, R. W.
**Journal:** Astrophysical Journal, vol. 142, p.419-421
**Bibliographic Code:** 1965ApJ...142..419P

# A MEASUREMENT OF EXCESS ANTENNA TEMPERATURE AT 4080 Mc/s

Measurements of the effective zenith noise temperature of the 20-foot horn-reflector antenna (Crawford, Hogg, and Hunt 1961) at the Crawford Hill Laboratory, Holmdel, New Jersey, at 4080 Mc/s have yielded a value about 3.5° K higher than expected. This excess temperature is, within the limits of our observations, isotropic, unpolarized, and free from seasonal variations (July, 1964–April, 1965). A possible explanation for the observed excess noise temperature is the one given by Dicke, Peebles, Roll, and Wilkinson (1965) in a companion letter in this issue.

The total antenna temperature measured at the zenith is 6.7° K of which 2.3° K is due to atmospheric absorption. The calculated contribution due to ohmic losses in the antenna and back-lobe response is 0.9° K.

A. A. PENZIAS
R. W. WILSON

May 13, 1965
BELL TELEPHONE LABORATORIES, INC
CRAWFORD HILL, HOLMDEL, NEW JERSEY

Penzias and Wilson shared the Nobel Prize in Physics (1978) for their discovery of the cosmic microwave background radiation.

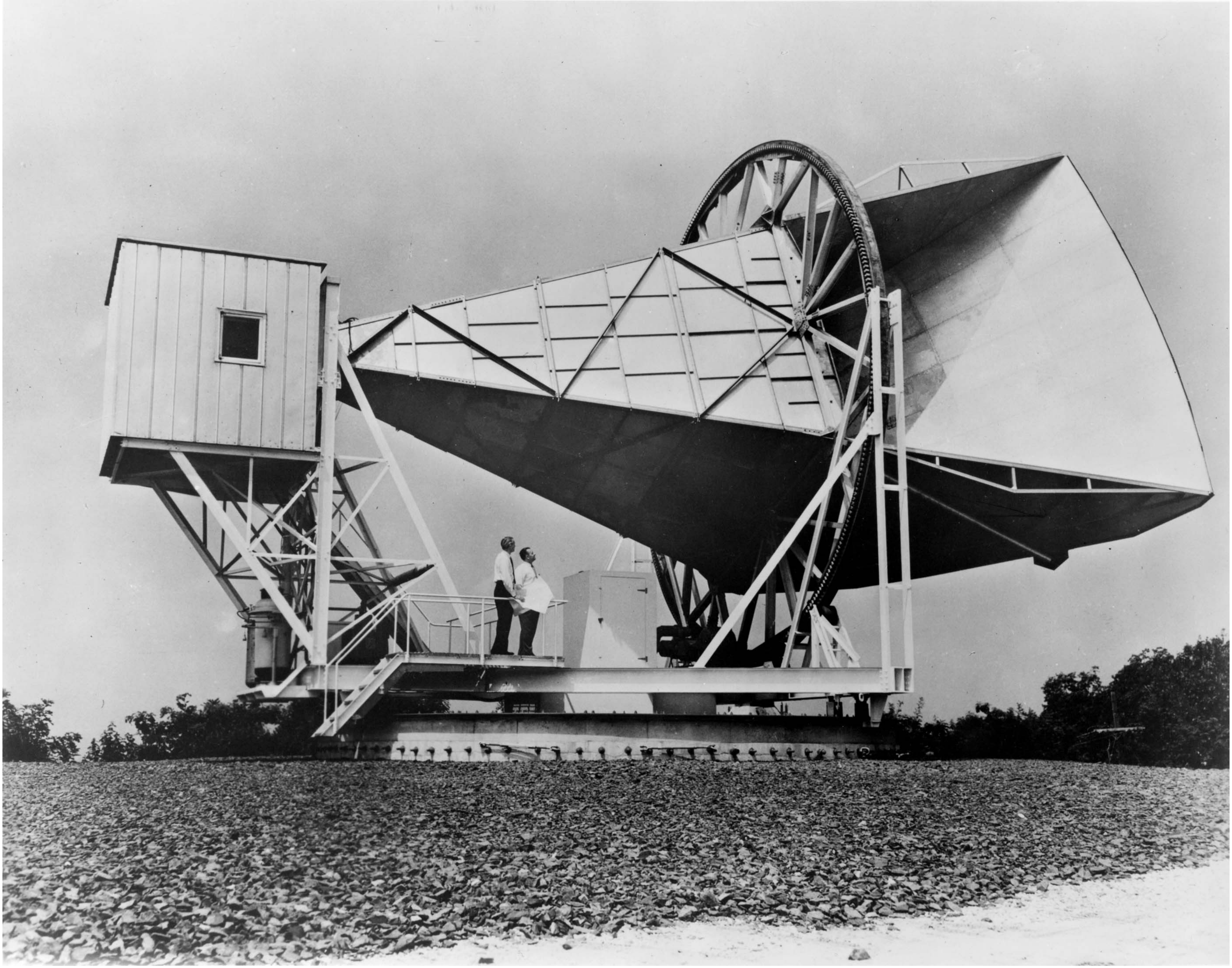

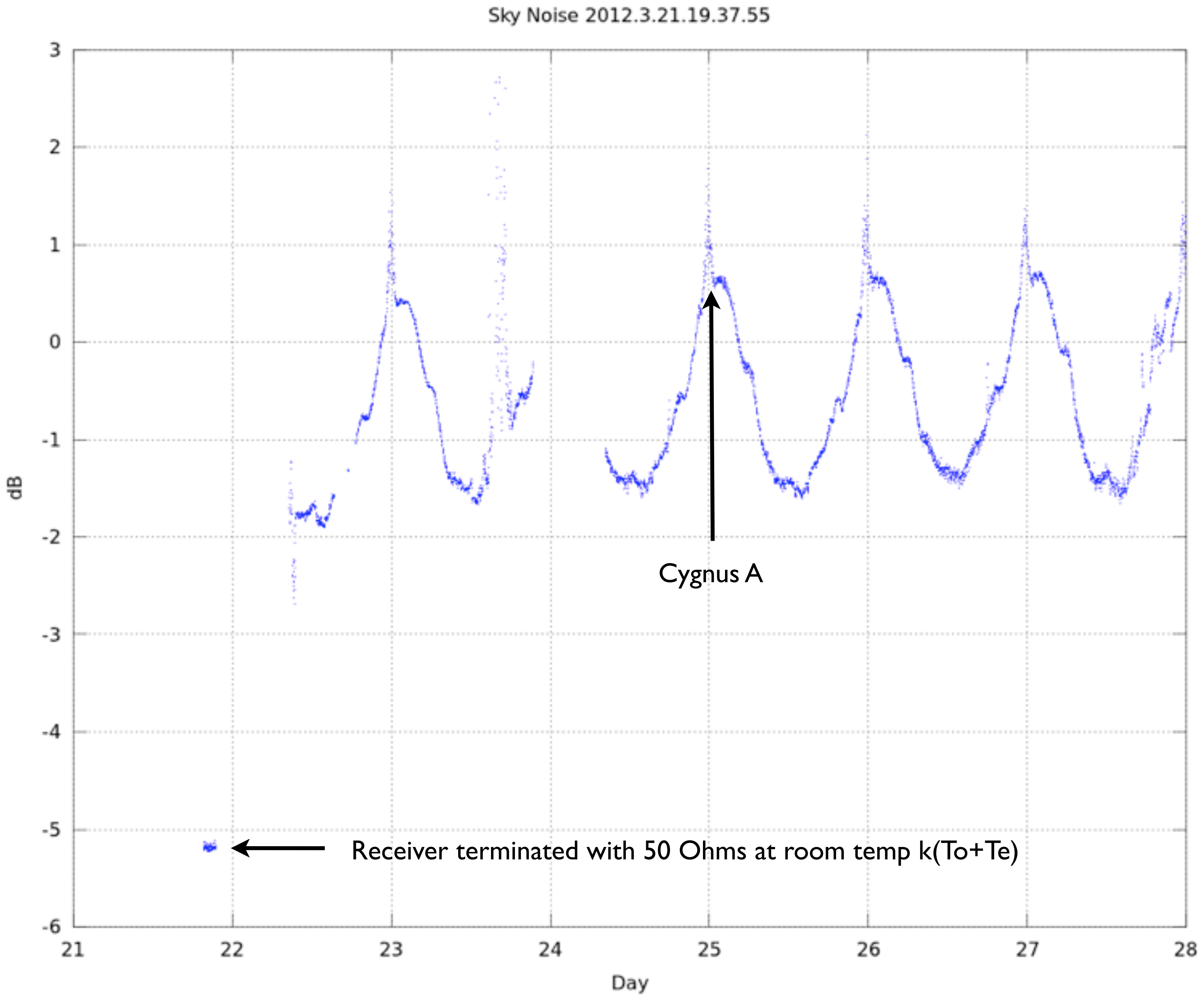
Sky Noise 2012.3.21.19.37.55
dB
3
2
1
0
-1
-2
-3
-4
-5
-6
Day
21
22
23
24
25
26
27
28
Cygnus A
Receiver terminated with 50 Ohms at room temp k(To+Te)

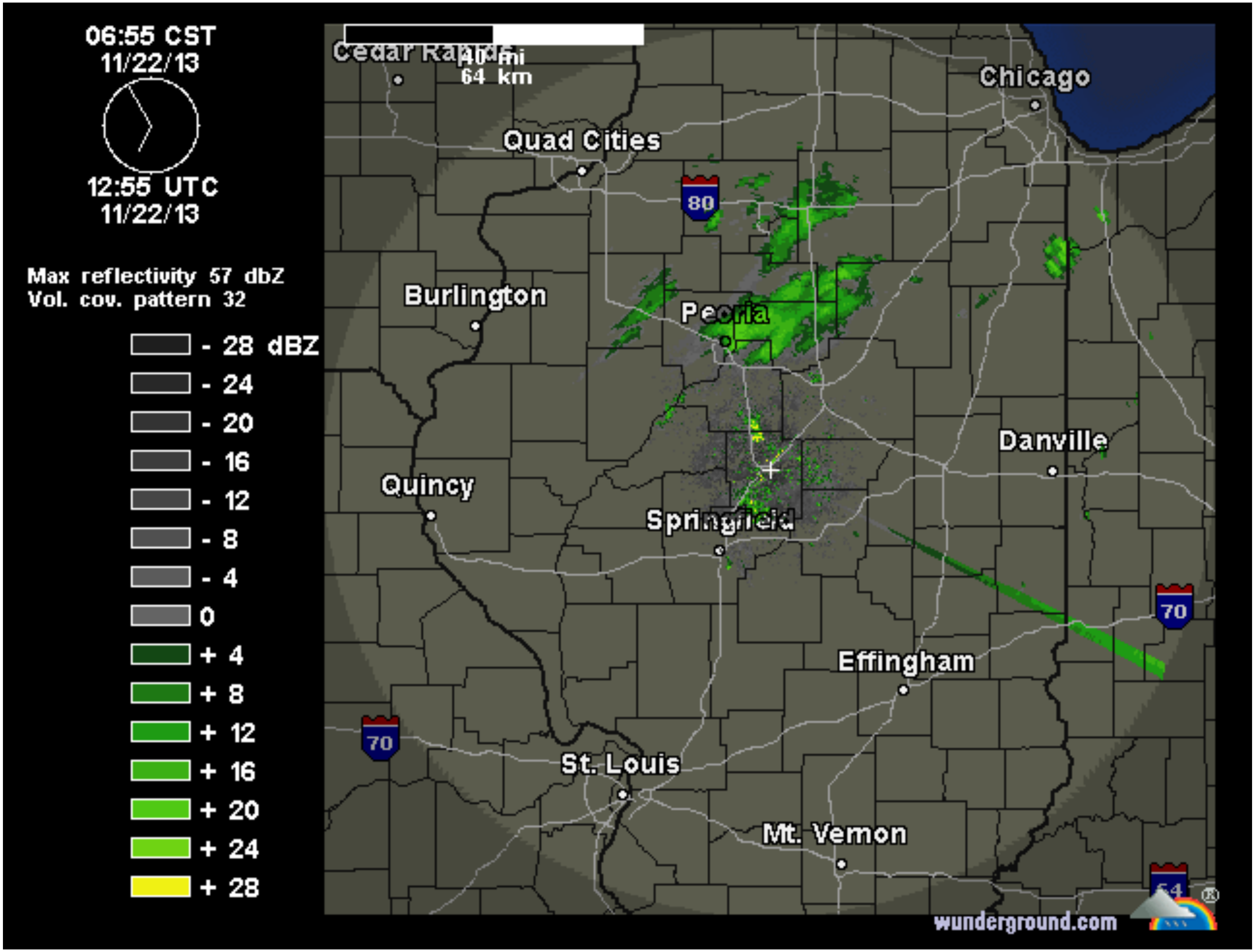
06:55 CST
11/22/13
12:55 UTC
11/22/13
Max reflectivity 57 dBZ
Vol. cov. pattern 32
- 28 dBZ
- 24
- 20
- 16
- 12
- 8
- 4
0
+ 4
+ 8
+ 12
+ 16
+ 20
+ 24
+ 28
40 mi
64 km
Cedar Rapids
Chicago
Quad Cities
80
Burlington
Peoria
Danville
Quincy
Springfield
70
Effingham
70
St. Louis
Mt. Vernon
64
wunderground.com

Effective input temperature, $T_e$, is used to refer, or re-assign, all 2-port noise to the source.

A more fundamental model re-assigns the 2-port noise to a noise voltage source and a noise current source at the input of the 2-port.

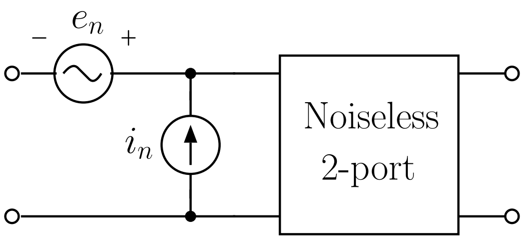

If the input-referred voltage and current sources are assigned to a noiseless source impedance ($Z_S$), then the noise power available from the source can be written in terms of the source impedance, rms voltage and current noise ($\sigma_e$, $\sigma_i$) and their complex correlation coefficient ($\gamma = \gamma_r + j\gamma_i$).

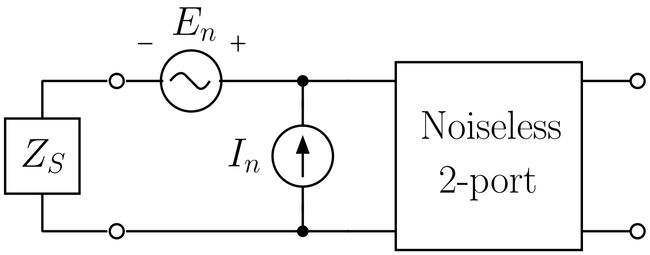

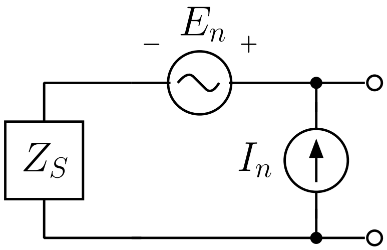

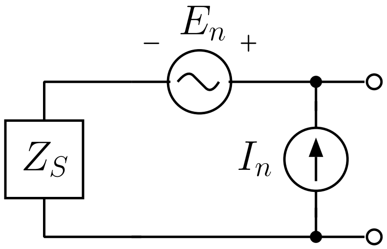

When $|Z_S| \to \infty$ all noise comes from current source.

When $|Z_S| \to 0$ all noise comes from voltage source.

When $|Z_S|$ is finite, both voltage and current noise contribute.

$$T_e = \frac{\sigma_i^2}{4kR_S}\{(R_S + \gamma_r \frac{\sigma_e}{\sigma_i})^2 + (X_S - \gamma_i \frac{\sigma_e}{\sigma_i})^2 + \frac{\sigma_e^2}{\sigma_i^2}(1 - |\gamma|^2)\}.$$

$$T_e = T_{e,min} + T_o G_n \frac{|Z_S - Z_{opt}|^2}{R_S}$$

$$Z_{opt} = R_{opt} + jX_{opt} = \frac{\sigma_e}{\sigma_i}\sqrt{1-\gamma_i^2} + j\gamma_i \frac{\sigma_e}{\sigma_i}$$

$$T_{e,min} = \frac{\sigma_e \sigma_i}{2k}\{\sqrt{1-\gamma_i^2} + \gamma_r\}.$$

$$G_n = \frac{\sigma_i^2}{4kT_o}.$$

$$\begin{aligned} T_e &= T_{e,min} + 4G_n Z_o T_o \tfrac{|\Gamma_s - \Gamma_{opt}|^2}{(1-|\Gamma_s|^2)|1-\Gamma_{opt}|^2} \\ &= T_{e,min} + 4\tfrac{R_n}{Z_o} T_o \tfrac{|\Gamma_s - \Gamma_{opt}|^2}{(1-|\Gamma_s|^2)|1+\Gamma_{opt}|^2} \end{aligned}$$

where

$$\Gamma_S = \frac{Z_S - Z_o}{Z_S + Z_o} = \text{ actual source reflection coefficient}$$

$$\Gamma_{opt} = \frac{Z_{opt} - Z_o}{Z_{opt} + Z_o} = \text{ optimum source reflection coefficient}$$

$$R_n = \frac{\sigma_e^2}{4kT_o} = \text{ noise resistance}$$

*Technical Data*

*MBC13900/D*
*Rev. 0, 06/2002*

*NPN Silicon*
*Low Noise Transistor*

MOTOROLA
intelligence everywhere™

digital dna™

# MBC13900

(Scale 2:1)

**Package Information**
Plastic Package
Case 318M
(SOT-343)

**Ordering Information**

| Device | Marking | Package |
|---|---|---|
| MBC13900T1 | 900 | SOT-343 |

Freescale Semiconductor, Inc.

The MBC13900 is a high performance transistor fabricated using Motorola’s 15 GHz $f_\tau$ bipolar IC process. It is housed in the 4-lead SC-70 (SOT-343) surface mount plastic package resulting in a parasitic effect reduction and RF performance enhancements. The high performance at low power makes the MBC13900 suitable for front-end applications in portable wireless systems such as pagers, cellular and cordless phones.

- Low Noise Figure, $NF_{min}$ = 0.8 dB (Typ) @ 0.9 GHz, 2.0 V and 5.0 mA
- Maximum Stable Gain, 22 dB @ 0.9 GHz, 2.0 V and 5.0 mA
- Output Third Order Intercept, OIP3 = 18 dBm (Typ) @ 2.0 V and 5.0 mA
- Ultra small SOT-343 Surface Mount Package
- Available Only in Tape and Reel Packaging

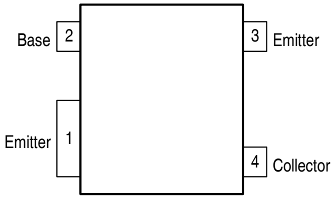

**Figure 1. Pin Connections**

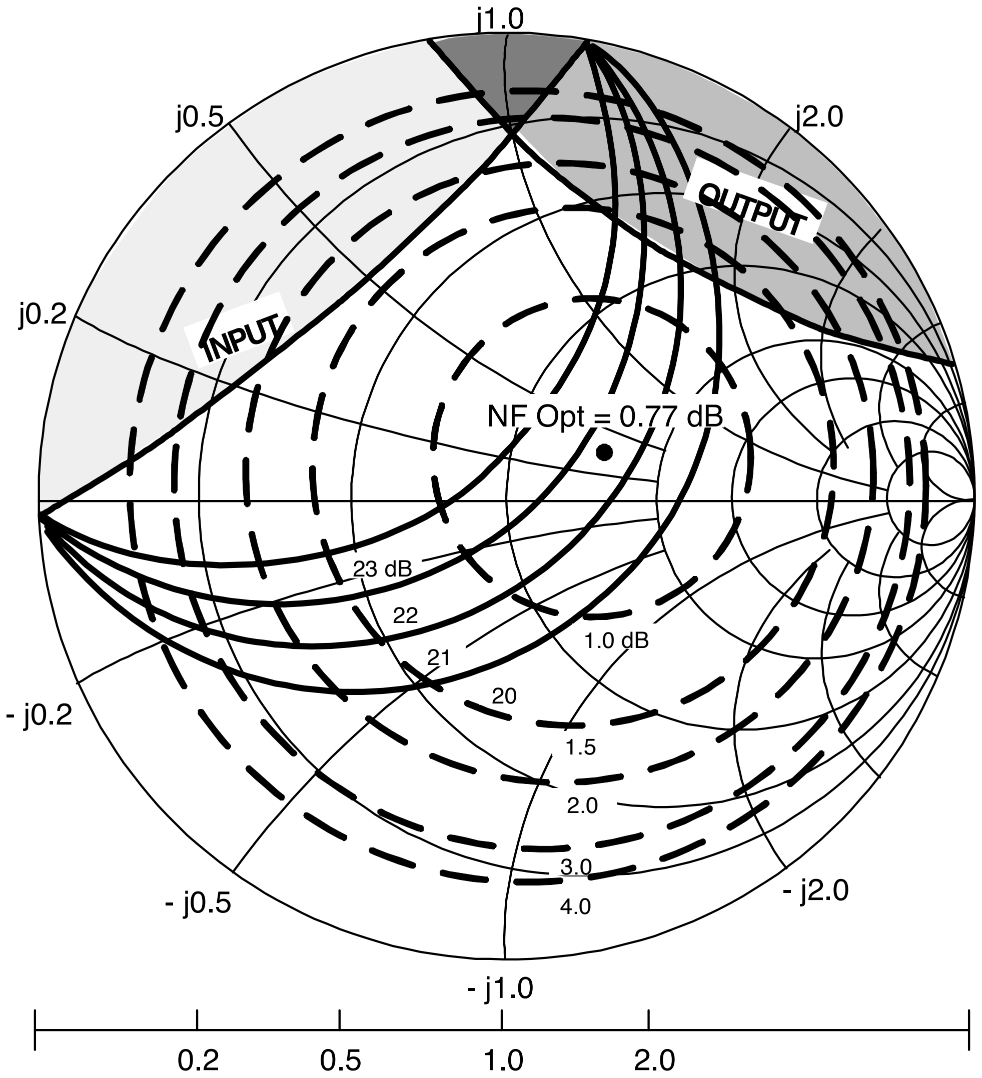

$V_{CE} = 2.0$ V

$I_C = 5.0$ mA

▨ ---Potentially Unstable

| f (GHz) | NF Opt (dB) | $\Gamma_O$ | Rn | K |
|---|---|---|---|---|
| 0.9 | 0.77 | $0.24 \angle 25.2^\circ$ | 8.5 | 0.48 |

**Figure 23. Constant Gain and Noise Figure Contours (f = 900 MHz)**

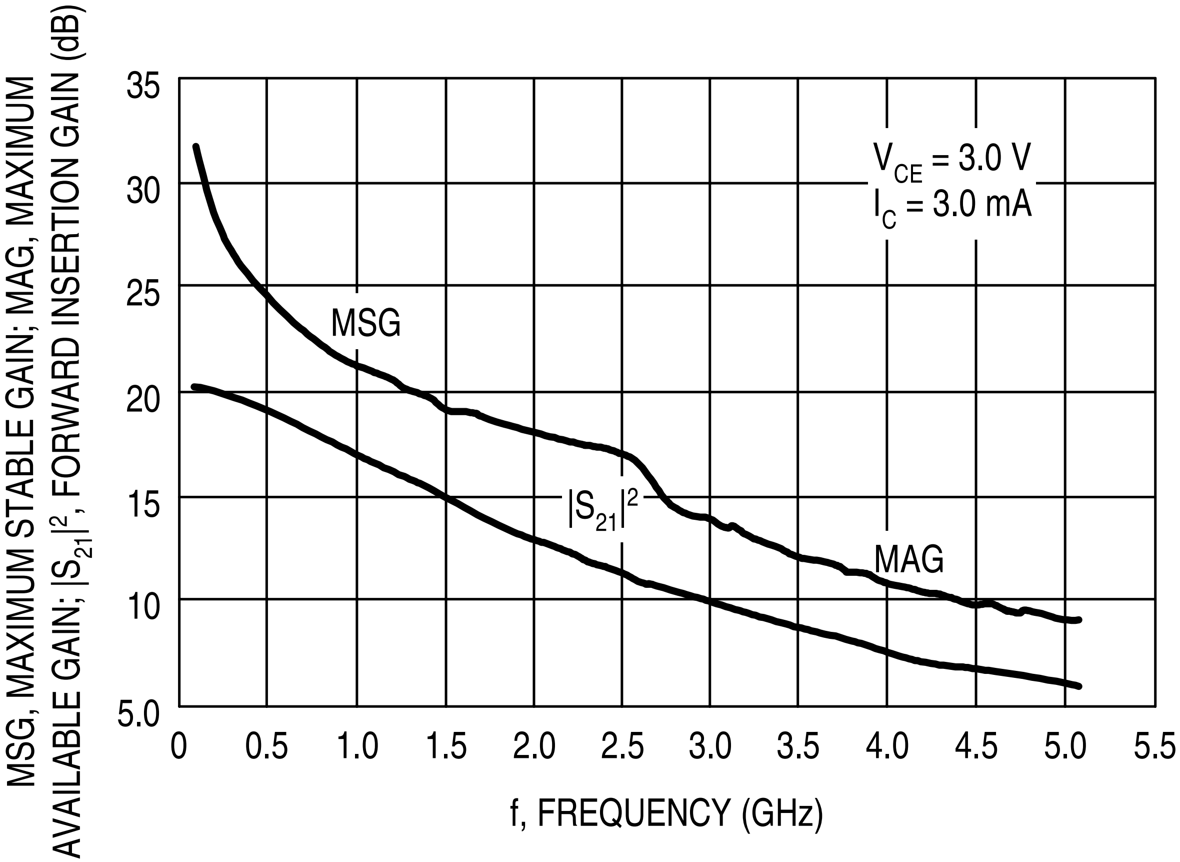

**Figure 7. Maximum Stable/Available gain and Forward Insertion Gain versus Frequency**

National Semiconductor

March 1987

# LM387/LM387A Low Noise Dual Preamplifier

## General Description

The LM387 is a dual preamplifier for the amplification of low level signals in applications requiring optimum noise performance. Each of the two amplifiers is completely independent, with an internal power supply decoupler-regulator, providing 110 dB supply rejection and 60 dB channel separation. Other outstanding features include high gain (104 dB), large output voltage swing ($V_{CC}$ − 2V)p-p, and wide power bandwidth (75 kHz, 20 Vp-p). The LM387A is a selected version of the LM387 that has lower noise in a NAB tape circuit, and can operate on a larger supply voltage. The LM387 operates from a single supply across the wide range of 9V to 30V, the LM387A operates on a supply of 9V to 40V.

The amplifiers are internally compensated for gains greater than 10. The LN387, LM387A is available in an 8-lead dual-in-line package. The LM387, LM387A is biased like the LM381. See AN-64 and AN-104.

## Features

| | |
|---|---|
| ■ Low noise | 1.0 $\mu$V total input noise |
| ■ High gain | 104 dB open loop |
| ■ Single supply operation | |
| ■ Wide supply range LM387 | 9 to 30V |
| LM387A | 9 to 40V |
| ■ Power supply rejection | 110 dB |
| ■ Large output voltage swing ($V_{CC}$ − 2V)p-p | |
| ■ Wide bandwidth 15 MHz unity gain | |
| ■ Power bandwidth 75 kHz, 20 Vp-p | |
| ■ Internally compensated | |
| ■ Short circuit protected | |
| ■ Performance similar to LM381 | |

# Typical Applications

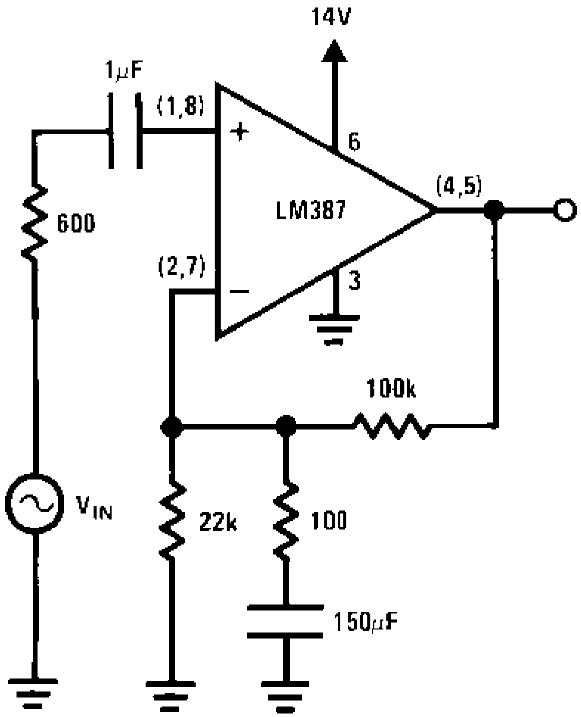
14V
1µF
(1,8)
+
6
(4,5)
LM387
600
(2,7)
−
3
100k
V_IN
22k
100
150µF

TL/H/7845–3

FIGURE 1. Flat Gain Circuit ($A_V = 1000$)

©1995 National Semiconductor Corporation

# Typical Performance Characteristics

$V_{CC}$ vs $I_{CC}$

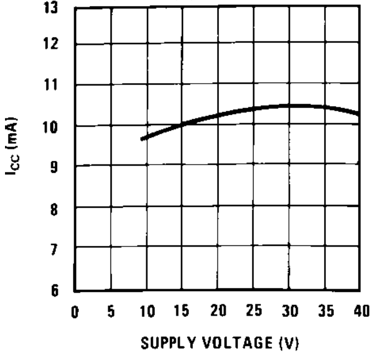

Gain and Phase Response

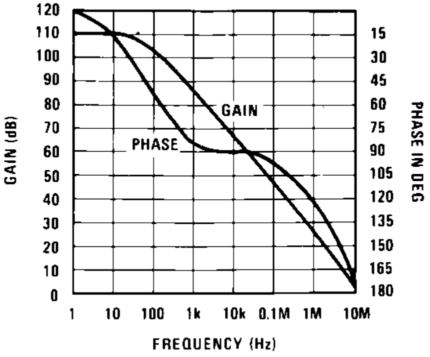

Large Signal Frequency Response

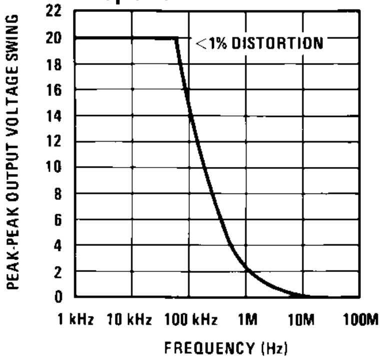

PSRR vs Frequency (Input Referred)

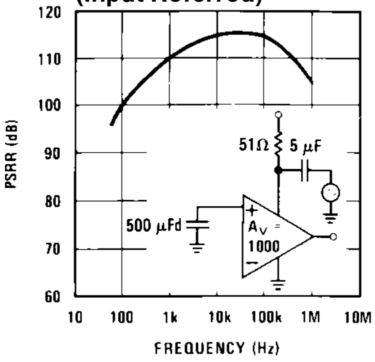

Channel Separation

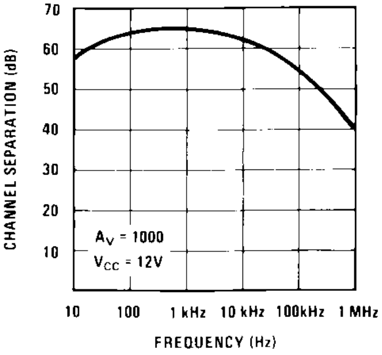

Distortion vs Frequency Non-Inverting Amplifier

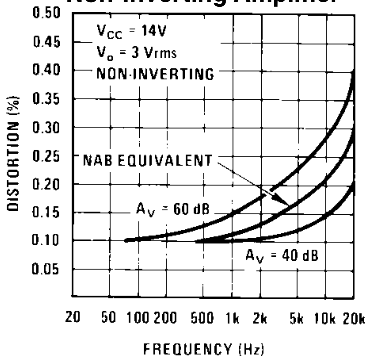

Noise Voltage vs Frequency

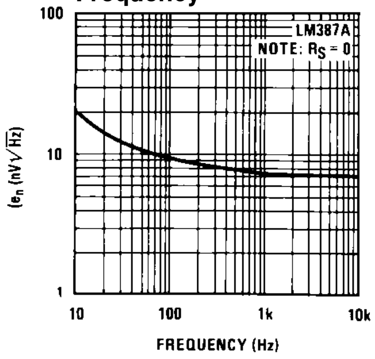

Noise Current vs Frequency

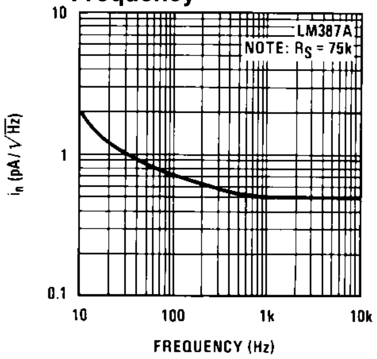

Distortion vs Frequency Inverting Amplifier

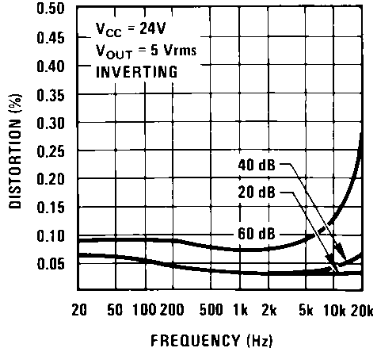

TL/H/7845–7

## Noise Voltage vs Frequency

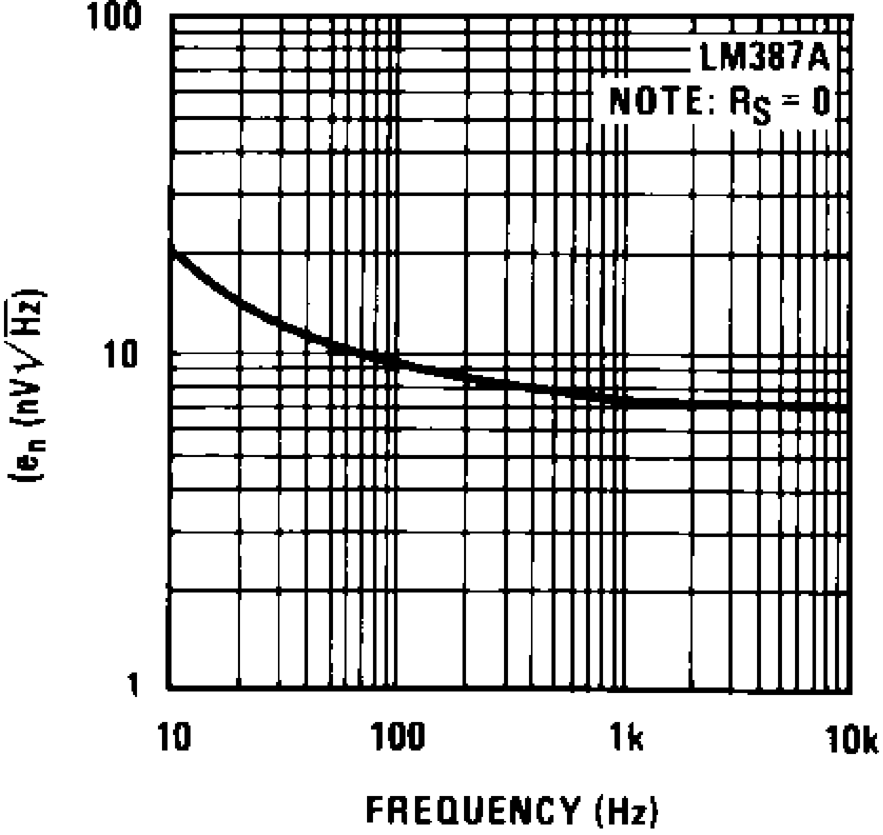

## Noise Current vs Frequency

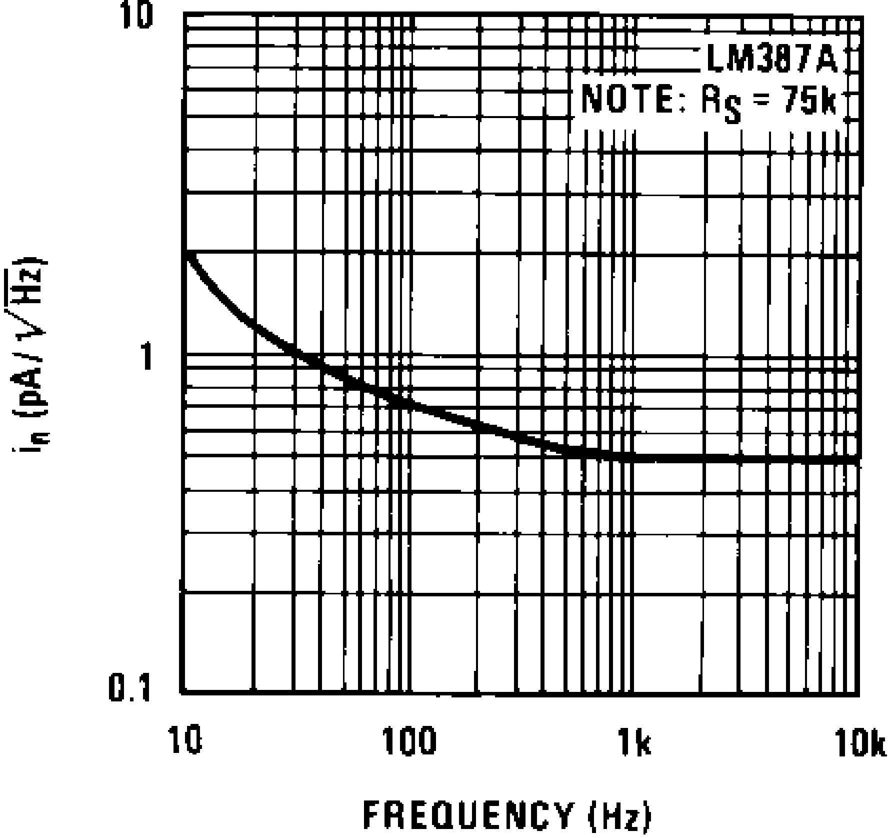

19-1303; Rev 0; 10/97

EVALUATION KIT
AVAILABLE

# Low-Cost Downconverter with Low-Noise Amplifier

## General Description

The MAX2406 low-noise amplifier (LNA)/downconverter mixer is designed for use over a wide range of frequencies and is optimized for communications systems operating at a frequency of 1.9GHz. Applications include PWT1900/DCT1900, DCS1800/PCS1900, PHS, and DECT. This device includes an LNA, a downconverter mixer, and a local-oscillator (LO) buffer in a low-cost, plastic surface-mount package. At 1.9GHz, the LNA has 2.5dB typical noise figure and a -9.5dBm input third-order intercept point (IP3). The downconverter mixer has a low 9.1dB noise figure and a 4.5dBm input IP3. Image and LO filtering are implemented off-chip for maximum flexibility.

The MAX2406 has a differential IF port that can be used in a single-ended configuration by tying the unused side to $V_{CC}$. The LO buffer can be driven differentially or in a single-ended configuration with only -10dBm of LO power. Power consumption is 60mW in receive mode, and typically drops to less than 1µW in shutdown mode.

For transceiver applications, the MAX2410 or MAX2411A both offer a transmitter along with a similar receiver.

## Applications

PWT1900/DCT1900
DCS1800/PCS1900
PHS/PACS
DECT

## Features

- **Integrated LNA/Downconverter**
- **3.2dB Combined Receiver Noise Figure:**
  - **2.5dB (LNA)**
  - **9.1dB (mixer)**
- **-12.5dBm Combined Receiver Input IP3:**
  - **-9.5dBm (LNA)**
  - **4.5dBm (mixer)**
- **LO Buffer**
- **+2.7V to +5.5V Single-Supply Operation**
- **60mW Power Consumption**
- **Low-Power Shutdown Mode**

## Ordering Information

| PART | TEMP. RANGE | PIN-PACKAGE |
|---|---|---|
| MAX2406EEP | -40°C to +85°C | 20 QSOP |

## Typical Application Functional Diagram

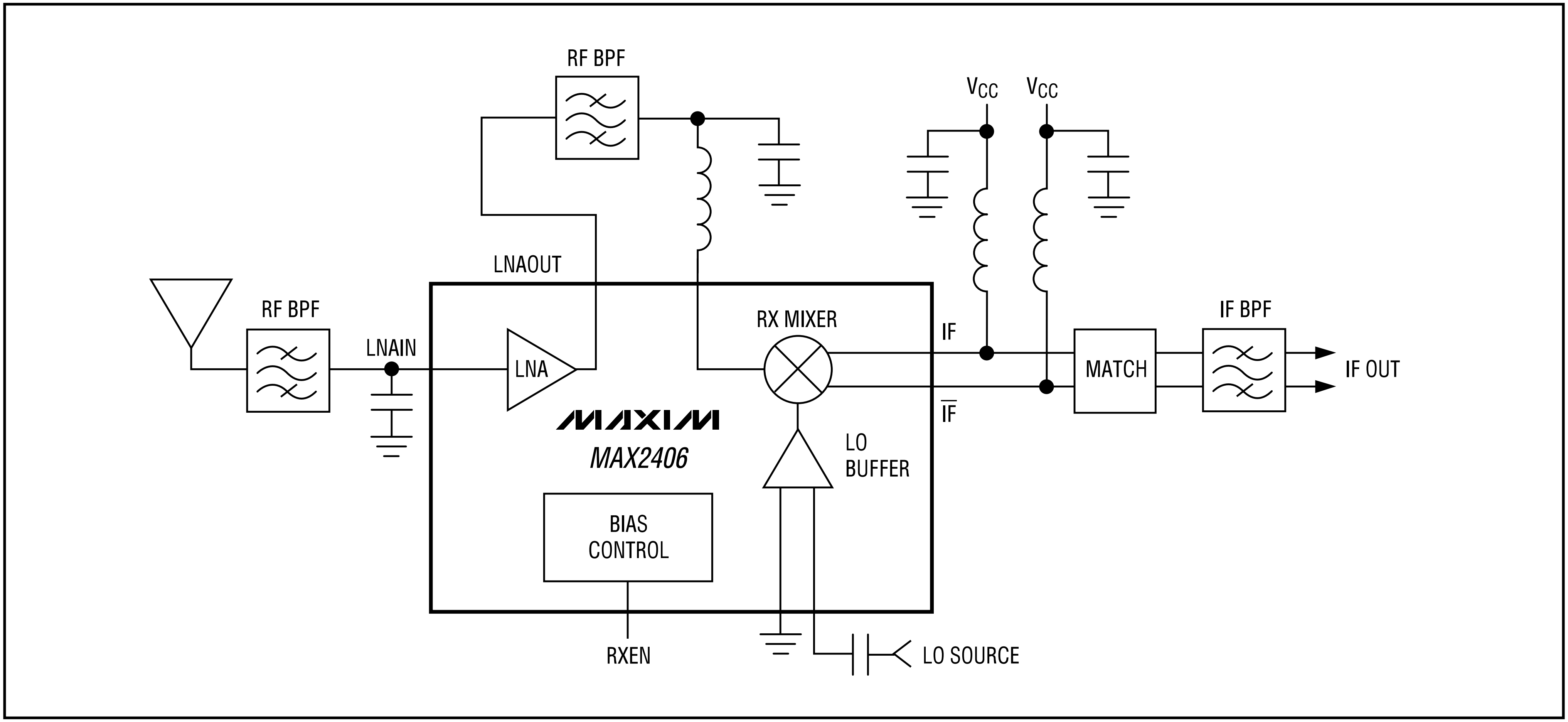
RF BPF
RF BPF
LNAIN
LNAOUT
LNA
MAXIM
MAX2406
BIAS CONTROL
RXEN
RX MIXER
LO BUFFER
LO SOURCE
$V_{CC}$
$V_{CC}$
IF
$\overline{IF}$
MATCH
IF BPF
IF OUT

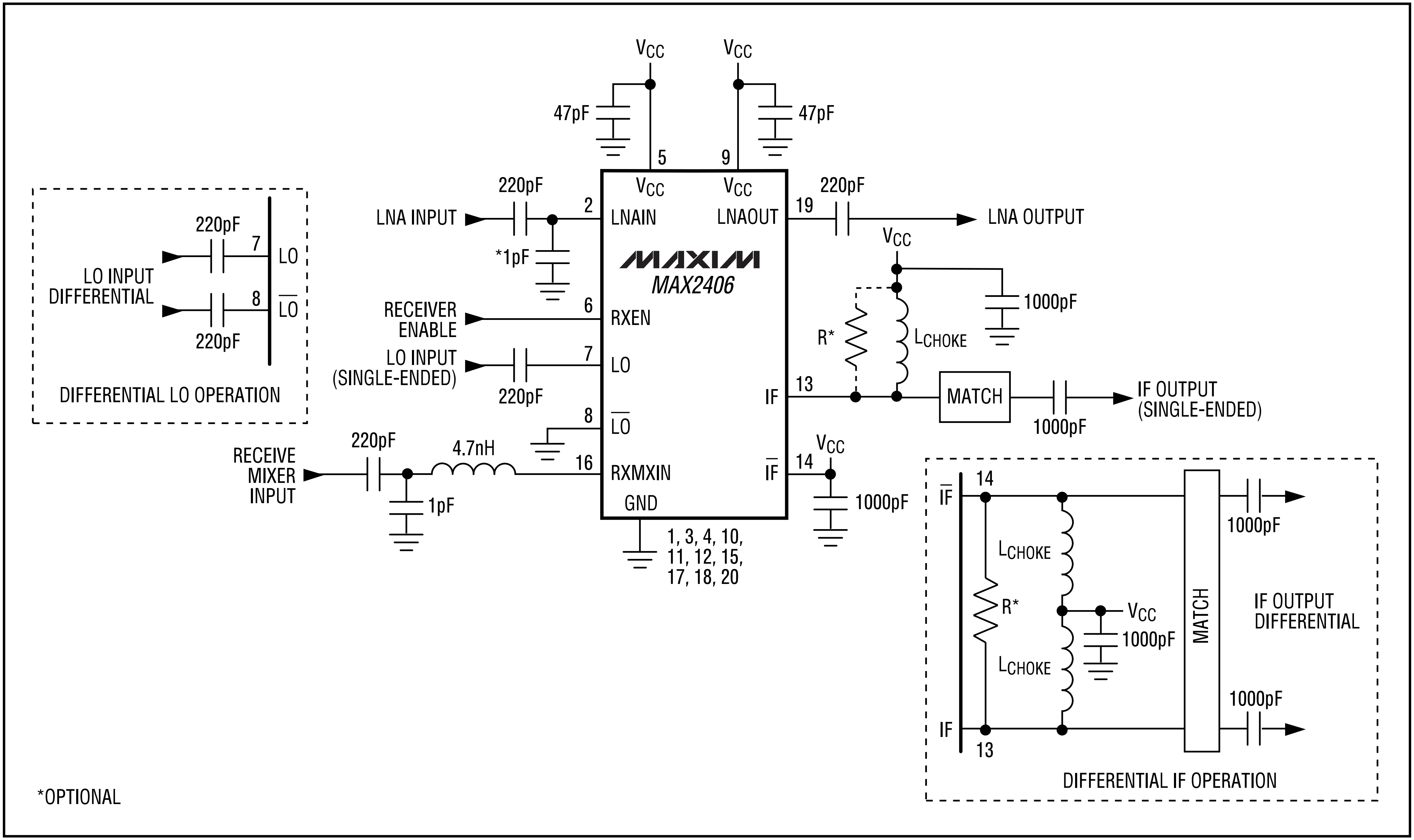
VCC
VCC
47pF
47pF
5
9
VCC
VCC
220pF
2
LNAIN
LNAOUT
19
220pF
LNA INPUT
LNA OUTPUT
*1pF
MAX2406
VCC
1000pF
RECEIVER ENABLE
6
RXEN
R*
LCHOKE
LO INPUT (SINGLE-ENDED)
7
LO
220pF
13
IF
MATCH
IF OUTPUT (SINGLE-ENDED)
1000pF
8
LO
RECEIVE MIXER INPUT
220pF
4.7nH
16
RXMXIN
IF
14
VCC
1pF
GND
1000pF
1, 3, 4, 10, 11, 12, 15, 17, 18, 20
220pF
7
LO
LO INPUT DIFFERENTIAL
8
LO
220pF
DIFFERENTIAL LO OPERATION
IF
14
1000pF
LCHOKE
R*
VCC
1000pF
MATCH
IF OUTPUT DIFFERENTIAL
LCHOKE
1000pF
IF
13
DIFFERENTIAL IF OPERATION
*OPTIONAL

*Figure 1. MAX2406 Typical Operating Circuit*

## AC ELECTRICAL CHARACTERISTICS

(MAX2406EVKIT, Rev. B, $V_{CC}$ = 3.0V, RXEN = $V_{CC}$, $f_{LO}$ = 1.5GHz, $f_{LNAIN}$ = $f_{RXMXIN}$ = 1.9GHz, $P_{LNAIN}$ = -30dBm, $P_{RXMXIN}$ = -21.5dBm, $P_{LO}$ = -10dBm, differential IF operation, 50Ω system, $T_A$ = +25°C, unless otherwise noted.)

| PARAMETER | CONDITIONS | MIN | TYP | MAX | UNITS |
|---|---|---|---|---|---|
| LNA Gain (Note 1) | $T_A$ = +25°C | 13.6 | 16 | 17.6 | dB |
| | $T_A$ = $T_{MIN}$ to $T_{MAX}$ | 12.2 | | 18.8 | |
| LNA Noise Figure | | | 2.5 | | dB |
| LNA Input IP3 | (Note 2) | | -9.5 | | dBm |
| LNA Output 1dB Compression | | | -5.6 | | dBm |
| Mixer Conversion Gain (Note 1) | $T_A$ = +25°C | 7.4 | 8.4 | 9.0 | dB |
| | $T_A$ = $T_{MIN}$ to $T_{MAX}$ | 6.2 | | 10.2 | |
| Mixer Noise Figure | Single sideband | | 9.1 | | dB |
| Mixer Input IP3 | (Note 3) | | 4.5 | | dBm |
| Mixer Input 1dB Compression | | | -7 | | dBm |
| Mixer Output Frequency | (Notes 1 and 4) | | | 450 | MHz |
| Receiver Turn-On Time | (Notes 1 and 5) | | 0.5 | 2.5 | µs |
| Minimum LO Drive Level | (Note 6) | | -17 | | dBm |
| LO to LNAIN Leakage | RXEN = high or low | | -49 | | dBm |

**Note 1:** Guaranteed by design and characterization.

**Note 2:** 1.9GHz and 1.901GHz tones at -30dBm per tone.

**Note 3:** 1.9GHz and 1.901GHz tones at -21.5dBm per tone.

**Note 4:** Mixer operation is guaranteed to this frequency. For optimum gain, adjust IF output match. See the IF Output Impedance (single ended) vs. Frequency graph in the *Typical Operating Characteristics.*

**Note 5:** Time from RXEN = low to RXEN = high, until the combined receive gain is within 1dB of its final value. Measured with 47pF blocking capacitors on LNAIN and LNAOUT.

**Note 6:** At this LO drive level, the mixer conversion gain is typically 1dB lower than with -10dBm LO drive.